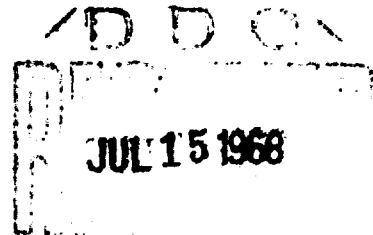Report No. 7489-2
(Unclassified)

SURVEY ON SEAPLANE

HYDRO-SKI DESIGN TECHNOLOGY

PHASE 2: QUANTITATIVE STUDY

by P. A. Pepper and L. Kaplan

Edo Corporation

28 March 1968

Distribution of This Document is Unlimited

Performed for the

OFFICE OF NAVAL RESEARCH and the
NAVAL AIR SYSTEMS COMMAND
DEPARTMENT OF THE NAVY
WASHINGTON, D. C., under Contract N00014-66-C0126

ACKNOWLEDGEMENT

TABLE OF CONTENTS

TABLE OF CONTENTS (cont.)

TABLE OF CONTENTS (cont.)

TABLE OF CONTENTS (cont.)

TABLE OF CONTENTS (cont.)

LIST OF FIGURES

LIST OF FIGURES (cont'd)

LIST OF FIGURES (cont'd)

ABSTRACT

This report covers the second part of a two-phase survey and analysis of hydro-ski seaplane technology. It contains quantitative correlations and parametric analyses of significant data used to define optimum hydro-ski size, ski location with respect to the strut and aircraft, ski and strut resistance, ski loads and load factors in waves, strut attachment to the aircraft, effects of strut size and length, and ski installation weight. The Phase I report previously issued, contains qualitative descriptions and correlations of the same information, as well as a complete bibliography of hydro-ski technology.

These two documents contain all of the background knowledge required before conducting general or specific design studies of hydro-ski configurations for a given set of design criteria, thereby eliminating the necessity for first reviewing the entire vast literature on seaplane hydro-skis. Simultaneously, they serve to define the state-of-the-art in this field and to indicate those specific areas requiring further investigation and definition.

SUMMARY

This report furnishes a complete description of all work done under Phase 2 of ONR Air Programs Contract N00014-66-C0126, thereby completing a survey of hydro-ski seaplane technology. The Phase 1 work for this contract, covering the qualitative survey, has been described in a companion report, Reference (1-1).

Phase 2 of this contract consists of a quantitative survey and related analyses. A prevalent feature of the present effort was in the systematic use of a digital computer for the more complex analyses covering the basic problem areas of hydro-ski seaplane dynamics. These were:

a) Fixed-trim, single impacts in waves;

b) Lower trim limits of stability in calm-water high-speed planing;

c) Two-degree of freedom response while traversing a train of waves at high speed.

For each of the areas investigated in this quantitative study, the existing empirical information was correlated with available analytical methods, including those developed during the course of this study.

As a result of the new analyses, successful correlations, and parametric studies described in this report, the final principal conclusion drawn from the Phase 2 effort is that present-day hydro-ski technology is sufficiently advanced so that the design of new hydro-ski seaplanes can be undertaken with a high degree of confidence and without danger from un-anticipated difficulties of an unusual nature. However, this high level of knowledge must still be augmented by an equally high level of skill and ingenuity on the part of the designer and, further, the analytical approaches emphasized herein must invariably be supplemented by suitable model tests.

The main findings of each of the analytical sections of this report are summarized below.

Section 3:   Steady-State Hydro-Ski Hydrodynamics

Adequate theoretical methods generally exist for calculating the steady-state hydrodynamic characteristics of basic hydro-ski forms in the fully wetted, ventilated, and planing regimes. Further experimental and theoretical studies are desirable for improving the calculation procedures for ventilated hydro-skis.

Section 4:   Strut Resistance Characteristics

Strut drag estimates can be confidently made for conditions at zero yaw angle. Further study is needed to adequately cover conditions with non-zero yaw.

Section 5:   Single Hydro-Ski Wave Impacts

An improved procedure has been developed for calculating the time history of fixed-trim single impacts in waves. The investigation revealed that, contrary to existing opinion, the maximum impact load does not occur when the initial contact is made on the mid-flank of a wave. Parametric analyses were also made to evaluate the effect of forward speed, wave height, and wave length on maximum loads and associated wetted lengths.

Section 6:   Dynamic Stability in Calm Water

The existing analytic method for calculation of the lower trim limit of stability applies only to chines-dry planing of a conventional-hull seaplane. A corresponding method was developed for the ski chines-wet planing of a hydro-ski seaplane. This linear analysis was converted to a digital computer program whose output defines the lower limit porpoising curve in the trim-speed plane. The correlations made with this program demonstrated its effectiveness for analyzing porpoising behavior during the preliminary design phase. The parametric studies indicated certain important beneficial and detrimental effects of various hydro-ski design parameters.

Section 7:   Wave Response of a Hydro-Ski Seaplane

To develop a rational method for selection of hydro-ski support strut length, a computer program was developed for calculation of the pitching and heaving response of a hydro-ski seaplane while traversing a wave train at constant speed, with the assumption that no hull impacts occur. The calculated results were compatible with theoretical expectations. The correlation with the available limited towing tank data was generally favorable and reasonable explanations were established for certain discrepancies.

As a result of the difficulties involved in programming this relatively complex non-linear analysis, it was found impractical, within the funds available for this contract, to conduct the desired parametric analyses.

Section 8:   Longitudinal Location of Hydro-Ski

The analysis of empirical data on hydro-ski longitudinal location indicated that the aircraft aerodynamic characteristics play a fundamental role in determining the optimum location of a hydro-ski. The computer programs developed in Sections 6 and 7 are considered useful for analysis of hydro-ski location in preliminary design work.

Section 9: Hydro-Ski Installation Weight

New and improved formulas were developed for correlating the weight data for skis and struts of previous full-scale ski installations. Some approximations are also provided for the weights of hull carry-through structure and ski retraction systems.

Section 10: Conclusions and Recommendations

As the principal result of this survey and analysis, it is concluded that hydro-ski seaplane design technology is sufficiently advanced so that the design of a hydro-ski seaplane for open ocean operation can be undertaken with confidence. Recommendations for further research are made for those areas where gaps in the knowledge still exist.

1. INTRODUCTION

This report covers the work done by Edo Corporation on Phase 2 of ONR Contract No. N00014-66-C0126. The basic purpose of this contract is to produce, by means of a survey and analysis, a single source document defining the present state of knowledge of seaplane hydro-ski technology.

The specific tasks assigned under this contract were as follows:

1. To conduct a literature search for all analytical and experimental data on aircraft hydro-skis and compile a bibliography;

2. To correlate qualitatively all data relating to optimum hydro-ski shape, spray characteristics, and longitudinal, lateral, and directional stability during take-off and landing of hydro-ski seaplanes;

3. To correlate quantitatively all data relating to hydro-ski size, ski location with respect to strut and aircraft, ski and strut resistance, ski loads and load factors in waves, strut attachment to the aircraft, effects of strut size and length, and ski installation weight.

The first two of these tasks, accomplished under Phase I of this project, have been reported in Reference 1-1.

The fundamental viewpoint underlying the entire Phase 2 quantitative study revolved around the adequacy of existing analytical methods and empirical data for the establishment of preliminary hydro-ski seaplane configurations. Based on this viewpoint, the complete range of hydro-ski technology was critically examined, beginning with the fundamental topic of the hydrodynamic lift of a planing surface and ending with the pitching and heaving motions of a hydro-ski seaplane in rough water. This review revealed that several important information gaps in hydro-ski technology still existed and that, correspondingly, a number of original analyses would be required.

A program plan was then established for the execution of the technical effort. This plan treated the dynamics of the hydro-ski seaplane in a progressively complex manner with respect to the aircraft's degrees of freedom and possible motions.

The program plan covered the following major problem areas:

A. Fundamental considerations in the design of hydro-ski installations, including principles of hydro-ski sizing and location;

B. Steady-state hydrodynamic characteristics of hydro-skis, i.e., lift, drag and center-of-pressure values for steady planing and submerged conditions;

C. Steady-state resistance characteristics of hydro-ski support struts;

D. Single impacts of fixed-trim hydro-skis (smooth and rough water conditions);

E. Planing stability of "skeleton" hydro-ski seaplanes (two degree-of-freedom linearized dynamics, smooth water condition);

F. Wave response of "skeleton" hydro-ski seaplanes (two degree-of-freedom non-linear dynamics, rough water condition);

G. Survey and analysis of hydro-ski installation weights.

For each analysis, the following general procedure was utilized:

a. Suitable analytic expressions, either previously established or newly developed, were defined, as required;

b. Where necessary or desirable for the particular analysis, a computer program was developed;

c. Calculations were then made using, as inputs, values for available test data;

d. Calculated values, such as loads, time histories, etc., were compared with the test results;

e. These correlations were then used to assess the validity of the analyses;

f. The computer programs were then used to perform pertinent parametric studies and the significant results of these studies were discussed.

It will be seen in the body of this report that these analyses have led to much further unification and amplification of hydro-ski knowledge and, further, have produced a number of results directly useful in design.

This report ends with a series of significant conclusions and specific recommendations for further experimental and analytical work in hydro-ski technology.

REFERENCES

1   Edo Report No. 7489-1: "Survey on Seaplane Hydro-Ski Design Technology. Phase 1: Qualitative Study," by P. A. Pepper and L. Kaplan, 23 December 1966.

2. FUNDAMENTAL CONSIDERATIONS IN THE DESIGN OF HYDRO-SKI INSTALLATIONS

2.1   INTRODUCTION

For the guidance of the hydrodynamics engineer, this section describes a number of fundamental considerations that must be made during the design of hydro-ski installations, as related to actual seaplane operations (take-off, landing and taxiing) in smooth and rough water, then presents the general sequence of design procedures, and finally discusses the analytical and/or experimental investigations that must be covered in the design phase. Among other things, this discussion explains the pertinence and use of the analyses and computer programs developed during this study contract. In addition, it proposes a new method whereby tank tests can be combined with computer calculations to obtain important information on hydro-ski seaplane hull loads, a subject not covered in the present state-of-the-art.

In keeping with the later sections of the report, emphasis is placed on the longitudinal characteristics which are obviously more basic than the others. A principal purpose of this discussion is to clarify the often conflicting hydrodynamic requirements for hydro-ski installation geometry in a systematic manner. It will be seen that most of the problem areas are susceptible to individual <u>analysis</u> but a standard procedure for the complete resolution and synthesis into an optimum system has not yet been achieved.

2.2   DESIGN PROCEDURE SEQUENCE GUIDELINE

Figure 2-1 presents a block diagram of the sequential procedures that will generally be followed during the hydrodynamic configuration development phase in the design of an operational hydro-ski configuration. Table 2-1 presents the associated nomenclature code. The analytical studies are seen to consist of a set of preliminary and final calculations.

The preliminary calculations establish approximate values for the hydro-ski size, the adequacy of the aircraft roll and yaw control in calm water conditions, and the hydro-ski load factor in high speed impacts. The latter calculation also determines the necessity for a "variable-area" hydro-ski if it is found that, using the ski size required for the desired unporting speed, the maximum load factors developed in high speed (landing) impacts exceed their desired design value. A variable-area hydro-ski utilizes a suitable mechanical arrangement to provide two different areas: a large one appropriate for speeds near unporting and a small one for speeds near getaway.

Utilizing the results of the preliminary calculations, more precise and definitive analyses of the longitudinal dynamic characteristics may be undertaken which will result in prediction of the lower trim limits of stability and the degree of rough water capability. Evaluation of the results for both the preliminary and final analytical studies will permit the final selection of the hydro-ski seaplane configuration on which dynamic model towing tank tests should be conducted.
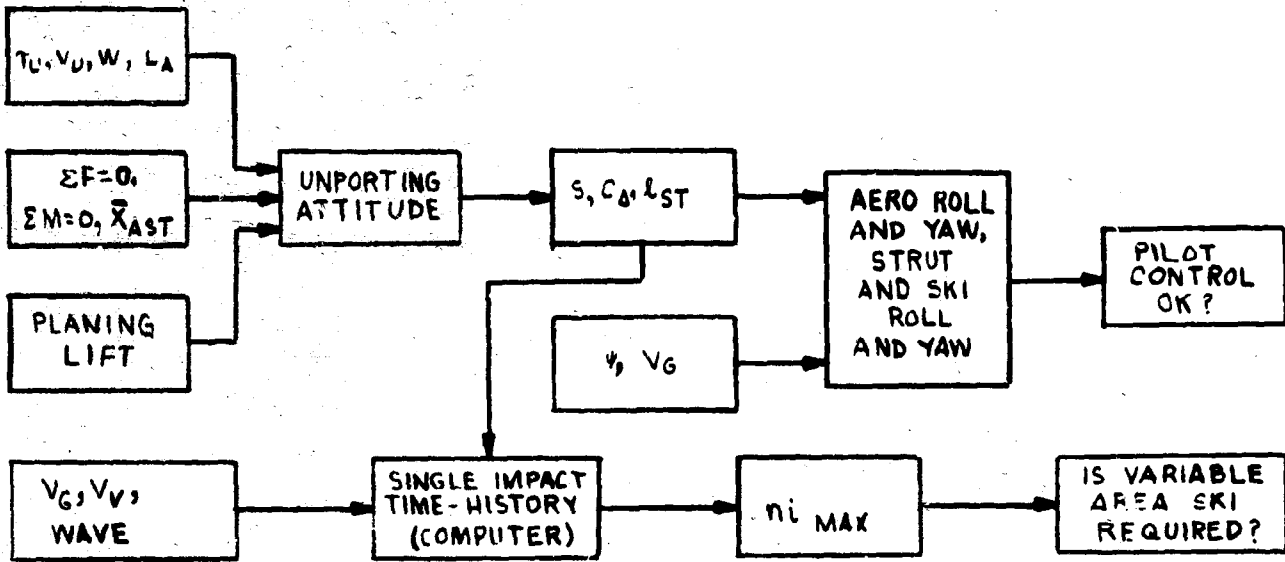
A. PRELIMINARY CALCULATION OF SKI SIZE AND STRUT LENGTH
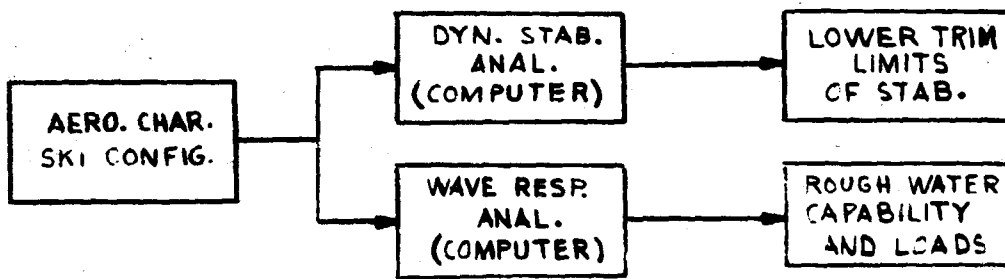
B. FINAL CALCULATION OF SKI AND STRUT CONFIGURATION
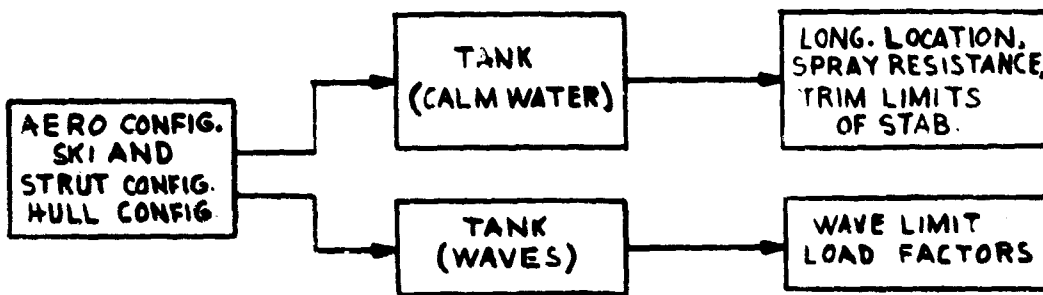
C. TOWING TANK TESTS

Figure 2-1. Hydrodynamic Design Sequence

TABLE 2-1

CODE FOR FIGURE 2-1(A)

τ_u = unporting trim

V_u = unporting speed

W = aircraft weight

L_A = aerodynamic lift

$(\Sigma F = 0)$ = lift equilibrium

$(\Sigma M = 0)$ = pitching moment equilibrium

$X_{A_S f}$ = distance from strut to hull afterbody step

S = hydro-ski area

C_{Δ_o} = beam loading coefficient

l_{ST} = strut length

Ψ = angle of yaw

V_G = getaway speed

V_v = sink speed

$n_{i_{max}}$ = maximum impact load factor

The primary purpose of towing tank tests is to serve as a check on the results of the theoretical investigation. As such, it can be anticipated that from these tests, some modifications to the configuration may result, particularly from those aspects of the flow characteristics, such as spray impingement effects, which cannot be readily considered in the mathematical model of the dynamic analysis.

The remainder of this report section furnishes a detailed description and explanation of the steps illustrated in Figure 2-1.

2.3 SELECTION OF UNPORTING SPEED AND SKI DIMENSIONS

2.3.1 Basic Problem Statement

Although some hydro-ski installations are optimized to permit calm-water take-offs because the basic aircraft configuration is inappropriate for a hull-type installation, the basic purpose of a seaplane hydro-ski is considered in this report from two fundamental viewpoints, both of which concern load alleviation in rough water. From one viewpoint, the primary function of a hydro-ski is to raise the hull clear of the waves in the high speed range. If this is not done, excessive loads and motions would occur under hull impacts. From another viewpoint, the primary function of a hydro-ski is to strike the water surface first so that, should the hull make contact, the sink speed would be greatly reduced, thereby resulting in only moderate hull impact loads. Basically, both concepts represent two ways of stating the same effect, but the former is more descriptive of a rough water take-off, while the latter describes the situation during a rough water landing. Both statements revolve around the fact that significant water impact accelerations can be developed in either situation. It follows that one of the primary concerns of the hydro-ski seaplane designer is the selection of the hydro-ski size for which, in the specified critical sea state, the design maximum loads for hydro-ski and hull impacts will be the same.

Thus, too large a ski will protect the hull from direct water impacts but hydro-ski impacts will be greater than they need be, while too small a ski will result in low hydro-ski impact loads but no substantial hull load reduction over that for a conventional seaplane. It will be evident from the following paragraphs that, in the present state-of-the-art, there is no straightforward solution to this fundamental design problem area.

2.3.2 Rough-Water Hull Loads vs. Speed

The variation of hull rough-water impact loads with speed and hydro-ski size is of obvious importance in connection with the selection of unporting speed and ski dimensions. However, primarily because of the scarcity of experimental data relating to this subject, definitive approaches to this problem area could not be established in the present project. Since data on hull impact loads are important for optimum structural design, a procedure is proposed below which will provide hull impact design load data for hydro-ski seaplanes.

A computer program is presented in Section 7 which calculates the hydro-ski loads, aerodynamic loads, and aircraft accelerations and motions generated on a skeleton (i.e., non-wetted hull) hydro-ski seaplane traversing a wave train at speeds above unporting. It is obvious that this computer program can be readily transformed into another which will determine the instantaneous hydro-ski and aerodynamic loads corresponding to a known time-history of aircraft motions relative to a wave surface.

Now, if the known time-history of aircraft motions (relative to a wave surface) fed into the computer program consists of recorded data from towing tank tests of a model hydro-ski seaplane, the computer can be utilized to establish the associated magnitudes of the hydro-ski and aerodynamic loads. However, as the accelerations recorded in the towing tank tests

also include the effect of hydrodynamic impacts on the hull, subtraction of the calculated hydro-ski and aerodynamic loads will permit the determination of the magnitude and location of the resultant hull impact loads.

As the hull bending moments are of primary interest for structural design, the towing tank model hydro-ski seaplane should also incorporate instrumentation for measuring the bending moment at selected stations or, as a minimum, for indicating the instantaneous location of hull wetted areas. These data will then allow the rational distribution of the resultant hull impact loads, especially if they are found to act simultaneously on separate forebody and afterbody regions. In this approach, it is assumed that any spray loadings on portions of the aircraft model are comparatively negligible, i.e., that hull wetting is primarily associated with direct hull impacts.

The procedure just described can be used for general parametric studies of ski-hull load equalization and/or studies of particular seaplane designs. Particularly in the latter case, it should be made an integral part of the model test procedure so that the effects of varying the ski parameters (as required for load equalization and which also automatically determine the unporting speed) on the other hydrodynamic qualities (planing stability, etc.) could be simultaneously assessed.

2.3.3 Rough-Water Ski Loads vs. Speed and Beam Loading

A basic problem confronting the hydro-ski designer is the selection of the hydro-ski size, or beam loading, compatible with reasonably low impact load factors. Since, under operational conditions, maximum hydro-ski impacts occur from wave contacts, analyses must be conducted to assure that excessive load wave impacts do not occur during the high-speed portion of the take-off or landing run.

As mentioned in Section 2.2, these analyses can be conducted from both a preliminary and final calculation aspect. in which single-impact time-history calculations are made in the preliminary phase. A computer program for these calculations is established in Section 5 of this report.

Although the fixed-trim wave-impact time-history calculations correlate well with experimental data, its use in hydro-ski seaplane configuration development is limited to the preliminary design phase only. The reason is that the approach parameters (sink speed and trim) for any single impact are arbitrarily selected and do not necessarily represent the natural dynamic response values that will occur when running through a train of waves. Rational calculations for landing in a wave train can be performed by the more complex two degree-of-freedom non-linear program developed in Section 7.

2.3.4 Unporting Speed and Ski Beam Loading

The hydro-ski unporting speed is a fundamental design parameter. When properly selected and achieved, it represents the speed above which a properly designed hydro-ski and strut combination will shield the hull from critical impacts in the design sea state. Although this implication is basic to unporting speed selection, unporting speeds have invariably been related to the calm water condition because of its relative analytical simplicity.

The standard procedure for calculation of the hydro-ski size, or beam loading, is to assume a "stick-fixed" take-off. That is, the side view drawing of the hydro-ski seaplane is laid out at that trim in which the level water line touches the ski bow and the afterbody step. From the considerations of static force and moment equilibrium, the required hydro-ski lift for various unporting speeds is established while accounting for the wing aerodynamic lift and the afterbody hydrodynamic lift. Having determined the required hydro-ski lift, the Shuford planing lift equation (with suitable modification as required for more complex ski shapes) (Section 3) can be employed to define the corresponding beam loadings associated with a range of hydro-ski lengths.

It may be found that the determined hydro-ski beam loading corresponding to the selected unporting speed is incompatible with the load factor limitation established as described in the preceding paragraph. Judicious adjustments in hydro-ski dimensions and/or the design unporting speed may then be considered to achieve the desired compatibility. It is sometimes necessary to employ a "variable area" hydro-ski to satisfy the conflicting beam loading requirements between unporting speed and maximum hydro-ski impact load factor.

2.3.5 Ski Area, Length, and Miscellaneous Parameters

It is now evident that several configuration parameters can be varied for the purpose of developing the desired performance characteristics. For example, hydro-ski lift may be increased by increasing the beam or incidence, or decreasing the deadrise. Each parametric variation may introduce detrimental effects under other conditions, so that trade-offs must be continuously evaluated.

Consider, for example, the situation in which it is desired to reduce the unporting speed by increasing the hydro-ski area. This may be accomplished either by increasing the hydro-ski beam or length. Because of aspect ratio effects, changing the beam is a more efficient way of accomplishing a change in lift. However, this approach will also invariably result in an increase in the maximum impact loads occurring in single impacts and in rough-water taxiing. Consequently, the final choice may involve an increase in hydro-ski length. Therefore, due to the complex relationships existing between the various hydro-ski parameters, with respect to their relative effectiveness, compromise adjustments in the hydro-ski configurations will be made, where more than one basic dimensional parameter is simultaneously varied in order to obtain the necessary or desired hydrodynamic characteristics. By referring to Sections 3, 5, and 6 of this report, considerable guidance for the quantitative effects of varying hydro-ski parameters may be obtained.

2.4 SELECTION OF SKI LOCATION

2.4.1 Unporting Trim Angle

The simple procedure described in para. 2.3.4 for preliminary estimation of the hydro-ski dimensions to accomplish unporting at a specified velocity involves drawing a profile of the hydro-ski seaplane in the unporting attitude. The geometry assumed is fairly representative of the actual attitude observed in towing tank tests, which, of course, simulates a fixed-stick take-off. This may not necessarily be the case under prototype operational conditions, since elevator control may be applied by the pilot to keep the bow down, so that there is no rapid pitch-up to the unporting attitude, and the hydro-ski is brought to the surface planing regime without the afterbody contacting the water.

For hydrodynamic design purposes however, the towing tank situation at unporting is considered, since its associated greater trim implies a conservative drag condition and the possibility of wing stalling will then be more closely examined. Furthermore, designing for a "two-point" unporting attitude reduces the pilot skill required for successful unporting.

2.4.2 Vertical Location

2.4.2.1 Hull Clearance

The vertical location of a hydro-ski (or, equivalently, the strut length), is obviously a primary factor affecting the rough water capability of hydro-ski seaplane configuration. Nevertheless, other considerations will limit the maximum strut length that may be designed for any particular aircraft. For example, it is obvious that, for any specific hydro-ski installation, a strut length can be reached which, because of the associated drag and bow-down moment, will prevent the trimming up motion necessary for ski unporting. As the bow-down moment is caused by the resultant force vector from the strut and hydro-ski passing too far aft of the c.g., it is sometimes possible to alleviate this situation by a further forward location for the ski.

The strut length is limited to that value for which corresponding unporting trim does not result in wing stalling. Otherwise, as the unporting attitude is approached, the wing lift will drop off, which increases the load on the ski and cause it to resubmerge, resulting in an emergence instability. The maximum strut length selected in accordance with this requirement (avoidance of wing stall at unporting) then must be investigated relative to the rough water capability when ski-borne, since its primary function is to keep the hull clear of wave impacts. The exact relationship between strut length and sea state negotiability has not been previously established either empirically or analytically.

The approximate "rule of thumb" relationship used in the past states that the wave height capability of a hydro-ski seaplane is equal to its strut length. In retrospect, as indicated in the Phase I report para. 4.3.2.2, it seems that this design guideline is more appropriate to a penetrating hydro-ski installation where, because of the high beam loading,

the aircraft tends to "plow through" the waves. With lower beam loadings (corresponding to large hydro-skis), the aircraft tends to rise over the waves so that for this type of installation the strut length can presumably be less than the negotiated wave height.

The foregoing empirical criteria may be used for estimating the proper strut length during the preliminary design phase of hydro-ski configuration design. During the later design phases, where investigations are conducted to ensure that the configuration will satisfy the specified rough water conditions, an analytical study of the seaplane's wave response characteristics based on the method presented in Section 7, should be undertaken.

2.4.2.2   Lateral Stability Effects

Having established a strut length for a particular hydro-ski which satisfies the rough water and longitudinal stability requirements, it may be found that when the aircraft is yawed, the rolling moment generated by the hydrodynamic side forces on the strut and ski is sufficiently large to introduce lateral stability problems.

To overcome the rolling tendency in yawed attitudes, adequate aerodynamic control is required. The two critical regimes for roll instability are at unporting and landing. In the first case, unporting may be difficult, even under a moderate amount of yaw, if ailerons are ineffective at the associated speed. In this case, it may be necessary to consider such design changes as increasing aileron size, decreasing the strut length, or increasing the unporting speed. In the second case, if a yawed landing is made, although ailerons are effective, it must be demonstrated that adequate restoring moment can be developed. Furthermore, it is also necessary to demonstrate, either by calculations or model tests, that, even though aileron control is adequate, the aircraft will not roll excessively in a moderately yawed landing before the pilot is able to respond and apply corrective control.

2.4.3   Longitudinal Location

2.4.3.1   Aircraft Longitudinal Control

Throughout the take-off regime, the hydro-ski and/or strut develops a continuously varying pitching moment about the aircraft center of gravity. It is clearly desirable that the hydro-ski be installed in such a position that the magnitude and direction of the moment naturally tend to assist the aircraft in maintaining a trim attitude variation which results in the shortest take-off run. As this ideal situation is unlikely to be realized in a stick-fixed take-off, the pitching moment generated by the hydro-ski and strut for the longitudinal position selected should at least permit pilot controllability of the trim. This aspect of the design is usually investigated in towing tank tests, where the effect of different elevator deflections on the take-off process can be evaluated.

2.4.3.2 Static Stability and Forward Location Limit

To counteract the moment from the drag forces acting on the submerged strut and hydro-ski, the longitudinal position of the hydro-ski is generally located somewhat forward of the aircraft center of gravity. The precise location of the hydro-ski is usually established from towing tank tests, wherein the stability characteristics for different fore and aft ski positions are observed, and the optimum location selected.

In a basic research tank test program on the effect of hydro-ski beam loading on rough water landing characteristics (Reference 2-1), it was established that, as the beam loading increases, a more forward position of the hydro-ski is required to prevent diving. This behavior is evidently a consequence of the increasing penetration afforded by higher beam loadings in which, because of the greater amount of strut wetting, the strut drag plays a greater part in the inclination of the resultant hydrodynamic force vector from the hydro-ski and strut. This towing tank investigation on the effect of systematically varying the hydro-ski beam loading demonstrated that, for any specific aircraft, the optimum longitudinal location of the hydro-ski is dependent on the value of the beam loading coefficient. In the study of Reference 2-1, landing tests in waves were conducted, and it was found that, for any longitudinal ski position, if the hydro-ski beam loading were too low, rapid pitch up motions would occur and that too high a beam loading would result in diving. It was therefore established that, as compared with large (low beam loading) hydro-skis, the optimum center of pressure locations for penetrating (high beam loading) hydro-skis, are further forward.

This result could have been anticipated since, for a constant strut length, with higher ski penetration, the greater the average wetting of the hydro-ski strut, thereby contributing a larger resistance component which increases the strut-ski resultant load inclination. The net effect is to apply a bow-down moment, so that to compensate, the ski has to be located in a somewhat more forward position. It is finally important to note that, with a ski in a relatively forward position, increasing ski incidence is also effective in preventing diving.

2.4.3.3 Dynamic Stability and Aft Location Limit

A well-known phenomenon in seaplane behavior is that of "lower limit" dynamic instability, commonly known as "porpoising". It is generally found that, as the static equilibrium planing trim is reduced (at a fixed speed), a trim value is reached below which a build-up in pitch and heave oscillations occurs. It is well-known that this instability is related to dynamic effects, and a relatively complex dynamic analysis (including aerodynamic contributions) is required to establish the precise location of the porpoising limit in the trim-speed plane.

A computer program for this analysis is presented in Section 6 of this report and shown to yield good agreement with test data. The study of that report section reveals the existence of a new factor conducive to porpoising. It is found that, for equilibrium trim angles in which the wetted area is entirely within the triangular region of a hydro-ski having a triangular stern planform, the stable portion of the planing region becomes severely

limited for a sufficiently aft location of the hydro-ski. It is thus deemed necessary to conduct the dynamic analysis of Section 6 for each specific aircraft employing a hydro-ski, and all the more so for skis with stern planform taper, to establish the range of aft ski locations which will cause this mode of dynamic instability.

2.4.3.4   High-Angle Porpoising

At any speed in the ski-borne range of a hydro-ski seaplane, there exists a trim at which getaway will occur provided that trim does not correspond to wing angles of attack in the stalled range. It is possible however that, before the flying trim is reached, the configuration is such that the hull afterbody contacts the water surface and initiates a porpoising action. This "high-angle porpoising" is less likely to occur in hydro-ski seaplanes because the strut places the hull at a substantially higher elevation than would be the case for conventional seaplanes at the same speed.

However, the possibility of high-angle porpoising should always be checked out in the course of the towing tank model test program because no method of analysis for this problem is available in the present state of the art. Reference 2-2 presents an example in which high-angle porpoising occurred in a hydro-ski configuration. This configuration consisted of a hydro-ski in an extreme forward location and a hull with an extreme aft step. The towing tank tests showed that the hydro-ski wake interacted with the hull bottom to cause unsatisfactory pitching behavior.

2.4.3.5   Directional Stability Effects

It can be generally assumed that when the aircraft is yawed and portions of the hydro-ski and strut are wetted, the center of pressure for the resulting side load will be forward of the aircraft center of gravity. This destabilizing effect introduces the possibility of directional instability.

This situation is usually evident on hydro-ski seaplanes during the landing run-out of a hydro-ski seaplane, when the forward speed is reduced sufficiently to cause submergence of the hydro-ski. At that time, because of the inadequacy of rudder control, a definite "hooking" motion will take place. Fortunately, because of the associated rapid deceleration, the only effect is one of personnel discomfort. However, there are two instances in hydro-ski seaplane operation where such a hooking tendency is less tolerable, one of which is potentially catastrophic.

The first case considered is that which can occur just prior to unporting. If an aircraft yaw attitude is developing as the unporting speed is being approached, the associated destabilizing moment may reach a magnitude sufficient to cause aborting the take-off because of the excessive drag resulting from the asymmetrical attitude by the yawing moment. Piloting techniques, such as selection of the initial heading with respect to the wind, are usually adequate to compensate for this effect.

A more serious design consideration is a yawed attitude in a rough-water landing in which the ski and strut can submerge at high speed. This has already been discussed with respect to lateral stability effects in para. 2.4.2.2. In this same situation, relatively forward locations of the hydro-ski and strut also tend to induce hooking at high speed which, of course, would be extremely dangerous. It is therefore necessary, in designing a penetrating hydro-ski installation, to insure that, when ski and strut submergence occurs at high speed, the pilot can bring the resulting unstable motion under control.

2.4.3.6 Correlation of Empirical Data on Longitudinal Ski Location

Although it is obvious from the preceding discussion that very many considerations enter into the choice of longitudinal ski location, it was hoped that an empirical correlation for this quantity could be established from existing geometrical data for previous ski installations. Such correlations, using single geometric parameters, were attempted, as described in greater detail in Section 8 of this report. These attempted correlations were unsuccessful and the lack of success was attributed to the multiplicity of parameters (particularly, the aerodynamic parameters) which actually affect ski location.

2.5 SPRAY CONSIDERATIONS

The spray characteristics of any seaplane configuration are of vital importance to its successful performance. Excessive spray can result in large drag increments, obscurement of pilot vision, structural damage and unstable behavior, any one of which, if appreciable, can render the aircraft unacceptable. The spray behavior of a hydro-ski seaplane configuration is generally evaluated in the course of the towing tank investigation.

It has frequently been found that the spray characteristics observed on hydro-ski seaplane tank models are optimistic with respect to prototype behavior. This situation can usually be attributed to the lateral and directional restraints generally imposed on the model during its tests. A clear example of this type was furnished by the Grunberg hydrofoil system on the JRF-5 airplane. This configuration employs a main supercavitating hydrofoil and two bow hydro-skis. The model tests of this configuration (Reference 2-3) showed very mild spray created by the bow-ski unporting, whereas the corresponding prototype spray was intolerably severe. This difficulty was overcome by reduction of ski incidence, elimination of the ski pointed trailing edges, and addition of chine strips.

Towing tank studies have been conducted to establish parametric relationships for the spray characteristics of planing surfaces. These studies are conducted for the utilization of their data for the prediction of full-scale geometry and associated effects. However, the results of these studies must be carefully interpreted, as shown by the following two specific instances of contradictory conclusions regarding the effects of certain hydro-ski design details on spray behavior.

The first case concerns the effect of horizontal chine flare on the height of the main spray. From the towing tank tests of prismatic planing surfaces in Reference 2-4 and 2-5, it was concluded that horizontal chine flare is ineffective in reducing the spray height

of the basic deadrise sections. Nevertheless, in the full-scale tests of Reference 2-6, the observations conclusively demonstrate that hydro-ski chine flare effectively minimizes the main spray height.

The second example concerns the effect of vertical chine strips on suppression of main spray height. From the tow tank test of Reference 2-4, it was reported that 2.2 to 5.5 percent beam width vertical chine strips are effective in reducing spray height. However, in the tow tank tests of Reference 2-5, where 4 percent beam width vertical chine strips were attached to the prismatic deadrise planing surface; it is reported that vertical chine strips have a relatively small effect. A further examination of these two references reveals that the conclusions of Reference 2-4 are based upon trims of 8, 12, and 15 degrees. The conclusions of Reference 2-5 are based upon trims of 6, 18, and 30 degrees, in which main spray height reduction at the lowest tested trim is noted in the body of the report.

From the foregoing, it appears that, pending further detailed investigation of the subject, both chine flare and vertical chine strips are effective in reducing main spray height at the trims generally associated with hydro-ski operation.

The spray burst associated with the unporting of a hydro-ski has also been a source of concern to the hydro-ski designer. For large, low-beam loading hydro-skis, a "slotted bow" has proven effective, (Reference 2-7), whereas this device resulted in no improvement when applied to a penetrating-type hydro-ski (Reference 2-8). It must be noted, however, that the unporting spray from the basic penetrating (high beam loading) hydro-ski was much less severe than that from the basic low-beam loading ski.

2.6   SKI INSTALLATION WEIGHTS

Of considerable importance in preliminary design work is the ability to make reasonable weight estimates for hydro-ski installations. For this purpose, a survey and analysis has been made of such weight information for previous ski installations. This area is covered in Section 9 of this report which describes new empirical formulas which furnish close correlations for the individual weights of skis and ski support struts. It is emphasized that these formulas are conservative because of the vast bulk of the previous installations used retrofitting of the skis to existing hull seaplanes.

REFERENCES

2-1   NACA RM L56I25a: "Tank Investigation of a Series of Related Hydro-Skis as Load-Alleviation Devices for Landing a Seaplane in Waves," by A. W. Carter, A. E. Morse, Jr, and D. R. Woodward, 19 December 1956.

2-2   Martin Company Report RM-54: "Hydrodynamic Study of Forward-Ski Aft Step Seaplane Alighting System," by D. A. King and M. G. Scheider.

REFERENCES (Continued)

2-3 NASA TN D-220: "A Brief Investigation of a Hydro-Ski Stabilized Hydrofoil System on a Model of a Twin-Engine Amphibian," by Sandy M. Stubbs and Edward L. Hofman, February 1960.

2-4 Davidson Laboratory Report R-678: "On the Main Spray Generated by Planing Surfaces," by D. Savitsky and J. P. Breslin, January 1958.

2-5 Davidson Laboratory Report R-768: "Final Engineering Report on Wake-Shapes of Planing Forms Associated with High-Speed Waterbased Aircraft," by R. L. Van Dyck, October 1960.

2-6 Thurston Erlandsen Corp. - Report 6502-1: "Final Summary Report Flight Test of the Hydro-Ski Research Vehicle (HRV-1) Equipped with TEC Skis No. 4 and No. 4A on Strut No. 2," by O. Erlandsen and D. B. Thurston, December 1965.

2-7 NATC PTR AD-366.1: "Evaluation of Hydrodynamic Characteristics of Model PBM-5S2 Airplane with a Modified Hydro-Ski, Report No. 1 Final Report," March 1958.

2-8 NATC PTR AD-366.2: "Evaluation of Hydrodynamic Characteristics of Model PBM-5S2 Airplane with a Small Variable Area Hydro-Ski, Report No. 1 Final Report," September 1961.

3. LONGITUDINAL HYDRODYNAMIC CHARACTERISTICS
OF ISOLATED HYDRO-SKIS

3.1 HYDRO-SKI FLOW REGIMES

In this report, a "hydro-ski" is defined as a hydrodynamic lifting surface of low total aspect ratio, as opposed to a hydrofoil which has a large total aspect ratio. In this definition, the aspect ratio A, is taken as the square of the maximum transverse dimension divided by planform area. The division between the two categories may be taken, somewhat arbitrarily, as A = 1.

Speaking most generally, the nature of the flow and, consequently, the pressures and loads developed by a hydro-ski, depends in a complex manner on a number of parameters. In addition to the parameters defining the ski geometry, of which the principal ones are the ski beam, total length, and deadrise, the type of flow varies with the speed (relative to still water), the trim, and the draft (depth of lowest point on ski). In this report section, attention will be limited to steady-state flow conditions in which the ski moves at constant speed parallel to the (still, horizontal) water surface and, also, to the condition of positive ski trim (angle between ski keel line and water surface).

The physical nature and the relations between these flow regimes have been investigated for a few hydro-ski shapes of simplified geometry. These investigations have served to indicate the principal types of flow regimes which may be described qualitatively, as follows:

1. PLANING

For drafts not exceeding the height of the total vertical ski projection, the ski acts as a planing surface and the flow at the forward portion of the water line is not affected by the proximity to the ski leading edge. This condition is maintained for all positive trim angles.

For slightly greater drafts (ski leading edge, L. E.) either directly above, at, or below the water line), the flow remains basically of planing type but can be affected by the details of the water flow around the ski L. E. and, therefore, is sensitive to the details of the ski L. E. geometry as well as the trim angle.

2. SUBMERGED

For still greater drafts, i.e. submerged ski, several different types of flow are possible, depending on ski draft, trim, and speed, as follows:

A. Fully Wetted Flow

At all drafts and relatively low speeds and trim angles, there occurs "fully wetted" flow wherein both upper and lower surfaces of the ski are wetted. In this condition, the flow is generally similar to that over a low aspect ratio airfoil. These flows are characterized by the presence of trailing vortices which, in the vicinity of the ski, take the form of a vortex sheet. Further downstream, the vortex sheet rolls up into two separate "tip" vortices or "vortex cores". At sufficiently shallow drafts, the reduced pressure inside the tip vortices is adequate to induce a flow of air from the surface into the core regions so that these vortices become aerated. However, at the lower trims, the spreading of the vorticity inside the vortex sheet near the ski prevents this air from reaching the ski itself. As the ski trim is increased, the aerated rolled up vortices approach the ski until, at some particular trim value, they reach the ski and the entrained air then spreads over the upper surface, finally resulting in a "ventilated flow" condition. The conditions associated with ventilation inception are discussed in more detail in Section 3.3.2.

B. Ventilated Flow

In the ventilated flow condition, the upper surface of the ski becomes completely exposed to the atmosphere. Except for a narrow sheet of water which is thrown over the ski L.E., this flow is very similar to the planing type of flow.

C. Cavitated Flow

At deeper depths, it becomes more difficult for air from the surface to reach the trailing vortices and the ski. In this case, the vortices tend to develop cavities which, instead of air, are filled with water vapor. Again, sufficient increase of trim and/or speed will spread the trailing cavities over the ski's surface until the latter is completely cavitated, i.e., covered by an underwater cavity (containing water vapor) of some finite extent. The length of this cavity is determined primarily by the "cavitation number", defined as the ambient static pressure divided by the dynamic pressure, and increases as the cavitation number decreases, for example, with increase of speed. It is obvious that, for comparable trims and speeds, the lift on a cavitated ski is greater than that on the same ski when ventilated because of the reduced pressure on its upper surface.

The preceding description of the main flow regimes has been deliberately restricted to the case of uniform horizontal motion of the ski. For most engineering purposes, it is sufficiently accurate to assume that, in the case of non-uniform motions, the latter are quasi-steady so that the flow regimes are the same as those prevailing under equivalent steady flow conditions. Some exceptions of this rule are utilized later on and will be justified when necessary.

3.2 PLANING CONDITION

The steady state force and moment characteristics of planing surfaces in uniform horizontal motion have been investigated many times in the attempt to formulate accurate analytical expressions for these quantities. The particular analytical expressions which furnish the closest approximation to the measured values appear to be those developed by Shuford in Reference 3-1. These are a set of semi-empirical formulas for the lift, drag, and pitching moment on planing surfaces of rectangular and triangular planforms and having constant deadrise.

According to Reference 3-1, the dynamic lift coefficient of such planing surfaces is given by:

$$C_L = L/qS$$

$$= C_{L1} + C_{L2}$$

where:

$$C_{L1} = \frac{\pi}{2}\left(\frac{A}{1+A}\right)\tau \cos^2\tau \ (1-\sin\beta_e)$$

$$C_{L2} = C_{D,\,C}\sin^2\tau \ \cos^3\tau \ \cos\beta_e$$

and: τ = trim angle, radians

β_e = effective deadrise angle, radians (angle between line joining keel and chine and the horizontal)

A = wetted aspect ratio, b/l_m

b = beam at waterline

l_m = mean wetted length

S = wetted area = bl_m, for prismatic surface,

= $bl_m/2$, for triangular surface

Also, $l_m = (l_k + l_c)/2$

where l_k = wetted keel length

l_c = wetted chine length

The quantity, $C_{D,C}$, is a cross-flow drag coefficient whose numerical value depends on the shape of the ski bottom cross-section. Figure 3, page 33, Reference 3-1, shows these values for various bottom shapes. Of particular interest is the value for surfaces with straight vee-bottoms and sharp chines:

$$C_{D,C} = 4/3$$

In addition to the dynamic lift coefficient, there is an additional static lift coefficient due to the effective buoyancy of the planing surface. This quantity, of importance under low speed conditions, is found to be one-half of the geometric buoyancy, where the latter is defined as the displacement of the wedge-shaped volume between the wetted lower surface of the ski and the undisturbed water line. The analytic form of this quantity for a prismatic ski with flat bottom is:

$$C_{L,B} = B/2qS$$

$$= \left(\frac{l_m}{b}\right)\left(\frac{1}{4C_V^2}\right) \sin 2\tau$$

where C_V = speed coefficient = $V/\sqrt{gb}$

The drag coefficient of the planing ski can be written as:

$$C_D = D/qS$$

$$= C_f + C_L \tan \tau$$

where C_f is the familiar skin friction coefficient dependent directly on the ski Reynolds Number:

$$R = V l_m / \nu$$

where ν = dynamic viscosity of water.

The center of pressure locations, measured from the ski trailing edge, are given by:

$$l_{cp}/l_m = \left[(7/8)C_{L1} + (1/2)C_{L2}\right] \Big/ (C_{L1} + C_{L2}) \text{ ,(rectangular planform)}$$

and $\quad l_{cp}/l_m = \left[C_{L1} + (2/3) C_{L2} \right] \Big/ (C_{L1} + C_{L2})$,(triangular planform)

While the foregoing equations are relatively simple in nature, their application in specific calculations is rendered difficult by the fact that the quantities, l_k and l_c, are not defined analytically in terms of the geometric parameters (draft, trim, etc.). More specifically, whereas l_k can be taken as approximately equal to $d/\sin \tau$, (d = draft) the value of l_c depends on the so-called "wave rise" effect, associated with the high pressure prevailing at the ski intersection with the waterline. If there were no wave rise, l_c would be defined by the purely geometric relationships, as:

$$\frac{l_k - l_c}{b} = \frac{1}{2} \frac{\tan \beta}{\tan \tau}$$

whereas, according to the well-known Wagner theory, the wave rise increases the wetted width in the chines dry region by a factor of $\pi/2$, so that:

$$\frac{l_k - l_c}{b} = \frac{1}{\pi} \frac{\tan \beta}{\tan \tau}$$

However, as shown in Figure 18, Reference 3-1, the experimental values of $(l_k - l_c)/b$ exhibit a complex dependence of this quantity on β and τ and, furthermore, they are also dependent on l_m/b. To simplify the application of Shuford's formulas, the experimental values of $(l_k - l_c)/b$ shown in Figure 18, Reference 3-1, can be (somewhat crudely) approximated, if desired, by the following expressions:

$$(l_k - l_c)/b = .085 \qquad (\beta = 0°)$$

$$\frac{l_k - l_c}{b} = \frac{n}{\pi} \frac{\tan \beta}{\tan \tau} \quad (\beta > 0°)$$

where, as shown here in Figure 3-1, the correction factor, n, depends only on β and τ .

It is obvious that, for hydro-skis, a precise knowledge of the wetted chine length, l_c, is only required for low values of l_k/b, for example, when planing very close to getaway speed or during the very initial stages of an impact process. Further, as will be demonstrated later in this report, most current practical interest is in hydro-skis of very high beam loadings which are not necessarily dependent on the addition of deadrise for their impact load alleviation capability. Finally, noting that, so far as can be established from available data, the correction factor, n, is less than one, it appears that a convenient approximation for the wave rise effect is to assume "full wave rise," i.e.
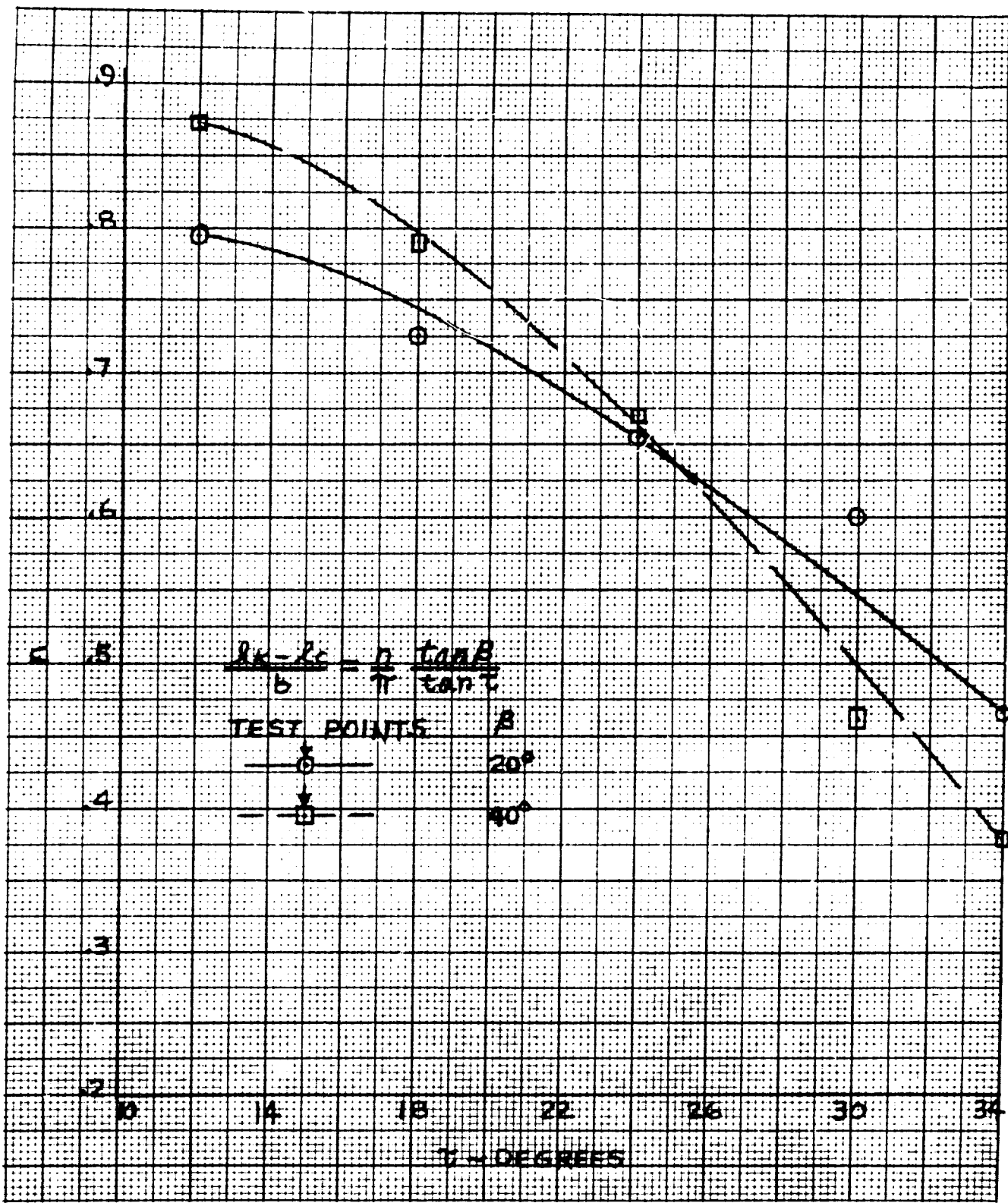
Figure 3-1. Empirical Correction Factors for Wagner Wave-Rise Formula

$$l_c = l_k$$

so that

$$l_m = l_k$$

Any substantial inaccuracy inherent in this approximation will then be limited to very low trim angles and/or very low wetted keel lengths.

This approximation has been used throughout the remainder of this report.

3.3 SUBMERGED CONDITIONS

3.3.1 Fully Wetted Condition

3.3.1.1 Lift Characteristics

A semi-empirical expression for the lift coefficient of a fully-wetted submerged ski has been derived and validated in Reference 3-2. This expression, valid only for flat (uncambered) skis with zero-deadrise and rectangular planform, is:

$$C_L = K_3 \left[\frac{2 \pi K_2 A}{(1 + A) + 2K_2} \tau + \frac{8}{3} \left(1 - \frac{A}{10} \right) \sin^2 \tau \cos \tau \right]$$

where $A = b^2/S$, and K_2 and K_3 are certain theoretical correction factors. K_2 depends on the draft and trim, while K_3 depends on draft, trim, and aspect ratio.

As most practical skis have $A < 1/3$, little accuracy is lost by neglecting the term, $(A/10)$, so that:

$$C_L \cong K_3 \left[\frac{2 \pi K_2 A}{(1 + A) + 2K_2} \tau + \frac{8}{3} \sin^2 \tau \cos \tau \right]$$

The function, K_2, is defined as:

$$K_2 = \frac{4f^2 + 8f \sin \tau + 1}{4f^2 + 8f \sin \tau + 2}$$

where

$$f = d \left[1 + \frac{\sin \tau}{4 (d + .05)} \right]$$

and d is the depth of the ski (flat plate) leading edge expressed as a fraction of the ski length.

As defined in Reference 3-2, K_3 is a complex function of f, τ, and A. However, for $A \leqslant 1/4$, the values of K_3 are nearly independent of A and, further, for $\tau < 20°$, are nearly independent of τ. Hence, in these parameter ranges, K_3 depends only on f and, for $0 < f < 1$, can be approximated closely by the simple expression:

$$K_3 = 1 - .5e^{-7.28f}$$

The preceding lift coefficient formula must be modified for application to more complex ski shapes. Of the more significant ski geometric parameters affecting ski lift, longitudinal camber has been the only parameter systematically investigated (Reference 3-3). This investigation covered the effects of adding upper surface camber to a flat plate of $A = 1/4$ on its hydrodynamic characteristics at a single depth/chord ratio of .42. The effects of upper surface camber on the ski lift curve at this depth are shown here in Figure 3-2. It is seen that, at the low angles of attack (trim angles), the upper surface camber produces the well-known effect of increasing the lift coefficient through a shift of the zero-lift angle but, unlike the case for high aspect ratio surfaces, this effect becomes reduced at higher trims.

Such geometric features as curved planforms and blunt (transom-type) trailing edges may be expected to have a substantial effect on ski fully-wetted hydrodynamic characteristics. Experimental data for a single ski embodying these two features are given in Reference 3-4 which also compares these values with those for a flat plate.

A certain amount of experimental data is available for the drag and pitching moment characteristics of fully-wetted submerged skis but, until now, no attempts have been made to correlate these values through suitable empirical formulas. As a principal purpose of this report is the quantitative correlation of available ski data, such analyses were made for a flat plate ski with rectangular planform and an aspect ratio of 1/4, as follows.

3.3.1.2 Drag Characteristics

If the fully-wetted lift coefficient is written as:

$$C_L = C_{L1} + C_{L2}$$

where

$$C_{L1} = \frac{2\pi K_2 K_3 A}{(1 + A) + 2K_2} \tau$$

and

$$C_{L2} = (8/3) K_3 \sin^2\tau \cos\tau$$
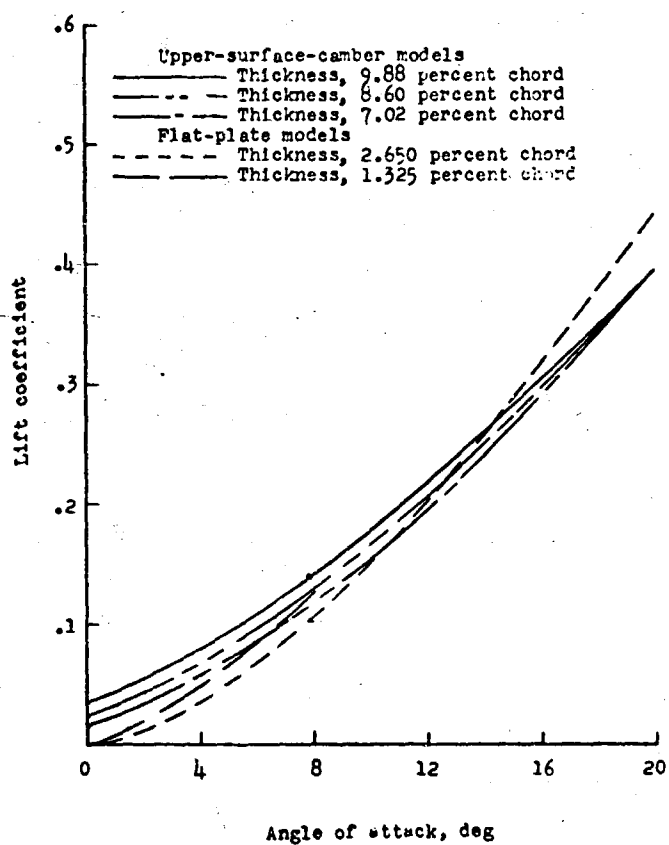
Figure 3-2. Effects of Upper Surface Camber on Lift Characteristics of a
Rectangular Flat-Bottom Ski

C_{L1} may be considered as a "circulation lift coefficient" and C_{L2} as a "cross-flow lift coefficient".

On the basis, it is logical to assume that the ski drag coefficient has the form:

$$C_D = C_{D0} + (C_{L1}^2/\pi A \eta) + C_{L2} \tan \tau$$

where: C_{D0} = profile drag coefficient (section value, primarily dependent on ski thickness, ratio and Reynolds Number).

$C_{L1}^2/\pi A \eta$ = induced drag coefficient, where η is the "Oswald efficiency factor", which may be depth dependent.

$C_{L2} \tan \tau$ = cross-flow contribution to ski drag.

As demonstrated in Appendix A of this report, analysis of the available test data for the 1/4 aspect ratio ski yielded a very reasonable value of C_{D0} and an equally reasonable curve for η as a function of depth-chord ratio. The resulting exceptionally close correlation of the experimental data is also included in Appendix A.

The effects of the ski drag characteristics of adding upper surface camber to a flat plate ski are described in Reference 3-3, according to which the maximum lift-drag ratio decreased with increasing camber and, also, moved to higher angles of attack. The reduction in the maximum L/D resulted both from the increased profile drag associated with the thicker (more cambered) skis and also from the reduced lift curve slopes.

Also, according to the data reported in Reference 3-4, the lift-drag ratio of an actual hydro-ski incorporating a non-rectangular planform, blunt transom, bow rise, and upper surface camber was lower than that of a flat plate of comparable aspect ratio.

3.3.1.3 Pitching Moment Characteristics

The pitching moment characteristics or, rather, their equivalent, the center of pressure values for the flat plate, rectangular ski of aspect ratio, 1/4, given in Figure 12 (b), Reference 3-5, were correlated by means of the semi-empirical formula:

$$\text{c.p.}(\% \text{ chord, forward of T. E.}) = (a + \frac{b}{C_{L1}}) \frac{C_{L1}}{C_L} + 0.50 \frac{C_{L2}}{C_L}$$

where "a" and "b" vary with depth-chord ratio. Figure A-8 of Appendix A shows the "best fit" values of "a" and "b" obtained in the correlation process. As shown in Figures

A-9 through A-12 of Appendix A, the correlations obtained in this manner were excellent.

3.3.2 Ventilated Condition

3.3.2.1 Ventilation Processes and Boundaries

The relatively high speed associated with a hydro-ski operating below the water surface will usually result in ventilated flow. In this flow regime, an aerated cavity extends aft from the unwetted upper surface of the hydro-ski. Although the mechanism of ventilation inception and development are known from model tests and may be physically described, an analytical treatment is not yet available to predict its occurrence under full-scale conditions. The following discussion will briefly describe the phenomena observed in model tests during the ventilation process. Pertinent experimental data are also included for guidance in assuming the existence of ventilated flow when performing hydro-dynamic calculations.

For the onset of ventilation, it is necessary that an air path be developed or provided to the upper surface of the hydro-ski. Such a path may be readily induced by the blunt base of a surface-piercing hydro-ski support strut.

If the depth of the ventilated pocket behind a strut extends down to the hydro-ski, it is likely that ventilated flow about the hydro-ski will be established. The depth of the ventilation pocket behind a base-vented strut may be estimated from the expression,

$$ h = V^2/10.25\,g \quad \text{(p. 10-15, Reference 3-6)} $$

The other mechanism of development of ventilated flow about a hydro-ski is by means of the air travelling along the path provided by the trailing vortices, when speed, angle of attack, and free surface proximity reach certain value combinations. At high angles of attack, in the lower speed range, the separated flow from the leading edge may reattach on the upper surface of the ski. The occurrence of this "partial bubble" type ventilation causes little or no change in lift. However, when the speed or angle of attack is increased so that the reattachment point reaches the trailing edge, there is an abrupt loss in lift. When ventilation occurs at the lower range of angles of attacks, the separated flow from the leading edge does not reattach, and there is also a sudden drop in lift.

The available correlations on the inception of vortex ventilation are presented here in Figures 3-3 through 3-5. Although limited, the information can provide semi-quantitative guidance for predicting the conditions required for complete ventilation. For example, the data presented in Figure 3-5 are for specific small-scale models at particular depths of submersion and utilize dimensional speed values.

Therefore, as the required scaling laws are presently unknown, it is necessary to rely on judgment in applying this information for predicting the nature of the flow about a prototype (full-scale) hydro-ski.

Figure 3-3. Details of Ski Models Used in Correlations of Ventilation Data
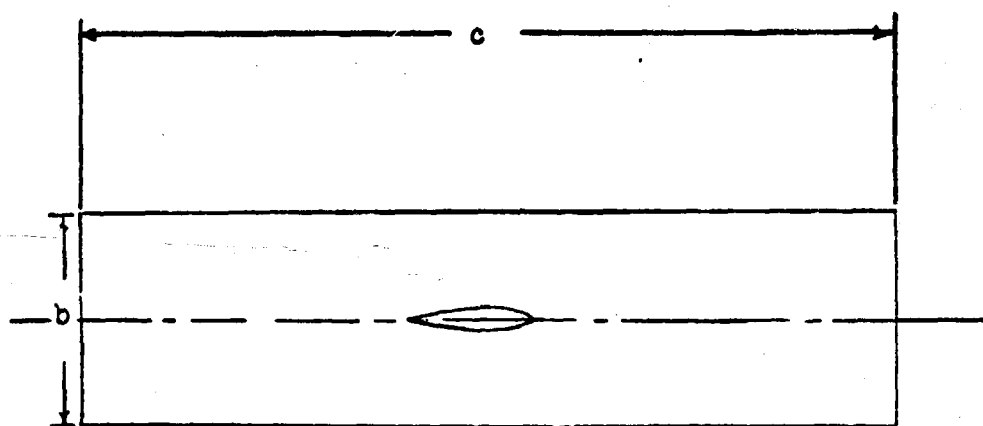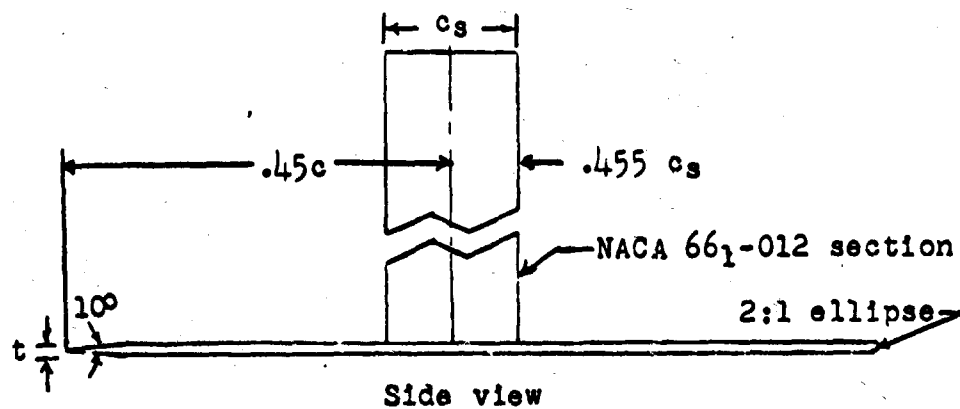
Model	c	b	t	c_s
Small	14.14	3.535	0.138	2.60
Large	36.00	9.000	.477	8.00
Thick	14.14	3.535	.375	4.00

DIMENSIONS ARE IN INCHES
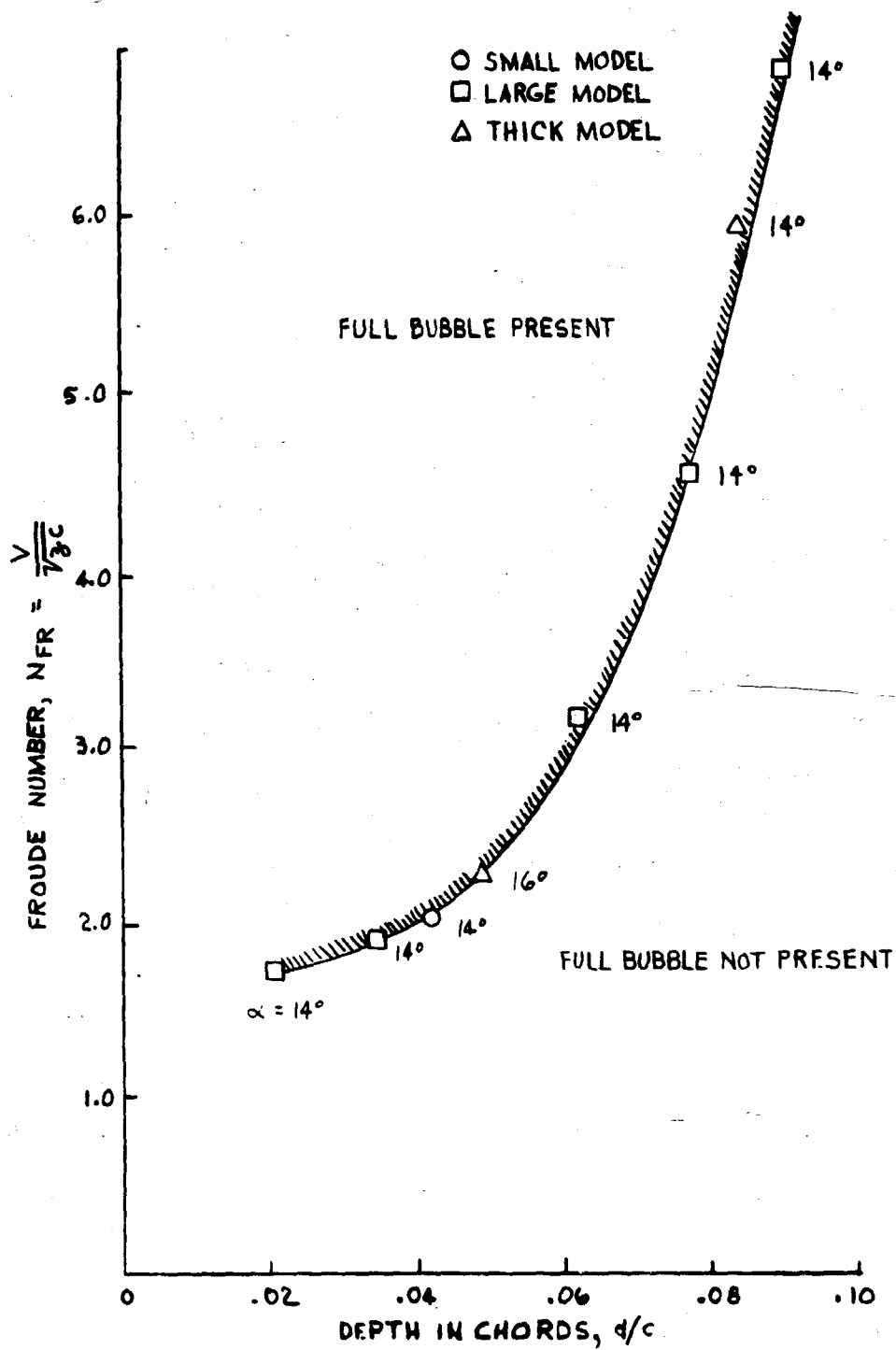
Figure 3-4. Correlation of Ventilation Speeds for the High-Angle Bubble
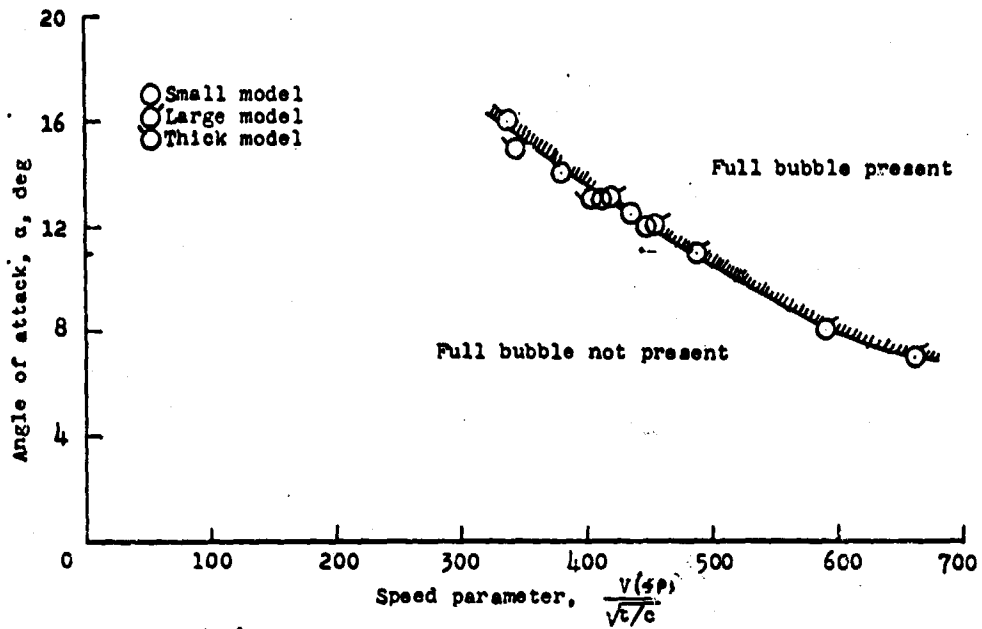
(a) Depth of submersion d, 0.5 inch.
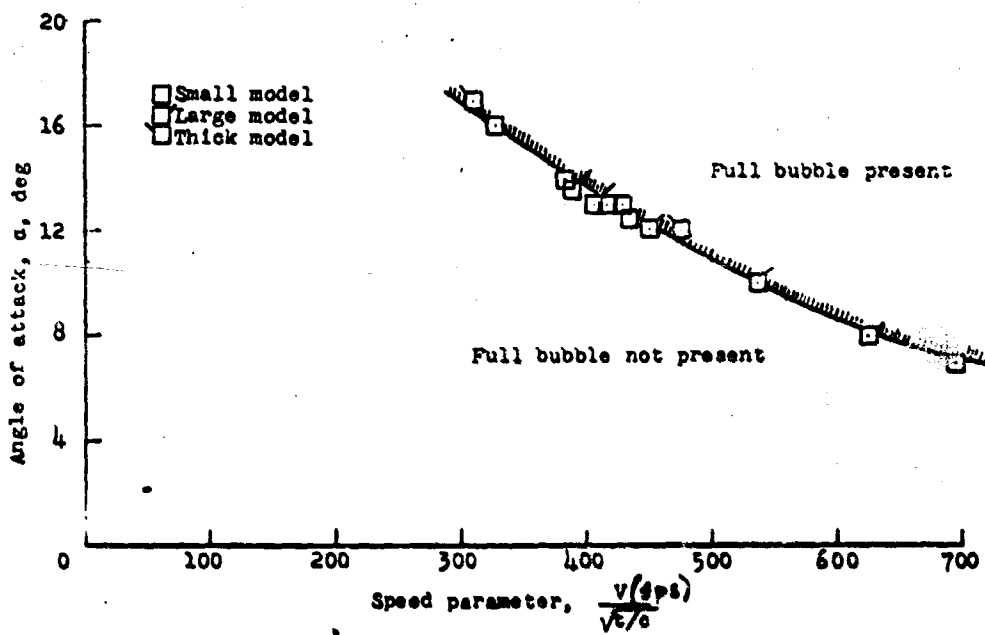
(b) Depth of submersion d, 1.0 inch.

Figure 3-5. Correlation of Ventilation Speeds for the Low-Angle Bubble

3.3.2.2   Flat Rectangular Skis

In Reference 3-7, Johnson has devised an essentially theoretical method for estimating the lift, drag, and center of pressure values for supercavitating hydrofoils of finite aspect ratio operating near the free water surface. Further, he has shown that these theoretical values agree extremely well with the limited available test data for hydrofoil aspect ratios greater than or equal to 1.

As the only technical difference between supercavitating and ventilated flow conditions is in the absolute value of the cavity pressure (i.e., water vapor pressure vs. atmospheric pressure), it appears that Johnson's theory should also be directly applicable to the ventilated flow case.

Whereas the Johnson analysis covers the more general case of longitudinally curved bottoms (bottom cambered hydrofoils), attention in the following will be restricted to the case of straight bottoms which is more representative of most practical hydro-ski shapes.

As presented in Reference 3-7, Johnson's analysis is awkward for practical calculation as it involves two separate iteration processes, one for lift coefficients and the other for drag and moment coefficients. To eliminate this difficulty and, simultaneously, to make this analysis more amenable for the later calculation of hydro-ski seaplane dynamics, Johnson's analysis has been converted into a digital computer program. Significant details of this conversion are given in Appendix B of this report. Incorporated in this program are certain purely empirical modifications used to provide closer agreement of calculated and experimental characteristics, as explained in Appendix B. The almost perfect agreement between the final calculated and the experimental characteristics for a ventilated ski of aspect ratio 1/4, is shown in Figures B-1, B-2, and B-3 of Appendix B.

3.3.2.3   Other Ski Geometries

References 3-3 and 3-4 present the results of steady-state tank tests of two hydro-ski models, both with upper surface camber. One of these had a rectangular planform and a flat bottom (Model A) while the other had a non-rectangular planform and a deadrise-type of bottom (Model B). In both cases, no ventilation was observed anywhere inside the ranges of the test parameters:

Model A: $0° < \tau < 20°$, $0 < d/c < .42$, $0 < V < 30$ fps

Model B: $0° < \tau < 20°$, $0 < d/c < .39$, $0 < V < 85$ fps

It appears that the absence of ventilation for these models can be attributed directly to the presence of the upper surface camber (airfoil-like profile) which tends to prevent flow separation at the ski leading edge.

3.3.3 Cavitated Condition

3.3.3.1 Cavitation Processes and Boundaries

As a hydro-ski seaplane accelerates from rest, the hydro-ski shape and attitude will induce pressure reduction over a region of its surface. With increasing speed, and depending upon the specific hydro-ski installation, cavitation may occur. This condition is possible if, at this same speed, the hydro-ski is submerged and no ventilation develops, either by the action of tip vortices or a strut-provided air path to the free water surface.

The cavitation number, based on local pressure, p , is defined as:

$$\sigma = (p_{\infty} - p) / (\rho/2) \, v^2$$

where
p_{∞} = free stream static pressure (varies with depth)

p = local pressure at any point on the hydro-ski surface

Cavitation begins when the local pressure value at some point reduces to p_v, the vapor pressure of water. The incipient cavitation number is, therefore:

$$\sigma_i = (p_{\infty} - p_v) / (\rho/2) \, v^2$$

The minimum pressure coefficient on a section is defined as:

$$C_{p\,min} = (p_{min} - p_{\infty}) / (\rho/2) \, v^2$$

or,
$$-C_{p\,min} = (p_{\infty} - p_{min}) / (\rho/2) \, v^2$$

t the inception of cavitation,

$$p_{min} = p_v$$

and, therefore:
$$\sigma_i = -C_{p\,min} = (p_{\infty} - p_v) / (\rho/2) \, v^2$$

The minimum pressure coefficient is dependent solely on the shape of the body and independent of its size, while the model and full-scale values of the free stream static pressure, p_{∞} , are close to each other under towing tank test and prototype conditions. Therefore, the cavitation inception speeds observed in the towing tank tests of hydro-ski models are approximately equivalent to the full-scale cavitation inception speeds. Consequently, the effects of cavitation development observed in towing tank tests of hydro-ski

seaplane configurations conducted in accordance with Froude scaling laws, will begin at a proportionately lower speed on the prototype aircraft.

Figure 3-6, taken from Reference 3-4, presents a comparison of towing tank tests results on cavitation boundaries for a flat plate and hydro-ski model. In both models, cavitation inception occurs at the leading edge upper surface. It is therefore evident that, unless prevented by ventilation effects, cavitation will occur on similar prototype hydro-skis somewheres inside their expected range of operational trims and speeds.

Reference 3-8 presents experimental data on the hydrodynamic characteristics of an aspect ratio 1/4, flat plate at several depths of submersion. From Figure 3-7, reproduced from Reference 3-8, the effects of cavitation are seen to be detrimental to hydro-ski performance. Since these effects occur in a gradual manner, no catastrophic motions are induced. However, these same curves also illustrate the sudden change in the hydro-dynamic force with the occurrence of ventilation, which developed in these tests by air entering the trailing vortices.

It is also noted that, at the higher trims, the ventilation tendency increases with proximity to the water surface. This attitude and location is representative of the situation that exists at the time of ski unporting during a seaplane take-off. In order to avoid un-stable aircraft behavior caused by the sudden loss in hydro-ski lift through ventilation as it approaches the water surface, hydro-ski ventilation can be induced at deeper submergence by utilizating a base-vented strut.

As has been made clear in Section 2 of this report, one of the most basic factors involved in the selection of hydro-ski dimensions is the lift developed just as the leading edge reaches the water surface during the take-off process (unporting condition). The flow then is definitely ventilated and the planing lift equations are used to establish the required hydro-ski area.

As the planing lift of a fully wetted lower surface hydro-ski is always less than its lift when fully wetted on both surfaces or under cavitating conditions, the hydrodynamic characteristics under cavitated flow conditions are of secondary concern in the basic design of a hydro-ski. However, an awareness of hydro-ski cavitation phenomena is important in appreciating possible performance discrepancies between model and prototype characteristics.
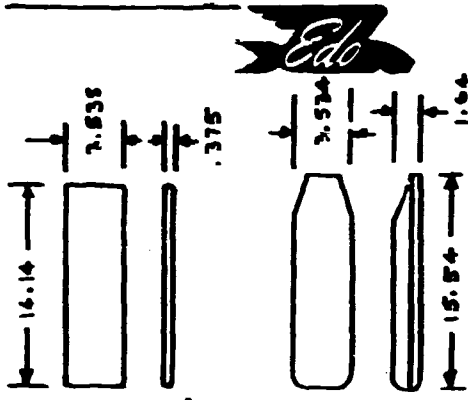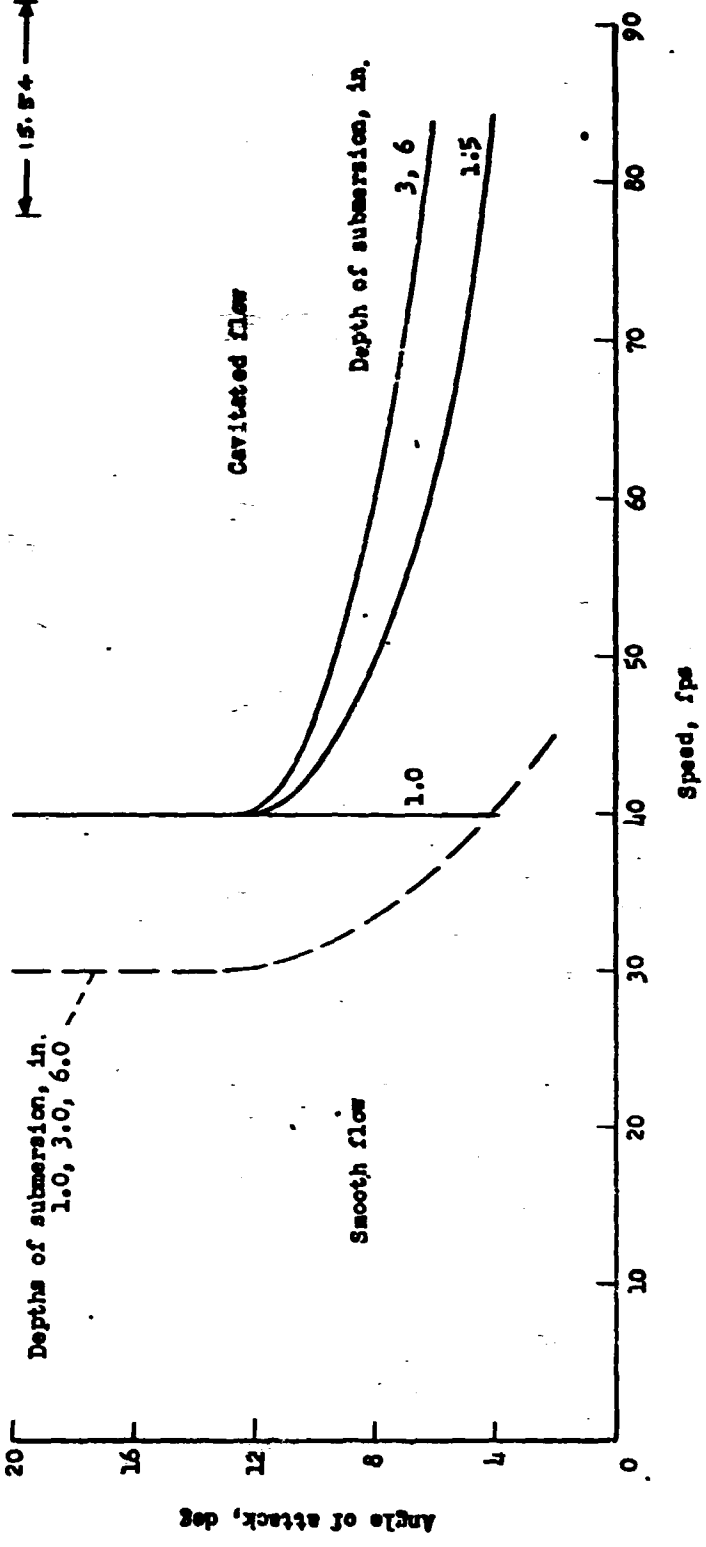
Figure 3-6. Comparison of Cavitation Boundaries at Various Depths of Submersion

(b) Depth of submersion, 1.0 inch.
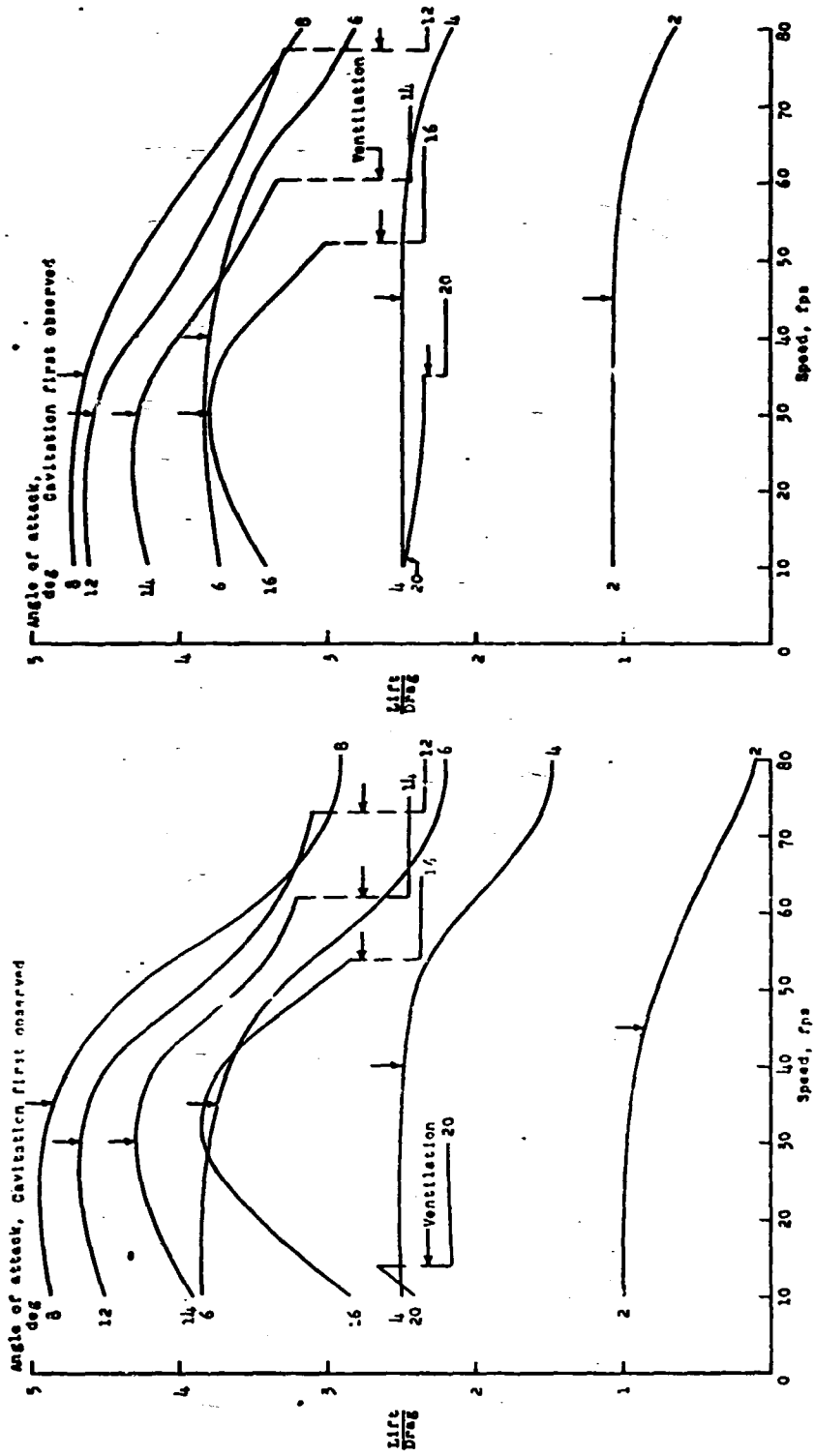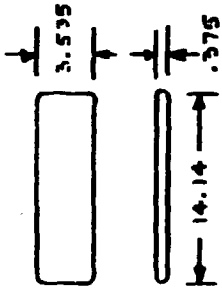
(a) Depth of submersion, 0.5 inch.

Figure 3-7. Effect of Flow Changes on the Lift-Drag Ratio of A Flat Hydro-Ski (Sheet 1 of 2)
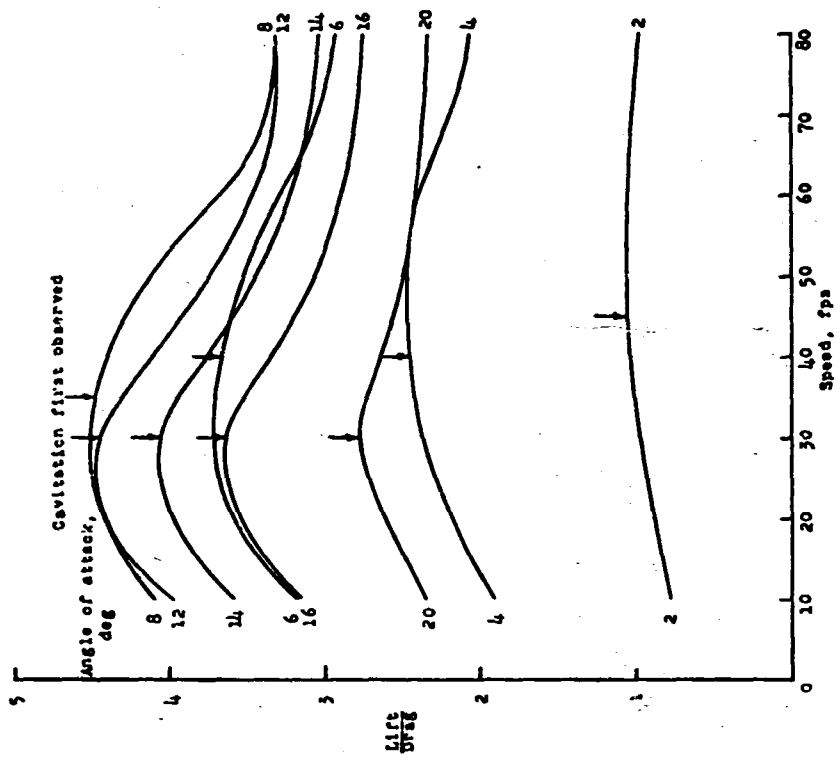
(c) Depth of submersion, 3.0 inches.
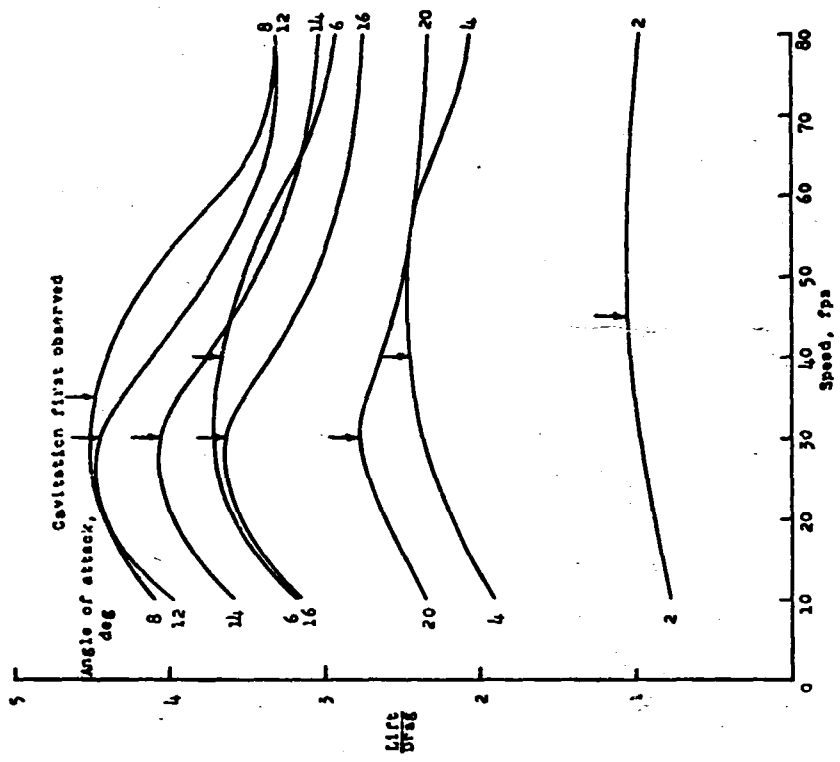
(d) Depth of submersion, 6.0 inches.

Figure 3-7. Effect of Flow Changes on the Lift-Drag Ratio of A Flat Hydro-Ski (Sheet 2 of 2)

REFERENCES

3-1   NACA TN 3939: "A Theoretical and Experimental Study of Planing Surfaces Including Effects of Cross Section and Planform," by C. L. Shuford, Jr., March 1957.

3-2.   NACA TN 4168: "A Method for Calculation of Hydrodynamic Lift for Submerged and Planing Rectangular Lifting Surfaces," by K. L. Wadlin and K. W. Christopher, January 1958.

3-3   NACA TN D-166: "A Hydrodynamic Investigation of the Effect of Adding Upper-Surface Camber to a Submerged Flat Plate," by V. L. Vaughan, Jr., November 1959.

3-4   NACA TN D-51: "The Hydrodynamic Characteristics of a Submerged Lifting Surface Having a Shape Suitable for Hydro-Ski Application," by V. L. Vaughan, Jr., October 1959.

3-5   NACA TN 3079: "The Hydrodynamic Characteristics of Modified Rectangular Flat Plates Having Aspect Ratios of 1.00 and 0.25 and Operating Near a Free Water Surface," by K. L. Wadlin, J. A. Ramsen, and V. L. Vaughan, Jr., March 1954.

3-6   "Fluid Dynamic Drag," by S. F. Hoerner, Published by the Author, 1965.

3-7   NACA RM L57I16: "Theoretical and Experimental Investigation of Arbitrary Aspect Ratio, Supercavitating Hydrofoils Operating Near the Free Water Surface," by V. E. Johnson, Jr., 12 December 1957.

3-8   NACA TN 3908: "Hydrodynamic Characteristics Over a Range of Speeds Up to 80 Feet per Second of a Rectangular Modified Flat Plate Having an Aspect Ratio of 0.25 and Operating at Several Depths of Submersion," by V. L. Vaughan, Jr. and J. A. Ramsen, April 1957.

4. STRUT RESISTANCE CHARACTERISTICS

4.1 FLOW CHARACTERISTICS

Just as the hydrodynamic characteristics of a hydro-ski are dependent upon the specific type of flow developed (e.g., fully-wetted, cavitated, or ventilated), the hydrodynamic force characteristics of hydro-ski support struts are related to the strut flow regime. Therefore, to calculate the resistance of a strut, it is first necessary to determine the nature of the strut flow.

At very low speeds, of course, all surface-piercing struts will be fully wetted, independent of the particular cross section. As speed is increased, the pressure drop associated with the flow about the strut section will cause a depression at the strut-level water line intersection. For most hydro-ski seaplane configurations, however, it is likely that, in this relatively low speed range, with the strut attached to the hull bottom and the keel still below the level water line, fully-wetted flow will exist. Consequently, the effect of moderate water surface depressions is usually of little or no interest in the drag estimation of hydro-ski support struts.

When the aircraft reaches the speed at which the strut-hull intersection clears the water surface, the flow about the strut can suddenly change from fully wetted to fully ventilated, as the hull bottom no longer blocks the development of an air passage down the strut. It is evident that this situation is particularly applicable to base-vented strut sections, although it is also possible that, prior to hull bottom emergence, such sections may already have a cavitation bubble extending aft of the blunt trailing edge.

It can usually be assumed that, because of the relatively high Froude numbers (based on strut depth) prevailing at the hull bottom clearance speed, a surface-piercing hydro-ski support strut will be completely ventilated. As the ventilated cavity static pressure is very close to atmospheric, the pressure acting on the aft portion of the strut is greater than that for either the fully wetted or cavitated conditions, so that the drag coefficient becomes markedly reduced. However, because of the hull bottom clearance, the surface-piercing configuration now introduces an additional drag component due to spray generation. This spray drag is usually considerably lower in magnitude than the reduction in base drag resulting from the occurrence of ventilation. Therefore, the net effect of ventilating a strut is to lower its resistance as compared with either the fully wetted or cavitated values. Thus, in addition to enhancing ventilation of the hydro-ski upper surface which precludes ski lift force breaks during unporting, this feature furnishes another reason for utilizing a base-vented strut section.

In general, the strut drag coefficient is dependent on various hydrodynamic parameters such as Reynolds number, Froude number, and cavitation number. As indicated

in the preceding discussion, the methods presented herein for engineering estimates of strut drag will cover only the fully wetted and cavity flow conditions.

4.2 DRAG ESTIMATION FOR FULLY WETTED STRUTS

The drag coefficient, based on frontal area, of a fully wetted faired strut section may be estimated by use of the expression:

$$C_D / C_f = 4 + 2 \left(\frac{c}{t} \right) + 120 \left(\frac{t}{c} \right)^3 \qquad \text{(P. 6-9, Reference 4-1)}$$

where C_f = skin friction drag coefficient

t/c = thickness/chord ratio

The skin friction drag coefficient in turbulence flow can be calculated from the well-known Schoenherr curve, or its simple approximation:

$$\frac{1}{\sqrt{C_f}} = 3.46 \log_{10} R_c - 5.6 \qquad \text{(P. 2-5, Reference 4-1)}$$

where: $R_c = Vc/\nu$ (Reynolds Number based on chord)

4.3 DRAG ESTIMATION FOR BLUNT-BASE STRUTS

Reference 4-2 develops theoretical curves for estimating the cavity (i. e., pressure) drag of several important strut sections having blunt trailing edges. The results therein are only applicable to flows in which the strut sides are fully wetted and a cavity extends aft from the base. As the cavity drag coefficient curves are also dependent on the cavitation number corresponding to the base cavity pressure, the results are applicable to both the fully submerged and surface-piercing conditions for a strut. The information given is not suitable for the speed range in which the strut base is also wetted. However, it is known that the blunt trailing edge will induce a base cavity at moderately low speeds, so that the results therein are generally applicable over the speed range of interest in hydro-ski design.

In utilizing the drag coefficient curves reproduced below, it must be remembered that the skin friction drag must be added to the estimated cavity drag and, if the strut pierces the water surface, spray drag must also be added.

The basic blunt base trailing edge strut sections for which theoretical cavity drag curves are presented in Reference 4-2 are:

a) Wedge:

$$y = \pm \frac{1}{2} \left(\frac{t}{c} \right) x$$

b)   Parabola:

$$y = \pm \frac{1}{2} \left(\frac{t}{c}\right) (xc)^{1/2}$$

c)   Modified Parabola with Zero Trailing Edge Slope:

$$y = \pm .75 \left(\frac{t}{c}\right) \left[(xc)^{1/2} - \frac{x^{3/2}}{3c^{1/2}} \right]$$

d)   Modified Parabola with Zero Cavity Drag:

$$y = \pm 2.17 \left(\frac{t}{c}\right) \left[\frac{(xc)^{1/2}}{2} - \frac{x^{3/2}}{3c^{1/2}} \right]$$

where: t/c = thickness ratio

                 x = chordwise distance, measured from leading edge

                 c = chord

Figure 4-1, reproduced from Reference 4-2, presents the theoretical cavity drag coefficients, based on the strut frontal area, of the foregoing sections. These values are considered to be suitable for engineering calculations, as good agreement with the test data of References 4-3 and 4-4 was obtained for practical strut thickness wedges and parabolic sections.

In Figure 4-1, $\sigma_b = \dfrac{p_\infty - p_c}{\rho V^2/2}$

where p_c = Pressure in base cavity

             p_∞ = absolute static pressure

From these curves, it is evident that the Zero Cavity Drag shape is superior to the others. However, this indication must be viewed by the designer with considerable caution since, if the "boattailing" in this strut section is made excessive, flow separation under some practical conditions may occur forward of the base, thus defeating the basic purpose of this design.

For engineering calculations, it is suggested that, in determining a base cavitation number, the absolute hydrostatic pressure of the average strut wetted depth be used for p_∞. If the strut is fully submerged, $p_c \approxeq 0$, while for a surface-piercing strut,

p_c = 14.7 psi.

ONE TERM MODIFIED PARABOLIC
STRUT, $M=0$, $C_{D_o}=0.22089$

PARABOLIC STRUT-
$C_{D_o}=0.3926$

WEDGE-
$C_{D_o}=0.6366$

ONE TERM MODIFIED
PARABOLIC STRUT $C_{D_o}=0$

$C_{D_o}=0$

ONE TERM MODIFIED PARABOLIC
STRUT, C_D BASED ON t_{MAX}
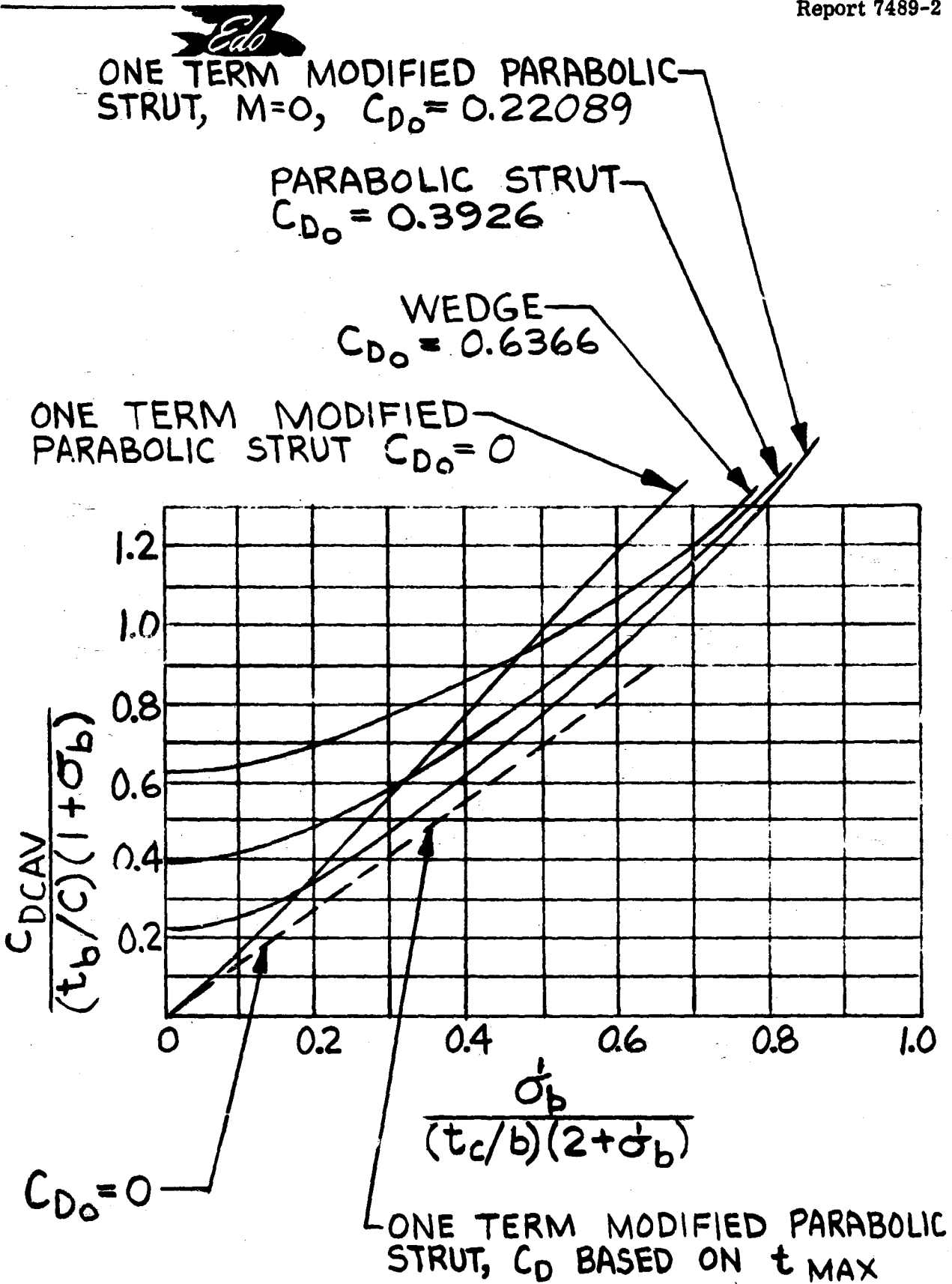
Figure 4-1. Cavity Drag Coefficient vs. Base Cavitation Number for Various Struts

Reference 4-2 also presents curves for estimating the cavity lengths of these same strut sections. These are based on two-dimensional theory and therefore the results do not account for the effect of gravity on the cavity shape. Consequently, the theoretical cavity length curves, reproduced here in Figure 4-2, only apply to fully submerged struts. However, they may be used for guidance in estimating the cavity length variation with depth, of surface-piercing base-vented struts, except in the region of the water surface. In this case, the base cavity pressure is:

$$\sigma_b = 2\,gh/V^2$$

where   h is the vertical distance from the water surface to a point on the strut.

Figure 4-2 may also be used for a preliminary estimate of the length of material annex that may be added to the base of a strut for increasing bending strength, while checking for cavity clearance. It is suggested in Reference 4-2 that a reasonable annex length is about 75 percent of the chord and that the annex length should not exceed about half the cavity length. Also, the notch depth should be at least 10 percent of the forebody thickness at the notch.

4.4   SPRAY DRAG ESTIMATION

Spray drag estimation may be based on the results of an experimental investigation conducted by the Davidson Laboratory. In the tests reported in Reference 4-5 it was found that the spray drag coefficient of a strut is, for practical purposes, dependent only on the strut thickness ratio. The effect of varying the leading edge radius is small and no effects of variations in the Reynolds and Froude numbers were found.

The empirical equation developed for the spray drag coefficient is:

$$C_{D_S} = \frac{D_s}{qct_{max}} = .03 + .08\left(\frac{t_{max}}{c}\right)$$

where: c = strut chord

t_{max} = maximum strut thickness
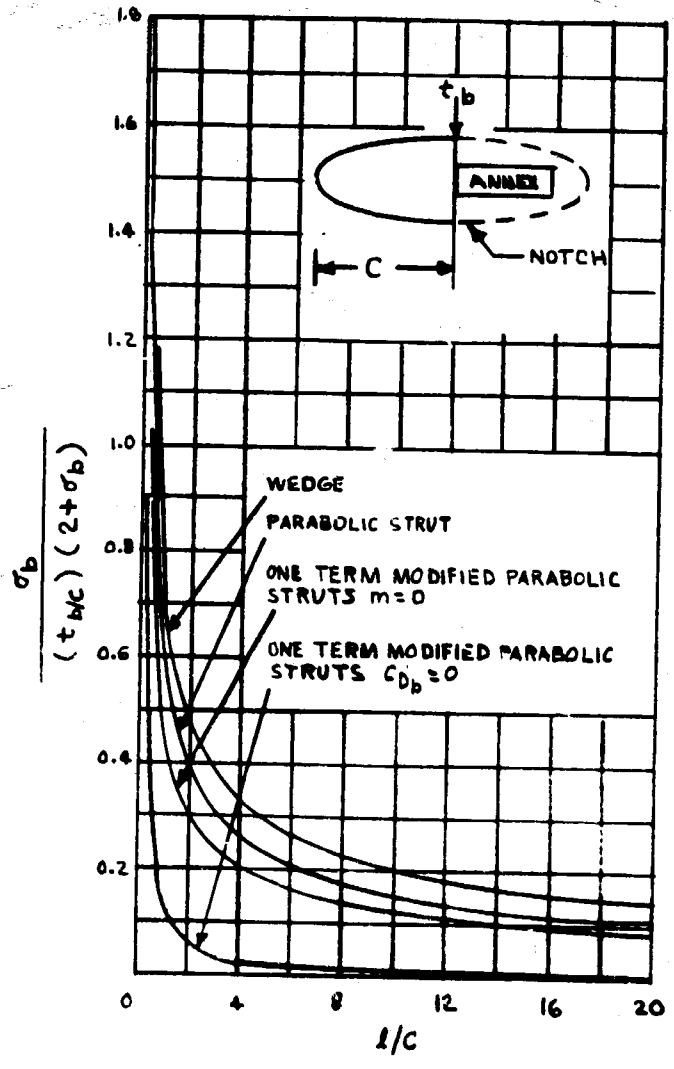
Figure 4-2. Cavity Length vs. Base Cavitation Number for Various Struts

REFERENCES

4-1   "Fluid-Dynamic Drag," by F. Hoerner, Published by the Author, 1965.

4-2   Hydronautics, Inc. Technical Report 001-16: "The Design of Base-Vented Struts for High Speed Hydrofoil Systems," by V. E. Johnson Jr. and S. E. Starley, September 1962.

4-3   California Institute of Technology Hydrodynamics Laboratory Report No. 97-4: "A Wake Model for Free Streamline Flow Theory: Part II. Cavity Flows Past Obstacles of Arbitrary Profile," by T. Y. Wu and D. P. Wang, May 1963.

4-4   Aerojet-General Corporation Report No. 2796: "Hydrodynamic Characteristics of Base-Vented and Supercavitating Struts for Hydrofoil Ships," by J. Levy, et al., August 1964.

4-5   Davidson Laboratory Report 1192: "Experimental Study of Spray Drag of Some Surface-Piercing Struts," by D. Savitsky and J. P. Breslin, December 1966.

5. SINGLE HYDRO-SKI IMPACTS WITH CONSTANT TRIM AND FORWARD SPEED

5.1 INTRODUCTION

It is obvious that one of the most fundamental aspects of hydro-ski design technology is the ability to predict ski impact loads. As will be emphasized later in this report, it is convenient to distinguish between the ski impact loads which occur while traversing a long train of waves such as in rough-water take-offs or taxiing, and those which occur during landings.

Unlike the conventional seaplane, where maximum hull landing loads tend to occur later in the landing process, the maximum landing loads on a hydro-ski tend to occur at the first wave impact. This difference is a consequence of the fact that, because of the smaller loads and the "centralized" ski location, the first wave impact of the hydro-ski seaplane does not generate the large pitching moments experienced during the comparable hull impacts. Fortunately for the hydro-ski designer, this fact provides him with relatively convenient methods for the estimation of maximum hydro-ski loads. These are of basic importance both in preliminary design, which often involves comparison of different ski geometries (dimensions, deadrise, etc.) and installation geometries (ski incidence, etc.) and in final design where the ski structure and the ski-strut attachment become defined by the maximum ski loads and associated pressure distributions.

Because of its fundamental importance, the subject of ski impact load prediction has received considerable attention in the past. As explained in Reference 5-1, these past efforts have been of two different kinds, as follows:

A) For use in preliminary design, attempts have been made to devise simple empirical formulas, in terms of fundamental parameters (ski beam loading and deadrise) and impact parameters (trim and initial flight path angle), for anticipated maximum impact loads in smooth water. The most sophisticated of these formulas is the one given by Mixson in Reference 5-2.

This formula, obtained by a regression analysis of test data covering large ranges of all the four parameters, has very substantial accuracy when properly restricted to the smooth water condition. Unfortunately, just as with the earlier cruder formulas, its utility is severely limited (if not destroyed) because it fails to distinguish between the maximum loads which occur while the ski is still planing (ski L.E. above the level water line) and those which occur simply because the L.E. has submerged, thus limiting the load build-up process. In effect then, the Mixson formula is self-defeating as it requires the designer to obtain auxiliary information on the effect of ski length. As this can only be done by calculation of impact time histories which also predict the maximum impact loads, the need for Mixson's (or any other) empirical formula becomes superfluous.

A further, closely related defect of the Mixson empirical formula is that it does not cover the case of wave impacts which is invariably the case of most practical interest. The problem of wave impacts will be treated in detail below where it will be shown that the conventional treatments of this problem are not only incorrect in principle, but also numerically inaccurate.

B) The other approach for prediction of maximum impact loads is through impact time-history calculation or, alternately, through suitable mathematical analysis of time-histories. As just indicated, these techniques have the virtue that they automatically include determination of the variation of ski wetted length during the impact process and, thus, of the effect of ski length in limiting maximum loads. The analysis of ski load time histories has a significant historical precedent in Milwitzky's successful analysis of the same problem for chines-dry hull loads (Reference 5-3) where all significant impact quantities were related directly to a single non-dimensional approach parameter.

An analysis of this type has been made by Markey in Reference 5-4. Unfortunately, this analysis shows very poor correlation with experiment for the values of the ski penetration (directly related to ski wetted length) at maximum acceleration, as shown clearly in Figure 7 of Reference 5-4. This result, attributed to his inadequate approximation for the virtual mass, means that any of his conclusions concerning ski wetted length are highly questionable. An even more important shortcoming of Markey's results in regard to practical ski design problems is that they cannot be exprapolated to the rough-water case by any simple procedure, as will be clearly demonstrated below.

For the foregoing reasons, the problem of single ski impacts is treated herein by purely numerical calculations, utilizing the "equivalent planing velocity" method. This method, utilized previously, is known to be equivalent, in principle, to the "virtual mass" method for beam loadings greater than 1.0 and is considerably simpler to apply as it does not involve analytic expressions for virtual mass.

5.2   SMOOTH WATER IMPACTS

5.2.1   Equation of Motion

For constant trim and forward speed, the single equation of motion can be written as:

$$(W/g)\ddot{d} = W - L_A - L_H$$

where: W = aircraft gross weight

g = acceleration of gravity

d = depth of lowest point on ski below level water line

L_A = aerodynamic lift

L_H = hydrodynamic (ski) lift

and where the dots signify differentiation with respect to time.

In the "equivalent planing velocity" method, the ski lift force is calculated from the equation:

$$L_H = C_{LH} (\rho V_{eq}^2 / 2) S$$

where: C_{LH} = ski lift coefficient

ρ = mass density of water

V_{eq} = equivalent planing velocity

S = ski wetted area

The essence of this method lies in the following two assumptions:

A. The instantaneous lift coefficient of the impacting ski is identical with that of a planing ski having the instantaneous geometry (i.e., trim and wetted length) of the impacting ski;

B. The equivalent planing velocity, V_{eq} is the fictitious horizontal velocity whose component normal to the ski keel is equal to the actual instantaneous velocity normal to the keel, i.e.,

$$V_{eq} \sin \tau = V_H \sin \tau + \dot{d} \cos \tau$$

or $$V_{eq} = V_H + \dot{d} \cot \tau$$

$$= V_H \left[1 + (\dot{d}/V_H) \cot \tau \right]$$

where: τ = trim angle (constant during impact process).

d = ski draft

Using the latter expression, the equation of motion becomes:

$$(W/g)\, \ddot{d} = W - L_A - C_{LH}\, (\rho V_H^2 / 2)\, \left[1 + (\dot{d}/V_H)\cot\tau\right]^2 S$$

All of the calculations of this report section use the Shuford formula for the ski planing lift coefficient, C_{LH}, described in Paragraph 3.2 of this report. However, to simplify the calculations with negligible loss of accuracy, the wave rise effect for skis with finite deadrise has been approximated by assuming "full wave rise", i.e.

$$l_c = l_k,$$

so that $A = b/l_k$ and $S = l_k b$.

For many purposes, it is convenient to rewrite the equation of motion in non-dimensional form. Letting

$$d = \delta b$$

and

$$t = \sigma (b/V_H)$$

where: δ = non-dimensional draft

          σ = non-dimensional time,

the equation of motion becomes:

$$\delta'' = \frac{1}{C_{VH}^2}\left(1 - \frac{L_A}{W}\right) - \frac{C_{LH}\,(1 + \delta'\cot\tau)^2\,\delta}{2\,(\sin\tau)\,C_{\Delta_0}} \qquad (5\text{-}1)$$

Here, C_{VH} = horizontal speed coefficient = $V_H / \sqrt{gb}$

L_A/W = "percent wing lift" expressed as a fraction

C_{Δ_0} = ski beam loading = $W / \rho g b^3$

C_{VH}, L_A/W, τ, and C_{Δ_0}, are parameters which are considered to be constant during the history of a particular impact process. The primes indicate differentiation with respect to δ. Also, the derivative, δ'', is related to the load factor, n, by the equation:

$$\delta'' = n / C_{VH}^2 \qquad (5\text{-}2)$$

5-4

Finally, if the quantity, L_A/W, the so-called "percentage wing lift" is designated as p, the equation of motion can be written as:

$$\delta'' = \frac{(1-p)}{C_{VH}^2} - \frac{C_{LH}(1+\delta'\cot\tau)^2\delta}{2(\sin\tau)C_{\Delta_0}}$$

(5-3)

Most previous analytic studies are restricted to the special case where p = 1 ("100% wing lift" case). The equation then reduces to:

$$\delta'' = -C_{LH}(1+\delta'\cot\tau)^2\delta/2(\sin\tau)C_{\Delta_0}$$

(5-4)

This case is of interest in several different respects. In the first place, it shows clearly that, during an impact, the hydro-ski acts as a non-linear spring device. Secondly, it is seen that this equation is independent of the speed coefficient and, therefore, particularly suited for parametric investigations. Lastly, although no use of this fact is made herein, this equation can actually be integrated analytically to obtain the "vertical velocity", δ', as a function of δ .

5.2.2   Correlation of Test Data

The equation for the "zero wing lift" case (eq. 5-3 with p = 0), was checked by comparison with available data. Reference 5-5 contains a series of experimental acceleration time-histories for smooth water impacts of rectangular skis. The tests included skis of 0° and 30° deadrise, and a ski beam loading range between 20 and 150.

Using eq. 5-3 in conjunction with Shuford's equation for C_{LH}, the corresponding theoretical time-histories were calculated on a high-speed digital computer. The comparisons of these theoretical curves with the experimental data are shown in Figures 5-1, 5-2, and 5-3.

It is seen that the theoretical curves correctly duplicate all of the significant trends of the experimental data and, with but one exception, furnish close approximations to the measured maximum accelerations and their associated time values. The exceptional case, shown in Figure 5-1 (B), is for a flat ski having a beam loading of 20. It may be noted that the discrepancy is only in the peak acceleration value and not in the times at which the peak acceleration occurs.

As explained earlier, it is not believed that this discrepancy can be attributed to the use of the equivalent planing velocity method. Because most current practical interest is limited to the higher loadings $(C_{\Delta_0}>50)$ for which the agreement is excellent, no further investigation of this discrepancy has been attempted.

These correlations show that the equivalent planing velocity technique is generally capable of predicting accurate time histories of highly loaded hydro-skis in smooth water
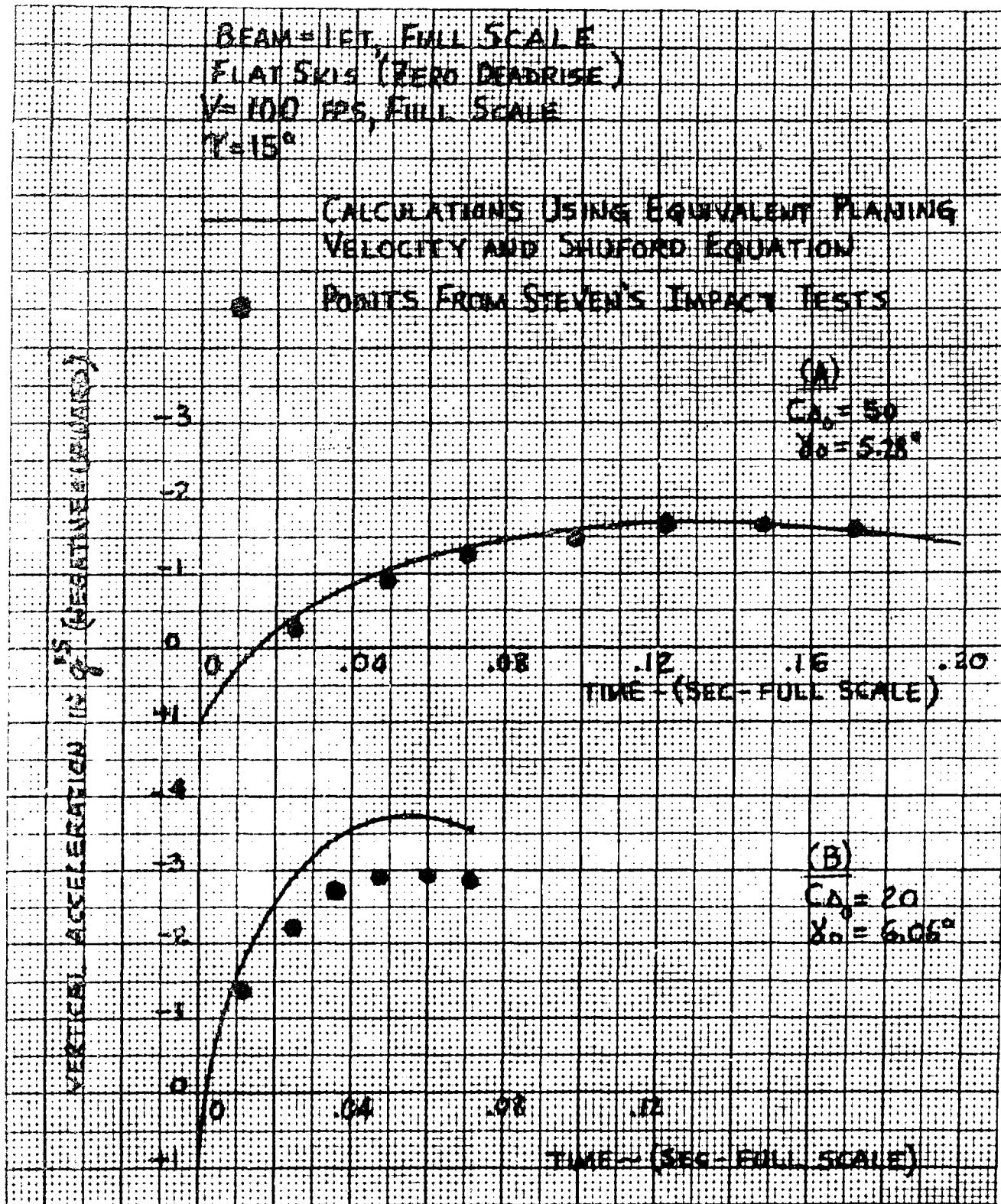
Figure 5-1. Acceleration Time Histories of Smooth Water Impacts:
Comparison of Impact Theory with Test Data
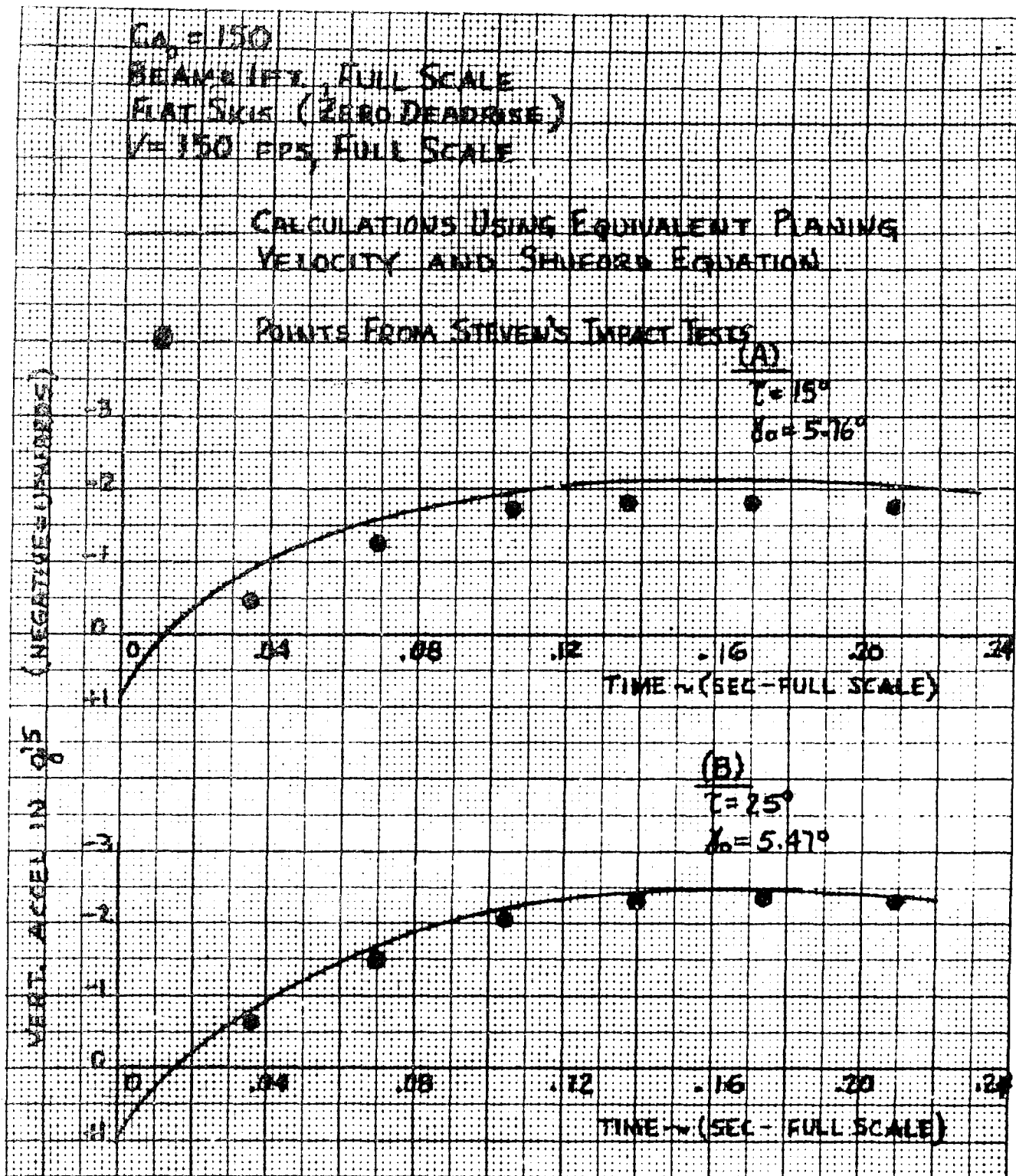
Figure 5-2. Acceleration Time Histories of Smooth Water Impacts:
Comparison of Impact Theory with Test Data
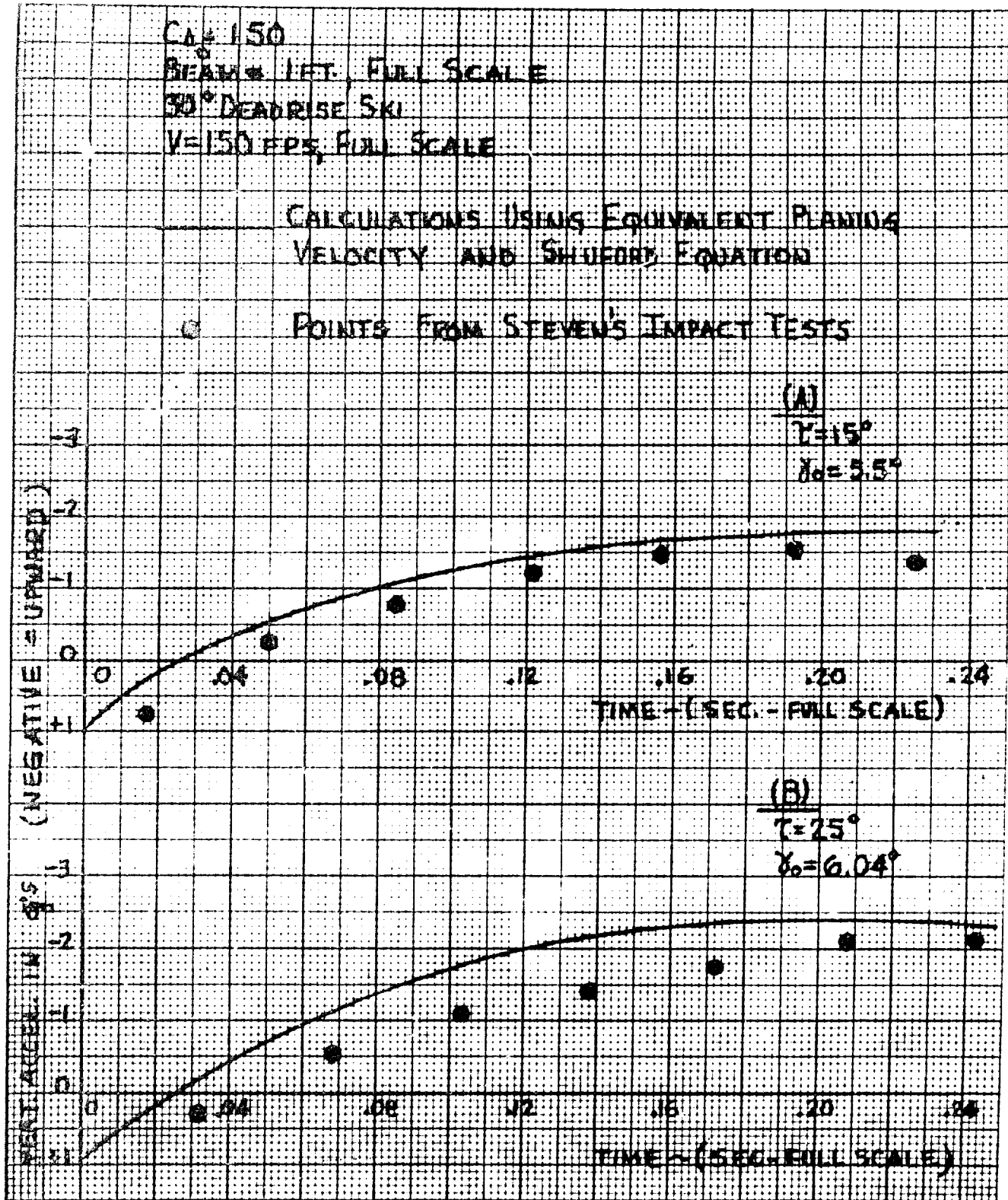
Figure 5-3.   Acceleration Time Histories of Smooth Water Impacts:
Comparison of Impact Theory with Test Data

impacts. It will be shown below that, when properly applied, it is equally capable of predicting time histories of rough water impacts. Before proceding with this rough water impact correlation, a number of significant parametric studies for the smooth water case will first be presented.

5.2.3 Effects of Beam Loading, Ski Length, and Deadrise on Impact Loads

The effects of these parameters on smooth water impact time histories were investigated by computing a number of such histories, using the static "100% wing lift" assumption. For this case, the equation of motion can be written as:

$$2\delta'' = \frac{2n}{C_{VH}^2} = -C_{LH} \frac{(1+\delta' \cot\tau)^2 \delta}{(\sin\tau) C_{\Delta_0}}$$

The time histories of the computed accelerations and the associated wetted length values are shown, in non-dimensional form, in Figures 5-4 and 5-5. In these charts, the ordinate is the non-dimensional "acceleration coefficient",

$$2n/C_{VH}^2$$

where n is the acceleration in "g" units, and the abscissa is the non-dimensional time:

$$\sigma = (V_H/b)t = \sqrt{g/b} \; C_{VH} t$$

The dashed lines represent constant values of the non-dimensional wetted length, l/b. In this form, the charts are independent of C_{VH} and may therefore be used directly to compute actual accelerations for any given C_{VH} value.

Figure 5-4 shows the acceleration time histories for flat skis having different beam loading coefficients, C_{Δ_0}, for a typical impact condition ($\tau = 10°$, $\delta_0 = 10°$). It clearly illustrates the powerful effect of increasing the ski beam loading or reducing the maximum impact load. It also illustrates the effects of ski length on load limitation for a given ski beam loading. Thus, at the low beam loading ($C_{\Delta_0} = 10$), practical ski lengths such as $l/b \cong 4$ will have no effect on the maximum load while at the very high beam loading ($C_{\Delta_0} = 200$), a length of $l/b = 4$ will reduce (the already low) maximum load by 30%.

Figures 5-5(A) and 5-5(B) show the effects of change in deadrise on the time histories for two different ski beam loadings. These charts serve to illustrate a very significant principle of ski design, i.e., the decreasing importance of deadrise in skis of high beam loading. Thus, for a beam loading of 10, the addition of 30° deadrise to a flat ski reduces the acceleration coefficient by .0180 (26% of the zero deadrise value) whereas for a
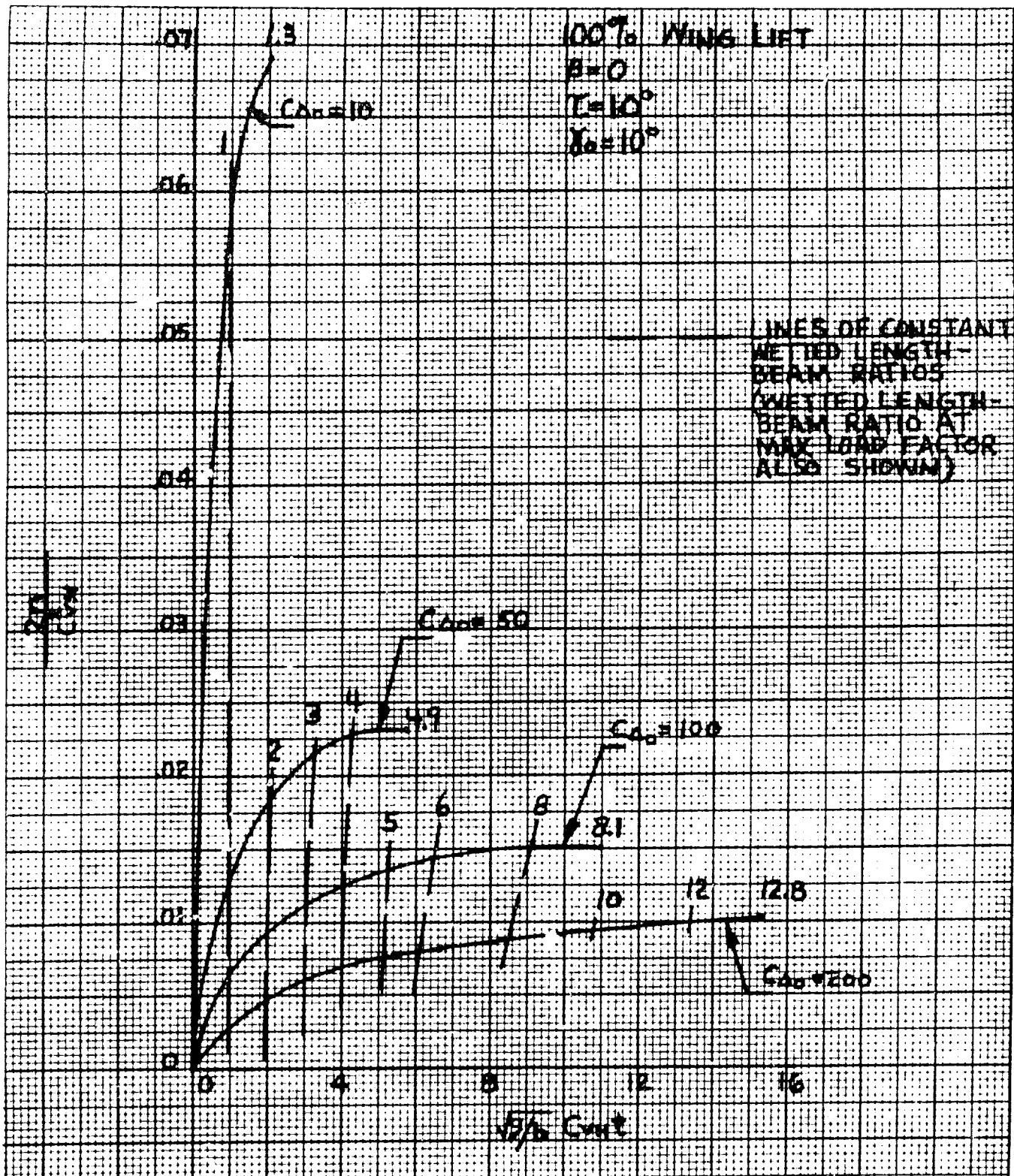
Figure 5-4. Theoretical Acceleration Time Histories of Smooth Water Impacts:
Beam Loading Variation
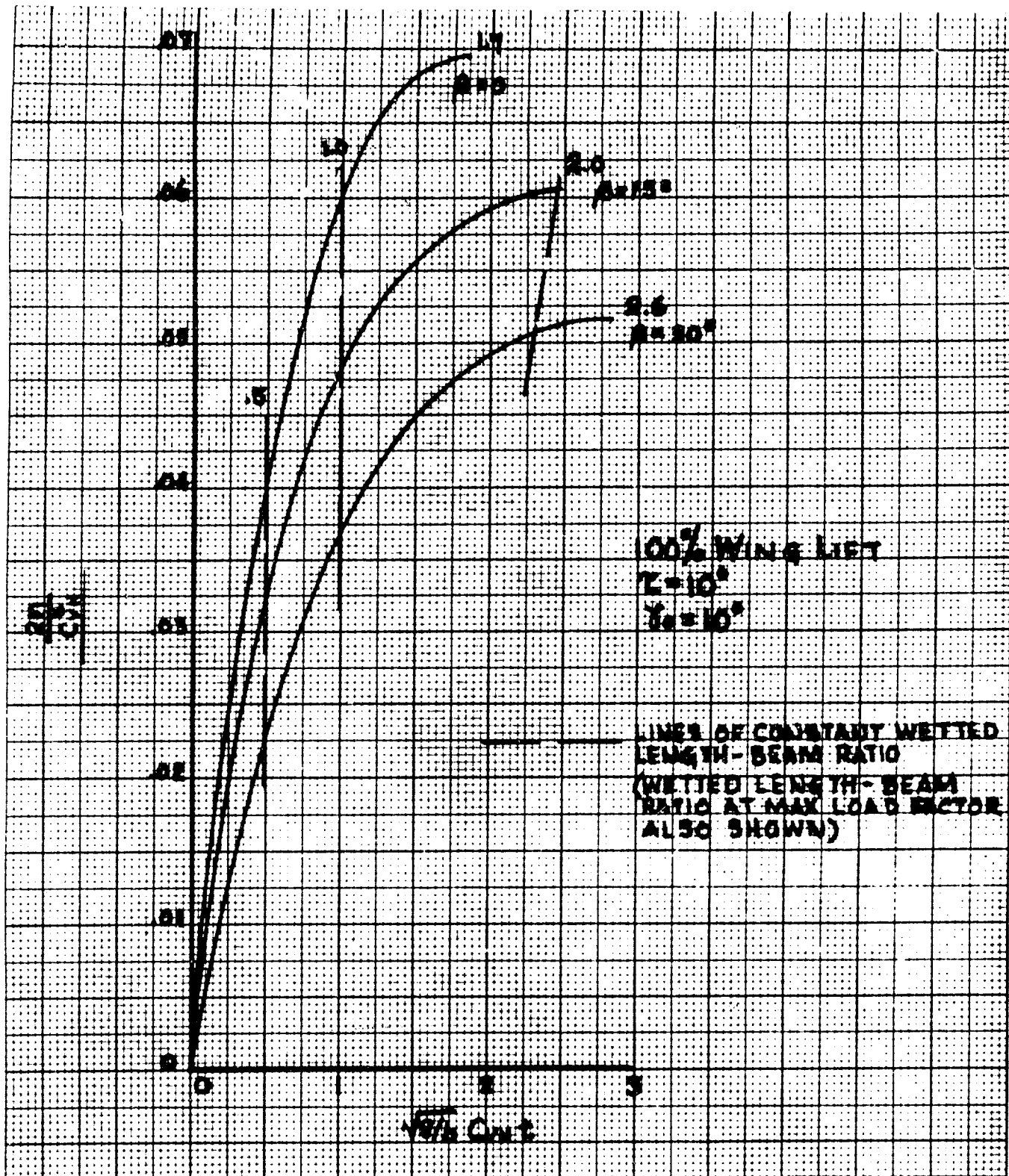
Figure 5-5(A). Theoretical Acceleration Time Histories of Smooth Water Impacts:
Deadrise Variation at Low Beam Loading: $C_{\Delta_0} = 10$
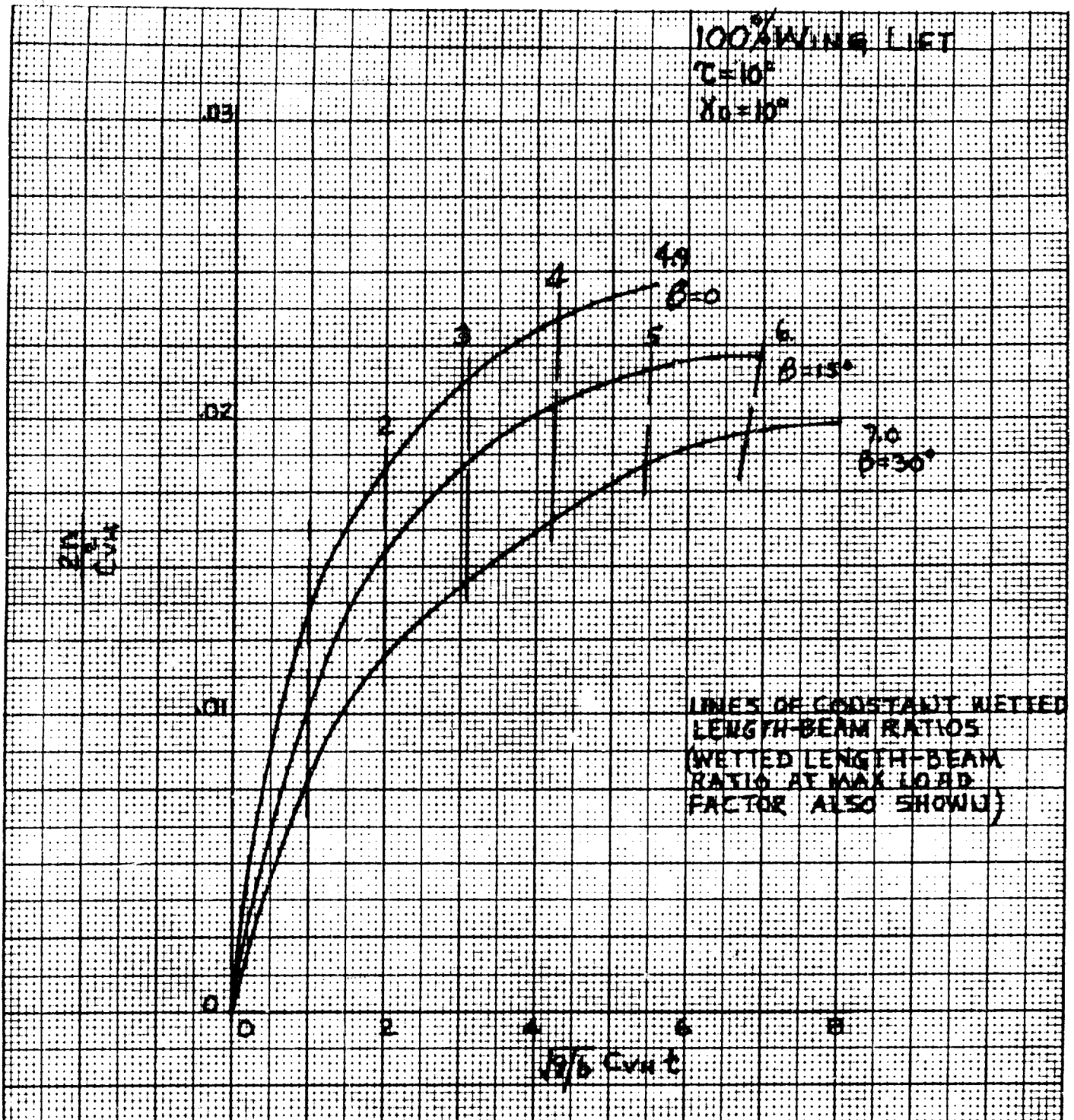
Figure 5-5(B). Theoretical Time Histories of Smooth Water Impacts:
Deadrise Variation at Medium Beam Loading: C_{Δ_0} = 50

beam loading of 50, the same increase in deadrise only reduces it by .0046 (19% of the zero deadrise value), i.e., only 1/4 of the absolute change for the $C_{\Delta_0} = 10$ case.

The effects of beam loading and deadrise variations on the _maximum_ accelerations are summarized in Figures 5-6 and 5-7 which clearly illustrate the main points of the preceding discussion. As a matter of interest, the corresponding curves obtained from Mixson's empirical formula (Reference 5-2) are compared with those obtained herein. While the trends are the same and the numerical values fairly close in all cases, the present values are probably more reliable. Thus, for a flat ski with $C_{\Delta_0} = 20$, the Mixson formula shows a maximum acceleration distinctly larger than that obtained in the present calculations. Thus, the Mixson formula would show an even greater discrepancy with the test data (Figure 5-1B, above) than do the present results.

5.2.4   Effects of Trim and Sink Speed on Impact Loads

Figures 5-8 and 5-9 show the calculated non-dimensional acceleration time histories of smooth water impacts of a flat ski for various trims and for various initial flight path (sink) angles, respectively, with typical values of the other parameters. Figure 5-8 illustrates several interesting effects, as follows:

1) The effects of varying trim on maximum accelerations is not very great. This means, for example, that in rough preliminary design calculations, the whole trim range need not be investigated. Further, for a fixed length-beam ratio, say 4.0, in the present example, the range of maximum accelerations would be further reduced.

2) In the typical case illustrated, a change of trim from 3° to 20° only changes the "peak load wetted length-beam ratio" from 7.0 to 3.5.

3) The constant l/b curves are not monotonic; that is, it is possible to obtain the same acceleration at the same wetted length at two different trim angles.

Figure 5-9 shows that, in the region of low sink angles (typical of conventional seaplanes), the maximum accelerations are nearly proportional to the magnitude of the sink angle. On the other hand, for large sink angles, which are more typical of certain types of STOL aircraft, the maximum load factor increases with sink angle at a much faster rate. Thus, in the particular example shown in Figure 5-9, doubling the sink angle (22.5° to 45°) multiplies the maximum acceleration by a factor of 4.3.

Figures 5-10 and 5-11 show the peak accelerations of Figures 5-8 and 5-9 plotted against the pertinent parameters. These charts serve to clarify some of the previous discussion. Figures 5-10 and 5-11 also show the comparable curves obtained from Mixson's empirical formula. Again, the trends are essentially the same. However, Figure 5-10 shows an appreciable discrepancy in numerical values. Again, the excellent correlation of the present calculations with the test results for $C_{\Delta_0} = 50$, as shown above
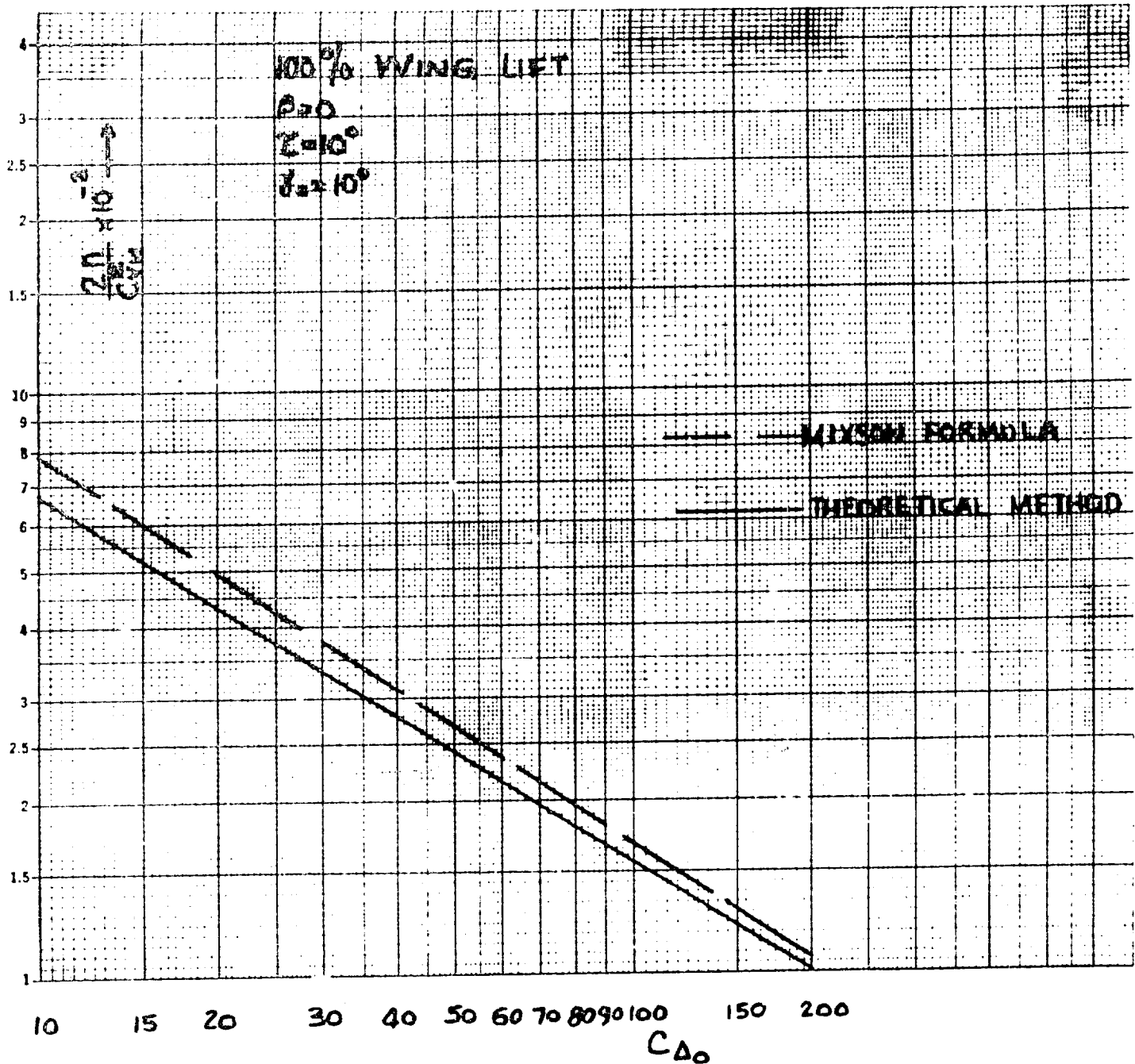
Figure 5-6. Theoretical Maximum Impact Acceleration in Smooth Water
vs Ski Beam Loading
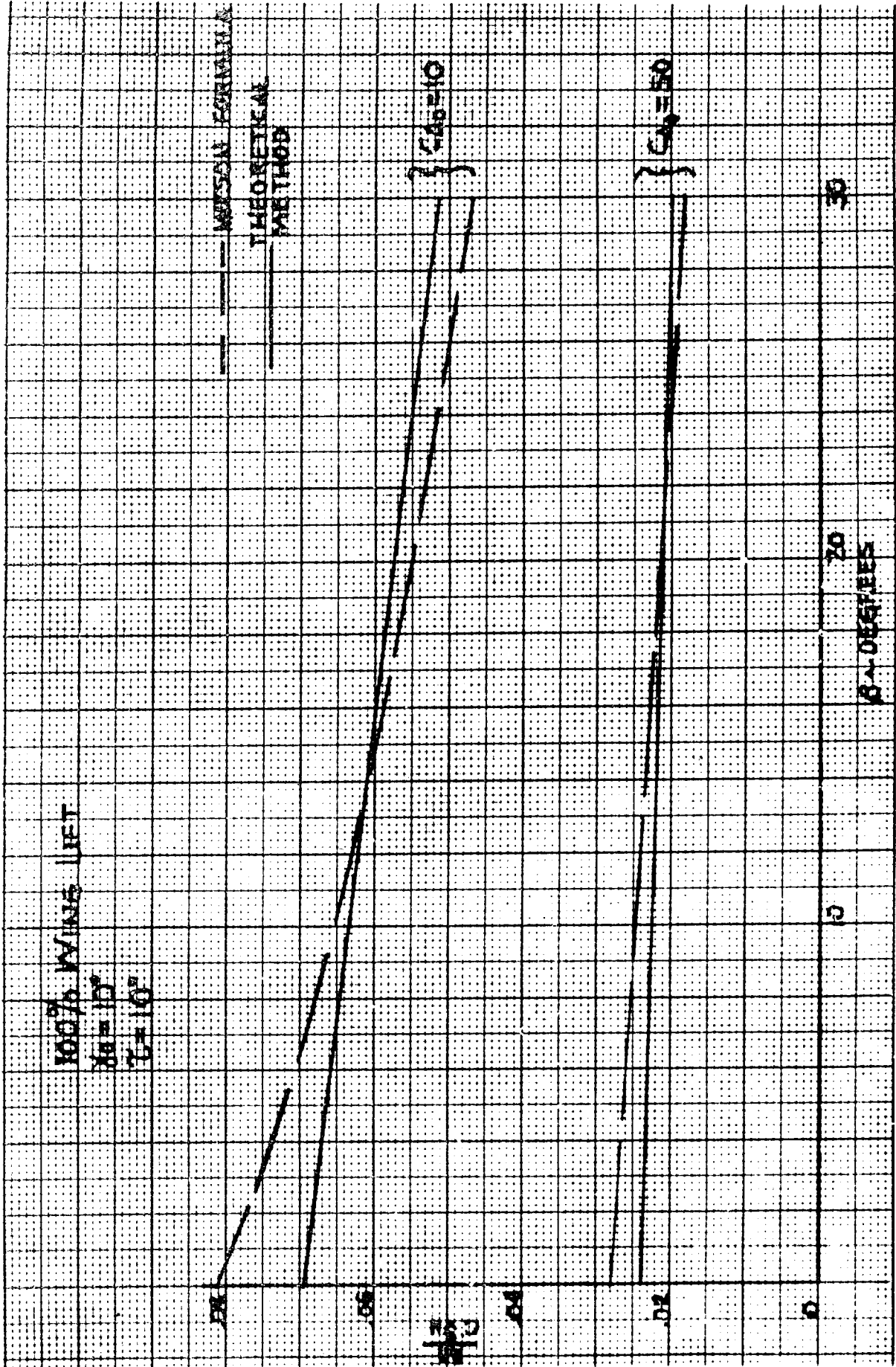
Figure 5-7. Theoretical Maximum Acceleration in Smooth Water vs Ski Deadrise Angle
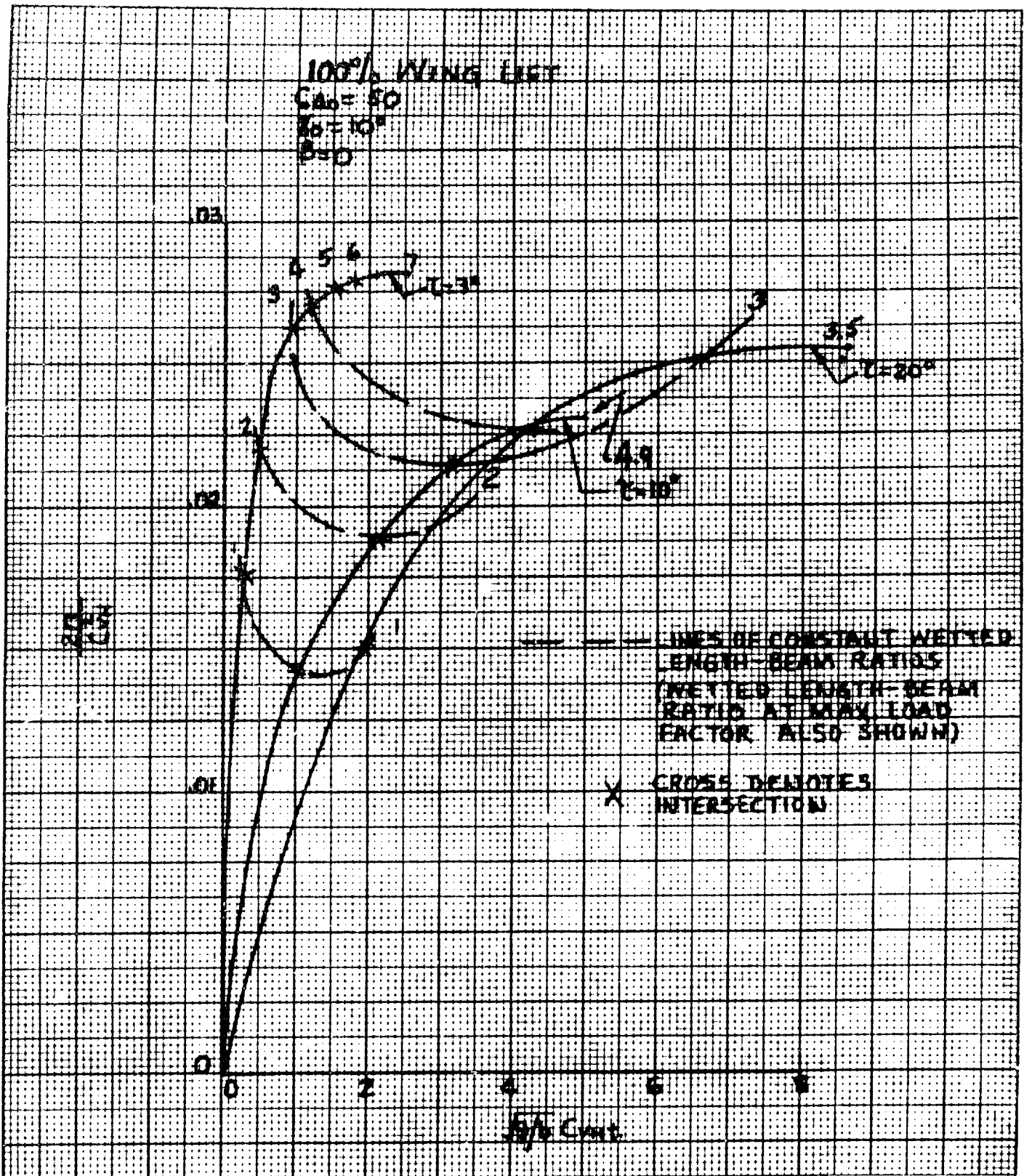
Figure 5-8. Theoretical Acceleration Time Histories of Smooth Water Impacts:
Ski Trim Variations
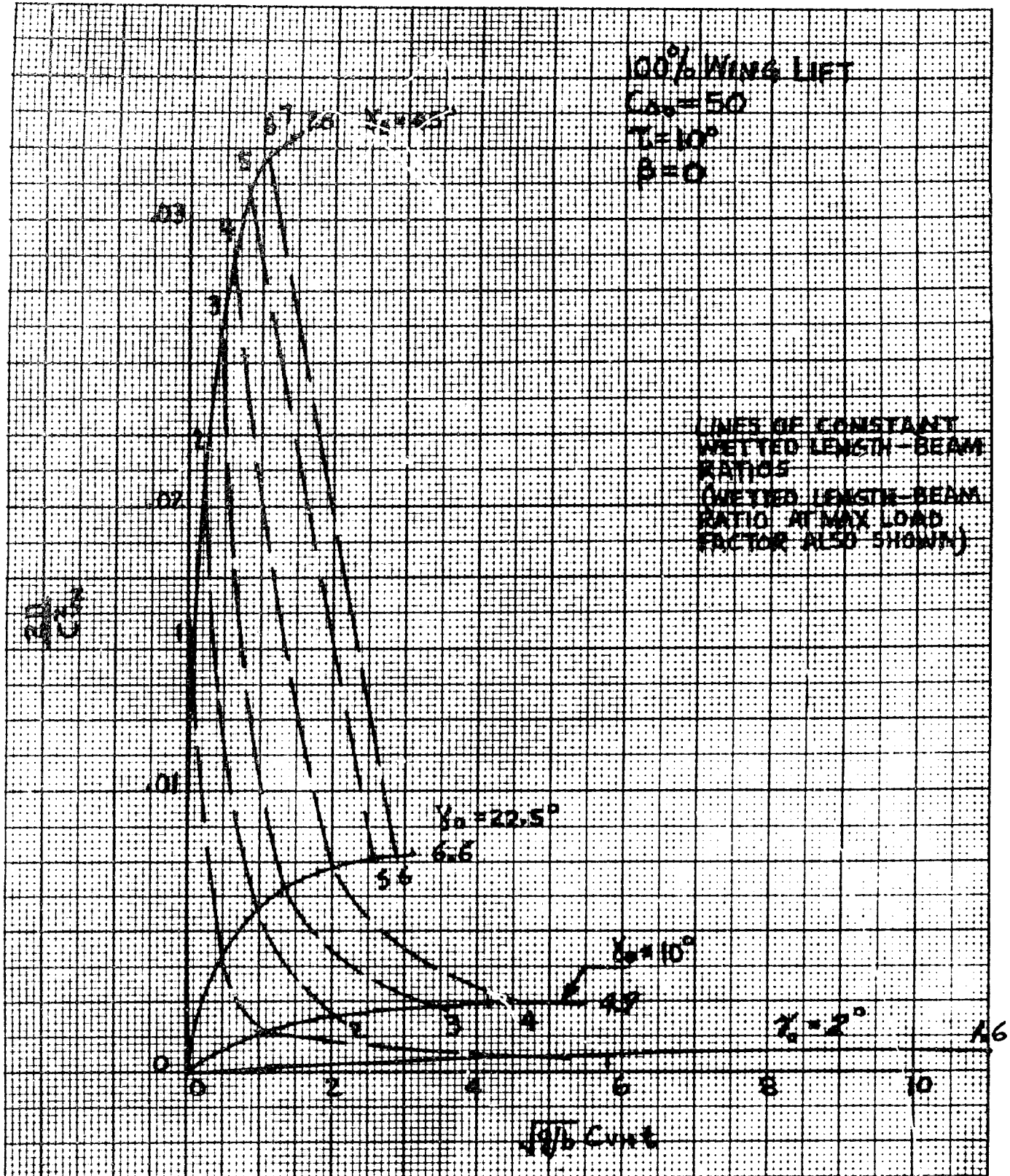
Figure 5-9. Theoretical Acceleration Time Histories of Smooth Water Impacts:
Flight Path Angle Variations
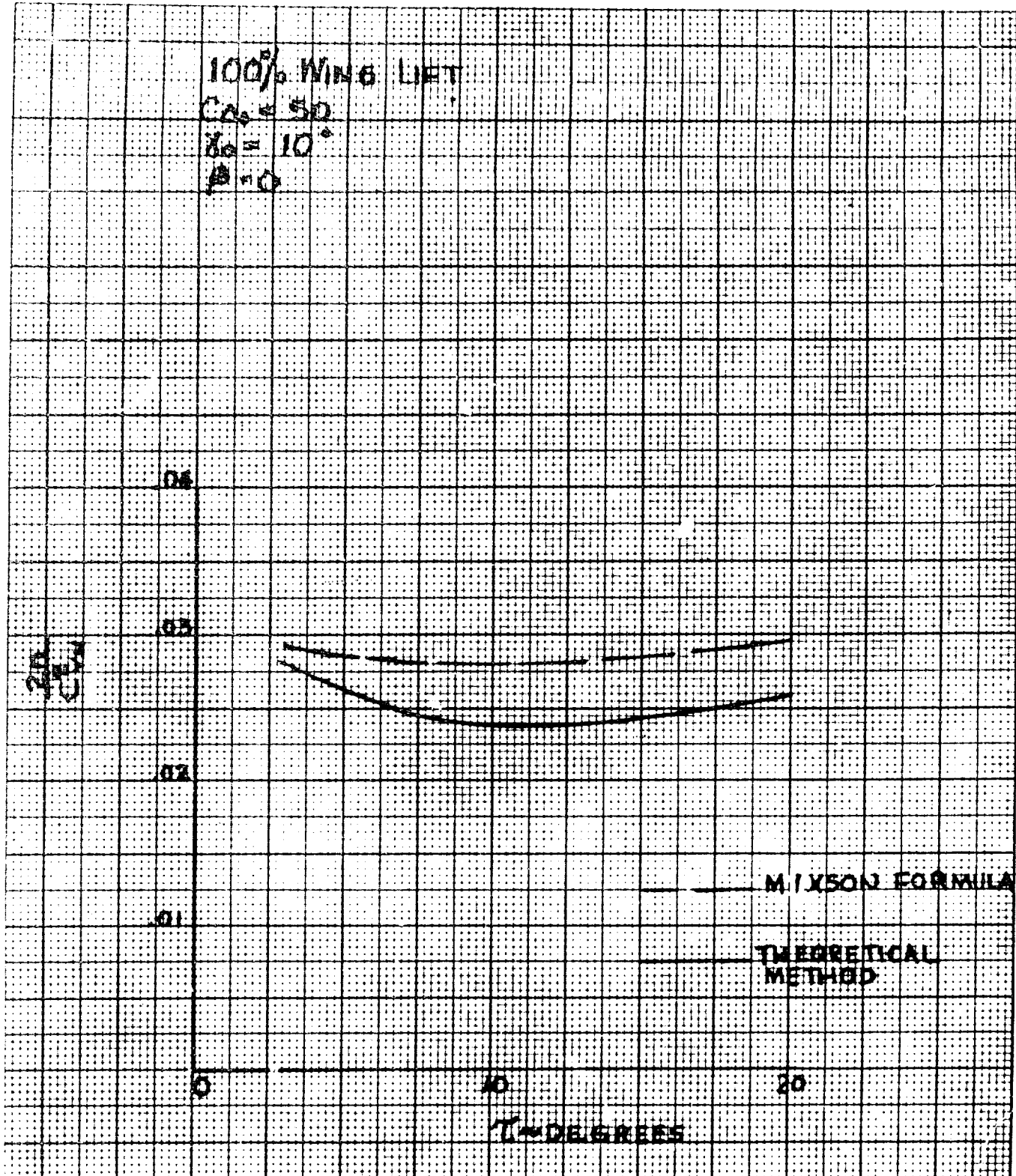
Figure 5-10. Theoretical Maximum Impact Acceleration in Smooth Water
vs Ski Trim Angle
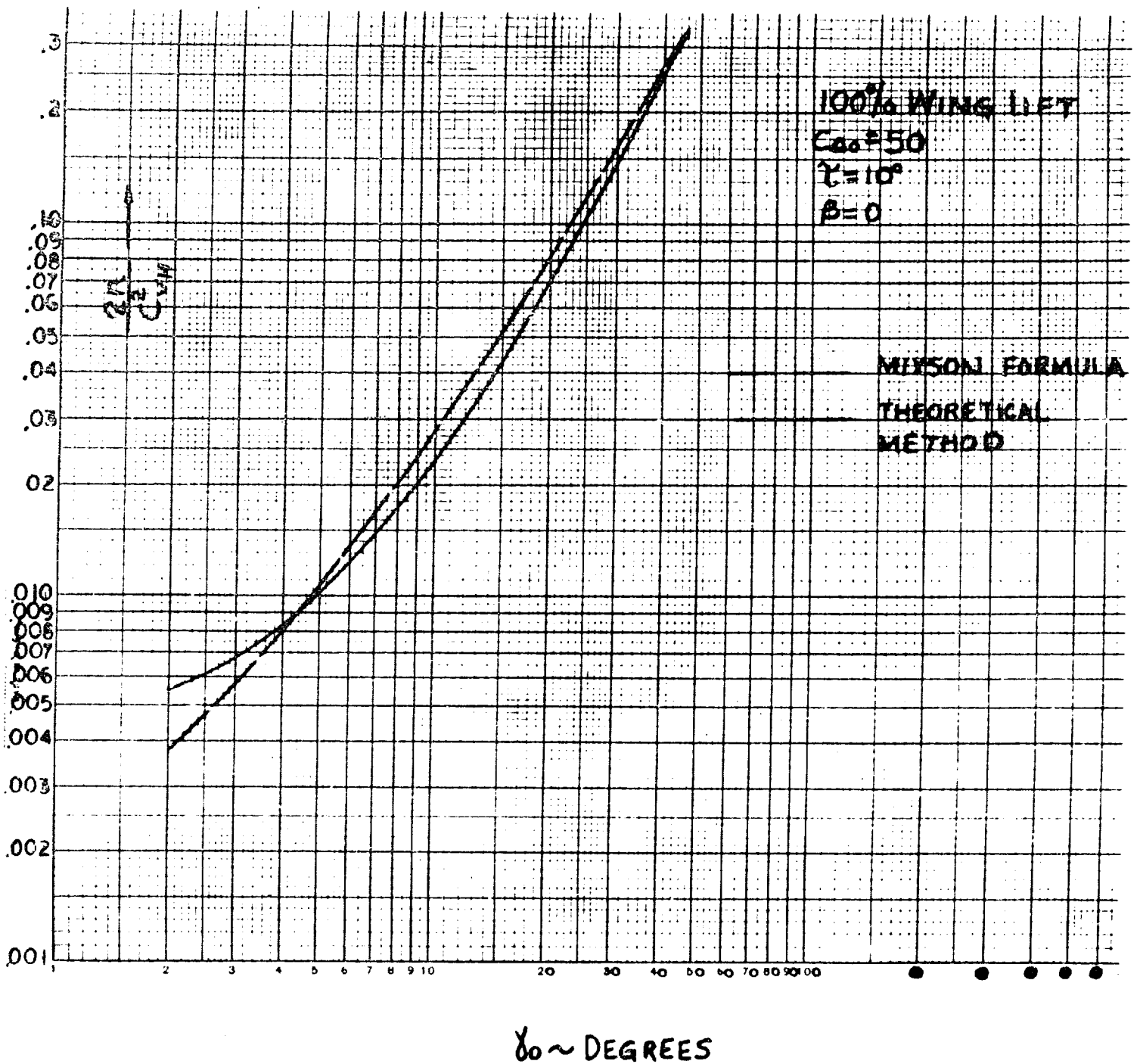
Figure 5-11. Theoretical Maximum Impact Acceleration in Smooth Water vs Flight Path Angle

in Figure 5-1A, indicates that the present results are more reliable than those obtained from the empirical formula. On the other hand, the agreement of the two curves in Figure 5-11 is very good.

5.2.5   Effects of Airplane Lift on Impact Loads

Figure 5-12 shows the calculated non-dimensional acceleration time histories of smooth water impacts of a flat ski for various values of the "wing lift" parameter, p, with typical values for all other parameters. These calculations are based on equation 5-3, above.

It is seen that there is a smooth dependence on "wing lift". The significant feature of these results is that the maximum acceleration values differ by amounts which are smaller than the initial differences, the latter representing the difference in "p" values.

5.3   IMPACTS ON WAVES

5.3.1   Introduction

For many years, it was thought adequate to analyze hydrodynamic impacts on head-sea wave flanks by use of an "advancing wedge" approximation. With this technique, the effect of the wave is approximated by assuming that the wave acts like an inclined straight wall of water moving with the true wave celerity, the slope of the "wall" being the actual wave slope at the initial contact point. In refined versions of this method, the effects of the wave orbital velocities are also taken into account.

With or without the orbital velocity effects, the advancing wedge approximation leads to the conclusion that, for impacts of a given ski on the flank of a given regular (head sea) wave under given approach conditions, the maximum impact loads will always occur when the initial impact point is the one having the maximum wave slope (i.e., lying midway between crest and trough).

This conclusion follows automatically from the manner used to account for wave slope in the impact process whereby the ski is endowed with an effective trim and an effective flight path angle given respectively by:

$$\tau_{eff} = \tau - \phi$$

$$\gamma_{eff} = \gamma + \phi$$

where ϕ is the wave slope. If the trim angles and flight path angles used in Figures 5-10 and 5-11 of this report are interpreted as effective quantities, it will be seen that the effect of wave slope in decreasing the effective ski trim is relatively negligible as compared with its effect in increasing the effective initial flight path angle. As the maximum accelerations
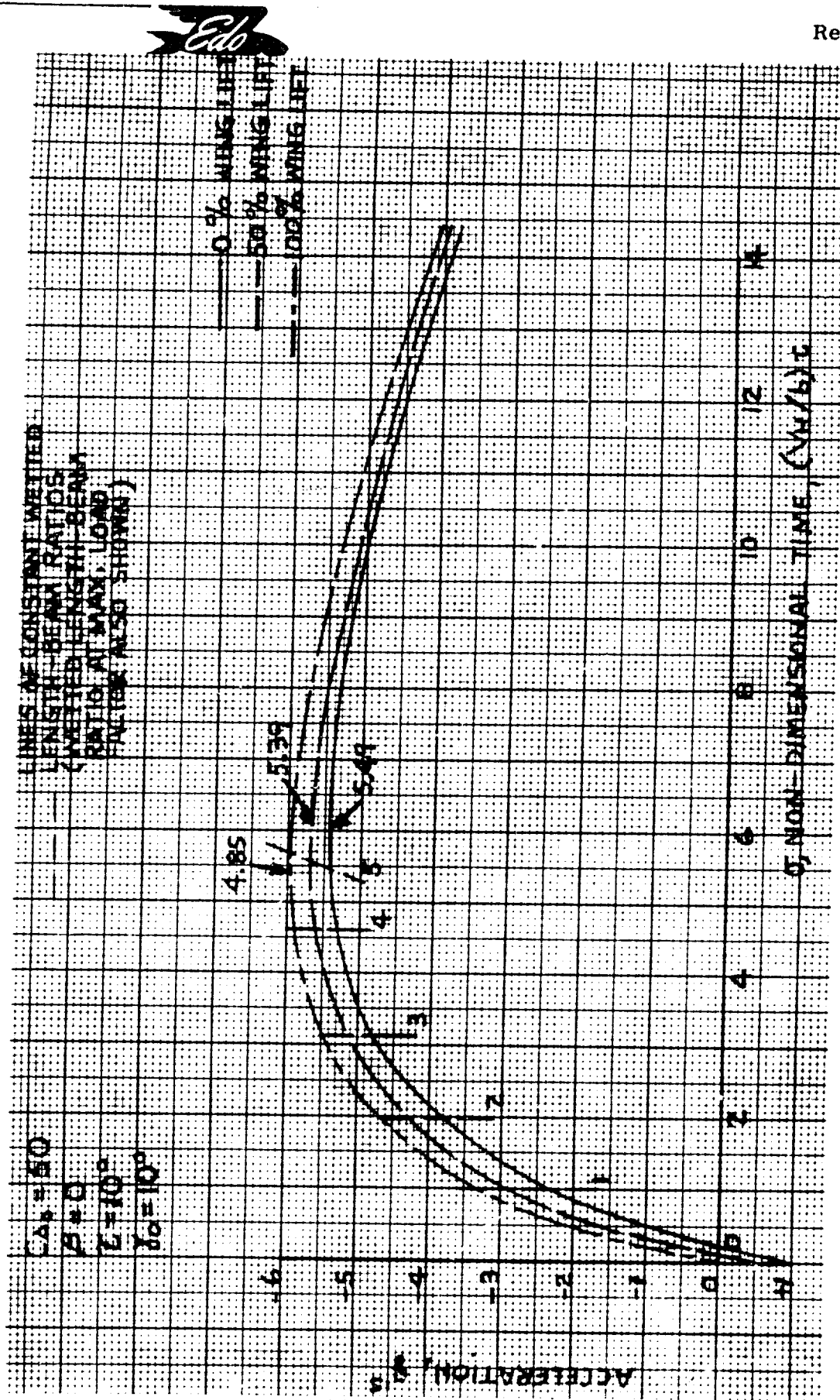
Figure 5-12. Theoretical Acceleration Time Histories of Smooth Water Impacts: "Wing Lift" Variation

increase very steeply with the effective flight path angle, it follows that the maximum peak accelerations will correspond to maximum wave slope.

It may be noted that the approach proposed in the Phase 1 report of this study, Reference 5-6, essentially agrees with this conventional concept. In that approach, the trim and initial flight path angles in Mixson's empirical formula for smooth water impacts would be replaced, in the wave impact case, by the _effective_ angles defined above, and would be taken simply as:

$$\phi = \phi_{max} = \tan^{-1}\left[\pi/(L/H)\right] ,$$

where H and L are the wave height and wave length. It is seen that this is simply one convenient way of utilizing the "advancing wedge" hypothesis and, as indicated earlier, still suffers from a lack of definition of wetted ski lengths.

The claim is now made that _any_ method utilizing the "advancing wedge" method cannot be correct (except by accident in particular cases) because this method embodies two different, but closely related, fallacies. Basically, this method is wrong because it does not account for the exact wave profile which affects the wetting of the ski, i.e., it replaces the actual profile by an infinite wedge. Precisely because it uses the wedge "approximation", it automatically leads to the condition that the maximum accelerations always occur for initial impact locations at the mid-point of the wave flank.

It will now be demonstrated that more accurate calculations can be made which account for the actual wave profile and that, when this is done, the maximum accelerations generally do _not_ correspond to initial impact locations at the flank mid-point, i.e., at the maximum wave slope locations.

5.3.2   Equations of Motion

Although the basic equation of motion is the same for wave impacts as for smooth water impacts, proper account must be taken of all wave effects, including geometric, kinematic, and dynamic effects. These effects may be summarized as follows:

1) The variation of both effective trim and effective flight path angle during the impact time history;

2) The variation of ski wetted length as affected by the true wave profile during the impact;

3) The variation of the orbital velocity dynamic effect during the impact.

All of these wave effects can be taken into account rather simply by using a coordinate system which moves horizontally with the ski at the latter's horizontal velocity, V_H.

In this system, the x-axis remains coincident with the level water line so that the origin stays vertically above or below the initial location of the ski trailing edge. In this system, the shape of a sinusoidal wave is given by:

$$y = \frac{H}{2} \sin \left\{ \frac{2\pi}{L} \left[x + (V_H + C) t \right] - \theta \right\}$$

where
H = wave height (trough to crest)

L = wave length

V_H = ski horizontal velocity (in space)

C = wave celerity = $\sqrt{g L/2\pi}$

θ = phase angle ($\theta = 2\pi x_o/L$, where x_o is the horizontal distance between mid-point of wave flank and initial impact point, taken as positive for impact points below mid-point)

The time is measured from the initial contact ($t = 0$ at $x = 0$) so that, by assigning different values to θ, the initial contact can be made to apply to any point along the entire wave flank. Figure 5-13 illustrates the pertinent values of θ.

Calculation of the instantaneous hydrodynamic force acting on the ski demands a knowledge of the wetted length or, alternately, the coordinates of the ski-wave surface intersection. The coordinates of the intersection are obtained from a consideration of the ski-wave geometry. Using the notation of the following sketch:
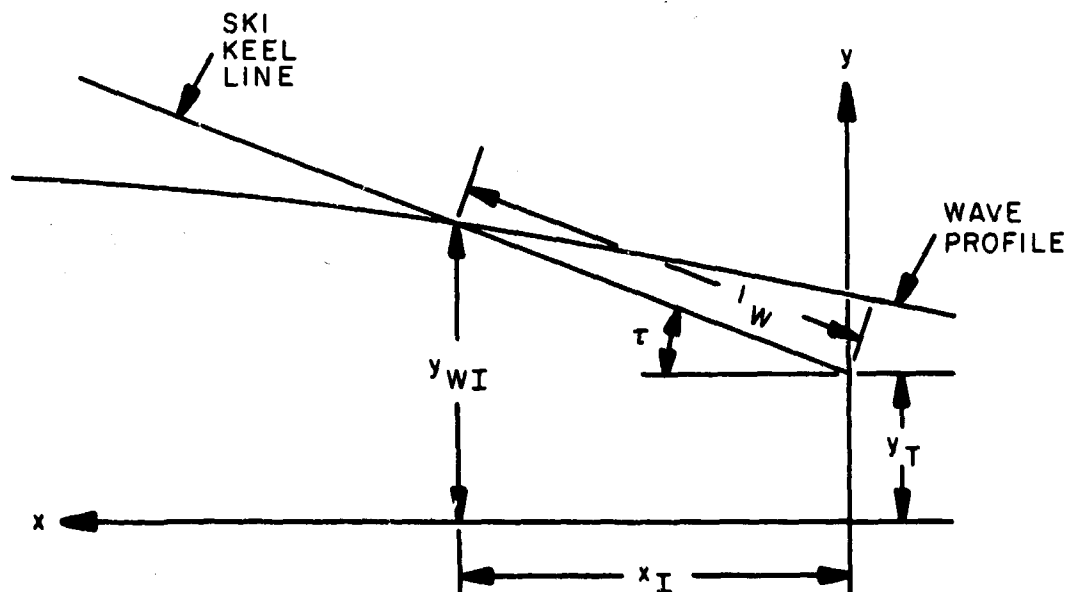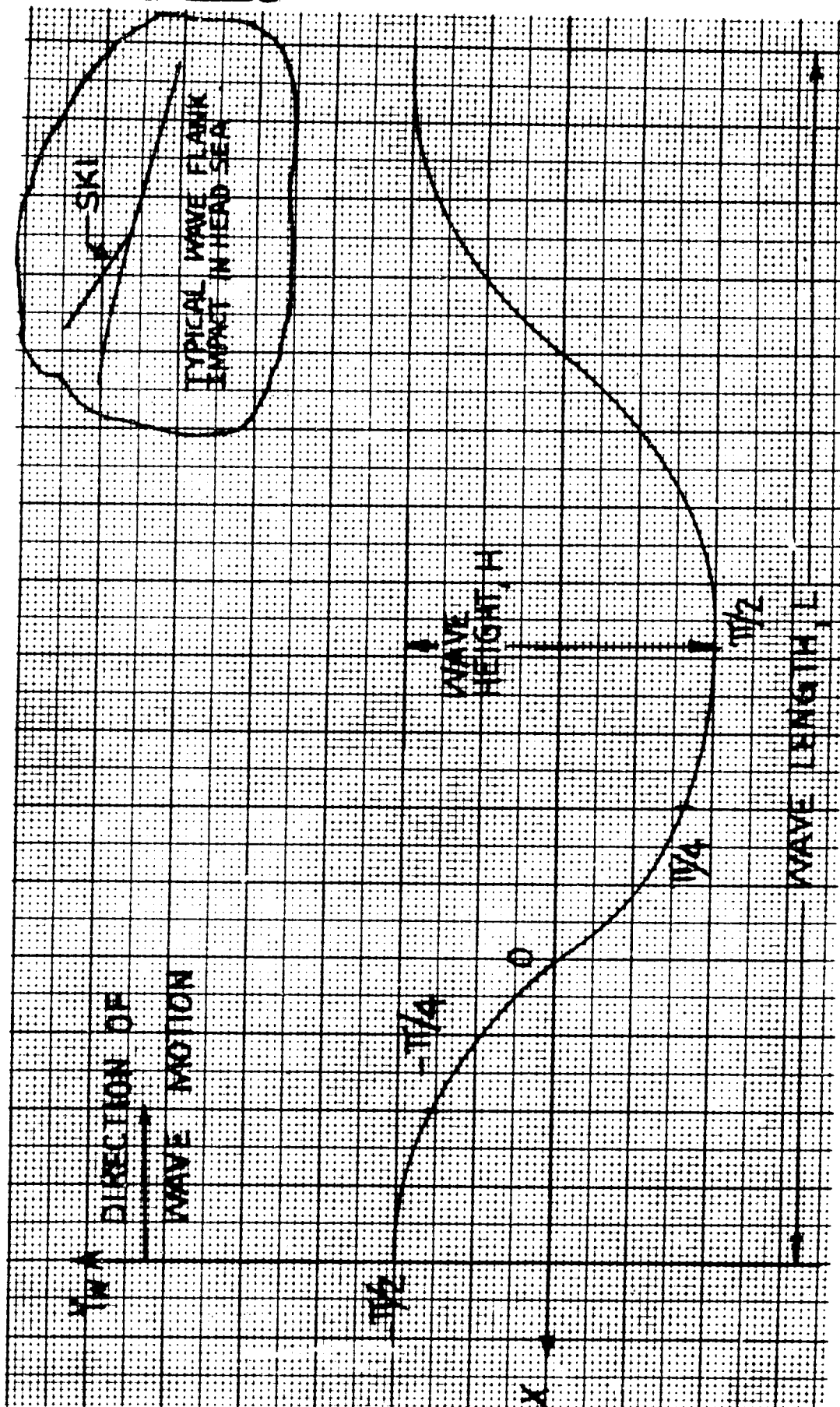
Figure 5-13. Sketch Illustrating Location of Initial Point on Wave Flank

it is seen that:

$$y_{WI} = y_T + x_I \tan \tau \qquad (I = \text{intersection})$$

But

$$y_{WI} = \frac{H}{2} \sin \left\{ \frac{2\pi}{L} \left[x_I + (V_H + C)\, t \right] - \theta \right\}$$

These two equations, in conjunction with the relation:

$$l_W = x_I / \cos \tau$$

and the equation of vertical motion (which basically defines y_T), serve to determine the instantaneous values of x_I and, thus, of l_W. It is seen that the quantity, y_{WI}, is actually irrelevant to the calculation.

What is relevant, however, is the quantity, ϕ_I, the instantaneous wave slope at the ski-wave intersection. This slope is given by:

$$\tan \phi_I = (dy/dx)_I$$

$$= \frac{\pi H}{L} \cos \left\{ \frac{2\pi}{L} \left[x_I + (V_H + C)\, t \right] - \theta \right\}$$

The present calculations use effective trim and flight path angles given by:

$$\tau_{eff} = \tau - \phi_I$$

$$\gamma_{eff} = \gamma + \phi_I$$

Finally, orbital velocity effects, although generally small, have been taken into account by inclusion of the instantaneous vertical component of the orbital velocity, where the pertinent orbital velocity is that at the ski-wave surface intersection.

The preceding approaches, accounting for all the known significant wave effects, were combined with the equation of motion and the "equivalent planing velocity" expression to form a single digital computer program using non-dimensional quantities. * This program was used for all of the calculated (theoretical) impact time histories described below.

* Actually, the smooth water impact calculations of Section 5.2, above, were obtained from the same wave impact computer program as a special case: wave height = 0.

5.3.3   Correlation of Test Data

The calculation technique outlined above was checked by comparison with available test data given in Reference 5-5. The latter contains a series of experimental time-histories for "zero wing lift" wave impacts of flat rectangular hydro-skis. Four of these time histories have been selected for comparison with the present theory. It must be explained that the test techniques used in obtaining these time histories was such that the precise location on the wave flank of the initial impact point could not be identified. Accordingly, in each case, the time histories were calculated for a variety of initial impact points. The family of curves thus obtained in each case was then compared with the experimental curve to determine whether the experimental curve is actually an interpolated "member of the family".

These comparisons are shown here in Figures 5-14 A, B, C, and D. Figure 5-14A shows that the test data belong to an initial impact point located approximately at $\theta = -\pi/8$. Figures 5-14B and C need no comment as the test data in each case are extremely close to one of the calculated curves ($\theta \cong -\pi/4$ in Figure 5-14B and $\theta \cong +\pi/2$ in Figure 5-14C). In Figure 5-14D, where the agreement for the total time history is not quite so good, the test data obviously correspond to a value between $+3\pi/8$ and $+\pi/2$. Even in this case, the error in the predicted maximum acceleration is only 6%.

These comparisons are considered to furnish a complete vindication of the present theoretical calculation technique.

5.3.4   Effects of Impact Location on Impact Loads

The results just presented are obviously of the utmost importance in connection with the prediction of hydro-ski impact loads. If for no other reason, they clearly contradict the traditional assumption that the maximum impact loads of a given ski in a given wave system under fixed approach conditions are always obtained when the initial impact point is that for maximum wave slope which, in present notation, is at $\theta = 0$. The foregoing results make it clear, in fact, that the maximum impact loads do not correspond to any single value of θ or, stated alternately, the value of n_{max} generally depends on the particular values of all significant parameters.

This statement is further clarified by Figure 5-15 which shows the dependence of n_{max} (calculated peak acceleration) on θ for the four cases illustrated in Figure 5-14. It is seen that, in these cases, the "absolute" maximum accelerations occur when the initial contact is made on the lower portion of the wave flank (and not at its center). A further point of the utmost practical significance is indicated by the l_w/b values shown on the curves of Figure 5-15. Just as in the case of smooth water impacts, it is obvious that the finite length of any actual practical hydro-ski will generally play a major role in limiting the maximum accelerations in rough water.
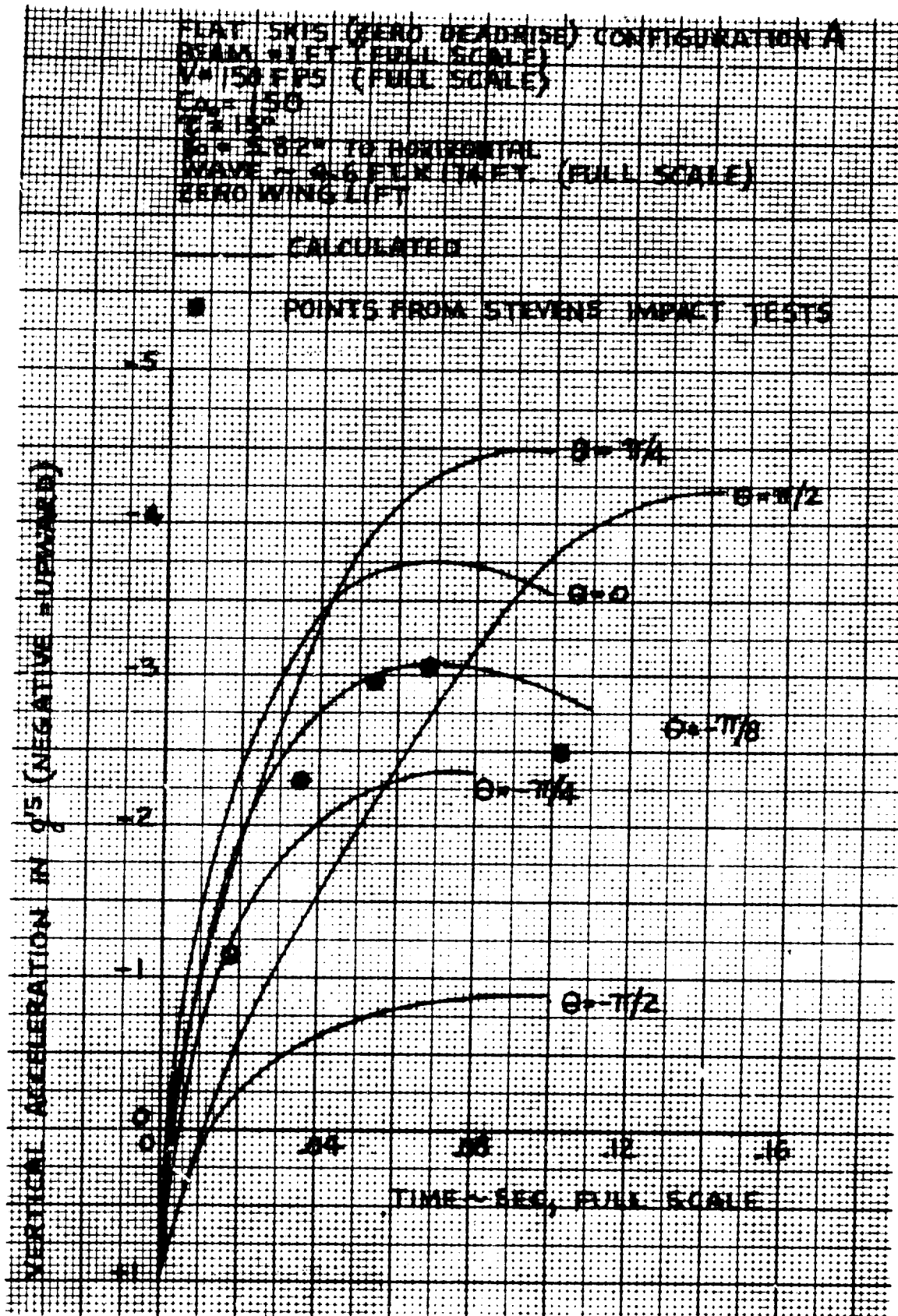
Figure 5-14(A). Acceleration Time Histories of Wave Impacts:
Comparison of Impact Theory with Test Data
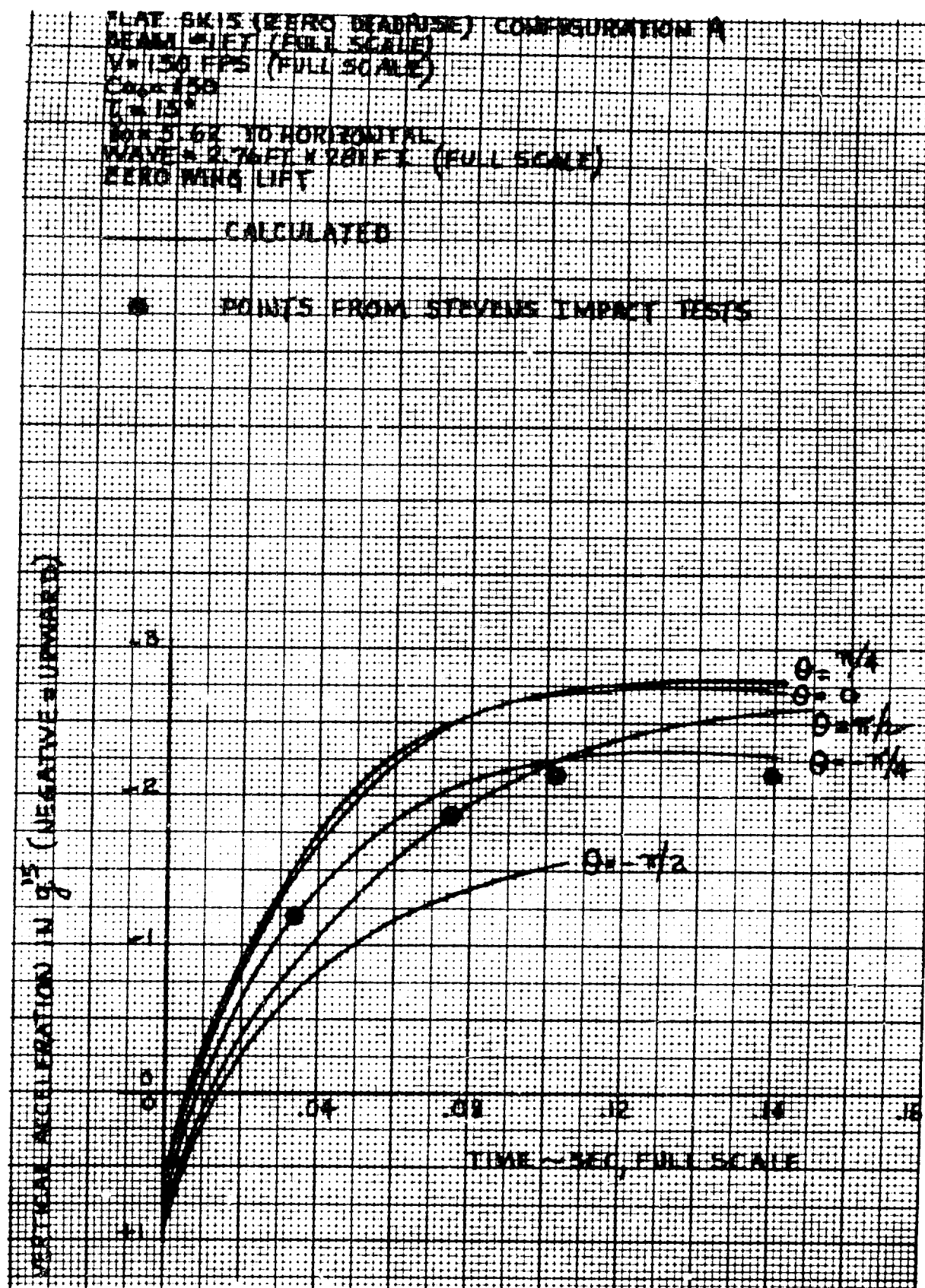
Figure 5-14(B). Acceleration Time Histories of Wave Impacts:
Comparison of Impact Theory with Test Data
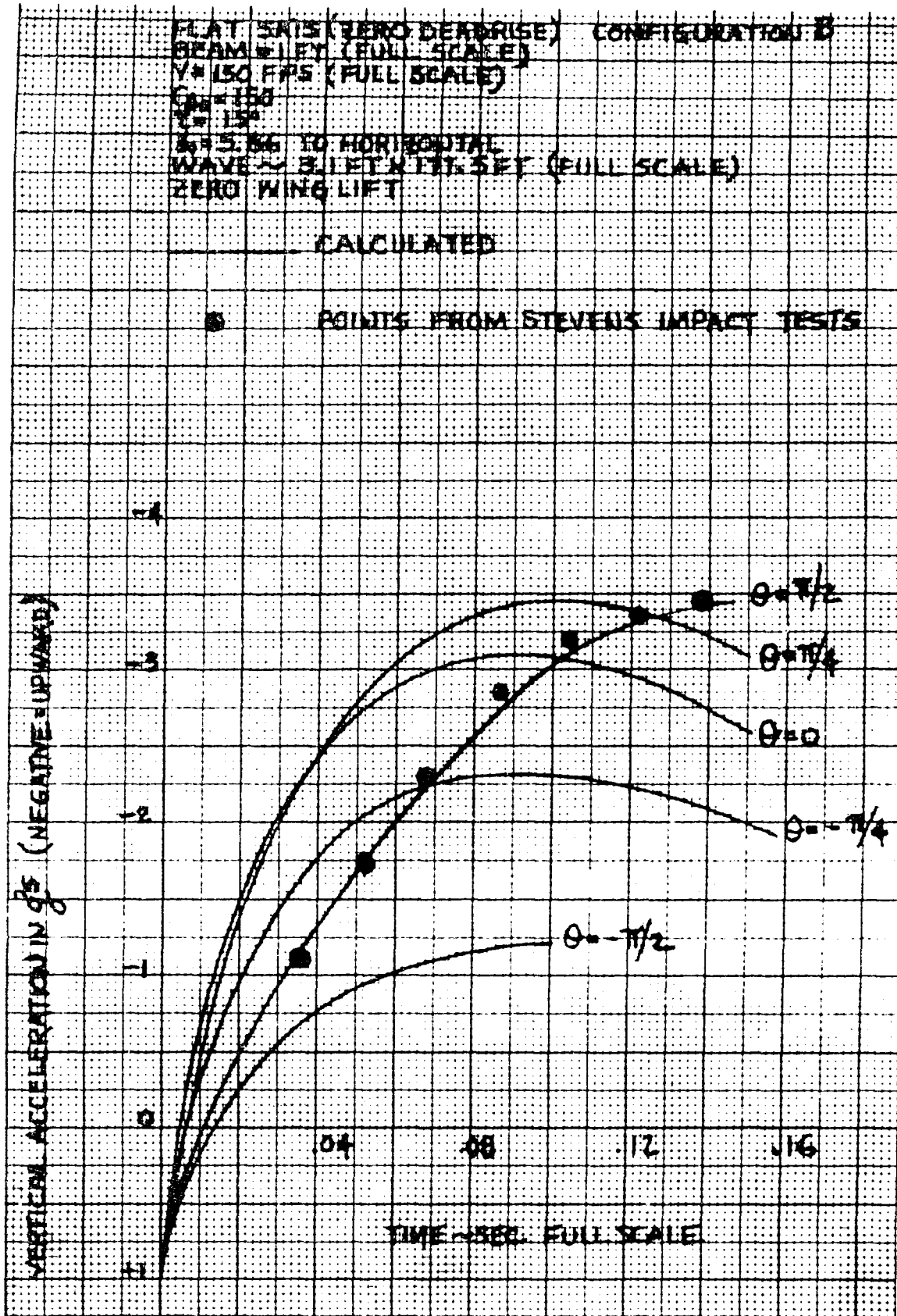
Figure 5-14(C). Acceleration Time Histories of Wave Impacts:
Comparison of Impact Theory with Test Data
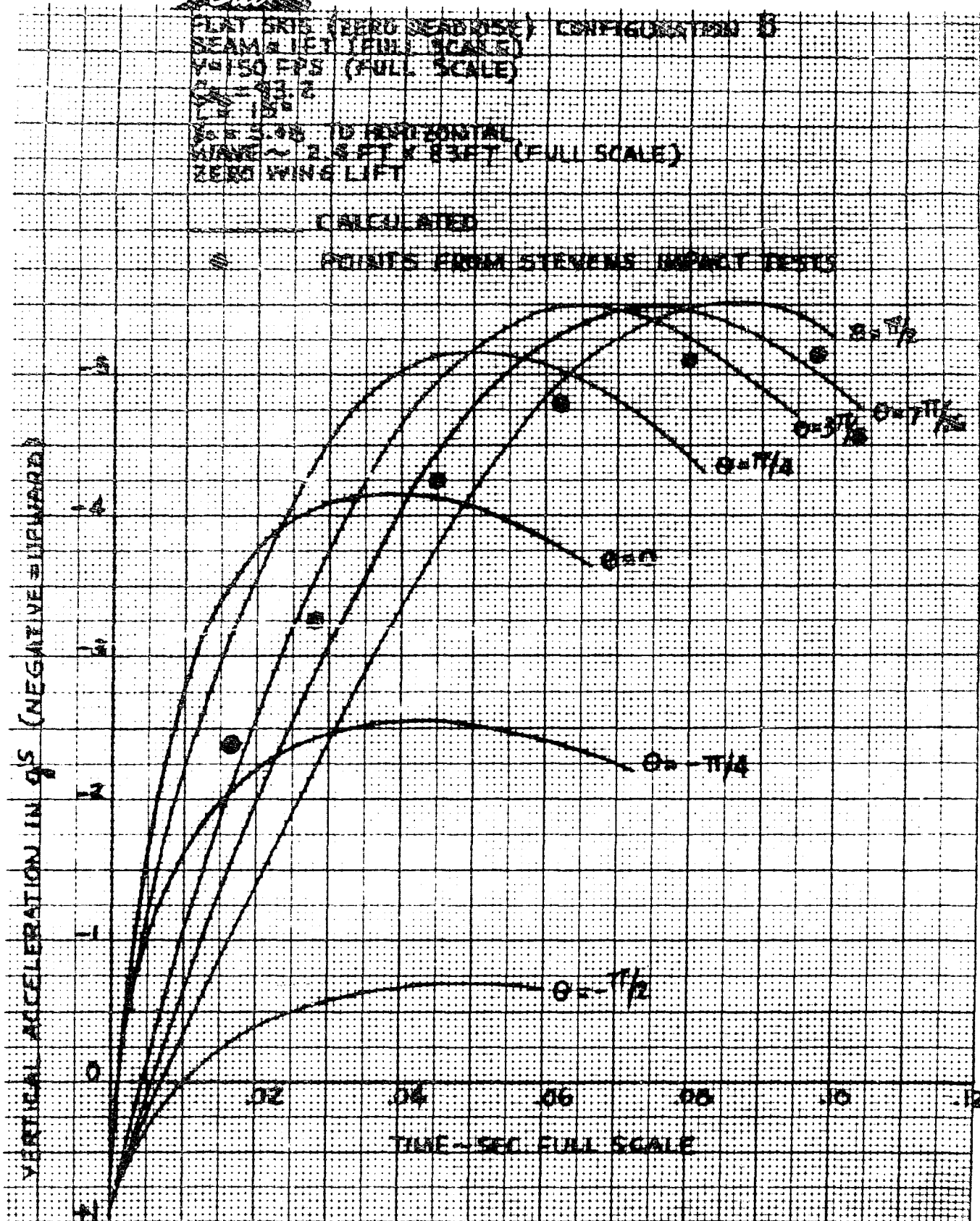
Figure 5-14(D). Acceleration Time Histories of Wave Impacts:
Comparison of Impact Theory with Test Data
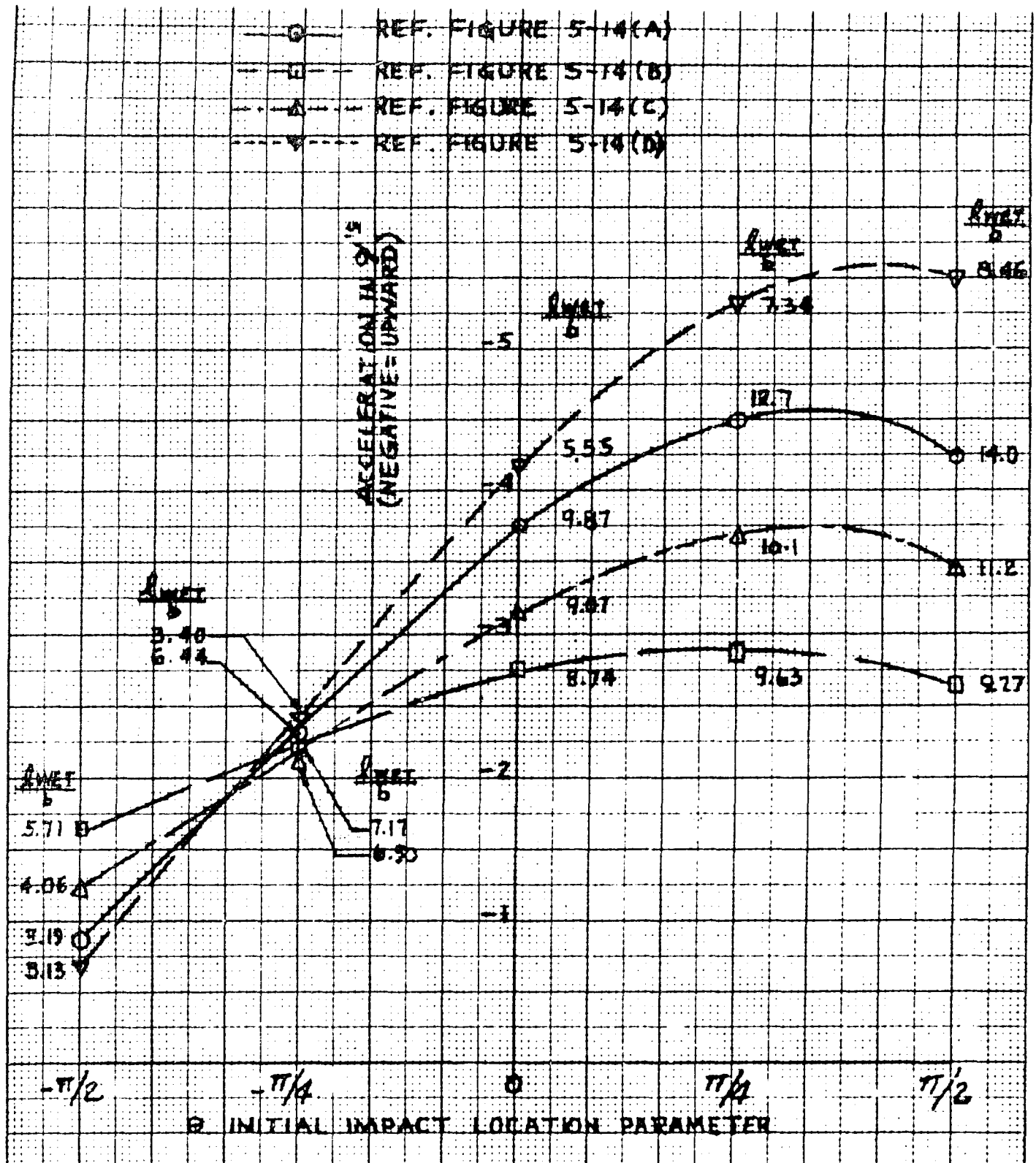
Figure 5-15.   Variation of Wave Impact Peak Acceleration with Initial Impact Location

In the present analysis, there are actually ten significant non-dimensional parameters, as follows:

Aircraft Aerodynamics:	"Percent Wing Lift", L_A/W
Hydro-Ski:	Beam Loading, C_{Δ_0}
	Deadrise Angle, β
	Length-Beam Ratio, l/b
Approach (Initial) Flight Condition:	Horizontal Speed Coefficient, C_{VH}
	Ski Trim Angle, τ
	Initial Flight Path (Sink) Angle, γ
Wave:	Wave Height/Ski Beam, H/b
	Wave Length/Ski Beam, L/b
	Initial Contact Point, θ

Because of the large number of these parameters, it was considered infeasible to conduct a complete parametric investigation of si gle ski wave impacts. Instead, primarily for illustrative purposes, a very limited parametric study has been made as will now be described.

5.3.5   Effects of Wave Geometry, Forward Speed, and Ski Length, on Impact Loads

The effects of wave geometry on hydro-ski impact loads are illustrated herein by a brief parametric study in which the wave height and wave length were varied independently. Further, to illustrate the effects of a significant aircraft characteristic, all of these calculations were made for two horizontal velocity values typical of conventional and STOL-type seaplanes.

To lend a note of realism, the non-dimensional parameters required for the computer program correspond to the following dimensional parameters:

Aircraft Gross Weight:	250,000 pounds
Hydro-Ski Beam:	3.40 feet
Hydro-Ski Deadrise Angle:	0 degrees

Ski Trim Angle:	10 degrees
Initial Vertical Velocity:	10 fps *
Horizontal Velocity (Conventional):	85 knots
Horizontal Velocity (STOL):	42.5 knots
Initial Flight Path (Sink) Angle (Conventional):	4 degrees
Initial Flight Path (Sink) Angle (STOL):	8 degrees

The calculations were made using the "100% wing lift" assumption, for the following full-scale wave dimensions:

CASE A. <u>H = 12 ft.</u> *

$\underline{L}$	$\underline{L/H}$ *
ft.	
240	20
3j0	30
480	40

CASE B. <u>L/H = 30</u>

$\underline{H}$	$\underline{L}$
ft.	ft.
9	270
12	360
15	450

* Per MIL-A-8864(ASG)

Note that, in Case B, instead of fixing a common wave length, a common value of L/H has been used. This choice has been made deliberately because, as explained in Paragraph 5.3.1, above, rough water accelerations computed with the traditional "advancing wedge" assumption would depend only on the (common) L/H value and not on the individual values of L and H.

In the same connection, the calculations were made without assuming any limitation on ski length but the effects of a typical limitation will be indicated. (With the unlimited length, the inherent differences between the present and "advancing wedge" computations are more readily appreciated). The "limited" ski length is chosen as 17.0 feet, corresponding to $l/b = 5.0$.

Summarizing the non-dimensional parameters:

"Wing Lift" Parameter:	$p = 1$
Hydro-Ski Beam Loading:	$C_{\Delta_o} = 100$
Hydro-Ski Deadrise Angle:	$\beta = 0$ degrees
Hydro-Ski Length-Beam Ratio:	$l/b = 5$ (when limited)
Hydro-Ski Trim Angle:	$\tau = 10$ degrees
Horizontal Velocity Coefficient (Conventional):	$C_{VH} = 13.75$
Horizontal Velocity Coefficient (STOL):	$C_{VH} = 6.88$
Initial Sink Angle (Conventional):	$\gamma_o = 4$ degrees
Initial Sink Angle (STOL):	$\gamma_o = 8$ degrees

CASE A. $\underline{H/b = 3.53}$

L/b	L/H
70.5	20
105.8	30
141	40

CASE B. $\underline{L/H = 30}$ $\underline{H/b}$ $\underline{L/b}$

                    2.65   79.5

                    3.53   105.8

                    4.42   132

The principal results of these computations are illustrated in Figure 5-16. In each of these plots, the peak acceleration obtained from the individual time histories have been plotted against the initial impact location. In each figure, the first chart is for V_H = 85 knots while the second chart corresponds to V_H = 42.5 knots.

Before discussing these results, it must be noted that some of them are approximate. This feature arises from the fact that, in connection with the "equivalent planing velocity" method, the approximation:

$$l_k = l_c,$$

has been retained even in regions of low effective trim angle, where it is known to be inaccurate (see Figure 3-1, Section 3). However, the errors inherent in this approximation are sufficiently small so that the conclusions drawn from the present calculations will not be appreciably affected.

The principal conclusions drawn from these results, most of which are of fundamental interest in the design of hydro-ski installations for rough-water seaplanes*, are as follows:

A. For the most part, the dependence of the peak accelerations on the wave geometry parameters follows the anticipated trends, i.e.:

        a. For constant wave height (Case A), the peak accelerations generally increase very rapidly with decreasing L/H, i.e., increasing wave slopes. This is true whether or not the ski length is limited.

        b. For constant L/H (Case B), the peak accelerations increase, but very slowly, with increasing wave height provided that the ski length is unlimited. For the case of limited ski length, the variation with wave height can be either increasing, constant, or decreasing, depending on other parameters, principally the initial contact point on the wave and, secondarily, on the forward speed.

*Note that, for "100% wing lift", the maximum hydrodynamic loads acting on the hydro-ski are directly proportional to the accelerations shown in Figure 5-16 and can be obtained by multiplying them by the aircraft gross weight.
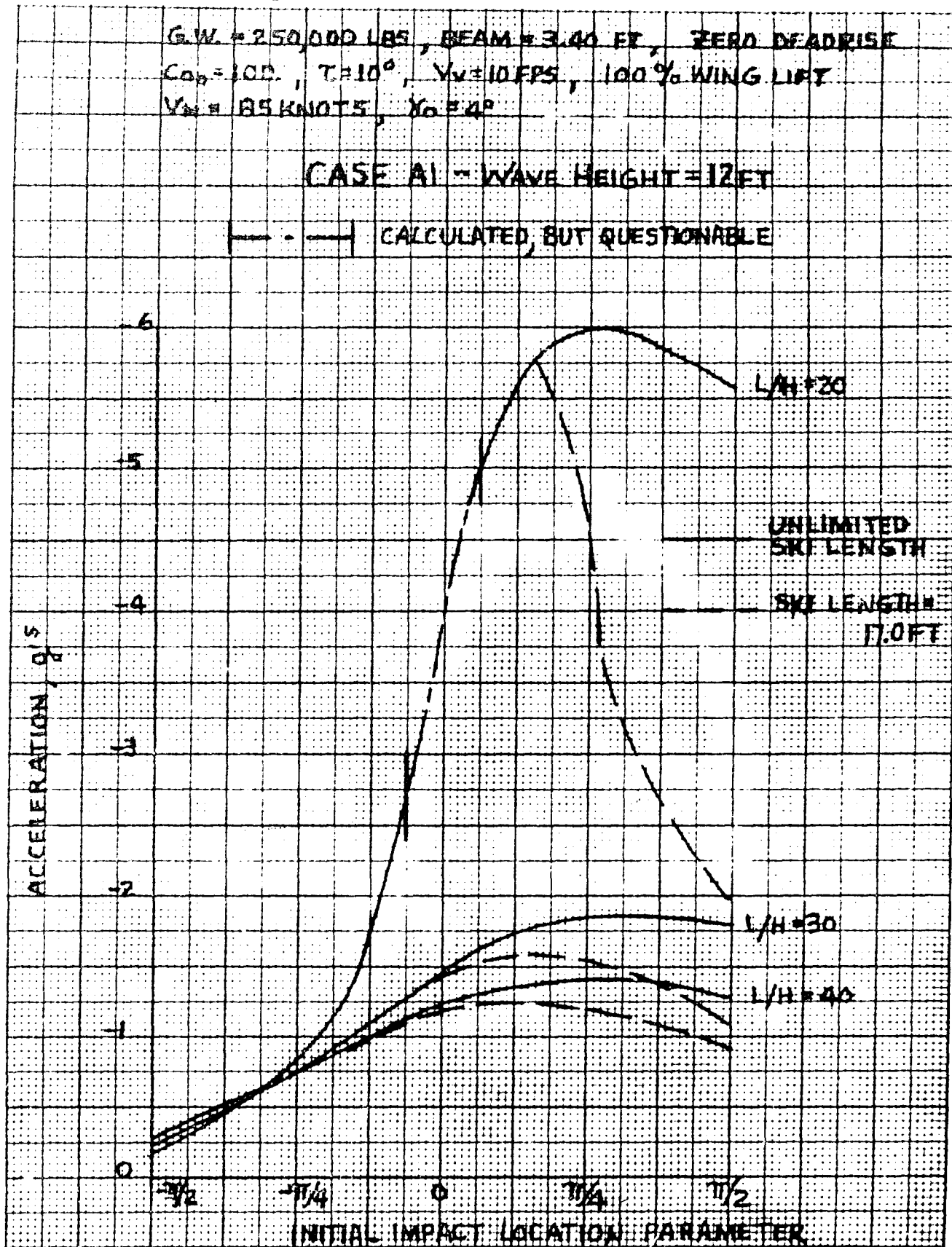
Figure 5-16A1. Theoretical Wave Impact Peak Acceleration vs Initial Impact Point Location
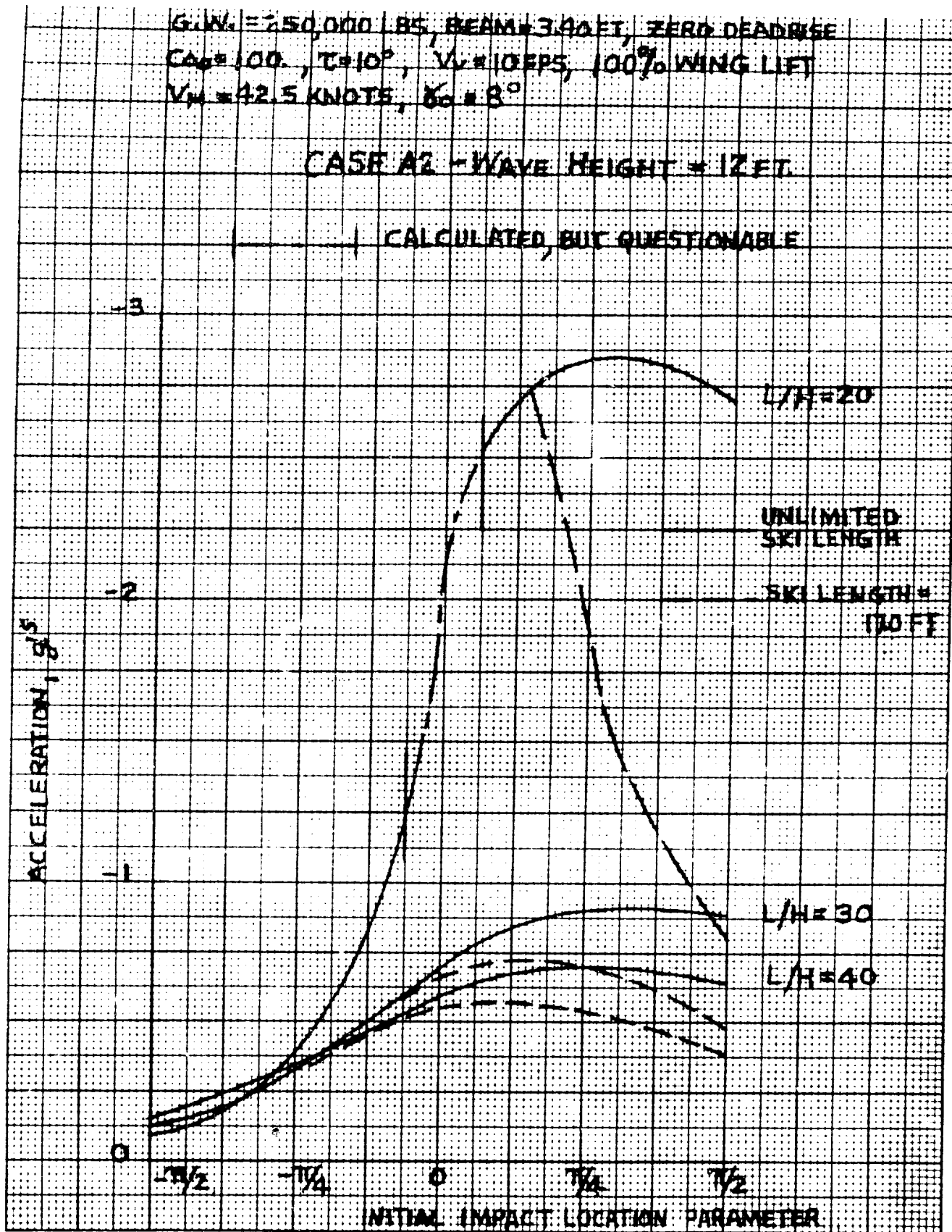
Figure 5-16A2. Theoretical Wave Impact Peak Acceleration vs Initial Impact Point Location
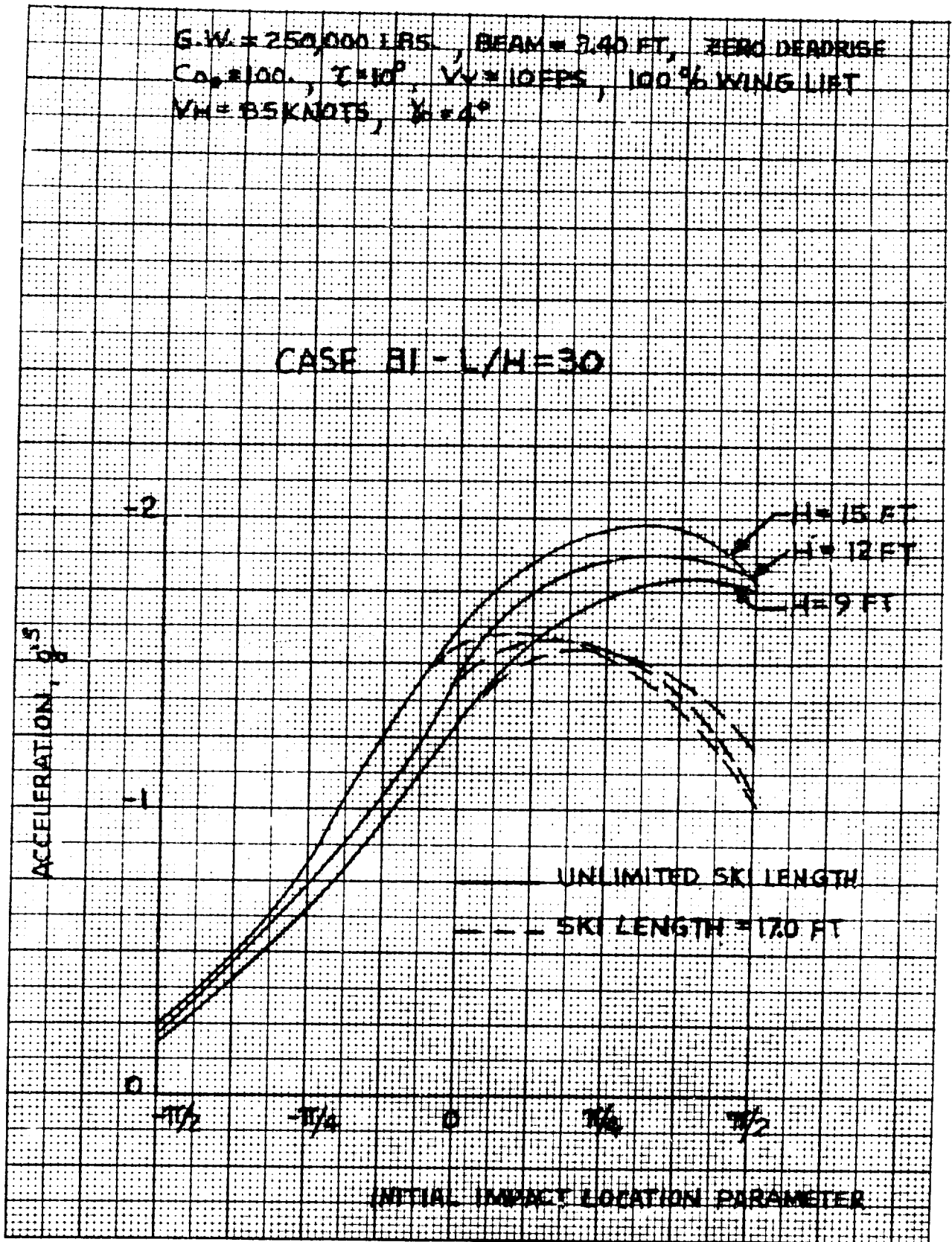
Figure 5-16B1. Theoretical Wave Impact Peak Acceleration vs Initial Impact Point Location
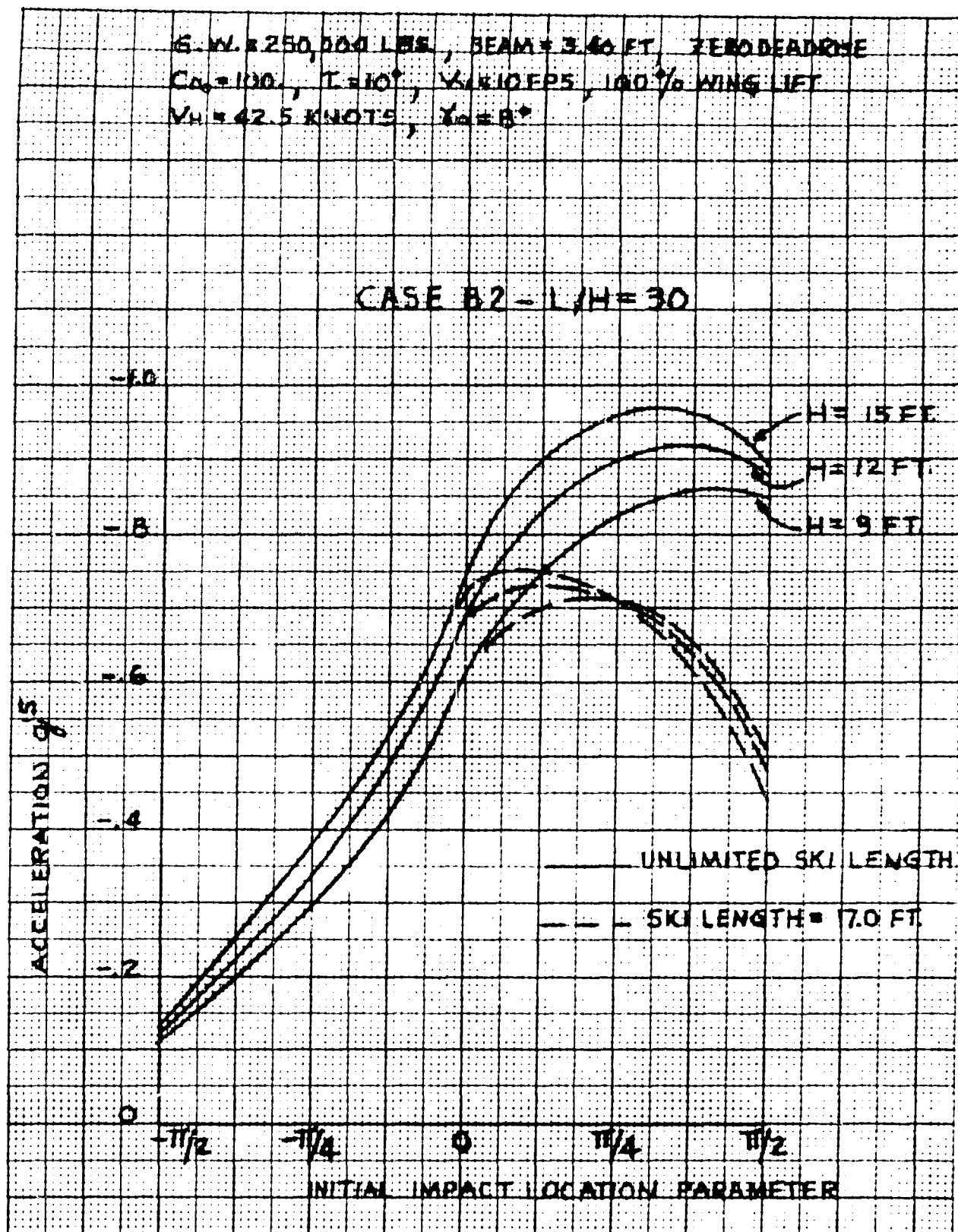
Figure 5-16B2. Theoretical Wave Impact Peak Acceleration vs Initial Impact Point Location

B. The effect of forward speed on the peak acceleration is very marked. In the present examples (based on constant sink speed), the peak accelerations are found to be, almost exactly, directly proportional to the forward speed.

C. Aside from the parametric aspects of this investigation, the numerical values have considerable interest in connection with the present specification requirements MIL-A-8864(ASG) . They show that a hydro-ski seaplane utilizing conventional aerodynamic and propulsion systems ($V_H = 85$ knots, in present example) can be expected to experience relatively high accelerations when landing under the specified rough-water conditions (H = 12 feet, L/H = 20), even with ski beam loadings as high as 100.

While these peak accelerations can be alleviated by one or more of several techniques such as increase of beam loading, decrease of ski length, incorporation of deadrise, no single one of these is nearly so effective as a substantial decrease in forward speed. Thus, it appears that, from the important standpoint of landing impact accelerations, there is much to be gained by use of STOL configurations in rough-water seaplanes.

REFERENCES

5-1   Edo Report No. 4439: "A Survey on Hydro-Ski Water Loads," by L. Kaplan,
       22 November 1957.

5-2   NASA MEMO 1-5-59L: The Effects of Beam Loading on Water Impact Loads and
       Motions," by J. S. Mixson, February 1959.

5-3   NACA TR 1103: "Generalized Theory for Seaplane Impact," by B. Milwitsky,
       30 October 1952.

5-4   NASA MEMO 2-10-59L: "A Generalized Hydrodynamic-Impact Theory for the
       Loads and Motions of Deeply Immersed Prismatic Bodies," by M. F. Markey,
       March 1959.

5-5   Convair Report No. ZU-2-002: "Presentation and Analysis of Hydrodynamic Tests
       at Stevens Institute of Technology on Isolated Skis and Ventrals," by
       R. E. Leadon and J. E. Piper, 24 November 1950.

5-6   Edo Report No. 7489-1: "Survey on Seaplane Hydro-Ski Design Technology.
       Phase I: Qualitative Study," by P. A. Pepper and L. Kaplan, 23 December 1966.

6. PLANING STABILITY OF THE SKELETON HYDRO-SKI SEAPLANE

6.1   INTRODUCTION

One of the most fundamental aspects of aircraft engineering is the determination of an airplane's longitudinal and lateral dynamic stability characteristics, which include such items as:

    A. Dynamic stability with fixed and free controls;

    B. Dynamic response to control surface displacements;

    C. Dynamic response to gusts.

Further, it is well-known that these problem areas can be successfully analyzed by use of linearized equations of motions. These equations involve a set of aerodynamic quantities ("stability derivatives") which are either estimated or obtained from suitable wind-tunnel tests, or both.

Problems of dynamic stability are also of importance in connection with seaplanes under waterborne conditions. Past experience has indicated that the principal dynamical stability problems of waterborne seaplanes, including both conventional hull and hydro-ski types, are those associated with "porpoising" motions.

As explained in more detail in Reference 6-1, there are two, basically different, types of porpoising motions, both occurring in the planing regime under "stick-fixed" conditions. Briefly described, at planing speeds, there is usually a stable range of (equilibrium) trim angles which is bounded by an "upper" and a "lower trim limit" of dynamic stability. Inside of the middle trim range, the seaplane is dynamically stable. At trims above the "upper limit", or below the "lower limit", the seaplane is dynamically unstable, the instability taking the form of so-called "porpoising" motions. Porpoising consists of coupled two-degree of freedom (heaving and pitching) motions involving undamped or, more accurately, negatively damped oscillations.

At trims above the upper limit, the porpoising is referred to as high-angle porpoising and, in the case of conventional hull seaplanes, these motions are associated with wetting of both hull forebody and afterbody. Similarly, in the case of the hydro-ski seaplane, it is possible to encounter high-angle porpoising involving wetting of the ski and the hull afterbody. However, because of the generally low location of the ski relative to the hull, high-angle porpoising on hydro-ski seaplanes, if it occurs at all, will generally take place at such high trim angles that the associated limitations on stable planing operations

are of little or no practical importance. In the present state of the art, there exists no analytical method (or the required input data) for the prediction of the occurrence of high-angle porpoising. This is true for both conventional and hydro-ski seaplane types. Furthermore, in the case of the hydro-ski seaplane, tank model-testing and full-scale flight testing have been too meager for the accumulation of test data adequate for the formulation of empirical relationships for such prediction.

The situation relative to low-angle porpoising is quite different. In low-angle porpoising, the coupled heaving and pitching motions involve only wetting of the hull forebody (alternately, hydro-ski) and, thus from the hydrodynamic standpoint, only the hydromechanics associated with unsteady planing conditions of a single "body". In one sense, the unsteady hydrodynamic problem is more complex than that treated in Section 5, above, because it involves two degrees of freedom. On the other hand, another basic feature makes for tremendous simplification: it is known from past experience with conventional hull seaplanes that very accurate predictions for the occurrence of low angle porpoising can be made with the use of linearized dynamics.

For the most part, past practice has utilized special tank testing techniques to establish the "lower porpoising limits" for particular seaplane configurations. Even for conventional seaplanes, there has never been, to our knowledge, a specific program, either experimental or analytical, investigating systematic variations in those parameters which are known to affect low angle porpoising.

Largely because of the ignorance surrounding this subject, it has assumed an unwanted significance in the design of hydro-ski installations. In the worst cases, ski installations satisfying all of the known "rule-of-thumb" design principles have been tested and found to yield unacceptable and still unexplained low angle porpoising limits. Further, a major portion of past experience has been with low beam-loading skis. The present trend, correctly, is towards high beam-loading skis and it is more than likely that this fundamental parametric change has a significant effect on the porpoising characteristics. This role may be either direct or, possibly, indirect as, for example, by requiring more stringent limitations on ski location, etc.

While low angle porpoising characteristics of specific hydro-ski seaplanes can always be determined by suitable model tank tests, it is obviously most desirable to have a method of predicting such characteristics in the earliest stages of a specific seaplane design. It is perhaps even more desirable to know which aerodynamic and hydrodynamic parameters are significant and what their specific effects are on porpoising behavior. This problem has been treated in this project by:

A. Establishing a computer program which, for a given "skeleton hydro-ski seaplane" configuration, simultaneously defines the entire range of trim-speed combinations for vertical equilibrium in the planing condition and also completely defines all stability boundaries within this region;

B. Comparing the theoretical stability boundaries computed in this manner with available towing tank measurements to demonstrate the accuracy of the theoretical method;

C. Using the computer program to perform certain basic parametric studies, in particular, of the ski design and installation parameters.

It will be seen that, in connection with Item B, the agreement between the theoretical and the experimental results is very satisfactory, thus clearly proving the validity of the theoretical approach.

6.2 BASIC EQUATIONS

6.2.1 General Dynamic Equations

The seaplane is considered to have freedom in heave and pitch, so that the general equations of its free motions are:

$$(W/g)\ddot{h} = L_H + L_A - W \qquad (6-1)$$

$$I\ddot{\tau} = M_H + M_A \qquad (6-2)$$

where W = airplane weight

I = airplane pitching moment of inertia relative to c.g.

h = heave displacement, positive upward

τ = trim angle of hull keel relative to horizon, positive nose up

L_H, L_A = hydro and aero lift forces

M_H, M_A = hydro and aero pitching moments

6.2.2 Planing Equilibrium

For equilibrium, i.e., steady state motion with constant forward speed, these equations reduce to:

$$L_{H_{eq}} + L_{A_{eq}} = W \qquad (6-3)$$

$$M_{H_{eq}} + M_{A_{eq}} = 0 \qquad (6-4)$$

It is assumed that eq. (6-4) can always be satisfied by application of suitable elevator deflection, i.e., unlimited elevator control is assumed to be available for this purpose. Further, the elevator deflections are assumed to have a negligible direct effect on the aerodynamic lift force.

Now consider a "skeleton hydro-ski seaplane" in an equilibrium planing condition. By this is meant a configuration in which the ski is the only planing element, i.e., there is no wetting of the hull. Thus, by the same token, the only hydrodynamic forces and moments are those arising from the wetting of the planing ski. It is now obvious that, in conjunction with the assumption concerning lift forces associated with the elevator deflection, if eq. (6-3) is considered as a relation between trim and forward speed, there is an entire range of trims for equilibrium at a given forward speed, within certain limits for a given "skeleton" configuration, the specific trim values being governed by the elevator deflections.

The nature of these limits can be readily understood by considering the "trim-speed" (τ vs. V) plane, as indicated by the sketch, Figure 6-1. The absolute trim limit, independent of all other restrictions, is taken as the keel trim angle corresponding to the stall angle of the aircraft. At this point, it should be mentioned that the principal practical aerodynamic configuration of interest in this analysis is that with power-on and with flaps, slats, etc., set for take-off.

The other two limits in the trim-speed plane consist of two curves, one corresponding to the "ski unporting" condition and the other to the "get-away" condition. The "unporting" curve represents those equilibrium trim-speed combinations corresponding to wetting of the entire ski bottom area, stated here as a condition on ski wetted length:

Ski Wetted Length = Total Actual Ski Length

or, simply:
$$l_W = l_{act}$$

Similarly, the get-away curve represents the limiting trim-speed combinations for which the wetted ski-length just becomes zero:

$$l_W = 0$$

Finally, there exists a practical upper limit to the get-away speed which, in present applications, is taken as the get-away speed corresponding to zero hull keel trim angle: $\tau = 0$. Thus, the entire planing region can be defined symbolically as:

$$0 \leqslant \tau \leqslant \tau_{st} \; ; \; 0 < l < l_{act}$$

Finally, it is obvious that the unporting and get-away boundaries are actually two particular curves belonging to the family of curves defined by constant values of wetted length:
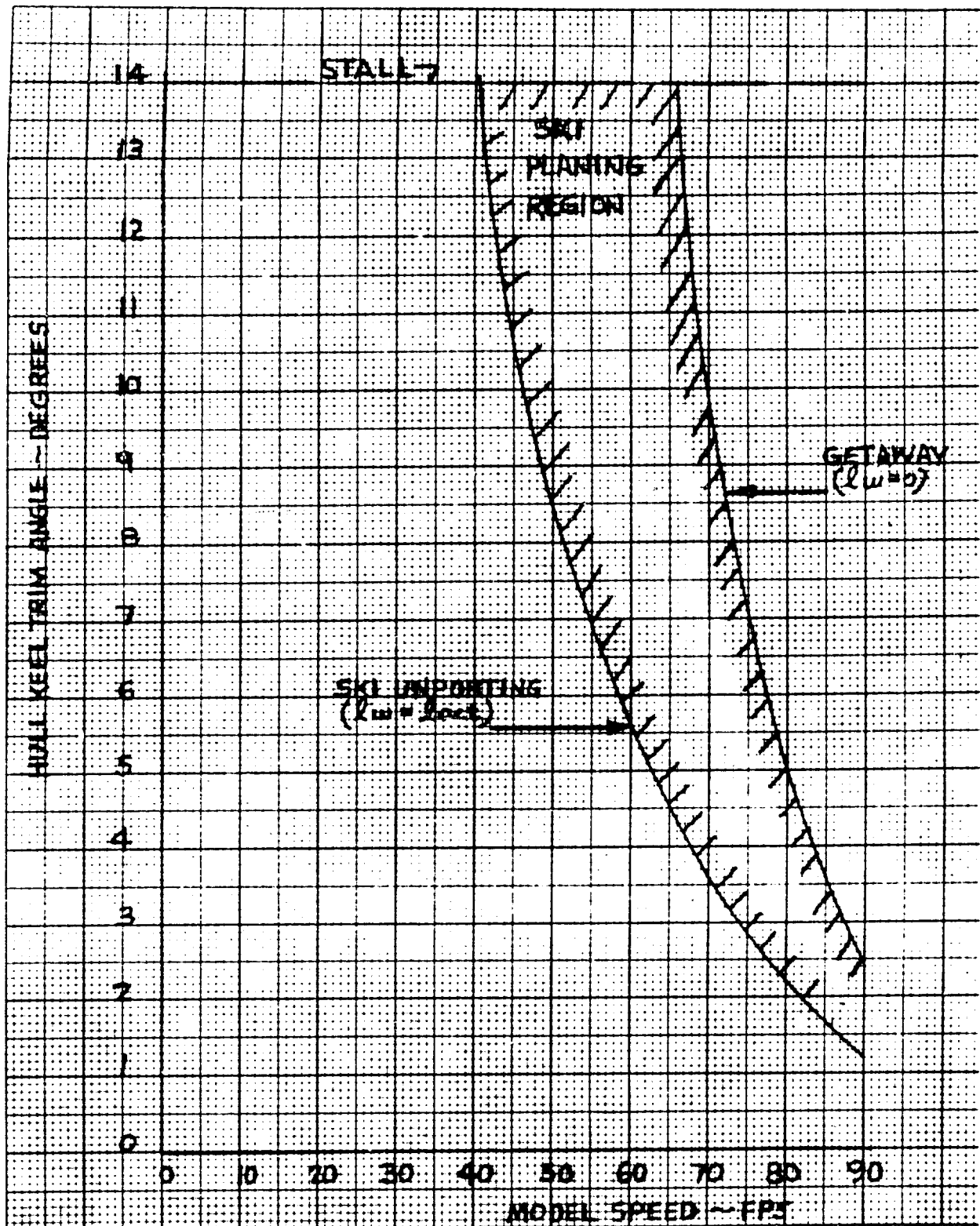
Figure 6-1. Sketch Illustrating Hydro-Ski Planing Region in Trim-Speed Plane

$$l_W = \text{const.}$$

The idealized construction just described must now be distinguished somewhat from actual aircraft behavior. It will be understood that the actual planing region for a specific seaplane may sometimes be somewhat more limited than that considered here. The two related principal reasons contributing to this difference are:

1) The limitations on elevator control, depending in turn on such items as c.g. location, ski location, power effects, etc., which may prevent achievement of certain trim-speed combinations;

2) As is typically the case with skis of large area, elevator control may be inadequate to permit ski unporting to occur at lower speeds without wetting of the hull afterbody (two-point unporting) and/or the hull forebody through spray thrown up by the ski. In such cases, the basic assumption of the "skeleton hydro-ski seaplane" is only applicable to a limited portion of the "ski planing" region described above.

While purely incidental in the present context, these remarks also serve to emphasize the most fundamental principle of hydro-ski system design, i.e., that such design must be completely integrated with the aircraft's aerodynamic characteristics.

The detailed equation defining the ski unporting curve (Figure 6-1) is not presented here but can be derived by utilizing Shuford's equation for the steady-state lift coefficient for the planing ski (see Section 3.2), together with the standard aerodynamic equation:

$$L_A = C_{LA} (\tau) \, q_A \, S_w,$$

in eq. (6-3). Similarly, the getaway curve is defined by:

$$C_{LA} (\tau) \, q_A \, S_w = W$$

6.2.3 Linearized Equations of Motion

Considering now a specific planing equilibrium condition, i.e., a specific combination of trim and speed inside of the planing region, let (h) and (τ) represent very small departures from their equilibrium values. Then, under stick-fixed conditions, i.e., elevators fixed at their trim settings for the equilibrium condition, the hydro and aero forces and moments will be those corresponding to small values of (h), (τ), and by the same token ($\dot{h}$) and ($\dot{\tau}$). Thus, their values can be approximated by using the first terms of the pertinent Taylor expansions, such as:

$$L_H \cong L_{H_{eq}} + (L_{Hh})(h) + (L_{H\tau})(\tau) + (L_{H\dot{h}})(\dot{h}) + (L_{H\dot{\tau}})(\dot{\tau}) \qquad (6-5)$$

with similar equations for L_A, M_H, and M_A.

In these Taylor expansions, the quantities in parentheses multiplying the variables are referred to as "stability derivatives." They actually represent true partial derivatives, i.e., for example:

$$L_{Hh} = \left(\frac{\partial L_H}{\partial h} \right)_{\tau, \dot{h}, \dot{\tau}}$$

Further, each such derivative generally depends on all four variables, thus:

$$L_{Hh} = f_1 (h, \tau, \dot{h}, \dot{\tau})$$

The essence of the present linearized theory is that, for very small departures from equilibrium, each stability derivative can be approximated by assigning it the constant value associated with the equilibrium condition, thus:

$$\left(\frac{\partial L_H}{\partial h} \right) = f_1 (h = h_{eq}, \tau = \tau_{eq}, \dot{h} = 0, \dot{\tau} = 0)$$

Now, if eqs. (6-5) are substituted into eqs. (6-1) and (6-2) and, further, if eqs. (6-3) and (6-4) are subtracted out, the linearized equations can be written in the abbreviated form:

$$
\left.
\begin{aligned}
a_1 (\ddot{h}) + a_2 (\dot{h}) + a_3 (h) + b_2 (\dot{\tau}) + b_3 (\tau) &= 0 \\
c_2 (\dot{h}) + c_3 (h) + d_1 (\ddot{\tau}) + d_2 (\dot{\tau}) + d_3 (\tau) &= 0
\end{aligned}
\right\} \quad (6\text{-}6)
$$

where:

$$
\left.
\begin{aligned}
a_1 &= W/g \\[6pt]
a_2 &= L_{A\dot{h}} + L_{H\dot{h}} \\[6pt]
a_3 &= L_{Ah} + L_{Hh} \\[6pt]
b_2 &= L_{A\dot{\tau}} + L_{H\dot{\tau}} \\[6pt]
b_3 &= L_{A\tau} + L_{H\tau} \\[6pt]
c_2 &= M_{A\dot{h}} + M_{H\dot{h}}
\end{aligned}
\right\} \quad (6\text{-}7)
$$

$$c_3 = M_{Ah} + M_{Hh}$$

$$d_1 = -I$$

$$d_2 = M_{A\dot{\tau}} + M_{H\dot{\tau}}$$

$$d_3 = M_{A\tau} + M_{H\tau}$$

$$\left.\begin{array}{c}\\\\\\\\\end{array}\right\} \quad (6\text{-}7)$$

Eqs. (6-6) represent the equations of the free transient motions of the seaplane following a slight disturbance from any particular equilibrium planing condition. If desired, they can be solved by selecting any arbitrary set of (small) initial values for the four quanti- ties: h, τ , $\dot{h}, \dot{\tau}$. What is of basic importance, however, is the <u>nature</u> of the free motions, which can be determined from the "natural modes".

The latter are obtained by substituting the "modal relations:"

$$h = h_0 e^{\lambda t}, \qquad \tau = \tau_0 e^{\lambda t} \qquad\qquad (6\text{-}8)$$

into eqs. (6-6) to obtain:

$$(a_1 \lambda^2 + a_2 \lambda + a_3) h_0 + (b_2 \lambda + b_3) \tau_0 = 0$$

$$(c_2 \lambda + c_3) h_0 + (d_1 \lambda^2 + d_2 \lambda + d_3) \tau_0 = 0$$

$$\left.\begin{array}{c}\\\\\end{array}\right\} (6\text{-}9)$$

Eqs. (6-9 can only be true for the particular values of λ defined by:

$$\begin{vmatrix} a_1 \lambda^2 + a_2 \lambda + a_3 & b_2 \lambda + b_3 \\ \\ c_2 \lambda + c_3 & d_1 \lambda^2 + d_2 \lambda + d_3 \end{vmatrix} = 0 \qquad (6\text{-}10)$$

Expanding this "characteristic" equation:

$$(a_1 \lambda^2 + a_2 \lambda + a_3)(d_1 \lambda^2 + d_2 \lambda + d_3) - (b_2 \lambda + b_3)(c_2 \lambda + c_3) = 0$$

or, $\quad A \lambda^4 + B \lambda^3 + C \lambda^2 + D \lambda + E = 0 \qquad\qquad (6\text{-}11)$

where:

$$A = a_1 d_1$$

$$B = a_1 d_2 + a_2 d_1$$

$$C = a_1 d_3 + a_2 d_2 + a_3 d_1 - b_2 c_2$$

$$D = a_2 d_3 + a_3 d_2 - b_2 c_3 - b_3 c_2$$

$$E = a_3 d_3 - b_3 c_3$$

(6-12)

Thus, the _nature_ of the free motion is determined by the roots of a fourth-order algebraic equation, (6-11), whose coefficients, defined by eqs. (6-12) and (6-7), are seen to be extremely complicated functions of the "stability derivatives" and the two inertia values, (W/g) and I.

Clearly, if desired, one could determine the nature of the free motions at any or all points of the aircraft's planing region. However, such labor is excessive as what is principally desired is the knowledge whether the free motions at a particular equilibrium point inside this region are stable or unstable. For this purpose, it is only necessary to subdivide the total planing region into "stable" and "unstable" sub-domains. The curves bounding these sub-domains are referred to as "stability boundaries" and are obtained from the following stability analysis.

6.2.4   Stability Analysis

If the leading coefficient, A, is positive, it is well-known that the necessary and sufficient conditions for the roots of an equation,

$$A \lambda^4 + B \lambda^3 + C \lambda^2 + D \lambda + E = 0$$

to represent stable motions, are:

$$B > 0, \ C > 0, \ D > 0, \ E > 0, \ R > 0, \qquad (6-13)$$

where R, known as Routh's Discriminant, is given by:

$$R = BCD - B^2 E - AD^2 \qquad (6-14)$$

(This statement constitutes Routh's Stability Theorem for which a concise proof is given on pp. 331-332 of Reference 6-2.)

Obviously, then, in general, there may exist a number of stability boundaries inside the planing region of a specific hydro-ski seaplane configuration which are defined, respectively, by the conditions:

$$B = 0, \quad C = 0, \quad D = 0, \quad E = 0, \quad R = 0 \qquad (6\text{-}15)$$

The two boundaries of most practical interest can be clearly defined, as follows:

a. The boundary, $E = 0$, separates a stable region ($E > 0$) in which one mode is a "subsidence" ($h = h_o e^{-at}$, $a > 0$) from an unstable region ($E < 0$) in which the corresponding mode is a "divergence" ($h = h_o e^{bt}$, $b > 0$);

b. The boundary, $R = 0$, separates a stable region ($R > 0$) in which one mode is a positively damped oscillation ($h = h_o e^{-at} \cos \omega_1 t$, $a > 0$) from an unstable region ($R < 0$) in which the corresponding mode is a negatively damped, i.e., divergent oscillation ($h = h_o e^{bt} \cos \omega_2 t$, $b > 0$). Referring back to Section 6.1, it will be seen that the "lower porpoising limit" is equivalent to the $R = 0$ boundary.

It is thus seen that determination of the stability boundaries in the trim-speed plane depends directly on the calculation of the hydro and aero stability derivatives.

6.3   STABILITY DERIVATIVES

Analytic expressions for the hydro and aero stability derivatives are derived in Appendix C of this report.

The hydrodynamic derivatives are for a hydro-ski* undergoing unsteady planing motions in calm water. They are derived by simple extensions of the "equivalent planing velocity" concept, introduced in Paragraph 5.2.1 of this report. This concept is used in conjunction with Shuford's expression for the planing lift coefficient, which has been extended to cover a type of ski planform not previously considered herein, namely, a basic rectangular planform with a pointed triangular tail area. This was found necessary for comparison of the theory with available test data.

Analytic expressions are also derived for the aerodynamic derivatives, using conventional approaches. The seaplane is assumed to be insensitive to ground effect, to have a conventional aerodynamic configuration and, further, no account is taken of power-on effects, either direct or indirect. It will be appreciated that these limitations are not fundamental, i.e., that the approaches utilized herein can be modified to account for such features as strong ground effects, unconventional configurations such as canard stabilizers, etc.

*These derivatives are also applicable to a seaplane hull in the chines-wet condition, provided that the wetted planform is of the type considered herein.

Regarding the aerodynamic derivatives, it is pointed out that the so-called "static" derivatives are best established from model test data obtained through either wind tunnel tests or the aerodynamic tests normally conducted on towing tank models. This is practically mandatory if it is desired to make stability calculations for power-on conditions as the accurate estimation of power-on aerodynamic characteristics is an exceptionally difficult task, particularly for propeller-equipped seaplanes. Similar considerations apply to ground effects.

Finally, it was found expedient to express all of the derivatives in dimensional form, rather than the non-dimensional form most often used in theoretical stability analyses. The conversion to non-dimensional form can, of course, be readily accomplished if so desired.

6.4   COMPUTER PROGRAM FOR PLANING STABILITY

Based on the foregoing considerations and analyses,   a computer program has been established for determination of the lower planing stability (porpoising) boundary. The fundamental nature of this program can be understood by reference to the following sketch:
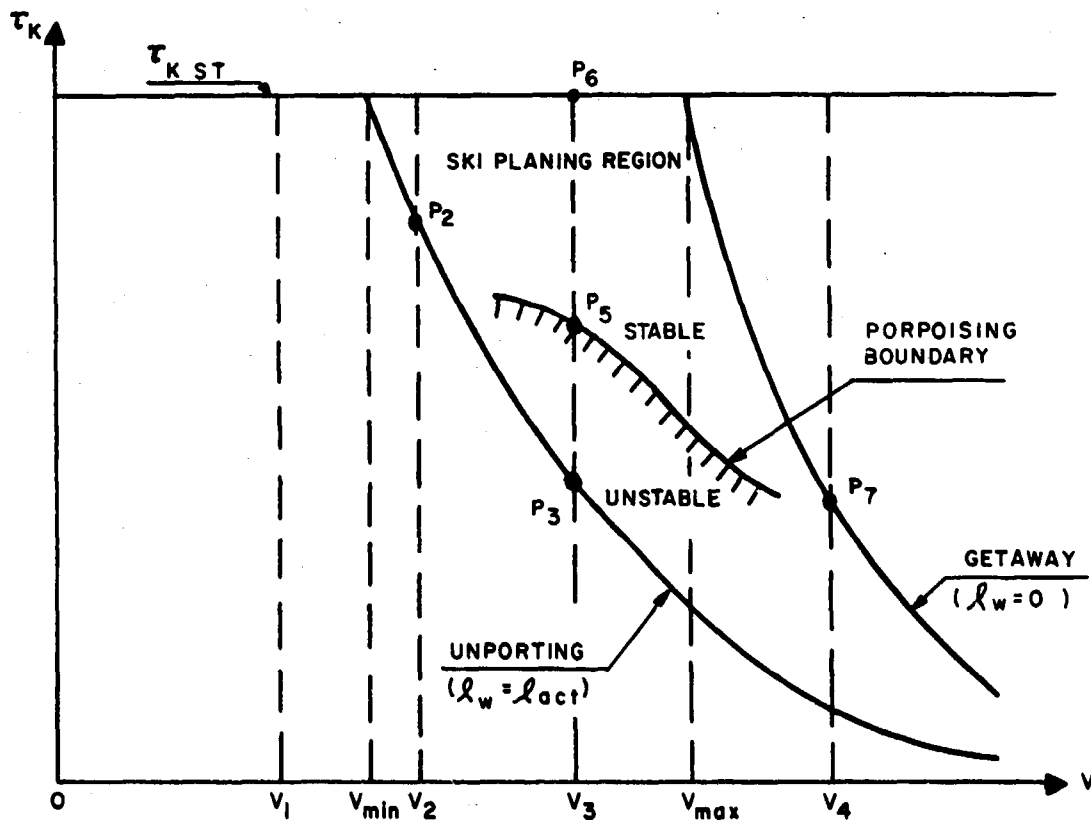
A. Numerical inputs consist of all aero and hydro characteristics of the specific hydro-ski seaplane necessary for the calculation of equilibrium values and stability derivatives, together with a series of preselected speeds.

B. At each speed, equilibrium conditions are calculated at various trim angles, using small trim angle increments and starting just above $\tau_K = 0°$ (zero hull keel trim). The first quantity calculated is the equilibrium wetted length. This value is compared with the actual (total) ski length. If $l_{W\,calc} < l_{act}$ this means that the ski is still submerged and the calculation proceeds to the next higher trim value, for which the equilibrium calculation is repeated. Two possibilities thus occur:

a) If the selected speed (such as V_1 in sketch) is less than V_{min}, the aircraft stall angle is reached before ski planing can occur. In this case, the calculations start all over again at the next higher (preselected) speed.

b) If the particular speed (such as V_2, V_3, or V_4) exceeds V_{min}, a trim will be reached at which the calculated wetted length is just slightly less than the actual ski length. This combination of speed and trim then represents a point (such as P_2, P_3, P_4) on the ski "unporting" curve. The computer then prints out the speed and trim values, together with the equilibrium wetted length. At this point, the computer also calculates the stability parameters, i.e., the coefficients, B, C, D, E of the stability equation and the corresponding value of R. In the usual cases, B, C, D, E, are all positive while R can be either positive or negative. If R is positive, then the point is inside the stable region, such as P_2 in the sketch. If R is negative, then the point is in the unstable region, such as P_3 in the sketch. The computer prints out these values (B, C, D, E, R) for each point encountered on the unporting curve.

c) After reaching a point on the unporting boundary, the trim angle is automatically increased and the equilibrium values and the stability parameters are calculated for the new trim. The computer then compares the signs of the stability parameters with those for the previous trim angle. If there is no change in any of these signs, the computer proceeds to the next higher trim angle. This process is repeated until such a sign change occurs. Only when this happens, the computer again prints out the speed, trim, ski wetted length, and the stability parameters. In the usual case, it is the sign of R that changes and the point at which this occurs represents a point on the "porpoising boundary", such as P_5 in the sketch.

d) In any case, the calculations are continued until the trim reaches either the stall angle (P_6 in sketch) or else a point on the "get-away" curve (P_7 in sketch). The "get-away" curve represents the condition at which the seaplane just becomes airborne, i.e., mathematically speaking, at which the ski wetted length just becomes zero. On

reaching points such as P_6 or P_7, the computer reports the corresponding fact in its print-out.

e) It is obvious that, by using sufficiently small increments both for speed and trim, the computer print-out will include all the information necessary for accurately plotting the ski unporting curve, the getaway curve (thus defining the boundaries of the entire ski planing region) and the stability boundaries (such as $R = 0$) inside of this region.

The computer program was written in Fortran IV language. Figure 6-2 is a flow diagram illustrating the program logic; Table 6-1 shows the code used; and Table 6-2 is the complete program statement.

It must finally be explained that the treatment of the aerodynamic characteristics used in this program assumes a prior knowledge of the aircraft lift and moment curve. Some generality has been introduced by assuming both of these curves to be parabolic, rather than linear.

START

READ
G1, G2, G3, G4,
G5, G6, G7, G8,
G9, G10,
AMASS,
AINER

READ
G11, G12, G13, G14,
G15, G16, G17,
G18, G19

READ
N, ELACT, STALL,
DTAU

STATEMENT 3

COMPUTE
TAUI, QW, QA

CALL AERO

COMPUTE
A4, A5, ELBB, A2

IF(A2)

WRITE
VV, TAU

GO TO 100

COMPUTE
A3, A1, ELWE₁

IF(ELBB-ELWE₁)

ELWET₁ = G1·ELWE₁

COMPUTE
ELWET₂

IF(ELWET-ELACT)

WRITE
VV, TAU

1

TAU = TAU + DTAU

2

CALL ROUTH

IF(ELWET-G10)

CASE I
STABILITY
DERIVATIVES

CASE II
STABILITY
DERIVATIVES

AERO DERIVATIVES
FOR CASE I
OR CASE II

COMPUTE
A1, A2, A3,
B2, B3, C2, C3,
D1, D2, D3

WRITE
A, B, C, D, E, R

3

WRITE
TAU
DD
A.

Figure 6-2.   Flow Diagram for

Figure 6-2   Flow Diagram for Planing Stability Computer Program

TABLE 6-1. FORTRAN IV CODE FOR PLANING STABILITY COMPUTER PROGRAM

ITEM	MATHEMATICAL NOTATION	FORTRAN NOTATION
maximum ski beam	b_{max}	G1
perpendicular distance from c.g. of aircraft to keel line of ski	p	G2
distance along ski from point at which p is measured to ski trailing edge (+ if aft)	q	G3
incidence angle of ski with respect to hull keel line	i_s	G4
ski deadrise angle	β	G5
wing area	S_w	G6
horizontal tail area	S_t	G7
distance from aircraft c.g. to quarter chord of tail	l_t	G8
mean aerodynamic chord	$\bar{c}$	G9
length of tapered portion of ski	l_b	G10
wing incidence with respect to hull keel line	i_w	G11
constants in C_L, $C_{L\alpha}$, C_M, $C_{M\alpha}$ aerodynamic equations		G12, G13, G14, G15, G16, G17, G19
downwash parameter	$d\epsilon/di_w$	G18

TABLE 6-1 (cont'd)

ITEM	MATHEMATICAL NOTATION	FORTRAN NOTATION
slope of aircraft lift curve	$C_{L\alpha}$	S2
slope of horizontal tail lift curve (based on tail area)	$C_{L\alpha t}$	S3
slope of aircraft moment curve	$C_{M\alpha}$	S4
number of velocities examined for each study		N
aircraft mass	W/g	AMASS
aircraft pitching moment of inertia, relative to c.g.	I	AINER
actual ski length	l_{act}	ELACT
stall angle of aircraft	(not used)	STALL
incremental change in aircraft trim	$\Delta\tau$	DTAU
aircraft (keel) trim	τ	TAU
index		J, K, L
aircraft speed	V_H	VV=V(J)
dynamic pressure (hydro)	q_w	QW
dynamic pressure (aero)	q_A	QA
non-dimensional length of tapered portion of ski	Λ_b	ELBB
non-dimensional wetted length of ski	Λ	ELWE

TABLE 6-1 (cont'd)

ITEM	MATHEMATICAL NOTATION	FORTRAN NOTATION
wetted length of ski	l_w	ELWET
coefficients of stability equation at $\tau = \tau$	A, B, C, D, E	A, B, C, D, E
coefficients of stability equation at $\tau = \tau + \Delta\tau$		AA, BB, CC, DD, EE
Routh Discriminant at $\tau = \tau$	R	R
Routh Discriminant at $\tau = \tau + \Delta\tau$		RR
derivatives of hydro lift force with respect to trim angle, pitching velocity, heave, and heave velocity	$L_{H\tau}, L_{H\dot{\tau}}, L_{Hh}, L_{H\dot{h}}$	HF(1), HF(2), HF(3), HF(4)
terms used in equations for Λ (See Appendix C)	b, c, N	A3, A1, A2
derivatives of hydro pitching moment with respect to trim angle, pitching velocity, heave and heave velocity	$M_{H\tau}, M_{H\dot{\tau}}, M_{Hh}, M_{H\dot{h}}$	HM(1), HM(2), HM(3), HM(4)
derivatives of aero lift force with respect to trim angle, pitching velocity, heave, and heave velocity	$L_{A\tau}, L_{A\dot{\tau}}, L_{Ah}, L_{A\dot{h}}$	AF(1), AF(2), AF(3), AF(4)
derivatives of aero pitching moment with respect to trim angles pitching velocity, heave, and heave velocity	$M_{A\tau}, M_{A\dot{\tau}}, M_{Ah}, M_{A\dot{h}}$	AM(1), AM(2), AM(3), AM(4)

TABLE 6-1 (cont'd)

ITEM	MATHEMATICAL NOTATION	FORTRAN NOTATION
heave, instantaneous height of c.g. above W. L.	h	H
coefficient of hydro lift	C_{LH}	CLH
wetted ski area	S_W	SW
instantaneous lift force on heaving and pitching ski	L_H	PLH
hydro moment arm	f	F
instantaneous moment acting on heaving and pitching ski	M_H	PMH
variation of ski wetted area with heave	S_{wh}	SWH
variation of hydro moment arm with heave	f_h	FH
variation of hydro lift coefficient with trim	$C_{LH\tau}$	CLHT
variation of ski wetted area with trim	$S_{W\tau}$	SWT
variation of hydro moment arm with trim	f_τ	FT

TABLE 6-2. FORTRAN IV STATEMENT OF PLANING STABILITY COMPUTER PROGRAM

```
// FOR
*LIST SOURCE PROGRAM
*NAME STABL
*IOCS(CARD, 1132 PRINTER)
      DIMENSION V(50)
      COMMON G1,G2,G3,G4,G5,G6,G7,G8,G9,G10,AMASS,AINER,
     1QW,QA,S2,S3,S4,G18,ELWE,ELWET,A4,A5,G19
      READ(2,10)G1,G2,G3,G4,G5,G6,G7,G8,G9,G10,AMASS,AINER
      READ(2,10)G11,G12,G13,G14,G15,G16,G17,G18,G19
10    FORMAT(8F10.5/4F10.5)
      WRITE(3,10)G1,G2,G3,G4,G5,G6,G7,G8,G9,G10,AMASS,AINER
      WRITE(3,10)G11,G12,G13,G14,G15,G16,G17,G18,G19
      READ(2,11) N,ELACT,STALL,DTAU
11    FORMAT(I2,3F10.5)
      WRITE(3,11) N,ELACT,STALL,DTAU
      READ(2,12)(V(J),J=1,N)
12    FORMAT(F10.5)
      DO 100  J=1,N
      TAU=.002
      K=1
      L=1
      VV=V(J)
3     TAUI=TAU+G4
      QW=.9938*VV**2
      QA=.00119*VV**2
      CALL AERO(TAU,CLEQ,S2,S3,S4,G11,G12,G13,G14,G15,G16,G17,G18,G19)
C  CALCULATION OF WETTED LENGTH AT EQUI
      A4=1.5708*TAUI*COS(TAUI)**2*(1.-SIN(G5))
      A5=1.333*SIN(TAUI)**2*COS(TAUI)**3*COS(G5)
C  A4 AND A5 ARE USED IN ROUTH
      ELBB=G10/G1
      A2=32.2*AMASS/(QW*G1**2)-.001196*G6*CLEQ/G1**2
C NOW COMES A TEST ON THE RHS OF WETTED LENGTH EQUATION
      IF(A2)37,37,28
37    WRITE(3,69) VV,TAUD
69    FORMAT(/'AT VELOCITY',F10.5,'FT/SEC THE GETAWAY TRIM IS,'F10.5,
     1'DEGREES'/)
28    CONTINUE
      A3=(A4+A5-.5*ELBB*A5-A2)/A5
      A1=(.5*ELBB*(A4+A5)+A2)/A5
C THIS EQUATION IS FOR THE CALC. OF WETTED LEN.. IN RECTANGULAR REGION
      ELWE= (-A3+ABS(A3)*SQRT(1.+(4.*A1/A3**2)))/2.
C  TESTING FOR FORMULA VALIDITY
      IF(ELBB-ELWE) 74,74,73
74    ELWET=ELWE*G1
      GO TO 75
C FORMULA FOR TRIANGULAR  REGION OF SKI
73    ELWE=SQRT(A2*2*(ELBB**2+1.)/(A4+(ELBB+1.)*A5))
      ELWET=G1*ELWE
75    IF(ELWET-ELAC)2,2,1
1     TAU=TAU+DTAU
      GO TO 3
2     GO TO (4,5),K
4     TAUD=TAU*57.3
      WRITE(3,200) VV,TAUD
200   FORMAT(/' AT THE VELOCITY',F10.5,'FT/SEC THE LOWER LIMIT PLANING
     1TRIM IS,'F10.5,'DEGREES'/)
      WRITE(3,205) ELWET
205   FORMAT(/' ELWET IS',F10.5/)
      K=2
```

TABLE 6-2 (cont'd)

```
C CALCULATION OF SKI STABILTY
5       CALL ROUTH(VV,TAU1,A,B,C,D,E,R,CLEQ)
        GO TO (6,7),L
6       WRITE(3,201) A,B,C,D,E,R
201     FORMAT(' AT THE LOWER LIMIT PLANING TRIM THE COEFICIENTS OF THE
       1STABILITY EQUATION ARE(ROUTH DISC IS LAST)'/6E15.4)
        AA=A
        BB=B
        CC=C
        DD=D
        EE=E
        RR=R
        L=2
        TAU=TAU+DTAU
        GO TO 3
7       TAUDD=(TAU-DTAU)*57.3
        TAUD=TAU*57.3
        IF(B*BB)23,23,8
8       IF(C*CC)23,23,9
9       IF(D*DD)23,23,20
20      IF(E*EE)23,23,21
21      IF(R*RR)23,23,22
23      WRITE(3,202) TAUDD,AA,BB,CC,DD,EE,RR,TAUD,A,B,C,D,E,R
202     FORMAT(/' AT A TRIM OF',F10.5,'THE COEF ARE(R IS LAST)'/6E15.4/'
       1 AT A TRIM OF',F10.5,' THE COEF ARE(R IS LAST)'/6E15.4/)
        WRITE(3,206) ELWET
206     FORMAT(/' ELWET IS',F10.5/)
22      AA=A
        BB=B
        CC=C
        DD=D
        EE=E
        RR=R
        IF(ELWET)27,27,24
27      TAUD=TAU*57.3
        WRITE(3,203) VV,TAUD
203     FORMAT(' AT THE VELOCITY',F10.5,'FT/SEC THE UPPER LIMIT PLANING
       1 TRIM IS',F10.5,' DEGREES'/)
        WRITE(3,207) ELWET
207     FORMAT(/' ELWET IS',F10.5/)
        GO TO 100
24      IF(TAU-STALL)25,26,26
25      TAU=TAU+DTAU
        GO TO 3
26      TAUD=TAU*57.3
        WRITE(3,204) VV,TAUD
204     FORMAT(' AT THE VELOCITY',F10.5,'FT/SEC THE PLANE STALLS AT
       1',F10.5,' DEGREES'/)
        WRITE(3,250) TAUDD,AA,BB,CC,DD,EE,RR,TAUD,A,B,C,D,E,R
250     FORMAT(/' AT A TRIM PRIOR TO STALL OF',F10.5,'THE COEF ARE
       1(R IS LAST)'/6E15.4/' AT THE STALL TRIM OF',F10.5,'
       2THE COEF ARE (R IS LAST)'/6E15.4/)
        WRITE(3,208) ELWET
208     FORMAT(/' ELWET IS',F10.5/)
100     CONTINUE
        CALL EXIT
        END

FEATURES SUPPORTED
    IOCS
```

TABLE 6-2 (cont'd)

```
// FOR
*LIST SOURCE PROGRAM
      SUBROUTINE ROUTH(VV,TAUI,A,B,C,D,E,R,CLEO)
      DIMENSION  HF(4),HM(4),AF(4),AM(4)
      COMMON  G1,G2,G3,G4,G5,G6,G7,G8,G9,G10,AMASS,AINER,
     10W,QA,S2,S3,S4,G18,ELWE,ELWET,A4,A5,G19
      IF(ELWET-G10)500,500,600
500   H=SIN(TAUI)*(G3+G2*COS(TAUI)/SIN(TAUI)-ELWET)
      CLH=(A4/(G10+1.))+A5
      SW=(G1**2/(2.*G10))*ELWE**2
      PLH=CLH*SW*QW
      F=(.75*(G2*COS(TAUI)/SIN(TAUI)-H/SIN(TAUI))-.25*G3)/COS(TAUI)
      PMH=F*PLH
      SWH=-(G1/(TAUI))*(ELWE/G10)
      FH=-.75/TAUI
      CLHT=1.5708*(1.-SIN(G5))*(1.-1.5*TAUI**2)/(G10+1.)+2.667*COS(G5)*(
     1TAUI-3.333*TAUI**3)
      SWT=-G1*(G2-H)/TAUI**2*ELWE/G10
      FT=-.75*(G2-H)/TAUI**2
      HF(3)=PLH*(SWH/SW)
      HM(3)=PMH*(SWH/SW+FH/F)
      HF(1)=PLH*(CLHT/CLH+SWT/SW)
      HM(1)=PMH*(CLHT/CLH+SWT/SW+FT/F)
      Z=VV*TAUI
      HF(4)=-2.*PLH/Z
      HM(4)=-2.*PMH/Z
      ZZ=VV*TAUI**2
      HF(2)=-2.*PLH*(G2-H)/ZZ
      HM(2)=-2.*PLH*(G2-H)/ZZ
      GO TO 700
600   H=SIN(TAUI)*(G3+G2*COS(TAUI)/SIN(TAUI)-ELWET)
      CLH=(A4/(ELWE+1.))+A5
      SW=G1**2*(ELWE-.5*G10)
      PLH=CLH*SW*QW
      F=(.75*(G2*COS(TAUI)/SIN(TAUI)-H/SIN(TAUI))-.25*G3)/COS(TAUI)
      PMH=F*PLH
      CLHH=A4/(G1*(ELWE+1.)**2*TAUI)
      SWH=-G1/TAUI
      FH=-.75/TAUI
      CLHT=1.5708*(1.-SIN(G5))*(G2-H)*(1.-.5*TAUI**2)/((ELWE+1.)**2*G1
     1*TAUI)+1.5708*(1.-SIN(G5))*(1.-1.5*TAUI**2)/(ELWE+1.)+2.6667*COS(G
     15)*(TAUI-3.3333*TAUI**3)
      SWT=-G1*(G2-H)/TAUI**2
      FT=-.75*(G2-H)/TAUI**2
      HF(3)=PLH*(CLHH/CLH+SWH/SW)
      HM(3)=PMH*(CLHH/CLH+SWH/SW+FH/F)
      HF(1)=PLH*(CLHT/CLH+SWT/SW)
      HM(1)=PMH*(CLHT/CLH+SWT/SW+FT/F)
      Z=VV*TAUI
      HF(4)=-2.*PLH/Z
      HM(4)=-2.*PMH/Z
      ZZ=VV*TAUI**2
      HF(2)=-2.*PLH*(G2-H)/ZZ
      HM(2)=-2.*PMH*(G2-H)/ZZ
700   AF(1)=S2*QA*G6
      AM(1)=S4*QA*G6*G9
      AF(2)=(1.+G18)*QA*S3*G7*G8/VV
      AM(2)=-(1.1+G18)*QA*S3*G7*G8**2/VV
      AF(3)=0.0
      AM(3)=0.0
      AF(4)=-AF(1)/VV
```

TABLE 6-2 (cont'd)

```
AV(4)=-AM(1)/VV
A1=-AMASS
A2=HF(4)+AF(4)
A3=HF(3)+AF(3)
B2=HF(2)+AF(2)
B3=HF(1)+AF(1)
C2=HM(4)+AV(4)
C3=HV(3)+AV(3)
D1=-AINER
D2=HM(2)+AV(2)
D3=HM(1)+AV(1)
A=A1*D1
B=A2*D1+A1*D2
C=A1*D3+A2*D2+A3*D1-B2*C2
D=A2*D3+A3*D2-B2*C3-B3*C2
F=A3*D3-B3*C3
R=-A*D**2+B*C*D-F*B**2
RETURN
END

CORE REQUIREMENTS FOR ROUTH
  COMMON     46  VARIABLES     100  PROGRAM   1214

END OF COMPILATION
```

TABLE 6-2 (cont'd)

```
// FOR
*LIST SOURCE PROGRAM
      SUBROUTINE AERO(TAU,CLEQ,S2,S3,S4,G11,G12,G13,G14,G15,G16,G17,G18,
     1G19)
      A=TAU+G11
      CLEQ=+G12*A**2+G13*A+G14
      S2=+G15*A+G13
      S4=G16*A+G17
      S3=G19
      RETURN
      END

CORE REQUIREMENTS FOR AERO
 COMMON        0  VARIABLES       4   PROGRAM        78

END OF COMPILATION
```

6.5 CORRELATION OF TEST DATA

Reference 6-3 presents the results of towing tank tests conducted on a 1/19-scale unpowered model of the Martin Model 329-C-2 Mach-2 patrol seaplane design. These tests, which covered separate evaluations of three different hydro-ski installations designed for this seaplane, included measurements of the lower limit porpoising boundaries. Two of these experimental boundaries will now be compared with the corresponding theoretical boundaries obtained from the computer program just described.

Table 6-3 lists the aerodynamic and related inputs for the computer program. It may be noted that the geometric values are those for the model while the aerodynamic values are those obtained from combined analyses and wind-tunnel tests of an earlier version of this seaplane design (Martin Model 329C-1). The resulting inaccuracies are believed to be negligible. Similarly, Table 6-4 lists the hydrodynamic inputs for the two hydro-ski installations investigated. * Both of those skis had the type of planform considered in Appendix C, i.e., essentially rectangular skis with triangular trailing edges. Further, both skis had leading edges curved in plan view. For the calculation of the ski unporting curves, the curved leading edges were replaced by straight ones located at the area centroids of the curved areas. This is reflected in the total ski length values listed in Table 6-4 which are slightly smaller than the geometric lengths.

Using the values listed in Tables 6-3 and 6-4 as inputs, the computer program just described was used to calculate the ski planing region boundaries and the lower limit (porpoising) boundary for each of the two hydro-ski seaplane configurations. The comparisons of the calculated and experimental porpoising boundaries are shown separately in Figures 6-3 and 6-4. In addition to the ski unporting and getaway curves which are furnished by the computer, these graphs show an additional intermediate trim vs. speed curve corresponding to the waterline location at the intersection of the rectangular and triangular portions of each ski. This particular waterline curve is of interest in interpreting the nature of the porpoising boundary and, as will be seen below, plays a fundamental role in determining the dynamic stability characteristics of certain ski configurations.

The general nature of the relation between the experimental and theoretical boundaries is very much the same for the two skis and is best described by the phrase: "semi-quantitative agreement." That is, the theoretical values are numerically close to the experimental ones but do not duplicate the details of the experimental curves, particularly the curvature reverses. Further, in the case of the Edo small ski (Figure 6-3), the

---

* The third ski installation ("Convair configuration") employs a hinged ski incorporating an oleo shock strut. Thus, the planing stability analysis for this type of configuration would necessarily involve a third degree of freedom (ski incidence). While the parameters for such an analysis can be readily determined from the information in this report, the analysis itself is relatively complex and was considered to be beyond the scope of this project.

agreement between the basic slopes is not too good but is better for the Martin small ski (Figure 6-4). However, generally speaking, the numerical agreement is about as close as that obtained in other analyses of seaplane hull porpoising. (See Reference 6-5, for example).

TABLE 6-3. AERODYNAMIC CHARACTERISTICS OF THE MARTIN 329C-2 SEAPLANE

(All values are for model scale: $\lambda = 1/19$)

Wing Area, S_w, sq. ft.	4.99 *
Wing M.A.C., $\bar{c}$, ft.	1.40 *
Wing Incidence (to Hull Keel, WLO), i_w, deg.	3° *
Horizontal Tail Area, S_t, sq. ft.	.868 *
Horizontal Tail Moment Arm, l_t, ft.	3.41 *
Gross Weight, pounds	39.4 *
Longitudinal Moment of Inertia, slug ft.^{2}	2.61 **

Aircraft Lift Curve: $C_{L_A} = -8.22 \, \alpha_w^2 + 6.71 \, \alpha_w$

$\qquad + .260$ ***

Aircraft Moment Curve: $C_{M_A} = 6.05 \, \alpha_w^2 - 1.76 \, \alpha_w - .0774$ ***

$d\epsilon/d\alpha_w$ .24 ****

* From Figure 5, p. 22, Reference C-4
** From p. 25, Reference C-3
*** Approximated from Figure 16, p.50, Reference C-4, for take-off condition (L.E. flaps @ 8°, T.E. flaps at 40°, in ground effect, $i_T = 0$), c.g. corrected to 32% MAC (tank model location)
**** From Figure 15, p. 48, Reference C-4, (α_w in radians)

TABLE 6-4. HYDRO-SKI INSTALLATIONS TESTED ON THE MARTIN 329C-2 SEAPLANE

(All values are for model scale: $\lambda = 1/19$)

SKI INSTALLATION:	MARTIN (Small Ski)	EDO (Small Ski)
Maximum Ski Beam b_{max}, ft.	.158	.203
Total (effective) ski length, l_{act}, ft.	2.11	.898
Length of Triangular T.E., l_b, ft.	.125	.278
Ski Deadrise Angle, β, deg.	0°	20°
Ski Incidence to Hull Keel, i_{SK}, deg.	7.72°	0°
Height of C.G. above Ski Keel Line, p, ft.	.711	.703
Distance of Ski T.E. aft $\perp$ from C.G., q, ft.	-.044	-.131

Although, as just indicated, the discrepancies between the theoretical and experimental boundaries are not terribly great, it was considered important to ascertain their probable cause. Generally speaking, if it is assumed that the analytic expressions for the stability derivatives used herein are accurate, then the discrepancies must be attributable either to omissions in the theory or else, to effects present in the model tests which violate the basic theoretical assumptions.

In connection with the first of these possibilities, the present analysis does not include the direct effect of ground proximity on the slopes of the aircraft wing and tail lift curves and on the downwash angle at the tail, all of which produce non-zero values of the two derivatives, L_{Ah} and M_{Ah}. Accordingly, expressions for these contributions, based on lifting line theory, were developed and included in the computer program which was re-run for the Edo small ski configuration. It was found that all of these contributions had an utterly negligible effect on the theoretical porpoising boundary. Based on this negative result, these contributions were then removed from the program.

Another possible contribution to the discrepancy can lie in aerodynamic non-linearities associated with elevator and/or stabilizer deflections, which was the method used in the tank tests for trimming the model in the planing region. That is, it is possible that the actual value of $C_{MA\tau}$ varies somewhat with elevator or stabilizer deflection.
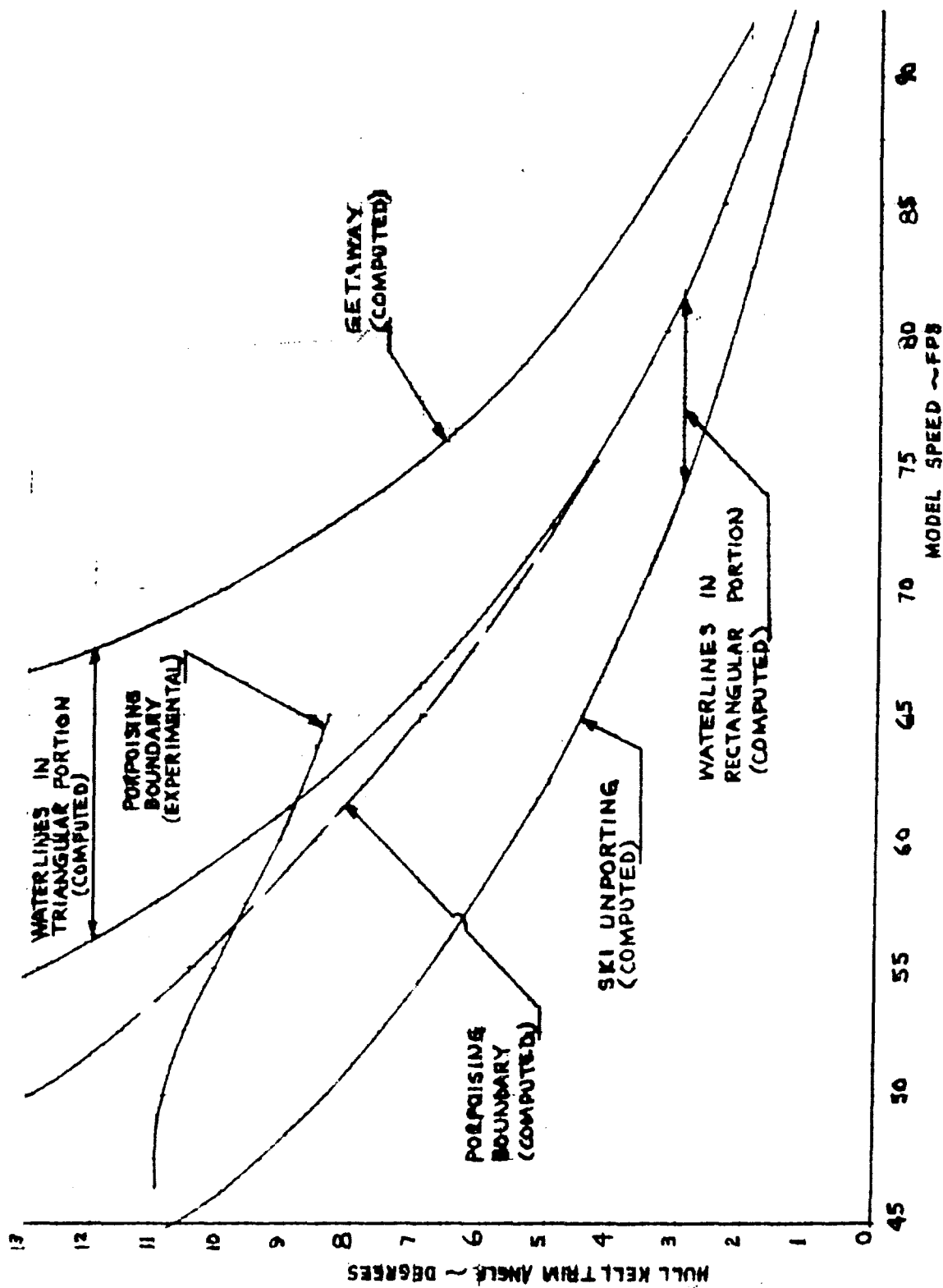
Figure 6-3. Comparison of Experimental and Theoretical Lower Limit Porpoising Boundary
Edo Small Ski on Martin 329C-2 Seaplane
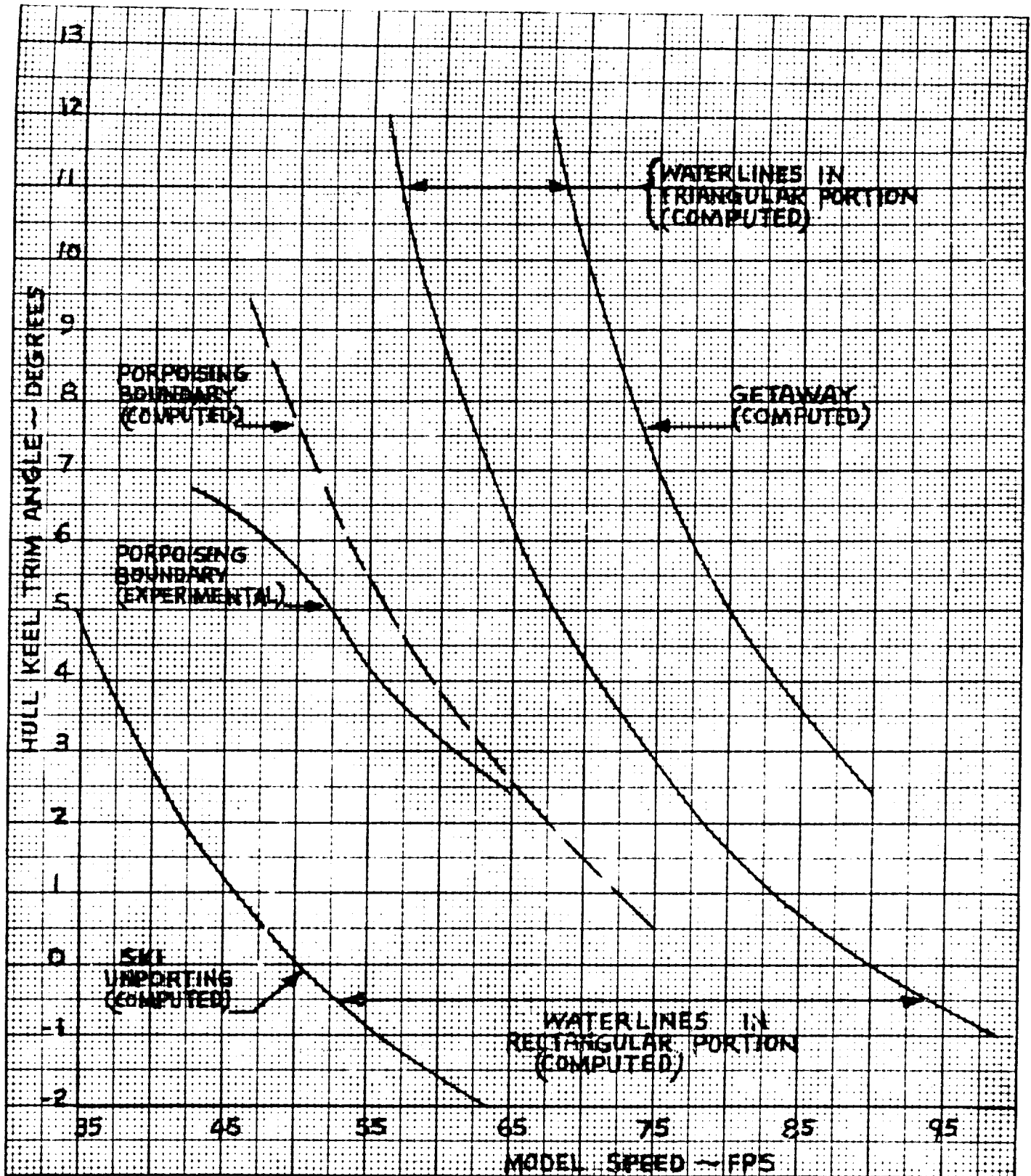
Figure 6-4. Comparison of Experimental and Theoretical Lower Limit Porpoising Boundary
Martin Small Ski on Martin 329C-2 Seaplane

Unfortunately, the basic aerodynamic data required for a direct check of this hypothesis were unavailable. However, a check of data for another seaplane (HU-16) indicated that this effect was probably too small to have any appreciable effect on the computed porpoising boundary.

It was finally concluded that the real major cause of the discrepancies between the computed and experimental porpoising boundaries must be the impingement of spray from the ski on various parts of the tank model. This phenomenon can be seen clearly in the photographs shown in Reference 6-3 and is specifically mentioned in the verbal description of the test results for both the Edo and Martin small skis. It is thus seen that this feature, present in the tank tests, violates the basic assumption utilized in the mathematical model that there is no wetting of the hull (or aerodynamic surfaces).

If this effect is accepted as the most plausible cause for the discrepancies, the actual agreement obtained must be considered very satisfactory. This means that any parametric studies based on the present computer program will be valid, both qualitatively and quantitatively, but only within the confines of the assumption that there is no wetting of the aircraft. From the standpoint of practical engineering design, it also follows that the results obtained with the present computer program will be useful in preliminary investigations of planing stability but cannot be accepted as necessarily realistic for any given configuration for which accurate values can only be obtained by tank tests. This restriction must be borne in mind in connection with the parametric studies presented in the remainder of this report section.

Using the computer program, a limited number of such parametric studies have been made and will now be described. While the effects on the planing stability of the aerodynamic parameters, particularly the static stability ($M_{A\tau}$) and pitch damping ($M_{A\dot{\tau}}$), are of great interest, the present investigations have been limited to variations of the principal hydrodynamic (ski) parameters, including ski beam, ski deadrise, ski incidence, and ski vertical and horizontal locations. It is obvious that variations in ski length obtained by changing the ski L.E. location while maintaining the same T.E. location, are of little inherent interest as their only effects are to alter the unporting boundary of the planing region and, accordingly, either extend or shorten the porpoising boundary curve.

For convenience in these studies, the aerodynamic characteristics of the Martin 329C-2 seaplane were retained and the ski installation characteristics considered were variations of those for the Edo small ski.

6.6   PARAMETRIC STUDIES OF PLANING STABILITY

6.6.1   Effects of Ski Beam Loading

The actual beam loading of the Edo small ski was 73.7. Additional computations were made for beam loadings of 50, 100, and 150, i.e., for new ski beams of .231 ft.,

.183 ft., and .160 ft. (model scale), with all other ski parameters unchanged. The resulting porpoising boundaries have been plotted in Figure 6-5.

It is seen that increase of beam loading has the distinctly undesirable effect of raising the porpoising boundary to higher trim values. Noting further that increased ski beam loading will, if anything, enhance upper limit porpoising as well, i.e., lower the upper porpoising boundary, it is apparent, in any case, that the net effect of increased beam loading is to reduce the stable range of trim-speed combinations for equilibrium. It is thus obvious that, to obtain the desired load alleviation characteristics inherent in skis of high beam loading, special attention must be given to the planing stability problem, i.e., it becomes necessary to compensate for the deleterious effects of the high beam loading on planing stability by careful selection of the other ski installation parameters.

6.6.2   Effects of Ski Deadrise Angle

The actual deadrise angle of the Edo small ski was 20°. Additional computations were made for deadrise angles of 0° and 10°, with all other ski parameters unchanged. The resulting porpoising boundaries have been plotted in Figure 6-6.

It is seen that increase of ski deadrise angle has the same unfavorable effect as increase of ski beam loading, i.e., it raises the porpoising boundary to higher aircraft trim values. Thus, the other principal characteristic conducive to impact load alleviation is found to be unfavorable from the porpoising standpoint, making it all the more mandatory to compensate by suitable choice of the remaining parameters.

6.6.3   Effects of Ski Incidence

The actual incidence of the Edo small ski with respect to the hull keel line was 0°. Additional computations were made for ski incidences of 5° and 10°, with all other ski parameters unchanged. More specifically, this means that the changes in ski incidence were obtained by a rigid body rotation of the ski about the c.g. in which "p", the perpendicular distance from the c.g. to the ski keel remains unchanged. (See the sketch of Appendix C.) The resulting porpoising boundaries have been plotted in Figure 6-7.

It is seen that increase of ski incidence has the distinctly favorable effect of lowering the porpoising boundary to smaller aircraft trim values. Further, while this effect cannot be precisely predicted, it can be anticipated that positive ski incidence will also have the effect of raising the aircraft trim values for the upper limit porpoising boundary (if any).

In practice, these significant advantages of ski incidence with respect to planing stability will, of course, be offset by its disadvantages relative to other hydrodynamic and/or design parameters. One obvious feature in the design category is the possible awkwardness in retracting a ski with incidence. More important are the anticipated adverse effects of excessive ski incidence on ski impact loads and on ski resistance, both in smooth and rough water. It is therefore obvious that, while a certain amount of incidence can be used very
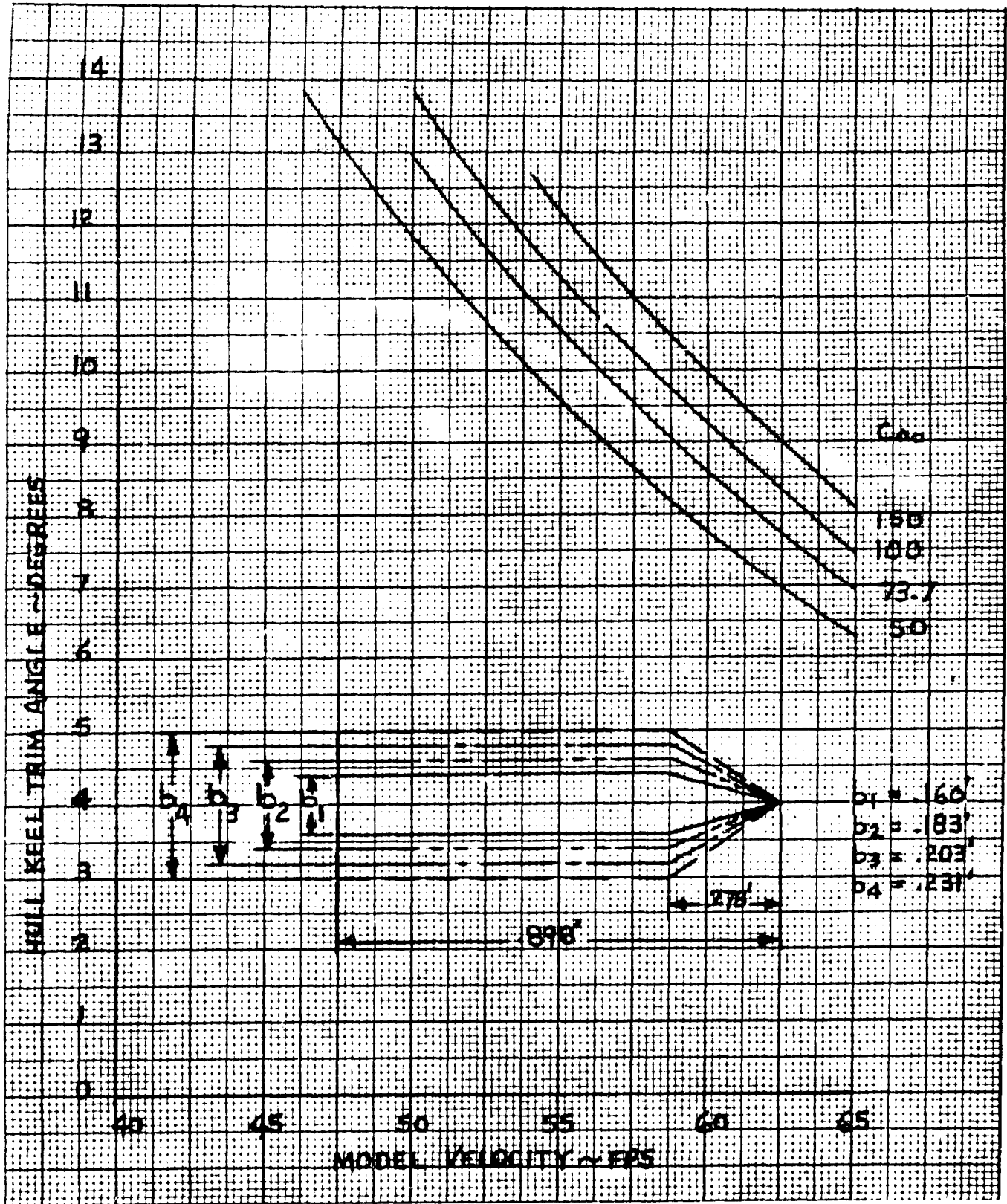
Figure 6-5. Effect of Hydro-Ski Beam Loading on Lower Limit Porpoising Boundary
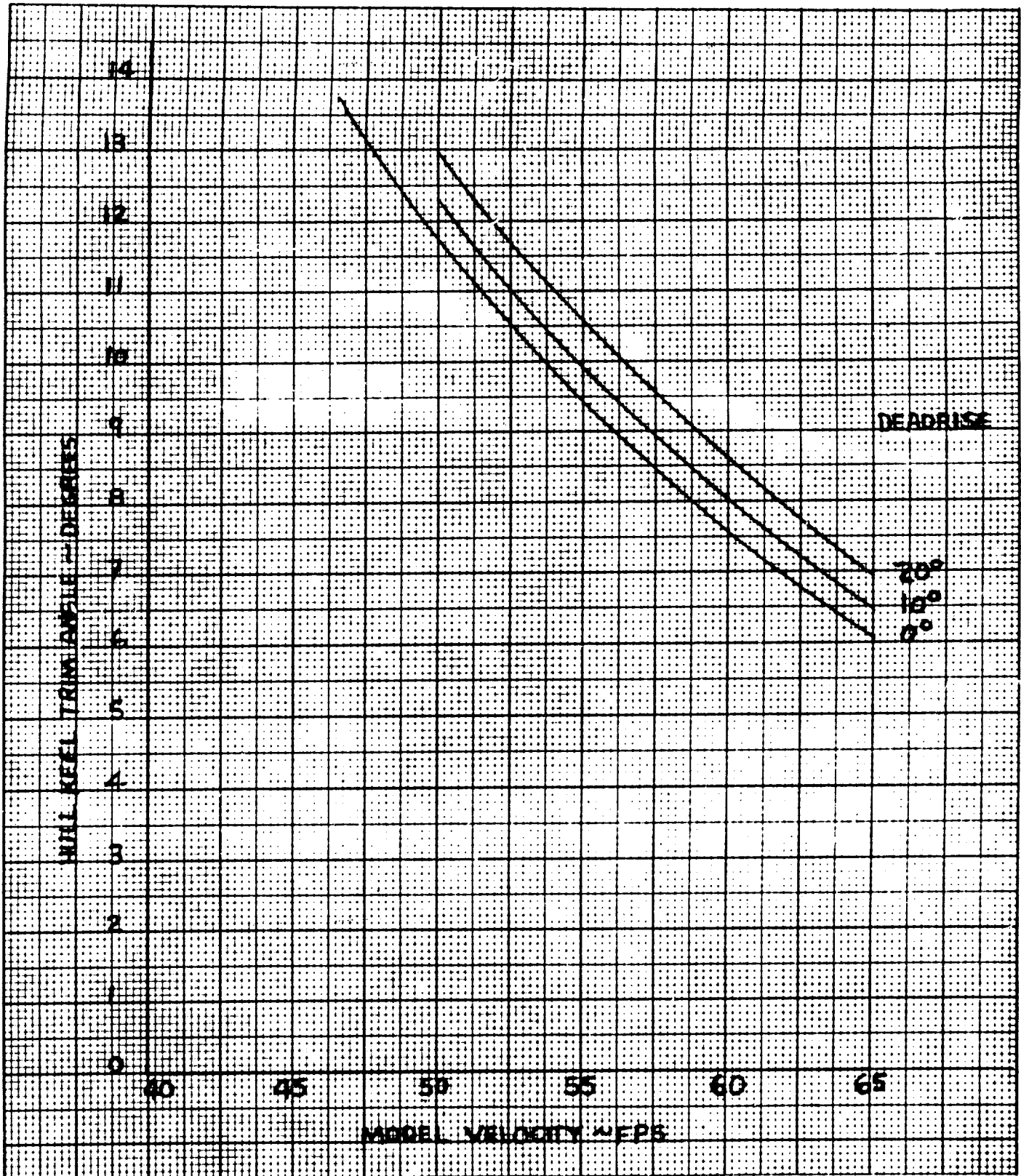
Figure 6-6. Effect of Hydro-Ski Deadrise Angle on Lower Limit Porpoising Boundary
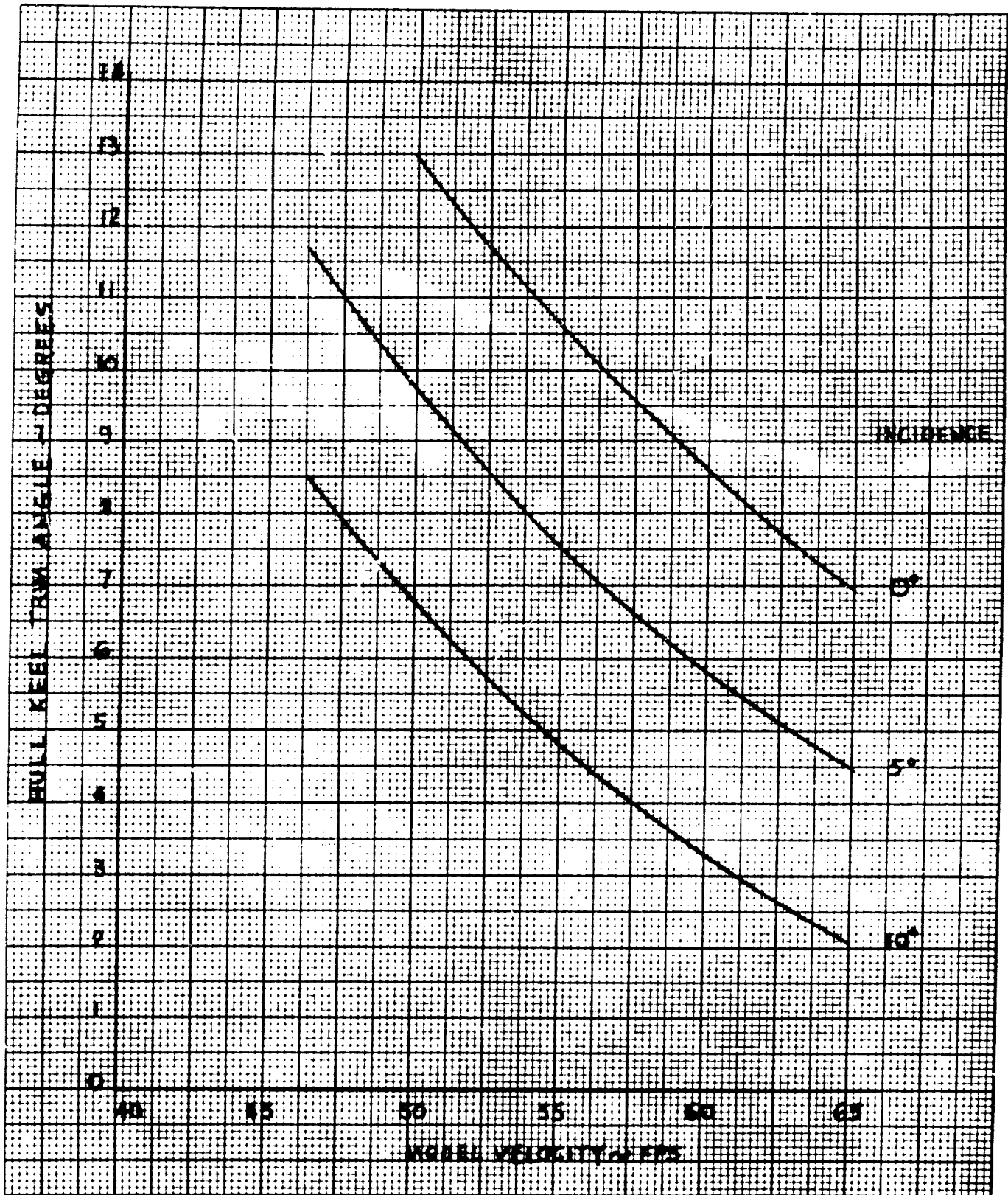
Figure 6-7. Effect of Hydro-Ski Incidence Angle on Lower Limit Porpoising Boundary

effectively to offset the harmful effects on planing stability of high beam loading and deadrise values, careful analysis is required to assure that other important limitations on the ski installation are satisfied.

6.6.4   Effects of Ski Vertical Location

While not precisely obvious from the expressions for the hydrodynamic stability derivatives given in Appendix C, it is intuitively apparent that the vertical location of the ski should have a negligible effect on planing stability. This assumption was checked by a calculation in which the actual strut length was doubled. The results (not plotted herein) showed that the lower limit porpoising boundary trim values were decreased by only .05°, thus clearly proving the correctness of the intuitive assumption.

6.6.5   Effects of Ski Longitudinal Location

Based on the tank test results, the optimum longitudinal location of the Edo small ski corresponded to the value, $q = .131$ ft. (model scale), where q is the distance to the ski T.E. from the foot of the perpendicular drawn from the c.g. to the ski keel line. Additional stability calculations were then made in which q was increased and decreased, respectively, by one whole ski length. Figure 6-8 shows the lower limit porpoising boundaries obtained from these calculations.

It is seen that, while the effects of these rather large shifts in the longitudinal location of the ski are not very great, shifting the ski in either direction has the favorable effect of lowering the trim values of the porpoising boundary and, further, a forward shift is slightly more favorable in this respect than an equal aft shift.

These particular calculations also served to reveal certain novel results concerning the planing stability characteristics of pointed hydro-skis which are illustrated in Figure 6-9. This graph shows that, for the aft ski location, there exist more than one planing stability boundary. More specifically, for this particular ski location, in addition to the usual "lower limit porpoising boundary," there are other boundaries (at higher trims) associated with changes of sign in several of the "stability coefficients." This novel result is explained as follows:

Examination of the mathematical expressions for the hydrodynamic stability derivatives in Appendix C shows that discontinuities in certain of these derivatives occur when the waterline passes the intersection of the rectangular and triangular portions of the ski. Further, the magnitudes of these discontinuities depend on the value of the geometric parameter, q, which defines the longitudinal location of the ski. For (relatively) forward ski locations, these discontinuities are not adequate to affect the basic nature of the planing stability characteristics, i.e., for such locations, there exists only one stability boundary for which $R = 0$ (lower limit porpoising curve) separating the unstable (lower) trims from the stable (higher) trims, irrespective of waterline location on the ski.
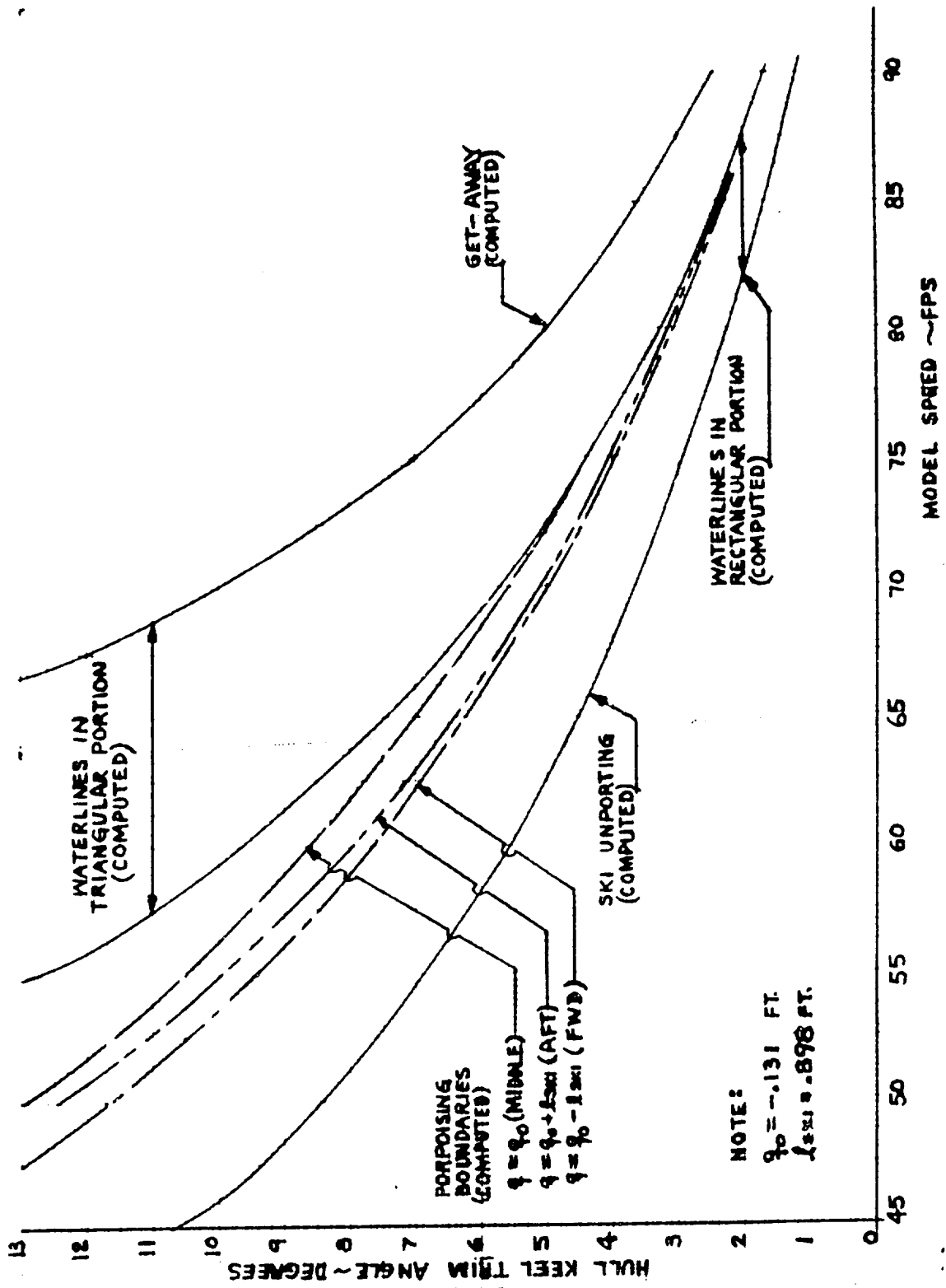
Figure 6-8. Effect of Hydro-Ski Longitudinal Location on Lower Limit Porpoising Boundary
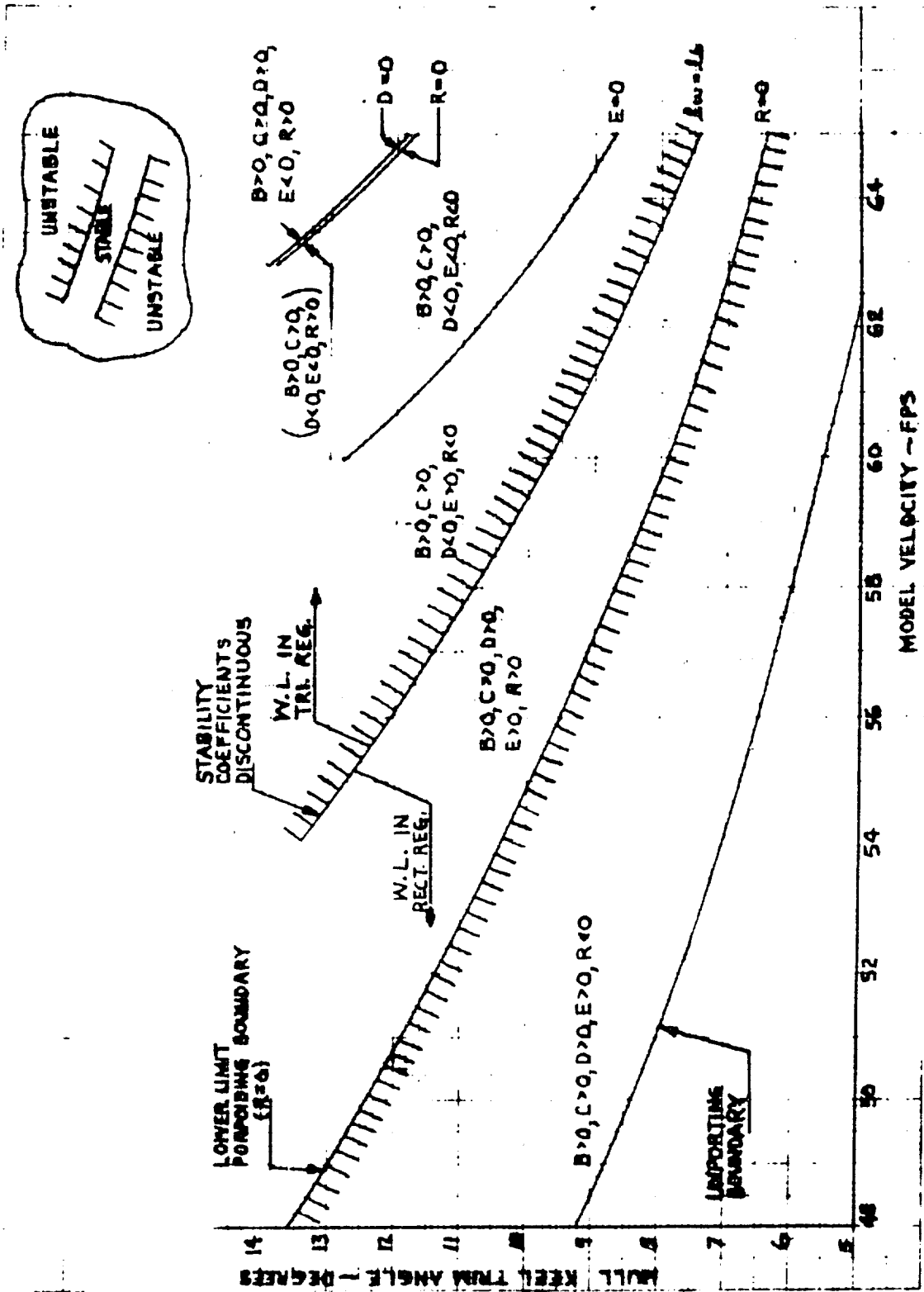
Figure 6-9. Dynamic Stability Boundaries for Aft Hydro-Ski Location

On the other hand, if the ski is sufficiently far aft, the discontinuities associated with the waterline location become sufficient to counteract the positive stability that would otherwise exist and then result in negative stability for _all_ waterlines in the triangular region. Thus, as clearly illustrated in Figure 6-9, the net _undesirable_ result is to limit the region of positive dynamic stability to a relatively narrow band, all totally apart from further possible limitations associated with upper limit porpoising. While it would obviously be of considerable interest to define more closely the precise aft location at which this novel phenomenon first occurs, this item was not investigated.

It is supposed that a kindred phenomenon occurs in the planing stability characteristics of seaplane hulls having pointed (so-called "faired") steps. Although its beam loading will generally be substantially lower than that of a ski, the two configurations may otherwise be considered comparable if the step "point" is identified with the ski T.E. If this analogy is indeed valid, then it could possibly account for the unusual "unstable 'islands' in the trim limits of planing stability" mentioned on p. 5 of Reference 6-1.

REFERENCES

6-1   NACA TN 1290: "Appreciation and Determination of the Hydrodynamic Qualities of Seaplanes," by J. B. Parkinson, May 1947.

6-2   Milne-Thomson, L. M. : "Theoretical Aerodynamics," 3rd Ed., Macmillan & Co., Ltd., London, 1958.

6-3   Convair (Division of General Dynamics) Report No. ZH-139: "Towing Tank Evaluation of Hydro-Ski Alighting Gear," by W. B. Barkley, October 1959.

6-4   Martin Company Report ER10501: "Summary of Mach-2 Patrol Seaplane Studies," by H. L. Meyer, November 1958.

6-5   ETT Unnumbered Report: "Analytical Determination of Lower Limit Stability of Flying Boats," by C. T. Froscher (LCdr, USN) and R. B. Greenwood (LCdr, USN), May 1951.

7. WAVE RESPONSE CHARACTERISTICS OF THE SKELETON HYDRO-SKI SEAPLANE

7-1 INTRODUCTION

As made clear by Figure 5-6 in Section 5 of this report, it is the high beam loading of the hydro-ski which gives rise to its load alleviation capability in single impacts, particularly as compared with the conventional seaplane hull. Equally dramatic and important is the ability of the hydro-ski to reduce the seaplane's motions and accelerations when planing in rough water. As has been further clarified in Section 2, above, this capability plays a fundamental role in the design of hydro-ski installations, thus making it mandatory for the designer to have available certain basic parametric studies relating to the wave response characteristics of hydro-ski seaplanes. Such data, covering as a minimum the effects of the principal ski installation and aerodynamic parameters, could be of two types:

A) Experimental data as obtained from towing tank model tests and/or, preferably, full-scale flight tests;

B) Conceivably, theoretical data, as obtained from a suitable computer program. Such a program would, of course, have the additional advantage of permitting calculations to be made for specific configurations in lieu of or, at least prior to model tests.

At this time, the vast expense and practical difficulties involved in flight testing have ruled out this source of information. Further, with but one exception, no genuine model test parametric studies have been sponsored nor is there presently in existence a computer program relating to this subject. Considering further that the establishment and validation of such a program, even with many inherent limitations, would be far more economical than model test studies. the achievement of this goal was established early during the current project. This report section gives:

A) A detailed description of this program;

B) A comparison of calculated wave responses with the few available experimental data.

Outputs of the computer program for determination of wave response furnishes certain important practical information for hydro-ski installation design. As in Section 6, this program is based on the assumption of a "skeleton" hydro-ski seaplane. thus neglecting wetting of the hull. For a given configuration, one of the program outputs is the maximum submergence of the ski below the wave surface. This quantity is directly related to the minimum strut length (alternately, the clearance between hull and ski) required to ensure that no hull wetting occurs during high-speed taxiing.

Thus, the program furnishes an important criterion for strut length requirements. It will, of course, be appreciated that this is only one of several criteria involved in the selection of strut length. Some of the others are:

1) The strut length required to avoid hull after-body wetting in smooth water at high trims (to eliminate high angle porpoising tendencies and to reduce drag);

2) Avoidance of excessive strut length to reduce strut drag prior to unporting;

3) Avoidance of excessive strut length to reduce directional instabilities, usually associated with forward ski locations;

4) The strut length required to reduce spray ingestion into engine intakes and/or propeller disks at or near unporting.

A more complete discussion of this entire problem area is given in Section 2 of this report.

Unlike the planing stability program described in Section 6, this computer program is very complex because it has been deliberately based on a highly non-linear mathematical model for the hydro-mechanics of the ski. Actually. a much simpler linear mathematical model might have been selected. Accordingly, an explanation of this choice is given in Section 7.2 prior to the description of the non-linear analysis.

7.2   WAVE RESPONSE THEORY

7.2.1   Linear Approach

In the preceding report section, the linearized, two degree-of-freedom equations of motion were used to analyze the problem of dynamic stability of the skeleton hydro-ski seaplane in smooth water. Using well-known procedures, the same equations of motion can also be modified to determine the motion of the planing hydro-ski seaplane in waves, _provided that the wave height is "sufficiently low"_.

If attention is restricted to the relatively simple case of regular, head-sea waves, the actual procedure is to consider the wave motion as a small perturbation of the smooth water condition and to determine analytically the associated periodic hydrodynamic forces acting on the moving ski. After a suitable linearization procedure, that is, the elimination of products of all small quantities (wave height, motion amplitudes and velocities), these periodic forces are then introduced on the right-hand side of eqs. (6-6). By well-known techniques, the resulting equations can be solved to yield the steady-state response solutions for $h(t)$ and $\tau(t)$, i.e., the persistent motions which follow the disappearance of the transient motions excited by any specific disturbance.

It is further obvious that the analytical determination of the steady-state response could have been established by a relatively simple extension of the analysis given in Section 6. This extension would consist of another computer program, involving the wave length L as an additional parameter.

It is equally obvious that there are very severe limitations on the applicability of this approach to the realistic prediction of wave response of hydro-ski seaplanes. While the motions of a ski-equipped seaplane in a given (regular) wave train may be assumed to be much gentler than those of a comparable hull-type seaplane (of similar gross weight, dimensions, and aerodynamic and propulsion characteristics), experience shows that even the ski-equipped vehicle will generally exhibit a non-linear response for waves of fairly small amplitude. It is readily appreciated, in fact, that totally apart from wave considerations, a planing hydro-ski is inherently a non-linear device for at least several reasons:

A) Even at constant trim, the ski lift and pitching moment do not depend linearly on its draft;

B) More generally, the ski lift and pitching moment are complicated non-linear functions of draft, trim, and their rates change, as can be seen directly from eq. (5-4);

C) The finite ski length gives rise to relatively sudden changes in lift and pitching moment at (or near) ski submergence.

Depending on wave height and wave length, some or all of these non-linear effects can be important in the wave response problem. Thus, whereas the linearized theory is capable of furnishing meaningful and practical information in the problem of the planing stability, it fails to do this for the wave response problem except in the uninteresting case of extremely small wave heights.

7.2.2   Non-Linear Approach

Based on the foregoing considerations, it was decided to establish a computer program for the calculation of the wave response motions of a skeleton hydro-ski seaplane which would account for all of the known non-linearities. It was appreciated initially that, at least in principle, certain difficulties are inherent in the interpretation of such calculations, for the following reason.

Whereas in the linearized approach, the steady-state response is completely independent of the initial conditions, this is no longer true when the equations and resulting motions become distinctly non-linear. For example, this means that, if a time history is calculated with one choice of initial conditions and is then repeated with all inputs the same except with different initial conditions, the "steady-state" motions (those prevailing after a sufficient time for the stable transient motions to damp out) may be distinctly different and show large discrepancies in such key features as impact acceleration magnitudes, diving tendencies, etc.

No "a priori" answer to this problem area can be provided at this time, in part because of the existing lack of experimental data required for comparison purposes. The approach taken in this report is a statistical one, wherein several "runs" are made for each case with different initial conditions. This procedure is essentially identical with that currently employed in towing tank tests for determining the planing (alternately, landing) behavior of seaplanes in rough water, wherein the moving seaplane model is dropped into the wave train in an arbitrary manner and a number of runs are repeated to obtain statistical data.

It is obvious that this approach requires some "rules-of-thumb" to insure validity and proper interpretation of the statistical data. In the past, it has been stated (without clear proof) that a minimum of seven runs for each case are required in tank tests to obtain valid test result samples. However, because of practical limitations, many programs have utilized as few as three or four runs.

Clearly, resolution of this problem area in this report would be entirely premature. Instead, the arbitrary decision has been made to restrict the number of runs to five for each case. Further, also following standard tank test procedures and runs are made with all (arbitrarily selected) initial conditions the same except for the initial location of the ski relative to the wave train. This selection has also been influenced in part by the results obtained in Section 5 of this report which have indicated the importance of this parameter in single ski impacts.

7.3 DESCRIPTION OF COMPUTER PROGRAM

7.3.1 General Description

The purpose of the program is to calculate the time history of the motions of a skeleton hydro-ski seaplane when planing through waves. Several restrictuons. previously used in the planing stability analysis of Section 6 and the ski impact analysis of Section 5, have been retained:

A. The seaplane's horizontal speed is maintained constant in each run and, correspondingly, there are only two degrees of freedom (heaving and pitching);

B. The longitudinal control setting (elevators, stabilizer, etc.) is maintained constant in each run and the pertinent aircraft aerodynamic characteristics are assumed to be independent of this control setting;

C. No direct account of power effects is taken in the aircraft's aerodynamic characteristics;

D. The wave train is assumed to consist of regular sinusoidal waves with the aircraft running in the head sea condition.

It may be noted that these assumptions readily permit accounting for accompanying head winds, if desired.

It will further be noted that the program is capable of being amended to remove practically all of these restrictions provided that the ensuing complications are acceptable. Even the "stick-fixed" restriction can be eliminated and replaced by an "autopilot-type" of mathematical model simulating a pilot's control actions.

The computational procedure followed in the program is as follows:

1. The entire program, including all inputs and computer print-out, uses non-dimensional quantities. The non-dimensionalization of all quantities, kinematic and dynamic, is effected through consistent use of two reference values as follows:

DIMENSION	REFERENCE
Length	Ski Beam, b
Time	Ski Beam/Horiz. Velocity, b/V_H

2. To permit calculation of the changes in the two coordinates, heave and pitch, and associated heaving and pitching velocities, inside of a small time interval, the two differential equations of motion are approximated by suitable difference equations.

3. The aero and hydro loads (i.e., forces and moments) are defined analytically in terms of the kinematic quantities. In the case of the hydro loads, these relations also depend on the geometric relations between the ski, the local wave surface, and the resultant velocity vector with special distinctions made between the various possible configurations (ski planing, ski submerged, and immersed bow), as explained in more detail below.

4. Starting with specified initial conditions, including a specified location of the wave relative to the ski, the equations of motion are solved step-by-step, using the load values from Step 2. Through use of the "Hamming-predictor-corrector" technique, the time increment used in each step is automatically made sufficiently small to insure continuity of the kinematic variables.

5. The computer print-out concludes the following instantaneous quantities (all non-dimensional):

a. Time;

b. Heave (height of c.g. above the level water line relative to equilibrium value);

c. Heave velocity;

d. Heave acceleration;

e. Trim angle (angle of hull reference line (keel line) relative to horizon;

f. Pitching velocity;

g. Pitching acceleration;

h. Bow vertical acceleration (at a specified distance forward of c.g.)

i. Ski Bow Submergence (vertical distance of bow below local wave surface);

j. Ski Draft (vertical distance of ski stern below local wave surface);

k. Ski wetted length;

l. Wave slope (relative to the level water line, measured at ski-water line intersection).

7.3.2   Equations of Motion

The basic equations of motion are identical with those used in the analysis of planing stability, i. e.:

$$(W/g) \, \ddot{H} \;=\; L_A + L_H - W$$
$$I \, \ddot{\tau} \;=\; M_A + M_H \tag{7-4}$$

where it is understood that the motions involve a constant horizontal speed and fixed aerodymanic controls. The particular control settings are those which furnish a particular equilibrium trim angle at the same horizontal speed. This equilibrium condition is described by the equations:

$$L_{A \, eq} + L_{H \, eq} \;=\; W$$
$$M_{A \, eq} + M_{H \, eq} \;=\; O \tag{7-5}$$

Subtracting eqs. (7-5) respectively from eqs. (7-4),

$$(W/g)\ddot{H} = (L_A - L_{A\,eq}) + (L_H - L_{H\,eq})$$

$$I\ddot{\tau} = (M_A - M_{A\,eq}) + (M_H - M_{H\,eq}) \tag{7-6}$$

In these equations, H represents the instantaneous height of the c.g. above the level water line. It was found more convenient to use as the vertical coordinate a quantity, h, defined by the relation:

$$h = H - H_{eq} \tag{7-7}$$

h is identical with the quantity, (h), used in Section 6 and the final basic form of the equations can be taken as:

$$(W/g)\ddot{h} = (L_A - L_{A\,eq}) + (L_H - L_{H\,eq})$$

$$I\ddot{\tau} = (M_A - M_{A\,eq}) + (M_H - M_{H\,eq}) \tag{7-8}$$

The horizontal motion of the wave train is taken relative to a vertical plane through the aircraft c.g. so that the general expression for the wave height can be written as:

$$y_w = \frac{H}{2} \sin\left[2\pi\left(\frac{x}{L} + \frac{t}{T}\right) - \theta\right] \tag{7-9}$$

where: x = horizontal coordinate relative to aircraft c.g., (positive for forward locations)

$$T = L / \left(V_H + \sqrt{(g/2\pi)L}\right)$$

θ = wave phase angle.

To obtain time histories of the aircraft motion, it is necessary to solve equations (7-8) subject to a set of four initial conditions, typically the initial values of h, τ, $\dot{h}$, and $\dot{\tau}$. In addition, it is possible to select a value of θ in eq. (7-9) so as to fix an initial wave phase relative to the aircraft in some particular manner. In the present program, only three of these five quantities are specified explicitly: these are τ_0, $(\dot{h})_0$, and $(\dot{\tau})_0$. Note that τ_0 is not necessarily identical with τ_{eq}.) The other two quantities, i.e., h_0 and θ, are

specified implicitly through the explicit specification of the initial values:

$$\left[y_w \,(@\,\text{ski T. E.}) \right] = (H/2)\,\sin\left[(2\pi/L)(p\,\sin\tau_0 \,-\, q\,\cos\tau_0) - \theta \right]$$

$$\left[\text{ski T. E. draft} \right]_0 = \left[y_w\,(@\,\text{ski T. E.}) \right]_0 + \left[p\,\cos\tau_0 + q\,\sin\tau_0 - H_{eq} - h \right]$$

(7-10)

where p and q are the quantities defined in the sketch of Appendix C.

Integration of the equations of motion, subject to the initial conditions just described, requires a knowledge of the explicit dependence of the aero and hydro loads on all of the pertinent geometric and kinematic variables. Essentially, the aero loads depend only on the kinematic variables and can be defined in the same manner in Section 6. The hydro loads are strongly dependent as well on the geometric variables locating the ski relative to the wave surface. It is obvious, in fact, that provisions must be contained in the program to cover a variety of possible ski-wave geometric configurations. For certain of these configurations, neither experimental nor analytic load values are presently available, even for the corresponding steady-state condition of uniform motion in smooth water. It therefore was necessary to devise entirely new expressions for such cases. Because of the resulting program complexity, it was decided to limit the analysis, for the submerged condition only, to skis of purely rectangular planform.

7.3.3 Aerodynamic Loads

Basically, the static airload variations with trim are assumed to resemble those measured on the unpowered HU-16 model. For this model, the lift curve is linear below the stall, exhibits a sharp break at the stall, and, above the stall, is again linear with a negative slope. For large up elevator angles and neglecting some slope reduction just below the stall, the moment curves can be closely approximated by straight lines throughout the entire positive trim range.

Then, consistent with the treatment of Appendix C, the airload terms in the equations of motion can be written as:

$$L_A - L_{A\,eq} = q_A \left\{ S_w C_L \left[\tau_K - (\dot{h}/V_H) \right] - S_w C_L \left[\tau_{eq} \right] + (1 + d\epsilon/d\alpha)S_t C_{L\alpha t} \cdot (\dot{\tau}\,l_t/V_H) \right\}$$

$$M_A - M_{A\,eq} = q_A \left\{ S_w \bar{c}\, C_{M\alpha} \cdot \left[\tau_K - (\dot{h}/V_H) - \tau_{eq} \right] - (1.1 + d\epsilon/d\alpha)S_t l_t C_{L\alpha t} \cdot (\dot{\tau}\,l_t/V_H) \right\}$$

Note that, below the stall, the lift equation takes the simplified form:

$$L_A - L_{A\,eq} = q_A \left\{ S_w C_{L\alpha} \cdot \left[\tau - (\dot{h}/V_H) - \tau_{eq} \right] \cdot (1 - d\epsilon/d\alpha) S_t C_{L\alpha t} \cdot (\dot{\tau}\, 1_t/V_H) \right\}$$

The present program format has been based on the specific types of lift and moment curves described above. However, the accommodation of more general types of aerodynamic curves (with or without power effects) can be readily effected, if desired, by obvious program modifications.

7.3.4   Hydrodynamic Loads

During the high speed portion of the rough-water landing or take-off run of a hydro-ski seaplane, the hydrodynamic loads on the hydro-ski can result from several distinctly different flow conditions. Speaking most generally, the loads developed depend on the relative ski-wave location, the ski trim relative to the wave surface, and the resultant velocity direction of the ski.

At the present time, theoretical and experimental data for prediction of hydro-ski impact load time-histories only cover those cases where the hydro-ski impacts the water surface at zero or positive trim. Further, although the existing analytical methods can account for variation of trim during the impact process, load calculation methods are not currently available for negative trim impacts, and/or negative angles of attack in the vicinity of the free water surface. Consequently, for a non-linear wave response computer program which is required to cover all realistic impact conditions, it was found necessary to develop analytic expressions for the hydro loads in those conditions which have not yet been considered in the literature.

Appendix D of this report furnishes a complete statement of the hydro-ski lift forces and moments used in the wave response program. Wherever novel expressions or values are used, they are believed to represent reasonable engineering approximations for what are, actually, relatively complex flow conditions.

While the individual expressions for the loads are considered realistic, the "transitions" between the flow regimes involve some artificiality in that they are taken as "sharp" ones. That is, the loads generally vary by finite amounts in crossing a "regime boundary", even though the differences in geometric and/or kinematic parameters may be very small. This results in (generally small) isolated discontinuities ("kicks") in the computer outputs which, of course, must be disregarded in the interpretation of the results.

Such discontinuities, of course, could be eliminated from the program by use of more refined (continuous) definitions of the boundaries separating the regimes. To have even attempted this in the present program would have increased the required effort by an infeasibly large factor. In addition, the resulting program complexity would probably have exceeded the capacity of this contractor's computer (IBM 1130). In short, while these discontinuities detract from the reality of the mathematical model, this defect is considered to be a tolerable one at the present stage of understanding of this problem area.

7.3.5 Program Details

Table 7-1 furnishes a complete definition of the Fortran IV code used in the computer program. Figure 7-1 is a program flow diagram intended to illustrate all of the logical decisions, including those which distinguish between the various ski flow regimes. Table 7-2 shows the statement of the program which is complete except for the "predictor-corrector" technique used to alter the time interval magnitudes. This feature has been omitted only because it is a standard computer subroutine.

Before describing the actual calculations made with this program, it may be pointed out that, in its present form, it effectively incorporates as special cases the program established in Section 5 for single fixed-trim ski impact loads in waves and the planing stability program of Section 6. These features may be briefly explained as follows:

TABLE 7-1. FORTRAN IV CODE FOR WAVE RESPONSE
COMPUTER PROGRAM

Item	Mathematical Notations	Fortran Notations
non-dimensional kinematic variables	h/b, $\dot{h}/V_H$, τ, $\dot{\tau}\, b/V_H$	V(1), V(2), V(3), V(4)
velocity parameter	V_H^2/gb	CV
ski incidence to hull keel	i	OMEGA
	$\dot{h}/V_H + i$	VV
initial value of kinematic variables	$(h/b)_o$, $(\dot{h}/V_H)_o$ $(\tau_o)_o$, $(\dot{\tau}\, b/V_H)_o$	YO(1), YO(2), YO(3), YO(4)
non-dimensional variables used in the Hamming-Predictor-Corrector numerical integration routine	$\left[\text{See program statement.}\right]$	F(1), F(2), F(3), F(4)
initial value of F(i) used in integration routine	–	F0
non-dimensional time	tV_H/b	X
non-dimensional total ski length	l/b	EL

TABLE 7-1. FORTRAN IV CODE FOR WAVE RESPONSE
COMPUTER PROGRAM (cont)

Item	Mathematical Notations	Fortran Notations
distance from perpendicular to ski through aircraft c.g. to trailing edge of ski (divided by ski beam) (+ if aft)	q/b	EDBAR
perpendicular distance from aircraft c.g. to ski keel (divided by ski beam)	p/b	ELD
ski aspect ratio	b/l	AR
horizontal distance from aircraft c.g. to leading edge of ski (divided by ski beam)	x_B/b	EXB
horizontal distance from aircraft c.g. to trailing edge of ski (divided by ski beam)	x_D/b	EXD
length of the triangular portion of the hydro-ski (divided by the ski beam)	l_b/b	ELBB
Hamming-Predictor-Corrector Numerical Integration Scheme	—	HAMM
crest to trough height of wave (divided by ski beam)	H/b	ABAR
wave length divided by ski beam	L/b	WLBAR
wave height above mean water surface (divided by ski beam)	y_w/b	YW
slope of wave at ski-wave surface intersection	ϕ	PHI
slope of wave at coordinate reference axis	ϕ_o	PHIG
equilibrium trim angle (of hull keel)	τ_{eq}	TAU
angle between ski and wave at coordinate reference axis	τ_o	TAUO

TABLE 7-1. FORTRAN IV CODE FOR WAVE RESPONSE
COMPUTER PROGRAM (cont)

Item	Mathematical Notations	Fortran Notations
non-dimensional period of wave encounter	T	T
angle between ski and wave slope at ski-wave surface intersection	τ_w	TAUW
estimated distance from coordinate reference axis to ski-water surface intersection (divided by ski beam)	x_1/b	EX1
distance between aircraft c.g. and ski-wave surface intersection (divided by ski beam)	x_2/b	EX2
maximum ski thickness (divided by ski beam)	–	SKITT
deadrise of ski	β	BETA
transcendental function used to solve for wetted length of ski in waves	–	FXX
derivative of FXX with respect to EX1	–	DFXX
wetted length divided by ski beam based on ϕ_o, τ_o	–	ELWO
equilibrium wetted ski length (divided by ski beam)	–	ABZ
wetted length (divided by ski beam)	l_w/b	ELWET
See Table 6-1	–	A1, A2, A3
area of horizontal tail/area of wing	S_t/S_w	SR
mean aerodynamic chord (divided by ski beam)	$\bar{c}/b$	CBAR
distance between aircraft c.g. and quarter chord of tail (divided by ski beam)	l_t/b	DTBAR

TABLE 7-1. FORTRAN IV CODE FOR WAVE RESPONSE COMPUTER PROGRAM (cont)

Item	Mathematical Notations	Fortran Notations
beam loading	C_{Δ_o}	CDELO
radius of gyration of aircraft divided by ski beam	k	GYBAR
downwash parameter	$1 + d\epsilon/d\alpha_w$	EF
non-dimensional ski wetted area	S_W/b^2	AWET
slope of aero pitching moment coefficient cursor	$dC_M/d\alpha$	CM
non-dimensional parameter (V_{eq} = equivalent planing velocity)	V_{eq}^2/V_H^2	COREQ
total aero lift coefficient	C_L	AERO
slope of (isolated) horizontal tail lift curve	$dC_{L_t}/d\alpha_t$	CLT
non-dimensional hydro force (See Program Statement)	L_{HYDRO}/WC_V^2	A, A10, A12
non-dimensional hydro moment (See Program Statement)	$N_{HYDRO}(b)/Wk^2C_V^2$	B, B10, B12
equilibrium hydro lift force	L_{Heq}/WC_V^2	EQUIF
equilibrium hydro moment	$N_{Heq}(b)/Wk^2C_V^2$	EQUIM
aero-hydro "density" parameter (ρ_A = air density, S_W = wing area)	$2W/\rho_A gS_W b$	CLCVG
orbital velocity at ski-water surface intersection (divided by V_H)	V_p	VP

TABLE 7-1. FORTRAN IV CODE FOR WAVE RESPONSE
COMPUTER PROGRAM (cont)

Item	Mathematical Notations	Fortran Notations
non-dimensional resultant linear velocity	V	VRCG
normal velocity component at leading edge of ski due to $\dot\tau$	$(V_N)_{LE}$	VNLE
horizontal component of resultant velocity at ski L. E.	$(V_H)_B$	VHB
vertical component of resultant velocity at ski L. E.	$(V_V)_B$	VVB
flight path angle of leading edge of ski with respect to horizon	γ	GAMMA
angle between VRCG and horizon	η	ETA
angle between EXCG and horizon	δ	DELTA
hypotenuse of the ELD-EXB triangle	–	EXCG
vertical distance between ski T. E. and water surface (divided by ski beam) (+ for T. E. below water)	D	DRAFT
vertical distance between ski L. E. and water surface (divided by ski beam) (+ for L. E. above water)	B	BOW
terms in Shuford planing equation	C_{L6}, C_{L7}	CL6, CL7
lift coefficient of submerged ski	$C_{L\,SUB}$	CLSUB
Shuford lift coefficient for planing ski	$C_{L\,SKI}$	CLSKI
distance to center of pressure of submerged ski from the T. E. (divided by ski beam)	–	XCPTE

TABLE 7-1. FORTRAN IV CODE FOR WAVE RESPONSE
COMPUTER PROGRAM (cont)

Item	Mathematical Notations	Fortran Notations
reduction in aircraft weight due to slipstream effect (specifically for HU-16 model)	$1 - (\Delta L/W)$	REDUC
moment arm of drag force acting on ski	–	DARM
horizontal distance between aircraft c.g. and center of pressure of submerged ski (divided by ski beam)		LHSUB
horizontal distance between aircraft c.g. and center of pressure of planing ski (divided by ski beam)	–	LHPLA
term reflecting Pierson virtual mass and Pabst aspect ratio correction factor	–	ASTAR
term in zero impact lift equation accounting for wave rise	–	ELHDM
vertical location of the ski T.E. with respect to the horizon	–	D
distance between aircraft c.g. and ski center of pressure for specific wave orientation	–	ELNOS
Bobyleff coefficient for ski upper surface	$.88 \ \mathrm{Cos} \ \beta_T$ $.88/\mathrm{Cos} \ \beta_T$	BOBYL
hydrodynamic moment arms used in zero trim impact calculation	– –	ELIMP ELIMM
distance from bow accelerometer location to aircraft c.g. (divided by ski beam)	–	ARM
bow vertical acceleration	–	BA

TABLE 7-1. FORTRAN IV CODE FOR WAVE RESPONSE
COMPUTER PROGRAM (cont)

Item	Mathematical Notations	Fortran Notations
vertical distance between ski T. E. and particular point on wave at time zero	–	DD
BOW/EL, for submerged ski	–	Y
subroutine based upon Johnson theory	–	CLCUB
effective angle of attack of ski with respect to horizon	α	ALPHA
parameters from Johnson theory	$f,\ c, \eta, \psi$	F, C, ZN, ZPSI
error above which integrating interval is halved	–	T1
error above which integrating interval is doubled	–	T2
minimum integrating interval beyond which program is terminated	–	T3
number of first order differential equations	–	N
printing time interval for output	–	HPR
stepping increment for integration scheme	–	H
final value of X	–	XEND
$(\pi/2)(\tau + i)\cos^2(\tau + i)(1 - \sin\beta)$	–	A4
$(4/3)\cos^3(\tau + i)\sin^2(\tau + i)\cos\beta$	–	A5
at equilibrium, horizontal distance from aircraft c.g. to center of pressure of ski (divided by ski beam)	–	ELHEQ
wave phase angle	θ	THETA
coefficients in computation of $(l_w/b)_{eq}$, for $l_w > l_b$	–	AA, BB, CC
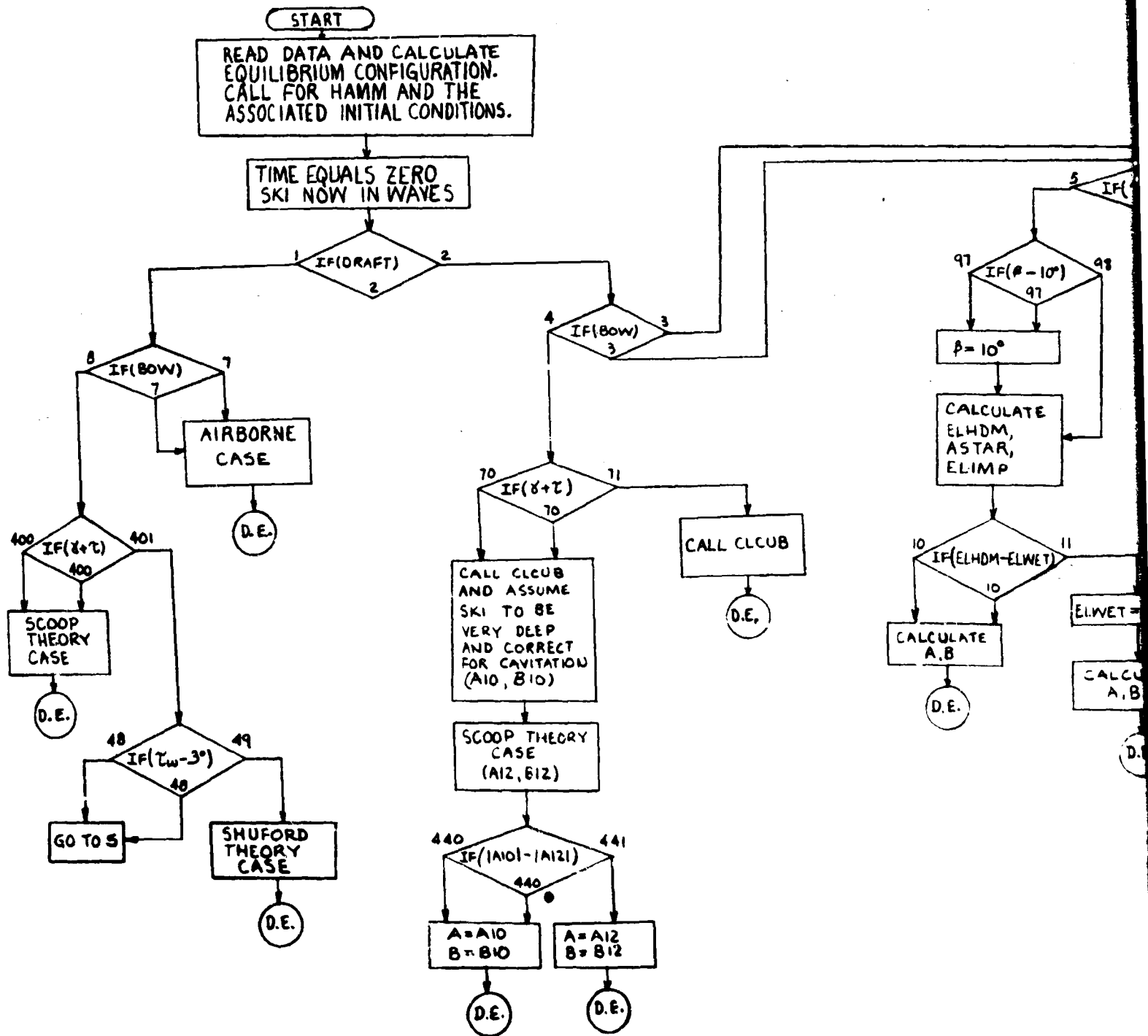
Figure 7-1. Flow Diagram
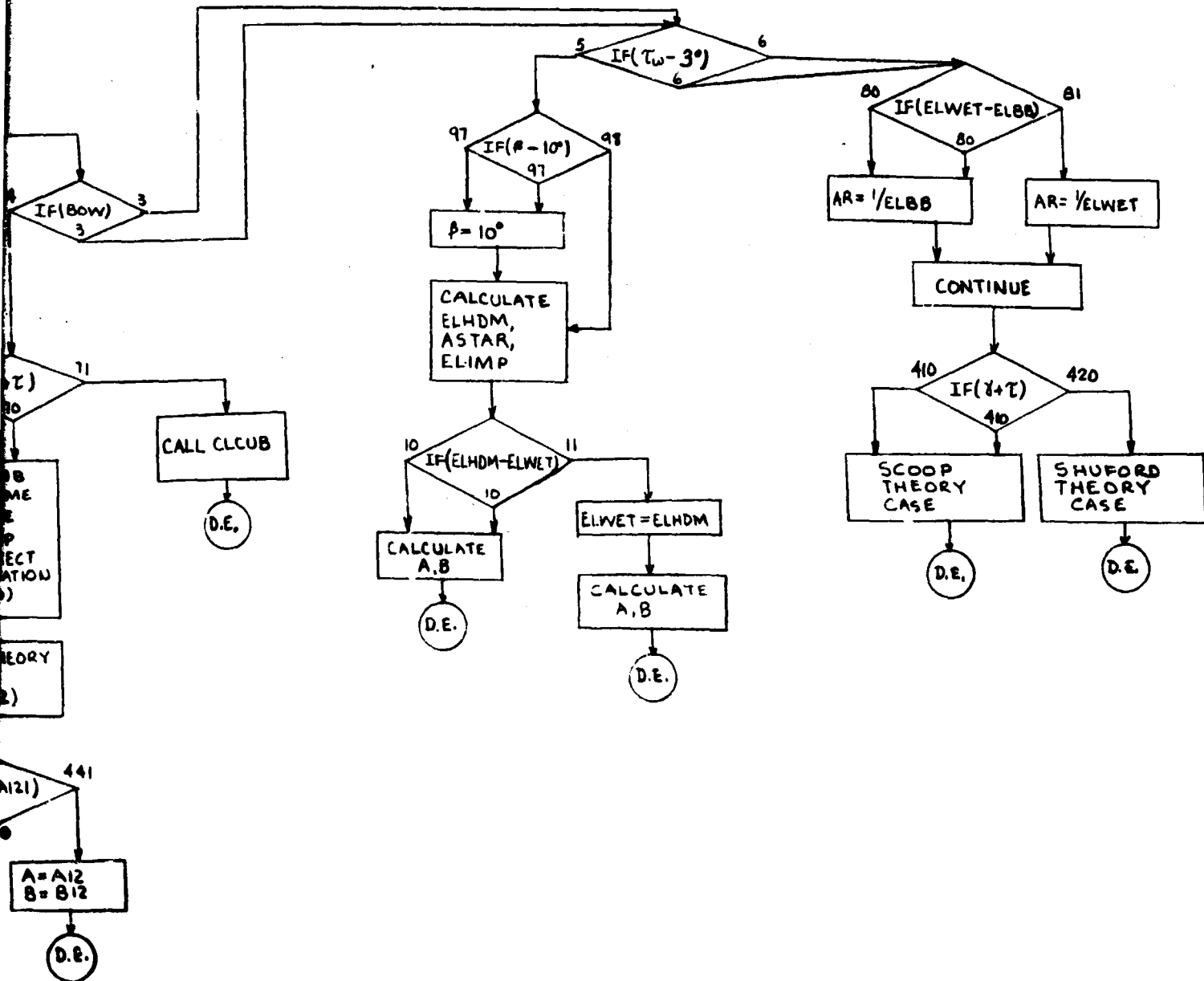
Figure 7-1.   Flow Diagram for Non-Linear Wave Response Program

Table 7-2. Fortran Statement of Wave Response Computer Program

```
     *  LIST SOURCE PROGRAM
     *  ONE WORD INTEGERS
     *NAME HYDRO
     *IOCS(CARD,1132 PRINTER)
           COMMON V(6),F(6),YO(6),FO(6),X
           COMMON ELWET,ROW,DRAFT,TAUW,WLBAR,CV,ABAR,EDBAR,EL,CDELO,GYBAR,
          1BETA,DTBAR,ELD,CLT,SR,CM,CBAR,CLCVG,EF,EQUIF,EQUIM,TAU,OMEGA,
          2AR2,ELRB,SKITT,G1,Y,REDUC,ARM,THETA,ETA,DYNAM,BA,BETAT,GAMMA,
          3RAN1,SL1,SL11,SL2,HEQB
           WRITE(9,911)
     911   FORMAT(1H1,'HYDROSKI IN WAVES, FREE TO PITCH AND HEAVE'//)
     C     READ INPUT PARAMETERS
           READ(2,100) EL,EDBAR,BETA,DTBAR,CBAR,SR,GYBAR,ELD,CLT,CDELO,
          1CM,CLCVG,EF,CV,WLBAR,ABAR
           READ(2,100)TAU,CLEQ,OMEGA,DYNAM
           READ(2,99)ELRB,SKITT,DRAFT,YWINT,REDUC,ARM,BETAT
           READ(2,99) RAN1,SL1,SL11,SL2
           READ(2,105)(YO(I),I=2,4),XEND,H,HPR,T1,T2,T3
     100   FORMAT(8F10.5/8F10.5)
     99    FORMAT(8F10.5)
     105   FORMAT(3F5.3,6E10.4)
     C     WRITE INPUT PARAMETERS
           WRITE(3,101)
           WRITE(3,102) EL,EDBAR,BETA,DTBAR,CBAR,SR,GYBAR,ELD
           WRITE(3,103)
           WRITE(3,102) CLT,CDELO,CM,CLCVG,EF,CV,WLBAR,ABAR
     101   FORMAT(' SKILENGTH/B  DISTCGTESKI/B    DEADRISE  DISTCG-TAIL/B   C
          1HORDW/B    ATAIL/AWING  RADGYABCG/B  PERPENDICULAR TO SKI/B ')
     102   FORMAT(8F13.6///)
     103   FORMAT(' COEFOFLIFTTAIL  WGTPARA  COEFOFMOMATCG  WGTCOEF        C
          1MP,PARA   VELPARA      WAVELENGTH/B WAVEAMP/B')
     C     CALCULATION OF EQUILIBRIUM CONFIGURATION
           A4  =1.5708*(TAU+OMEGA)*COS(TAU+OMEGA)**2*(1.-SIN(BETA))
           A5  =1.3333*COS(TAU+OMEGA)**3*SIN(TAU+OMEGA)**2*COS(BETA)
           A2=2.*CDELO*(REDUC/CV-CLEQ/CLCVG)
           A3=(A4+A5-.5*ELRB*A5-A2)/A5
           A1=(.5*ELRB*(A4+A5)+A2)/A5
     C     THIS EQUATION IS FOR THE CALCULATION OF WETTED LENGTH IN RECT REG
           AR2=(-A3+ABS(A3)*SQRT(1.+(4.*A1/A3**2)))/2.
     C     TESTING FOR FORMULA VALIDITY
           IF(ELRB-AR2)74,74,73
     74    GO TO 75
     C     FORMULA FOR TRIANGULAR REGION OF SKI
     73    AR2=SQRT(A2*2.*(ELRB**2+1.)/(A4+(ELRB+1.)*A5))
     75    EQUIF=REDUC/CV-CLEQ/CLCVG
           IF(AB2-ELRB)912,912,914
     912   AR=1./ELRB
           GO TO 915
     914   AR=1./AR2
     915   CONTINUE
           CL6=A4*(AR/(1.+AR))
           CL7=A5
           FRACT=(.875*CL6+.5*CL7)/(CL6+CL7)
           ELMEQ=(AR2*FRACT-EDBAR)*COS(TAU+OMEGA)+ELD*SIN(TAU+OMEGA)
           EQUIM=EQUIF*FLMEQ/(GYBAR**2)
     C     CALCULATION OF YO(1)
           XD=-EDBAR*COS(TAU+OMEGA)+ELD*SIN(TAU)
           THPTA=6.283* XD/WLBAR=ATAN(2.*YWINT/SQRT(ABAR**2-1.*(YWINT**2)))
```

Table 7-2. Fortran Statement of Wave Response Computer Program (cont'd)

```
        DEQ=AB2*SIN(TAU+OMEGA)
        HEQF=ELD*COS(TAU)+EDBAR*SIN(TAU+OMEGA)-DEQ
        DD=YWINT+DRAFT
        YO(1)=DEQ+DD
C       WRITE CALCULATED VALUES
        WRITE(3,106)
        WRITE(3,107)AB2,ELHEQ,EQUIF,EQUIM,TAU,CLEQ,OMEGA
        WRITE(3,111)G1,(YO(I),I=1,4)
111     FORMAT(1H 'EFF BEAM=',3F8.3,3X,'YO=',3F8.3,3X,'YODOT=',3F8.3,3X,'TAU=
       1',F8.5,3X,'TAUDOT=',F8.5//)
        WRITE(3,98) ELBB,SKITT,DRAFT,YWINT,REDUC,ARM,BETAT
98      FORMAT(1H 'LB/B=',F7.4,3X,'SKI TH/B=',F7.4,3X,'INT DRAFT=',F7.4,3X
       1,'INT WAVE=',F7.4,3X,'REDUC=',F7.4,3X,'ARM=',F7.4,3X,'BETAT=',F7.4
       2//)
        WRITE(3,169)THETA,DYNAM
169     FORMAT(1H 'THETA=',F8.5,3X,'DYNAM=',F10.5//)
        WRITE(3,170) RAN1,SL1,SL11,SL2
170     FORMAT(1H 'RAN1=',F8.4,3X,'SL1=',F8.4,3X,'SL11=',F8.4,3X,'SL2=',F8
       1.4//)
        WRITE(3,104)
106     FORMAT(1H 'EQUI WETTED L/B  DIST TO CP/B   EQUI F      EQUI M
       1EQUI TRIM     EQUI CL      OMEGA     ')
107     FORMAT(7F13.6 //)
104     FORMAT(//' TIME,Tv/B HEAVE/B   VSKI/V    ASKI/VV/B TRIM       ANG
       1 VFL  ANG ACCEL  LWET/B      ROW/B      DRAFT/B    TAUW    BA'//)
        N=4
        CALL HAMM(N,XEND,H,.0,HPR,T1,T2,T3)
        STOP
        END

FEATURES SUPPORTED
ONE WORD INTEGERS
IOCS

CORE REQUIREMENTS FOR HYDRO
COMMON    134  VARIABLES    56  PROGRAM    1168

END OF COMPILATION
```

Table 7-2. Fortran Statement of Wave Response Computer Program (cont'd)

```
*LIST SOURCE PROGRAM
* ONE WORD INTEGERS
      SUBROUTINE FOFXY
      REAL LMPLA,LHSUB
      COMMON V(6),F(6),YO(5,),FO(6),X
      COMMON ELWET,ROW,DRAFT,TAUW,WLBAR,CV,ABAR,EDBAR,EL,CDELO,GYBAR,
     1BETA,DTBAR,ELD,CLT,SR,CM,CBAR,CLCVG,EF,EQUIF,EQUIM,TAU,OMEGA,
     2AB2,ELBR,SKITT,G1,Y,REDUC,ARM,THETA,ETA,DYNAM,BA,BETAT,GAMMA,
     3RAN1,SL1,SL11,SL2,HEOB
C     WAVE PARAMETERS
      VV=V(3)+OMEGA
      SS=SIN(V(3))
      CC=COS(V(3))
      S=SIN(VV)
      C=COS(VV)
      T=WLBAR/1.398*SQRT(WLBAR/CV)+1.1
      YW=.5*ABAR*SIN(6.283*X/T-THETA)
      PHIO=3.1416*ABAR/WLBAR*COS(6.283*X/T-THETA)
      TAUO=VV-PHIO
      ELWO=(YW-V(1))*COS(PHIO)/SIN(TAUO)
      EX1=ELWO*C
      D=ELD*C -(HEOB+V(1))*C/CC+EDBAR*S
311   FXX=.5*ABAR*SIN(6.283*(EX1/WLBAR+X/T)-THETA)-(EX1-ELD*SS)*S/C
     1+D-EDBAR*S
      DFXX=3.1416*ABAR/WLBAR*COS(6.283*(EX1/WLBAR+X/T)-THETA)-S/C
      EX2=EX1-FXX/DFXX
      IF(FXX/(DFXX*EX1)-.001) 310,309,309
309   EX1=EX2
      GO TO 311
310   ELWFT=(FX2-ELD*SS)/C+EDBAR
      EXD=-EDBAR*C+ELD*SS
      EXB=EL*C+EXD
      DRAFT=.5*ABAR*SIN(6.283*(EXD/WLBAR+X/T)-THETA)+D
      ROW=EL*S-D-.5*ABAR*SIN(6.283*(EXB/WLBAR-X/T)-THETA)
      PHI=3.1416*ABAR/WLBAR*COS(6.283*(EX2/WLBAR+X/T)-THETA)
      TAUW=VV-PHI
      ST=SIN(TAUW)
      CT=COS(TAUW)
C     CALCULATION OF PARAMETERS USED SEVERAL TIMES IN THE PROGRAM
      FACT=ST*C+S*(1.-CT)
      SB=SIN(BETA)
      CB=COS(BETA)
      IF(EL-ELWET) 20,20,22
20    ELWET=EL
22    IF(ELWET-ELBB)31,31,32
31    AWET=.5*(ELWET)**2/ELBB
      GO TO 21
32    AWET=(ELWET-ELBB)+0.5*ELBB
21    CONTINUE
      VRCG=SQRT(1.+(V(2))**2)
      ETA=ATAN(-V(2))
      EXCG=SQRT((ELD)**2+(EL-EDBAR)**2)
      DELTA=ATAN((EL-EDBAR)/ELD)
      VNLE=EXCG*V(6)
      GAMMA=ATAN((VRCG*COS(ETA)+VNLE*COS(DELTA))/(VRCG*SIN(ETA)+VNLE*SIN
     1(DELTA)))
C A AND B DETERMINE TERMS TO BE USED IN DE
      IF(DRAFT) 1,2,2
```

Table 7-2. Fortran Statement of Wave Response Computer Program (cont'd)

```
      2     IF(ROW) 4,3,3
      4     IF(GAMMA+V(3))70,70,71
      C     THIS IS THE SUBMERGED REGION
     70     Y=2.
            CALL CLCUR(CLSUB,XCPTE)
            LHSUB=ELD*SS+(XCPTE*EL-EDBAR)*C
            VP=7.1*ABAR/SQRT(32.2*CV*WLBAR)*COS(6.283*(LHSUB/WLBAR+X/T))
            1*EXP(6.283*ROW/WLBAR)
            DARM=ELD*CC-(XCPTE*EL-EDBAR)*S
            A10 =CLSUB*AWET*(1.+(V(2)+V(4)*LHSUB-VP)**2)/(2.*CDELO)
            R10=A10*(LHSUB-DARM*(S/C))/GYBAR**2
            ELNOS=.7*ELWET-EDBAR
            COREQ=((S+(VP-V(2)-V(4)*ELNOS)*C)/ST)**2
            IF(BETAT)77,77,78
     77     ROBYL=.RB/COS(BETAT)
            GO TO 79
     78     ROBYL=.RB*COS(BETAT)
            DARM=ELD*CC-(XCPTE*EL-EDBAR)*S
     79     A12=ROW*COREQ*FACT*ROBYL/CDELO
            R12=A12*(LHSUB-DARM*(S/C))/GYBAR**2
            IF(ABS(A10)-ABS(A12))440,440,441
    440     A=A10
            R=R10
            GO TO 9
    441     A=A12
            R=R12
            GO TO 9
     71     CALL CLCUR(CLSUB,XCPTE)
            LHSUB=FLD*SS+(XCPTE*EL-EDBAR)*C
            VP=7.1*ABAR/SQRT(32.2*CV*WLBAR)*COS(6.283*(LHSUB/WLBAR+X/T))
            1*EXP(6.283*ROW/WLBAR)
            DARM=ELD*CC-(XCPTE*EL-EDBAR)*S
            A=CLSUB*AWET*(1.+(V(2)+V(4)*LHSUB-VP)**2)/(2.*CDELO)
            R=A*(LHSUB-DARM*(S/C))/GYBAR**2
            GO TO 9
      C     THIS IS THE ZERO TRIM IMPACT REGION
      3     IF(TAUW-.0523) 5,6,6
      5     IF(BETA-.1745)97,97,98
     97     BETA=.1745
            GO TO 98
     98     CONTINUE
            ASTAR=7.7516*(.2459*(BETA)**2-.7446*(BETA)+.8024)*(1.-.5/ELWET)
            1*CB**2/SB**2
            ELIVP= FLWET/3.-EDRAR
            ELHDW=.3183*SB*CT/(CB*ST)
            ELIWW=ELWET-.666*ELHDW-EDBAR
            IF(FLHDW-ELWET)10,10,11
     11     ELHDW=ELWET
            A=ASTAR*(VV-V(2)-V(4)*ELIWP)**2*ELWET*DRAFT/CDELO
            GO TO 12
     10     A=ASTAR*(VV-V(2)-V(4)*ELIWW)**2*ELWET*SKITT/CDELO
            DARM=ELD*CC-ELIWP*S
     12     R=A*(ELIWP-DARM*(S/C))/GYBAR**2
            GO TO 9
      C     THIS IS THE PLANING REGION
      6     IF(FLWFT-ELRB) 80,80,81
```

7-21

Table 7-2.   Fortran Statement of Wave Response Computer Program (cont'd)

```
80      AR=1./ELBA
        GO TO 82
81      AR=1./ELWET
82      CONTINUE
        IF(GAMMA+V(3))410,410,420
C       THIS IS THE SCOOP REGION
410     ELNOS=FDBAR-.3*ELWET
        VP=7.1*ABAR/SQRT(32.2*CV*WLBAR)*COS(6.283*(ELNOS/WLBAR+X/T))
        COREQ=((S+(VP-V(2)-V(4)*ELNOS)*C)/ST)**2
        DARM=FLNOS*S+ELD*CC
        A=+ROW*COREQ*FACT*(.88*1./COS(BETAT)/CDELO
        B=A*(ELNOS-DARM*(S/C))/GYBAR**2
        GO TO 9
C       THIS IS THE SHUFORD PLANING REGION
420     CL6=1.5708*AR*TAUW*CT**2*(1.-SIN(BETAT)/(1.+AR)
        CL7=1.3333*ST**2*CT**3*COS(BETA)
        CLSKI=CL6+CL7
        FRACT=(.875*CL6+.5*CL7)/CLSKI
        LHPLA=TELWET*FRACT-EDBAR)*C+ELD*S
        VP=7.1*ABAR/SQRT(32.2*CV*WLBAR)*COS(6.283*(LHPLA/WLBAR+X/T))
        COREQ=((S+(VP-V(2)-V(4)*LHPLA)*C)/ST)**2
        DARM=ELD*CC-(FRACT*ELWET-EDBAR)*S
        A=CLSKI*COREQ*AWET/(2.*CDELO)
        B=A*(LHPLA-DARM*(S/C))/GYBAR**2
        GO TO 9
1       IF(ROW)8,7,7
8       VP=7.1*ABAR/SQRT(32.2*CV*WLBAR)*COS(6.283*(EX2  /WLBAR+X/T))
        IF(GAMMA+V(3))400,400,401
C       THIS IS THE SCOOP REGION
400     FLNOS=(FL-EDBAR)-.3*ELWET
        COREQ=((S+(VP-V(2)-V(4)*ELNOS)*C)/ST)**2
        IF(BETAT)87,87,88
87      ROBYL=.BB/COS(BETAT)
        GO TO 89
88      ROBYL=.BB*COS(BETAT)
        DARM=-FLNOS*S+ELD*CC
89      A=ROW*COREQ*FACT*ROBYL/CDELO
        B=A*(ELNOS-DARM*(S/C))/GYBAR**2
        GO TO 9
401     IF(TAUW-.0523)48,48,49
48      GO TO 5
49      FLNOS=(FL-FDBAR)-.7*FLWET
C THIS IS THE REVERSED SHUFORD PLANING REGION
        AR=1./ELWET
        CL6=1.5708*AR*TAUW*CT**2*(1.-SIN(BETAT)/(1.+AR)
        CL7=1.3333*ST**2*CT**3*COS(BETA)
        CLSHU=CL6+CL7
        COREQ=((S+(VP-V(2)-V(4)*ELNOS)*C)/ST)**2
        DARM=-FLNOS*S+FLD*CC
        A=CLSHU*COREQ*AWET/(2.*CDELO)
        B=A*(ELNOS-DARM*(S/C))/GYBAR**2
        GO TO 9
7       A=0.
        B=0.
C THE BASIC EQUATIONS OF MOTION
```

Table 7-2.   Fortran Statement of Wave Response Computer Program (cont'd)

```
      9     CONTINUE
            IF(V(3)-V(2)-RAN1)300,300,302
    300     AERO=SL1*(V(3)-V(2)-TAU)
            GO TO 305
    302     AERO=SL11+SL2*(V(3)-V(2))-SL1*TAU
    305     CONTINUE
            F(1)=V(2)
            F(2)=AERO/CLCVG+A-EQUIF+CLT*V(4)*DTBAR*SR*EP/CLCVG
            F(3)=V(4)
            F(4)=CM*(V(3)-V(2)-TAU)*CPAR/(CLCVG*GYBAR**2)+B-EQUIM-(EP    *CLT
           1*SR*(DTBAR/GYBAR)**2*V(4)/CLCVG
            RA=F(2)+ARM*F(4)
            RETURN
            END

      FEATURES SUPPORTED
        ONE WORD INTEGERS

      CORE REQUIREMENTS FOR FOFXY
        COMMON    134  VARIABLES     126   PROGRAM   2262

      END OF COMPILATION
```

Table 7-2. Fortran Statement of Wave Response Computer Program (cont'd)

```
* LIST SOURCE PROGRAM
* ONE WORD INTEGERS
      SUBROUTINE CLCUB(CLSUB,XCPTE)
      COMMON V(6),G(6),YO(6),FO(6),X
      COMMON ELWET,BOW,DRAFT,TAUW,WLBAR,CV,ABAR,EDBAR,EL,CDELO,GYBAR,
     1THETA,DTBAR,ELD,CLT,SR,CM,CBAR,CLCVG,EF,EQUIF,EQUIM,TAV,OMEGA,
     2AR2,ELRR,SKITT,G1,Y,REDUC,ARM,THETA,ETA,DYNAM,BA,BETAT,GAMMA,
     3PAN1,SL1,SL11,SL2,HEQB
      AP=1./FL
      Y=-ROW/EL
      ALPHA=V(3)+OMEGA-V(2)
      F=3.1416*(1.-.344*Y**.2125)
      C=.3183/(AR+1.)
      ZN=ALPHA/(2.29*C*COS(ALPHA))
      ZPSI=(1.+C*F*COS(ALPHA))/(4.58*C*COS(ALPHA))
      CL1=3.1416*AR*((ALPHA-ZPSI)+SQRT(ZPSI**2-ZN))
      CL2=.88*SIN(ALPHA)**2*COS(ALPHA)/(AR+1.)
      CL=CL1+CL2
      XCP=(.3125*CL1+.5*CL2)/CL
      XCPTE=1.-XCP
      CLSUB=CL
      RETURN
      END

FEATURES SUPPORTED
ONE WORD INTEGERS

CORE REQUIREMENTS FOR CLCUB
COMMON    134  VARIABLES    28  PROGRAM    206

END OF COMPILATION
```

Table 7-2.   Fortran Statement of Wave Response Computer Program (cont'd)

```
* LIST SOURCE PROGRAM
* ONE WORD INTEGERS
      SUBROUTINE OUTPT
      COMMON V(6),F(6),YO(6),FO(6),X
      COMMON ELWET,BOW,DRAFT,TAUW,WLBAR,CV,ABAR,EDBAR,EL,CDELO,GYBAR,
     1THETA,DTBAR,ELD,CLT,SR,CM,CBAR,CLCVG,EP,EQUIF,EQUIM,TAU,OMEGA,
     2AR2,ELBR,SKITT,G1,Y,REDUC,ARM,THETA,ETA,DYNAM,BA,BETAT,GAMMA,
     3RANI,SL1,SL11,SL2,HEQB
      WRITE(3,100)X,V(1),V(2),F(2),V(3),V(4),F(4),ELWET,BOW,DRAFT,TAUW,
     1AA
100   FORMAT(1H ,F10.3,11F10.7)
      RETURN
      END

FEATURES SUPPORTED
   ONE WORD INTEGERS

CORE REQUIREMENTS FOR OUTPT
   COMMON    134  VARIABLES       4   PROGRAM       46

END OF COMPILATION
```

A. FIXED-TRIM IMPACT LOADS

In the present program, the fixed-trim condition can be achieved most readily by assigning an arbitrary extreme high value to I, the aircraft moment of inertia, thus effectively making $\ddot{\tau} = 0$, so that τ retains its initial value. The remaining initial conditions can then be selected to represent any desired landing impact, including the initial contact point on the wave flank. In that case, the initial portion of the time history furnished by the present program will be coincident with that given by the program of Section 5.

B. PLANING STABILITY

The smooth water condition is, of course, a special case where the wave height is taken as zero and any finite arbitrary wave length is used. With these restrictions, the applicable initial conditions for the present program can be conveniently taken as:

$$\dot{h} = \dot{\tau} = 0, \ \tau = \tau_{eq} + \Delta\tau, \quad d = d_{eq}$$

Here, d_{eq} is the draft at τ_{eq} (at the selected speed), and $\Delta\tau$ is some small arbitrary angle, say 1/4 degree.

Using these initial conditions, a run is made wherein the trim time history takes the form of an oscillation with either divergent, constant, or subsident amplitudes. For a fixed forward speed, it is a simple matter to vary τ_{eq} to obtain that value of τ_{eq} corresponding to oscillations of constant trim amplitude. This then represents a point on the lower neutral dynamic stability boundary (R = 0 curve).

While this is not difficult to do, the separate program of Section 6 for calculating the R = 0 curve is considered preferable to the procedure just described which requires the intervention of the engineer.

7.4   CORRELATION OF TEST DATA

7.4.1   Description of Test Data

References 7-1 and 7-2 describe a series of towing tank tests of several hydro-ski installations on a 1/16 dynamic scale model of the HU-16 (Grumman Albatross) seaplane. Of the three skis tested, attention will be centered herein on Skis Nos. 1 and 2 which had beam loadings of 60 and 100, respectively, deadrise angles of 22 1/2°, and respective length-beam ratios of 5.20 and 5.48.

Among several other items, the tank tests included take-off runs in regular waves (4 ft. x 120 ft., full-scale). Among the test data are the vertical accelerations, obtained in the (full-scale) speed range of 60-80 knots, measured at the c.g. and at the bow (1 ft. forward of c.g., model scale). Aside from a few details of minor importance, such

as the presence of small longitudinal accelerations in the model tests, it was assumed that the present computer could correctly simulate the high speed portions of the model runs which, in view of the relatively low accelerations recorded, were assumed to involve no genuine wetting of the hull (aside from spray). Thus, in effect, complete agreement between the model tests and present calculations would be indicated provided both of the following conditions were met:

      a. Using plausible interpretations of the calculated values, the calculated and measured c.g. and bow accelerations were reasonably close;

      b. The calculations showed ski immersions not exceeding the model strut length.

7.4.2   Computer Calculations

      Calculations were made for a full-scale speed of 70 knots using an equilibrium (hull keel) trim angle of 11.3° (figure 15, p. 37, Reference 7-2, for V_M = 30.3 fps). This trim angle is the free-to-trim value for the chosen speed and an elevator angle of −25 degrees, as measured in the tank, and includes the effects of the fixed unloading and pitching moment values applied to the model to simulate slipstream effects. Furthermore, it is known from the tank tests that no porpoising occurred at this speed-trim combination, thus making it unnecessary to perform a planing stability check.

      In accordance with the discussion at the end of Section 7.2, the calculations included five runs made with four of the five initial conditions the same:

$$\text{Ski T.E. Draft} = \dot{h} = \dot{\tau} = 0, \ \tau = \tau_{eq} = 11.3°,$$

but with varying initial locations on the wave flank of the ski T.E., i.e., wave heights at the ski T.E.:

$$y_w (T.E.) = -H/2, \ -H/2\sqrt{2}, \ 0, \ +H/2\sqrt{2}, \ +H/2$$

where: $y_w (T.E.) = (H/2) \sin\left[(2\pi/L)(p \sin \tau_{sk} - q \cos \tau_{sk}) - \theta\right]$

and p and q are defined by the sketch of Appendix C.

      Each run was made for a duration of ten (10) full wave cycles, with surveillance of the print-out process to ascertain the presence of physically unacceptable values of trim and/or ski draft because no limitations on these two quantities had been built into the program. This number of wave cycles far exceeds the number of waves encountered by the towing tank model in the high speed portion of a take off run.

7.4.3   Principal Features of Computed Time Histories

The print-outs of the computed wave response time histories (not included in this report) were carefully reviewed to:

A.   Obtain an overall picture of the general nature of the motions for each ski beam loading; and

B.   Extract significant data (particularly maximum accelerations and strut drafts) together with associated information on ski-wave geometry and kinematical quantities.

The data, and their correlation with the towing tank measurements will be presented below, while the following discussion covers the gross aspects of the computed time histories.

Briefly stated, the calculated motions and accelerations for the HU-16 with the C_{Δ_o} = 60 ski are appreciably more severe than those for the same aircraft with the

C_{Δ_o} = 100 ski.   As typical examples, both the maximum c.g. and maximum bow vertical

accelerations are greater, the maximum ski drafts are appreciably greater, and both the airborne vertical excursions and airborne dwelling time are greater for C_{Δ_o} = 60.

The total trim range is also appreciably larger, and includes frequent occurrence of stalling. These basic results can be explained with following manner.

As a direct consequence of the lower beam loading, the impact loads in the early portion of the C_{Δ_o} = 60 ski run-outs are relatively large and so are the associated

pitching moments.   These give rise to relatively larger values in the later impacts.   The greater trim motions generated by the larger pitching moments create substantially larger trim ranges for the lower ski beam loading.   Thus, on the one hand, the larger high trim values result in higher positive accelerations which are, of course, further aggravated by aircraft stalling (if present).   On the other hand, the reduced lower trim values, in conjunction with the specific wave impact location and flight path angle, are occasionally capable of producing such low load impacts that relatively considerable ski submergence occurs.

As will be seen below, the average trim change in the higher beam loading ski run-outs was only two degrees.   This result correlates with past qualitative observations that very high beam loading skis produce a "plowing through the waves" effect.

However, it is important to emphasize that the comparative behavior of this same aircraft with the two different skis is not necessarily due exclusively to the difference in the ski beam loading, but may depend in part on the specific aerodynamics, specific wave conditions, and specific speed selected.   Thus, considerably more parametric study is required before genuinely valid claims can be made.

7.4.4 Significant Data from Computed Time Histories

Significant data from the computed time histories is summarized in Table 7-3A. All values listed are for full-scale. In addition to the values obtained from the individual runs, this table also includes the averaged, i.e., statistical values. In addition to the features discussed above, maximum sink speed values are listed. These values are also appreciably higher for the low beam loading ski. Lesser acceleration values were also tabulated (not included herein) to ensure that the maximum values obtained are statistically realistic.

Thus, there is no question that, at least from a qualitative standpoint, the computer results agree with the general empirical experience that high beam loading skis alleviate motions and accelerations in rough water.

7.4.5 Comparison with Tank Data

For convenience, the available tank data, taken from Reference 7-2, is listed in Table 7-3B. It is seen, in the first place, that any attempt at correlation is limited because the only quantities measured in the tank were the two vertical accelerations. Specifically, no draft measurements were made nor is there any other way of telling whether the tank maximum accelerations involved hull impacts. This feature is discussed at greater length below.

It is equally important to note that the tank data are for a finite speed range while the computer data are for one specific speed (midpoint of tank speed range). This difference can possibly confuse the correlation as the effect of forward speed on the computed results has not been determined and cannot be readily predicted.

Finally, it is noted again that the computer runs were made using arbitrary <u>mild</u> initial conditions. It is entirely plausible to suppose that, for both skis, the motions would be more severe had less mild conditions been used, for example, by assuming some finite (non-zero) initial sink speeds.

With these important reservations in mind, the closest possible explanation for the discrepancies appear to be the following. Considering first the $C_{\Delta_o} = 100$ ski, the

computer showed lower vertical accelerations than did the tank tests, and also indicated no strut wetting in any run. (The actual full-scale strut length is 4.0 feet for both ski installations.) The discrepance in the vertical loads is likely due to one or both of the two reasons just cited (speed range and initial conditions). The severe motions from these causes would give somewhat larger submergence which, for the actual hull configuration, would be adequate to create hull impacts and thus further exaggeration of the accelerations. This explanation, of course, assumes that the maximum tank accelerations obtained with this ski were, in fact, associated with hull impacts. Finally, it may be noted that, while appreciable numerical differences exist between the comparable average accelerations, their differences are identical (.56 - .57g). This result is considered to lend credibility to the preceding explanation.

TABLE 7-3. HIGH-SPEED PLANING DATA: HU-16 HYDRO-SKI INSTALLATIONS IN 4 FT. x 120 FT. WAVES

A. COMPUTER PROGRAM DATA (V = 70 KNOTS, NO WIND)

Run No.	Init Ski Loc	SKI NO. 1, C_{Δ_o} = 60, l/b = 5.20						SKI NO. 2, C_{Δ_o} = 100, l/b = 5.48					
		Max C.G. Accel (g)	Max Bow Accel (g)	Max Ski Draft (ft)	Max Keel Trim (deg)	Min Keel Trim (deg)	Max Sink Speed (fps)	Max C.G. Accel (g)	Max Bow Accel (g)	Max Ski Draft (ft)	Max Keel Trim (deg)	Min Keel Trim (deg)	Max Sink Speed (fps)
1		.87	1.35	4.0	15.8	9.3	7.6	.44	.66	4.0	11.2	9.8	1.7
2		1.14	1.89	5.4	16.3	7.8	8.8	.52	.77	3.0	11.0	10.8	3.9
3		1.03	1.76	3.4	15.4	9.2	6.3	.50	.82	2.1	11.3	10.4	1.0
4		.99	1.68	4.5	16.9	5.4	9.2	.58	.77	2.5	12.2	9.0	2.4
5		1.06	1.80	3.3	15.0	9.1	6.3	.61	.94	3.0	13.0	8.7	3.6
AVERAGE:		1.02	1.67	4.1	15.9	8.0	7.6	.53	.79	2.9	11.7	9.7	1.9

B. TANK DATA FOR 1/16 -SCALE MODEL (V = 60 - 80 KNOTS, NO WIND)

Run No.	Init Ski Loc	SKI NO. 1						SKI NO. 2					
		Max C.G. Accel (g)	Max Bow Accel (g)	Max Ski Draft (ft)	Max Keel Trim (deg)	Min Keel Trim (deg)	Max Sink Speed (fps)	Max C.G. Accel (g)	Max Bow Accel (g)	Max Ski Draft (ft)	Max Keel Trim (deg)	Min Keel Trim (deg)	Max Sink Speed (fps)
1	*	1.20	2.05	*	*	*	*	1.30	1.50	*	*	*	*
2	*	1.05	1.55	*	*	*	*	1.10	1.40	*	*	*	*
3	*	1.05	1.40	*	*	*	*	1.00	1.40	*	*	*	*
4	*	1.00	1.15	*	*	*	*	1.00	1.10	*	*	*	*
AVERAGE:		1.08	1.54	*	*	*	*	1.10	1.35	*	*	*	*

* Unknown   NOTE: Full-scale strut length = 4.0 feet

The exceptionally close agreement between both the ranges and average values of computed and measured c.g. and bow accelerations for the C_{Δ_o} = 60 ski installation

requires very little further comment. The one point requiring explanation is that two of the computed maximum ski drafts exceeded the actual strut length. It might thus be anticipated that the tank model could generate higher accelerations than those given by the computer. The actual fact is that the large ski drafts occurred only a few times in the computer runs and it is possible that they were "missed" in the tank runs because of the very limited number of impacts occurring therein.

Alternately, it is also conceivable that hull impacts did occur in the tank runs but, since a hydro-ski can effectively reduce the hull impact velocities, hull impact accelerations did not exceed the hydro-ski impact accelerations.

7.4.6 Discussion

It is obvious that, while these particular HU-16 tank tests remain as the only available test data, their correlation with the computer runs will remain unclear. This difficulty can only be resolved by conducting a series of towing tank tests on a skeleton hydro-ski seaplane model. With such tests, procedures and measurements could be used to permit far more direct correlation with the computer program results.

Although some of the results of the computer program are subject to further examination, either because of the simplified mathematical model or lack of suitable comparative towing tank data, further parametric studies could have been made to establish the relative effects of the operational environment on hydro-ski seaplanes in the high-speed range. Of particular interest would have been computer runs to ascertain the effects of variation in wave height and wave length. Unfortunately, as a result of the technical effort involved in developing the computer program, no time and funds were available within the present contract to conduct these investigations. This subject is pursued further in Section 10 of this report.

REFERENCES

7-1   Davidson Laboratory Letter Report LR-976: "Development Tests of HU-16 Hydroski Aircraft," by R. L. Van Dyck, October 1963.

7-2   Grumman Aircraft Engineering Corp., Report No. XA 111-108-4: "Hu-16 Hydroski Development," by T. B. Street, February 1964.

8. HYDRO-SKI LONGITUDINAL LOCATION

As part of the present survey, attempts were made to correlate actual hydro-ski longitudinal locations, as determined from towing tank tests, with the most significant hydrodynamic ski parameters, such as ski beam loading. If successful, a correlation of this type would substantially reduce the preliminary design effort currently necessary for the establishment of an optimum hydro-ski location. For this purpose, an examination was made of all available geometric data on towing tank models (and full-scale hydro-ski configurations) exhibiting satisfactory hydrodynamic characteristics.

The approaches used in these attempted correlations were based on the successful, but limited, correlation shown in Figure 5 of Reference 8-1. These results, which correlate the longitudinal locations of ski centers of pressure with ski length, are for a variety of skis tested on a single seaplane model (one gross weight), the tests covering only rough-water landings.

A variation of this approach was first attempted, in which the basic parameters were non-dimensionalized as follows:

1) The "longitudinal location parameter" was taken as the angle between a line joining the aircraft c.g. and the ski c.p. (taken, as in Reference 8-1, at 2/3 ski length forward of ski T.E.) and the perpendicular from the c.g. to the ski keel;

2) Instead of the ski length, the "ski size parameter" was taken as the ski beam loading.

The "correlation" of these two quantities, shown in Figure 8-1, covers eighteen different model and prototype aircraft (some with several skis). These configurations are identified in Table 8-1. It is seen that, although there is a general trend of increasing inclination angle with increasing beam loading, the data spread is much too large to permit construction of a representative curve, or even a representative band of values. In brief, the correlation is considered to be much too poor for practical use in preliminary design work.

Further attempted correlations were then made using various other combinations of non-dimensional "longitudinal location" and "ski size" parameters. In all cases, these attempts were equally unsuccessful. As a principal result of these studies, it was concluded that other configuration parameters have significant effects on optimum ski location and would thus have to be accounted for in the correlation process. It is reasonable to assume that, in addition to possible geometric parameters such as ski length-beam ratio and ski incidence, the correlation must account for the aircraft aerodynamic parameters, particularly such items as longitudinal static stability and control parameters (say,

$(\partial C_M / \partial C_L)_{\delta_e}$ and $(\partial C_M / \partial \delta_e)_{C_L}$ maximum elevator deflections, etc.
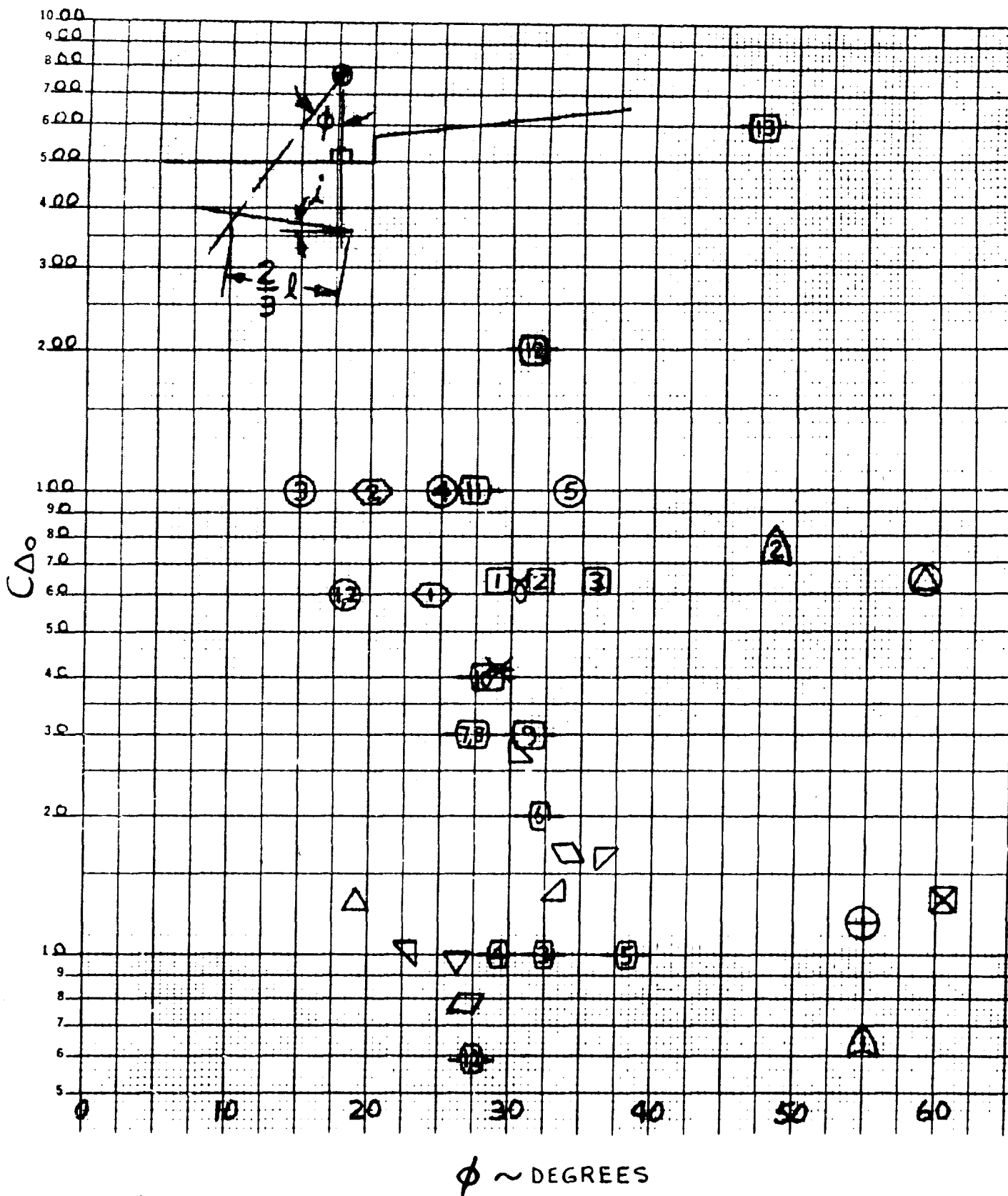
Figure 8-1. C_{Δ_0} vs ϕ for Various Hydro-Ski Seaplanes

TABLE 8-1

IDENTIFICATION CODE FOR FIGURE 8-1

CODE	REFERENCE	A/C	l/b	i (DEGREES)
—①—	8-1	1/12 scale Dynamic Model	3.25	0
—②—	8-1	1/12 scale Dynamic Model	2.81	0
—③—	8-1	1/12 scale Dynamic Model	5.12	0
—④—	8-1	1/12 scale Dynamic Model	4.23	0
—⑤—	8-1	1/12 scale Dynamic Model	6.12	0
—⑥—	8-1	1/12 scale Dynamic Model	6.12	0
—⑦—	8-1	1/12 scale Dynamic Model	5.69	0
—⑧—	8-1	1/12 scale Dynamic Model	5.30	0
—⑨—	8-1	1/12 scale Dynamic Model	6.12	0
—⑩—	8-1	1/12 scale Dynamic Model	6.12	0
—⑪—	8-1	1/12 scale Dynamic Model	6.12	0
—⑫—	8-1	1/12 scale Dynamic Model	6.12	0
—⑬—	8-1	1/12 scale Dynamic Model	6.12	0
△	8-2	Hypothetical Jet Propelled Airplane	4.00	4.5
▽	8-3	Grumman JRF-5	4.00	0
�	8-4	Convair Skate 7 Seaplane	6.12	2
◿	8-5	Edo Model 142 Hydro-Ski Research Airplane	5.50	0
◹	8-6	Grumman JRF-5	3.476	0
▽	8-7	1/24 scale Dynamic Model Seaplane	4.00	0

TABLE 8-1 (Cont'd)

CODE	REFERENCE	A/C	1/b	i (DEGREES)
⟋⟍	8-8	Martin PBM-5 Seaplane	3.462	0
⬡	8-9	1/24 scale Dynamic Model Seaplane	4.00	0
⊕	8-10	Supersonic Multijet Bomber	5.78	2
1	8-11	Thurston-Erlandsen Hydro-Ski Aircraft	3.466	0
2	8-11	Thurston-Erlandsen Hydro-Ski Aircraft	3.466	0
3	8-11	Thurston-Erlandsen Hydro-Ski Aircraft	3.466	0
①	8-12	Grumman HU-16	5.198	0
②	8-12	Grumman HU-16	5.198	0
③	8-12	Grumman HU-16	5.474	0
④	8-12	Grumman HU-16	5.474	0
⑤	8-12	Grumman HU-16	5.474	0
⬟	8-13	XF2Y-1	6.00	3
⟨1⟩	8-14	Grumman HU-16	5.198	0
⟨2⟩	8-14	Grumman HU-16	5.198	0
⊠	8-15	Supersonic Multi-Jet Aircraft	7.33	2
✳	8-116	PBM-5S	3.47	0
△1	8-17	Martin 329C-2	4.07	0
△2	8-17	Martin 329C-2	4.65	0
γ	8-18	HRV-1	3.46	8

Further investigation of this problem area was considered infeasible, partly because of the large additional effort involved, and partly by the lack of (readily available) required aerodynamic data for most of the aircraft. Although some of the aerodynamic parameters could have been estimated, it was felt that such effort was not warranted because of the inability to estimate accurately such features as power-on effects for prototype aircraft, ground effects for both prototype and model aircraft, etc.

Consequently, until much better correlations are achieved, towing tank model tests are still considered to furnish the only practical method for final determination of optimum hydro-ski longitudinal locations. In addition to the usual take-off and landing runs, such tank tests should also include rough-water constant-speed taxi tests covering the applicable speed range.

REFERENCES

8-1   NACA RM L56I25a: "Tank Investigation of a Series of Related Hydro-Skis as Load-Alleviation Devices for Landing a Seaplane in Waves," by A. W. Carter, A. E. Morse, Jr., and D. R. Woodward, December 1956.

8-2   NACA RM L7I04: "Preliminary Tank Tests of NACA Hydro-Skis for High-Speed Airplanes," by J. R. Dawson and K. L. Wadlin, 26 November 1947.

8-3   NACA RM L9K29: "Tank Investigation of the Grumman JRF-5 Airplane Fitted with Hydro-Skis Suitable for Operation on Water, Snow and Ice," by K. L. Wadlin and J. A. Ramsen, 12 June 1950.

8-4   NACA RM SL51F07a: "Hydrodynamic Investigation of a 1/13-scale model of the Consolidated Vultee Skate 7 Seaplane Equipped with Twin Hydro-Skis," by R. E. McKann, C. W. Coffee, and D. D. Arabian, 12 September 1951.

8-5   NACA RM SL51I24: "Tank Investigation of the Edo Model 142 Hydro-Ski Research Airplane," by J. A. Ramsen, K. L. Wadlin, and G. R. Gray, 24 September 1951.

8-6   NACA RM SL52D17:   "Tank Investigation of the Grumman JRF-5 Airplane Equipped with Twin Hydro-Skis," by J. A. Ramsen and G. R. Gray, 10 April 1952.

8-7   NACA RM L53F04:   "A Brief Hydrodynamic Investigation of a Navy Seaplane Design Equipped with Hydro-Ski," by L. J. Fisher and L. Hoffman, 1 September 1953.

REFERENCES (Continued)

8-8   NACA RM SL55L15: "Tank Tests of a 1/8-Size Powered Dynamic Model
       of the Martin PBM-5 Seaplane Equipped with a Single Edo Hydro-Ski,"
       by C. W. Coffee, Jr., 6 January 1956.

8-9   NACA RM L56D26: "Comparison with Theory of Landing Impacts of a Model
       of a Seaplane Incorporating a Hydro-Ski with and without a Shock Absorber,"
       by E. L. Hoffman, 11 July 1956.

8-10   NACA RM L57G05: "Aerodynamic and Hydrodynamic Characteristics of a
       Proposed Supersonic Multijet Water-Based Hydro-Ski Aircraft with a Variable-
       Incidence Wing," by W. W. Petynia, F. Hasson, and H. Spooner, 23 October
       1957.

8-11   Davidson Laboratory, S.I.T. R-934:   "Development Tests of Thurston-
       Erlandsen Hydroski Aircraft," by R. L. Van Dyck, March 1963.

8-12   Davidson Laboratory, S.I.T. LR-976: "Development Tests of HU-16
       Hydroski Aircraft," by R. L. Van Dyck, October 1963.

8-13   Convair Report ZC-2-065:   "Small Ski Research Program on the XF2Y-1,
       Airplane," by F. H. Sharp and E. E. Whigham, October 1957.

8-14   Grumman Report XA 111-108-3: "HU-16 Hydroski Development," by T. B.
       Street, August 1963.

8-15   NACA Memo 10-13-58L: "Low Speed Aerodynamic and Hydrodynamic
       Characteristics of a Proposal Supersonic Multijet Water-Based Hydro-Ski
       Aircraft with Upward Rotating Engines " by W. Petynia, D. R. Croom,
       and E. E. Davenport, October 1958.

8-16   Davidson Laboratory, S.I.T. R-681: "To Evaluate the Hydrodynamic
       Characteristics of the PBM-5S on a Small Penetrating Hydro-Ski," by
       G. Fridsma, 14 March 1958.

8-17   Convair Report ZH-139: "Towing Tank Evaluation of Hydro-Ski
       Alighting Gear," by W. B. Barkley, October 1959.

8-18   Thurston-Erlandsen Corp. Report 6302-4: "Final Summary Report Flight Test
       of the Hydro-Ski Research Vehicle HRV-1 Equipped with the PBM Type Ski,"
       by D. B. Thurston, 25 November 1963.

9. SURVEY OF HYDRO-SKI INSTALLATION WEIGHTS

9.1 GENERAL

For the preliminary weight estimation of new operational hydro-ski seaplane configurations, it is desirable to have a background of weight data on previous installations, including the separate contributions of the hydro-ski, its support strut, and the hull carry-through structure. Although several full-scale seaplanes have been flown with hydro-skis installed, all of these installations were basically experimental in nature where the primary consideration was the development of a "working" configuration that could safely explore and advance hydro-ski seaplane technology.

With only one exception, all full-scale hydro-ski seaplanes flown to date have been conversions of existing aircraft. The single exception was the Convair XF2Y "Sea Dart" and even this aircraft had two subsequent modifications in its basic hydro-ski configuration.

The early developmental stage in the state-of-the-art, combined with the desire to minimize engineering and manufacturing costs, admittedly resulted in very conservative structural design approaches for these hydro-ski installations. It can therefore be anticipated that, for new operational aircraft, the hydro-ski installation weight fraction (percent of aircraft gross weight) should be distinctly improved over those indicated in the present weight survey. In this connection, it is obvious that the method presented in Section 5 of this report for the estimation of rough-water impact loads constitutes the foundation of an accurate and rational method for the structural design of hydro-skis and, thus, for the development of rational ski weight formulas.

9.2 HYDRO-SKI WEIGHT

Table 9-1 lists the hydro-ski weights for previous installations, together with the parameters which appear in the hydro-ski weight formula proposed by the Martin Company in Reference 9-1. This formula is:

$$W_{ski} = .112 \, (n_1 \, \Delta_0 \, l_{sk}^2)^{1/2}$$

where: Δ_0 = aircraft design gross weight, lbs

n_1 = design ultimate load factor

l_{sk} = hydro-ski length (ft)

TABLE 9-1

HYDRO-SKI WEIGHTS

Martin Formula: $W_{SKI} = .112(n_1 \Delta_o l_{sk}^2)^{1/2}$
Edo Formula: $W_{SKI} = K(n_1 \Delta_o l_{sk})$

$K = .000443$ (single skis), $.000774$ (twin skis)

AIRCRAFT	REMARKS	W_{SKI} (actual) lbs	n_1 —	Δ_o lbs	l_{sk} ft	W_{SKI} (Martin) lbs	W_{SKI} (Edo) lbs
OA-9(Goose I)	Single, also designed for snow and ice	185	5.3	8400	9.33	220	184
JRF-5(Goose II)	Single	135	4.89	8400	8.67	197	158
JRF-5(Goose III)	Twin (actual weight less wheels)	141	5.15	4200	6.75	111	113
PBM-5 (Large Ski)	Single, strut location not optimum	1581	5.68	55000	16.2	1020	2242
PBM-5 (1/3 Area Ski)	Single, strut at ski stern	1000	3.75	55000	9.36	475	855
YF2Y-1	Twin	389	4.5	8250	18.85	408	542
XF2Y-1	Single large ski	979	5.1	19100	22.5	787	970
OTTER	Twin, non-buoyant aircraft	159	4.5	4000	9.58	143	133
OE-1	Twin, non-buoyant aircraft	28	5.13	1215	6.86	61	33
HRV-1 (Ski #1)	Single ski, Al. Al. casting	24	5.42	2700	2.92	40	19
HRV-2 (Ski #2)	Single, "bent-plate" ski	18	5.42	2700	2.79	38	18

The data in table 9-1 is graphically presented in Figure 9-1. It can be seen that the points in the left hand portion are above the range of good agreement, while those on the right side tend to be below. A revised hydro-ski weight formula is therefore suggested which, as illustrated in Figure 9-2, results in a significant correlation improvement.

The revised hydro-ski weight formula is:

$$W_{SKI} = K(n_1 \Delta_o l_{sk})$$

where: n_1, Δ_o and l_{sk} are as above,

and, $K = .000443$ for single ski installations

$K = .000774$ for twin ski installations

It should be noted that neither the Martin nor the Edo expressions for hydro-ski weight account for the location of the support strut or struts, although most hydro-skis can be categorized as beam-type structures. Accordingly, an even further refinement in the hydro-ski weight formula could probably be obtained if strut location were to be considered.

9.3 HYDRO-SKI STRUT WEIGHT

Weight data for hydro-ski support struts are contained in Table 9-2. The ski strut weight formula proposed by the Martin Co. in Ref. 9-1, is:

$$W_{STRUT} = .001 (n_1 \Delta_o l_{st})$$

where: n_1 and Δ_o are as above,

and, $l_{st} = $ exposed strut length

From Figure 9-3, it is seen that the correlation between the actual strut weights and those given by the Martin formula is unacceptably poor. For this reason, a new formula has been developed. This is:

$$W_{st} = .262 (n_1 \Delta_o l_{st}^2)^{1/2}$$

which, as can be seen from Figure 9-4, generally results in a much improved agreement, except in the region applicable to lightweight aircraft (2000 lbs. — 5000 lbs.).
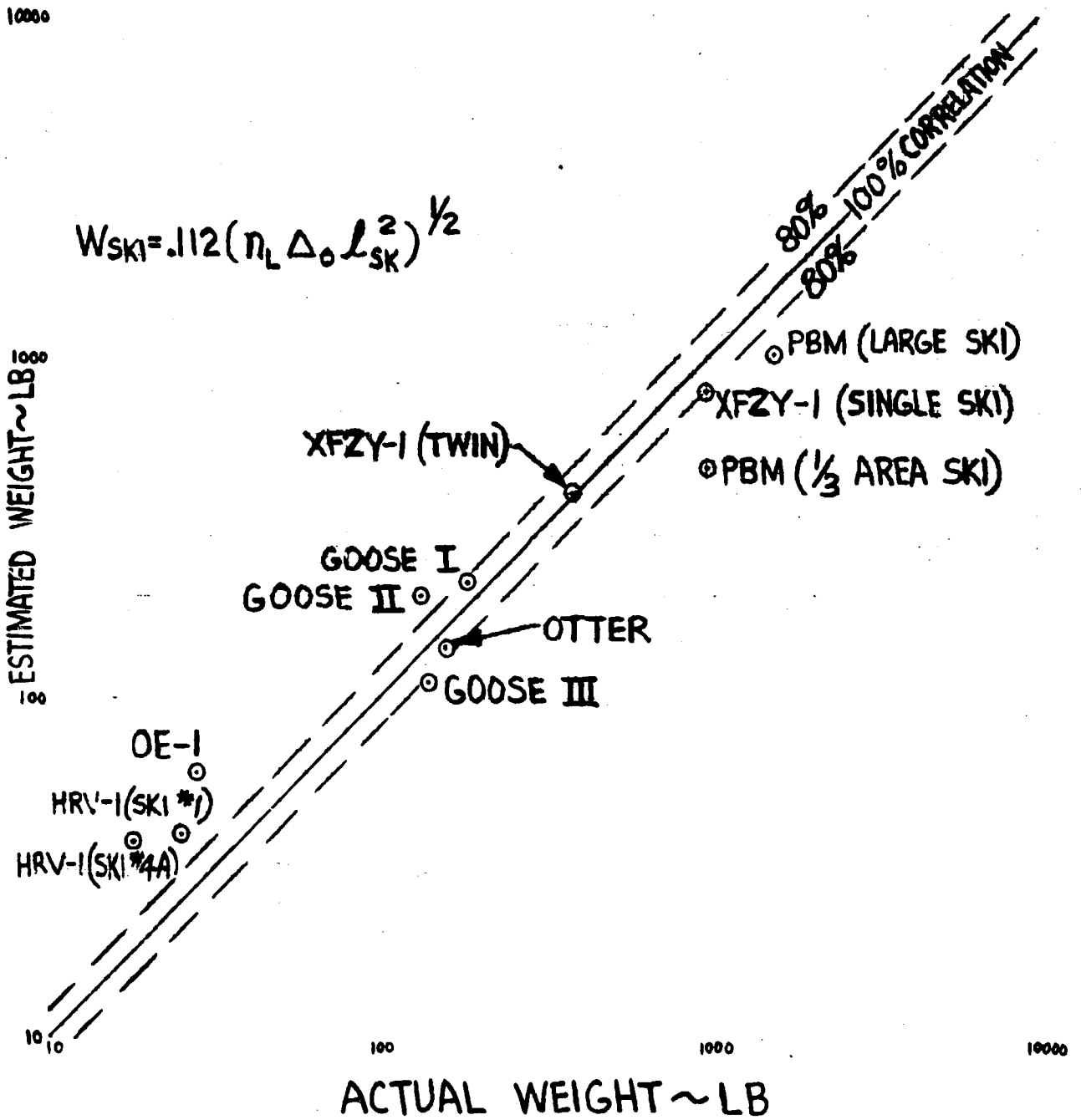
$$W_{SKI} = .112 \left(n_L \, \Delta_o \, \ell_{SK}^2 \right)^{1/2}$$

Figure 9-1. Comparison of Actual Ski Weights with Martin Formula Values

$$W_{SKI} = K (n_L \Delta_o l_{SK})$$

K = .000443 (SINGLE SKI)
K = .000774 (TWIN SKI)
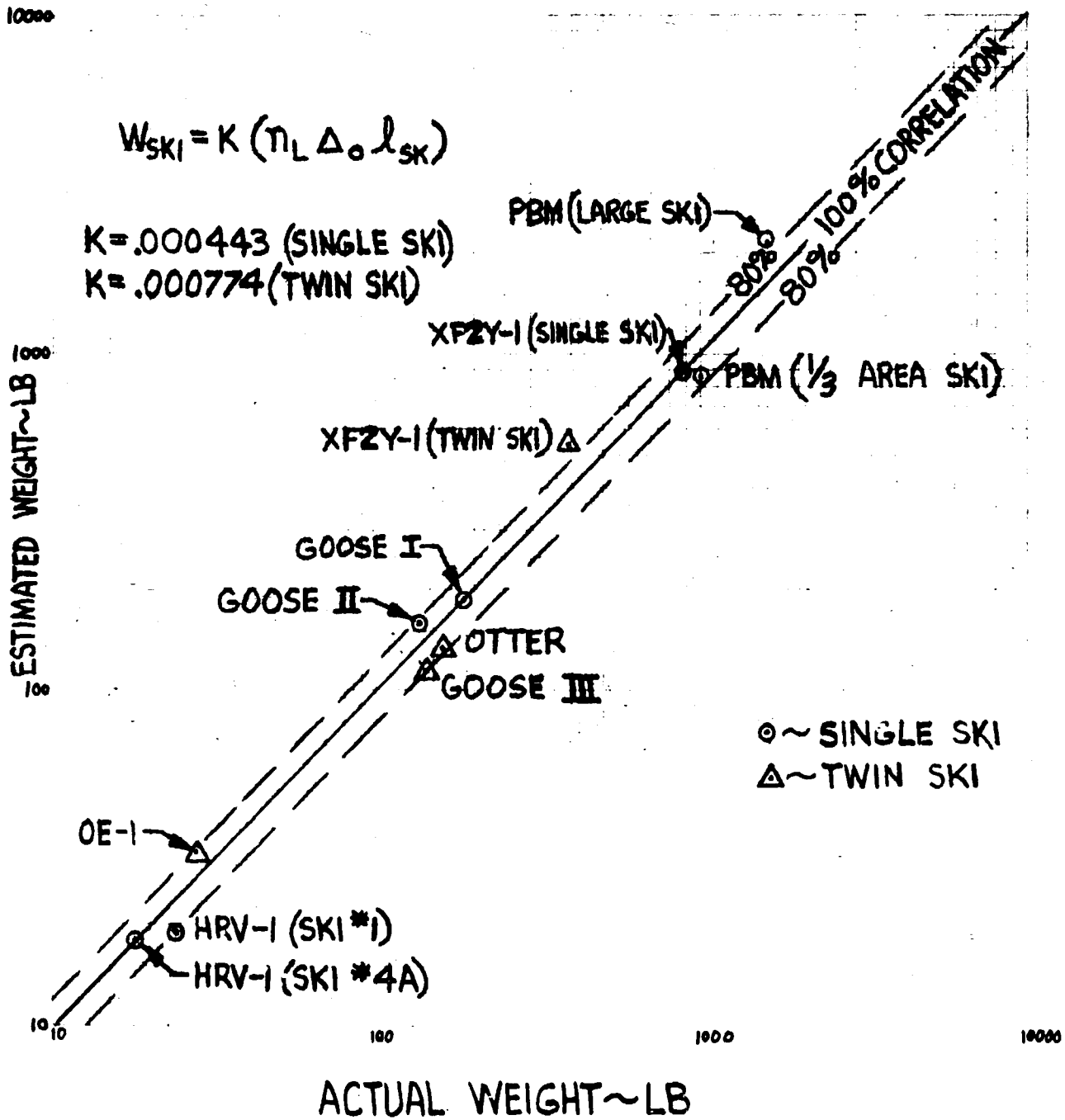
Figure 9-2. Comparison of Actual Ski Weights with Edo Formula Values

$$W_{STRUT} = .001 (n_l \, \Delta_o \, \ell_{ST})$$
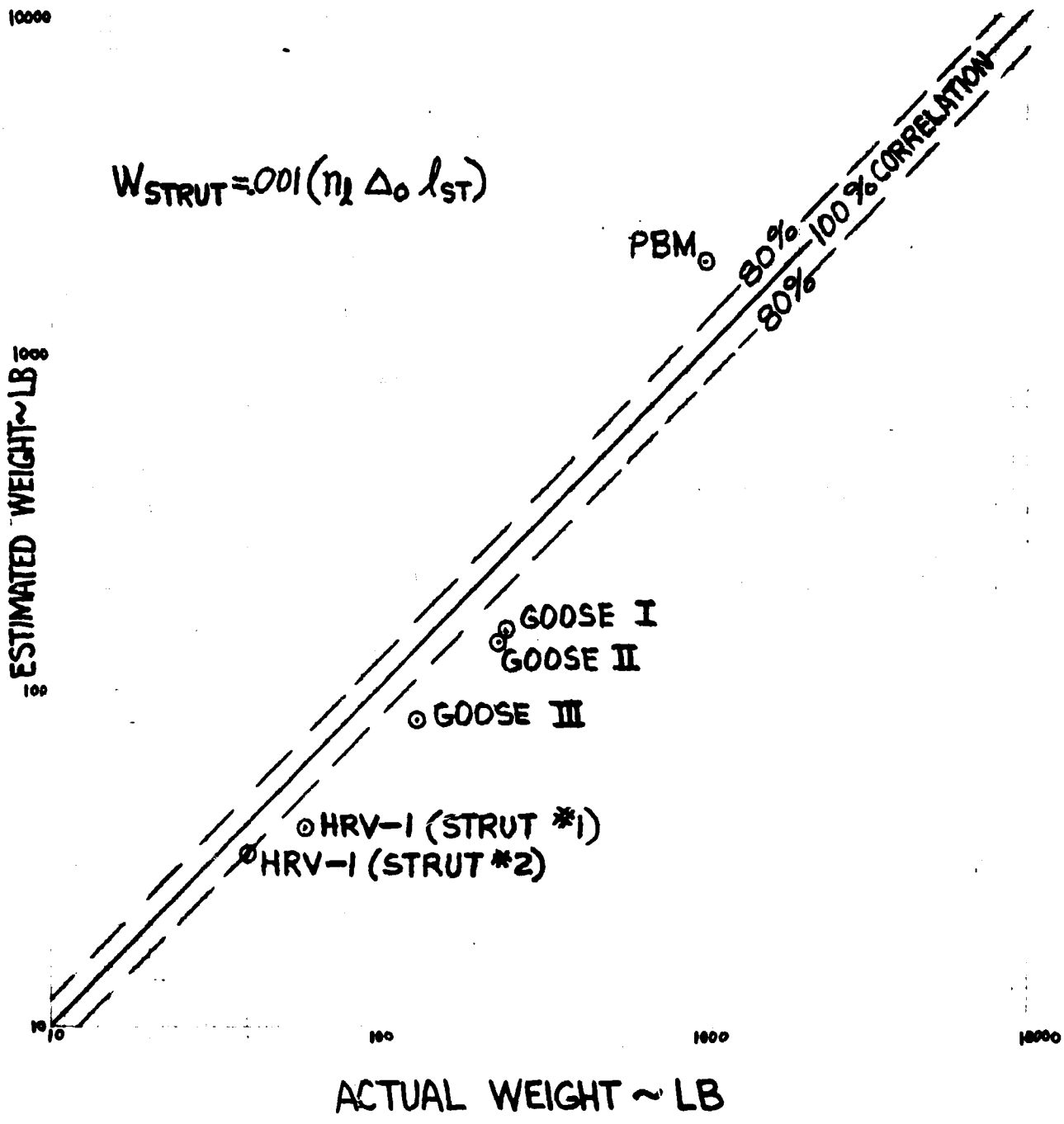
Figure 9-3. Comparison of Actual Strut Weights with Martin Formula Values

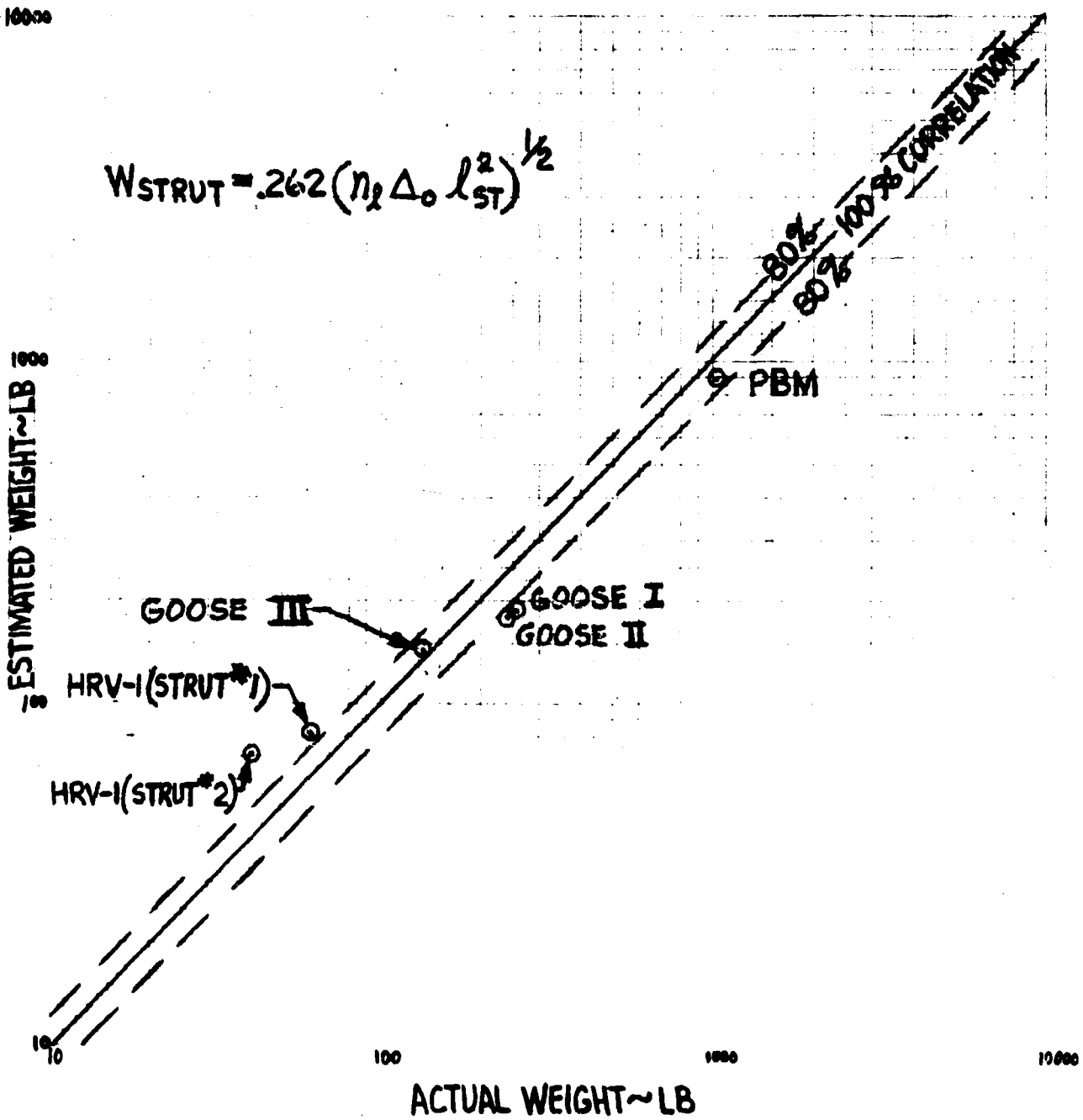$$W_{STRUT} = .262\left(n_\ell \Delta_o \ell_{ST}^2\right)^{1/2}$$

Figure 9-4. Comparison of Actual Strut Weights with Edo Formula Values

TABLE 9-2

STRUT WEIGHTS

Martin Formula: $W_{st} = .001 (n_1 \Delta_o l_{st})$

Edo Formula: $W_{st} = .262 (n_1 \Delta_o l^2_{st})^{1/2}$

AIRCRAFT	W_{st} (act)	n_1	Δ_o	l_{st}	W_{st} (Martin)	W_{st} (Edo)
	lbs.	-	lbs	ft.	lbs.	lbs.
OA-9(Goose I)	253	5.3	8400	3.42	152	189
JRF-5(Goose II)	237	4.89	8400	3.42	141	182
JRF-5(Goose III)	133	5.15	4200	3.73	81	144
PBM-5	1019	5.68	55,000	6.0	1875	879
HRV-1 (Strut #1)	61	5.42	2700	2.66	39	84
HRV-1 (Strut #2)	40	5.42	2700	2.25	33	71

9.3   HULL REINFORCEMENT WEIGHT

As the hydro-ski support strut applies concentrated loads to the aircraft at its attachment to the hull, hull structural reinforcement is necessarily provided in this region to carry through and distribute the loads into the basic hull structure.

The available information on hull reinforcement weight is presented in Table 9-3 below:

TABLE 9-3

HULL REINFORCEMENT WEIGHT

Installation	(1) Hull Reinforcement Weight	(2) Strut Plus Hydro-Ski Weight	(1)/(2)
OA-9	97	438	.22
JRF-5 (Single Ski)	100	475	.22
JRF-5 (Twin Ski)	135	670	.20
PBM-5 (Large Ski)	2726 *	2600	1.05
HRV-1	28 *	85	.35

*Exclusive of ski retraction mechanism

It is observed in the foregoing table that the hull reinforcement weight fraction relative to the sum of ski and strut weights is fairly constant for the "Goose" modifications. For the PBM-5 and HRV-1 hydro-ski modifications, this weight fraction has a different order of magnitude. One reason for this discrepancy lies in the fact that, for the latter two cases, the hydro-ski extension could be adjusted.

More important, the extremely high value for the hull reinforcement weight for the PBM can be accounted for by the fact that, since ballast was required to achieve the desired operating gross weight, structural components were designed and analyzed to minimize manufacturing costs and engineering effort at the expense of weight and bulk. Accordingly it is suggested that, for a fixed hydro-ski installation, 20% of the hydro-ski and strut weight be allocated for hull reinforcement. For a retractable hydro-ski installation, it is suggested that 40% is a reasonable value. Furthermore, based on the only available data (PBM-5), the ski retraction mechanism weight can be estimated to be 10% of the strut-plus-ski weight.

REFERENCES

9-1   Martin Co. Report ER9433: "Preliminary Design Data for Water-Based
        Aircraft with Hydrofoils or Skis," by E. G. U. Band and J. W. Cuthbert,
        June 1957.

10. FINAL CONCLUSIONS AND RECOMMENDATIONS

10.1   INTRODUCTION

This report has presented a quantitative study, together with related analyses, of principal problem areas involved in the design of seaplane hydro-ski installations. The scope of these analyses was necessarily subject to certain limitations of which the following are considered to be most important:

1. Only the significant longitudinal seaplane characteristics were treated.

2. Only those problem areas were treated which were either independent of, or required no detailed knowledge of the aircraft's aerodynamic longitudinal control characteristics and/or hull hydrodynamics.

The particular studies and analyses presented in this report follow a distinct logical sequence relative to problem complexity. In each individual study, the results of the associated analysis have been correlated with pertinent available data to affirm the validity of the analysis and, by implication, the particular assumptions utilized therein. With but one exception, these correlations have been uniformly successful. These successful correlations ensure the validity of the parametric studies accompanying the individual analyses.

The present studies, analyses, and associated computer programs constitute a unified body of knowledge which, as made clear in Section 2 of this report, can be used to great advantage in the preliminary design and analysis of seaplane hydro-ski installations. At the same time that these results unify and augment existing hydro-ski technology, they also serve to indicate that certain problem areas still remain unanalyzed and that further analytical and/or experimental efforts are highly desirable. The remainder of this report section describes the conclusions drawn from the present study and presents a list of detailed recommendations for such further efforts. Conclusions and recommendations are presented first for each of the separate topics covered in this report and an additional list of recommendations is furnished for those topics not covered. Wherever necessary, the conclusions and recommendations are accompanied by brief explanations of their significance and importance.

10.2   STEADY-STATE HYDRO-SKI CHARACTERISTICS (SECTION 3)

10.2.1   Planing Characteristics

It has been verified that the semi-empirical expressions for the steady-state hydrodynamic characteristics of hydro-skis established by Shuford in Reference 10-1 yield

accurate results even when the gross approximation of "full wave rise" is utilized. This subject is not considered to require any further investigation.

10.2.2   Submerged, Fully-Wetted Characteristics

The existing semi-empirical analysis for the hydro-ski lift in this flow condition has been extended to cover drag and pitching moment characteristics. Extremely close agreement with the experimental data for skis of aspect ratio, 1/4, has been obtained.

While not considered vital, it would be desirable to extend the correlation to cover at least one other ski aspect ratio. The necessary experimental data for skis of aspect ratio, 1/8, are presently available for this purpose (Reference 10-2).

10.2.3   Submerged, Ventilated Characteristics

The existing method for calculating these characteristics is that given by Johnson in Reference 10-3. As presented therein, this method is awkward as it involves a "manual" iteration procedure for one quantity and a "manual" interpolation procedure for another. This awkward approach has been replaced in this report by an equivalent accurate digital computer program which can also serve as a subroutine in dynamical problems.

In Reference 10-3, Johnson showed that his method, essentially theoretical in nature, gave accurate correlations with experimental data for a flat plate hydrofoil of aspect ratio, 1.0. In this report, using the equivalent computer program, the theoretical characteristics of a flat plate of aspect ratio, 1/4, were calculated and compared with available test data. This correlation showed certain discrepancies which were attributed to the fact that the test data were for a "modified" flat plate having a bevelled trailing edge. Suitable, simple empirical correction factors were established to account for these discrepancies. When the computer program was revised accordingly, excellent agreement with the test data was obtained.

It is firmly recommended that further investigations of this problem area be made, as follows:

A.   Using the existing program (including the empirical corrections), the correlation between calculated and existing experimental values for bevelled skis of aspect ratio, 1/8, should be obtained;

B.   Even more important, tank test data should be obtained for both unbevelled flat plate and deadrise skis of two aspect ratios (typically, 1/4 and 1/8). This will permit:

a)   A more direct check of the Johnson theory for low aspect ratio surfaces;

b)   Establishment of suitable empirical factors for the deadrise effect.

10.3 STRUT RESISTANCE CHARACTERISTICS (SECTION 4)

In Section 4. the survey on strut resistance characteristics demonstrated that adequate methods are presently available for hydro-ski strut drag estimation under the following conditions:

a)   zero yaw angle;

b)   fully wetted or base-vented;

c)   surface-piercing or completely submerged.

In some high-speed towing tank tests utilizing base-vented struts, it has been observed that a "choking" phenomenon occurs, which closes off the cavity opening to the atmosphere. This effect is ascribed to the pressure reduction at the side spray walls associated with the high velocity air entering the cavity. (A report, Reference 10-6, has recently been published, which includes a theoretical method for predicting the occurrence of base cavity choking. Unfortunately, this report did not arrive in time for including its results herein.)

Although the contents of Section 4 deal only with the drag performance of hydro-ski support struts at zero yaw, their side force characteristics are also of concern to the hydro-ski configuration designer. In addition to affecting the strut structural design and its weight, hydro-ski strut side forces are an important factor in establishing the lateral and directional stability and control characteristics during yawed attitudes with the strut immersed. The applicable information on this topic is sparse and it is recommended that further theoretical and empirical studies be conducted to permit prediction of the hydrodynamic characteristics of yawed submerged and surface-piercing struts in the fully-wetted and ventilated flow conditions.

10.4 SINGLE HYDRO-SKI WAVE IMPACTS (SECTION 5)

Using the "equivalent planing velocity" concept in conjunction with Shuford's expression for lift coefficient, an original computer program has been devised for the calculation of the time histories of vertical accelerations and associated wetted ski lengths experienced by hydro-skis in fixed-trim impacts on head-sea wave flanks. This program permits variation of the initial location of the ski relative to the wave surface. This analysis and the associated program have been validated by the following procedures:

A.   Smooth water impact time histories calculated with the present method were successfully compared with experimental values.

B.   Sample parametric studies were made for smooth water impacts and the results successfully compared with those given by Mixson's empirical formula (Reference 10-4). This computer program also furnishes the very important wetted length values which are not included in Mixson's analysis.

C. Calculations were then made for certain specific (head sea) wave impacts for comparison with experimental data obtained in tank tests. In each case, for otherwise specified conditions, the calculations covered variations in the initial location of the ski relative to the wave surface. Successful correlations were obtained but only through proper definition of this "initial location parameter" which had not been measured in the conduct of the tank tests.

The calculations for Item C, above, also served to demonstrate the novel remarkable result that, contrary to existing belief, maximum impact loads do not occur when the initial wave contact is made on the point of maximum wave slope but invariably occur for lower initial locations on the wave flank. Furthermore, these same examples show that the differences in the (relative) maximum impact loads for these two locations could be very appreciable. It is thus concluded that the rational estimation of maximum impact loads must include the effects of this vital "initial location parameter." Furthermore, these same calculations served to indicate that the ski length was a significant parameter in single wave impacts, i.e., for certain combinations of ski-wave parameters and initial conditions, the finite length of an actual ski could play an important role in limiting the maximum accelerations.

By way of sample parametric studies, the computer program was then utilized to estimate maximum impact loads for two hypothetical large hydro-ski equipped seaplanes in open ocean operation. The two seaplanes had the same weight but different landing speeds: 85 knots for the conventional seaplane and 42.5 knots for the STOL-type seaplane. The wave conditions covered those specified for open ocean seaplanes in the current applicable specification, MIL-A-8864(ASG). It was found that:

A. For a given seaplane landing in waves of fixed height, maximum impact loads vary non-linearly with wave length-height ratio, i.e., a reduction in L/H from 40 to 30 results in a relatively small change of 0.45g whereas a reduction from 30 to 20 results in a relatively large change of 4.15g.

B. For a given seaplane landing in waves of fixed length-height ratio, maximum impact loads are relatively insensitive to wave height, at least for sufficiently large wave height values.

C. Maximum impact loads are very strongly affected by the (horizontal) landing speed. In the case investigated, where the landing speed of the STOL seaplane was assumed to be half that of the conventional seaplane, the maximum impact loads (based on a common sink speed) were found to be approximately proportional to the landing speed. This important result shows that the STOL aircraft has a distinct inherent advantage over the conventional aircraft in regard to single wave impacts when both are equipped with the same hydro-ski.

It is concluded that the new approach to the calculation of impact load character-istics (trim histories, maximum loads, wetted lengths) for the single fixed-trim impacts of a ski in waves, wherein realistic account is taken of the initial location on the wave flank, is inherently superior to present methods and provides extremely accurate values. It can therefore be used with considerable confidence in parametric studies and/or ski structural design.

Owing to the central importance of the impact problem, it is recommended that:

A. Correlation be made with the remainder of the existing test data;

B. Further test data be obtained to cover wider ranges of the pertinent para-meters and the theory correlated with these;

C. Special experimental and analytical investigations be made of impacts in-volving low relative trim angles to establish suitable methods of impact load prediction. These investigations should cover both flat and deadrise skis. The analytic methods should include the "zero trim impact" approach for the deadrise skis and, if feasible, the effect of trapped air, as treated in Reference 10-5, for the flat skis.

10.5 ── PLANING STABILITY OF THE SKELETON HYDRO-SKI SEAPLANE (SECTION 6)

Using linearized ("small motion") theory, an original computer program has been established for the calculation of planing stability boundaries of a "skeleton" hydro-ski seaplane, defined herein as one for which there is no wetting of the hull.

Using this program, calculations were made for the lower trim limits of planing stability (lower limit porpoising) for two hydro-ski installations on the Martin 329 C-2 sea-plane and the results compared with the experimental values obtained in towing tank mea-surements. These comparisons showed that numerical values were reasonably close but that the calculated values failed to reproduce the detailed features of the experimental por-poising boundaries. Further analyses, made with the hope of improving the agreement, proved fruitless and it was concluded that the principal source of the discrepancies was the wetting of the hull and aerodynamic surfaces in the model tests, a feature necessarily omitted from the computer program. It was further concluded that, if allowance were made for this effect, the theoretical results could be used with confidence in parametric studies but, for detailed application, should always be checked by suitable model tests.

Parametric studies were made to establish typical effects of varying the basic parameters of the hydro-ski installation. The results of these parametric studies which for the most part are novel ones, are as follows:

A. Those hydro-ski features which are known to be most beneficial for impact load alleviation, namely high beam loadings and large deadrise angles, have distinctly ad-verse effects on the lower limit porpoising boundary, i.e., they raise the lower trim stability limits;

B.   A hydro-ski installation feature which is known to have an adverse effect on hydrodynamic resistance, namely ski incidence, has a distinctly favorable effect on the lower limit porpoising boundary;

C.   The lower limit porpoising boundary is insensitive to large changes in strut length;

D.   The lower limit boundary can be somewhat improved (lowered) by shifting the ski location either forward or aft from a specific "central" location. However, in the case of skis having pointed trailing edges, a sufficiently far aft shift can have the distinctly unfavorable effect of limiting the stable portion of the planing region to a very narrow band of trim angles, totally aside from other possible limitations associated with high angle porpoising.

It is concluded that:

A.   Satisfaction of the fundamental criterion of planing stability generally imposes severe limitations on practically all of the significant hydro-ski configuration parameters;

B.   These limitations are, in fact, so severe that other important system criteria will usually have to be compromised;

C.   It follows that suitable detailed trade-off studies will have to be performed in the preliminary design of specific configurations;

D.   Because the planing stability characteristics are dependent on the seaplane's aerodynamic characteristics, it may even be necessary and/or desirable to include these characteristics in the trade-off studies.

Because planing stability is such a fundamental hydrodynamic criterion and because of the remarkable results obtained in the brief parametric studies reported herein, it is recommended that:

A.   Further wide-range experimental parametric studies be made, covering the effects of both hydrodynamic and aerodynamic parameters, including independent variations of ski beam loading, deadrise, incidence, vertical and horizontal locations, and T.E. shape, as well as aerodynamic static stability and damping (equivalently, horizontal tail size and moment arm);

B.   Design studies and tank tests be used to establish feasible "variable-area" ski configurations which will specifically overcome the poor planing stability characteristics of highly loaded skis without compromising their impact load alleviation qualities;

C.   Suitable analytic studies be made to compare the planing stability characteristics of STOL and conventional hydro-ski seaplanes.

10.6   WAVE RESPONSE CHARACTERISTICS OF THE SKELETON HYDRO-SKI SEAPLANE (SECTION 7)

An original computer program was established for the calculation of the heaving and pitching motions of a "skeleton" hydro-ski seaplane traversing a train of waves at constant forward speed. Unlike the treatment of planing stability, this program accounts for the (generally) highly non-linear dependence of the ski's hydrodynamic loads on the ski-wave geometry and ski kinematics. As a matter of fact, for certain of these conditions involving submerged skis. it was found necessary to establish entirely novel and, as yet. unverifiable expressions for the loads.

The only quantitative test data relative to this problem area are the accelerations of a tank model of the hydro-ski HU-16 seaplane experienced in the high speed portions of rough-water take-offs. Accordingly. for each of two hydro-skis of different beam loading, a series of five computer runs were made to simulate the high speed portions of these tank tests. The five computer runs involved variations in the location of the initial ski contact point on the wave flank, with all other (arbitrary) initial conditions the same.

In the case of one ski having a beam loading of 60, the agreement between the measured and computed c.g. and bow maximum vertical accelerations, both with respect to range and average values. was remarkably close. This significant result is considered to furnish basic validation of the computer program. For this ski, an apparent inconsistency between the actual strut length on the tank model and the maximum computed ski drafts was explained in two alternate plausible ways.

In the case of the second ski which had a beam loading of 100, there were large, but consistent discrepancies between the measured and computed vertical accelerations. Tentative but thoroughly plausible explanations were advanced to explain these differences. For this ski, the calculations showed a very narrow trim range and ski drafts less than the actual strut length. These results are consistent with the known behavior of high beam loading skis.

The determination of wave response characteristics is actually a central one in the design of hydro-ski installation. At this time, there is almost a complete lack of quantitative data pertinent to this problem area. Accordingly, the following substantial program is recommended to eliminate this deficiency.

A towing tank test program on a model skeleton hydro-ski seaplane should be conducted to permit more specific correlation with the computer program developed in this investigation. Accordingly, all the aerodynamic and hydrodynamic characteristics and derivatives required for the program should first be obtained by suitable model tests. For example, aerodynamic coefficients well above the stall should be obtained, as well as ski planing lift coefficients at negative trims, etc.

The model skeleton hydro-ski seaplane should be systematically tested under various wave conditions, including calm water, with the runs being made at constant speed to conform with the existing computer program. In addition to the usual bow and c.g. accelerometers, the model instrumentation should also incorporate a means for measuring the instantaneous hydro-ski draft.

It is to be noted that the successful correlation for the wave response of a skeleton hydro-ski seaplane is a necessary prerequisite for the rational determination of the hull loads in accordance with the procedure presented in Section 2. (See paragraph 10.9, below.)

10.7   HYDRO-SKI LONGITUDINAL LOCATION (SECTION 8)

Attempts to establish purely empirical correlations between actual hydro-ski longitudinal location and certain inherent hydro-ski parameters, such as beam loading, proved unsuccessful. These negative results tended to confirm an opinion generally shared by hydro-ski design engineers that the behavior of a hydro-ski seaplane in the high speed planing regime can be strongly influenced by the aircraft's aerodynamic characteristics, which would therefore play an important role in affecting optimum ski longitudinal locations.

Although no simple empirical relationship for defining optimum ski longitudinal locations is presently available, the effects of changing this location on a seaplane's dynamic stability can be investigated with the computer program of Section 6 and, similarly, the effects of such changes on the seaplane's wave response characteristics can be investigated with the computer program of Section 7. To do these things in a manner meaningful for preliminary design, it is obviously important to relate these investigations to the aircraft's aerodynamic control characteristics covering, at least, the control available vs. the control required for trimming the aircraft in particular planing equilibrium conditions.

Although no specific details are presented herewith, it is felt that a "pilot" program of the type just described is well warranted for an initial conclusive demonstration of this approach toward definition of ski location.

10.8   SURVEY OF HYDRO-SKI INSTALLATION WEIGHTS (SECTION 9)

A survey has been made of actual weight values for previous hydro-ski installations. Separate comparisons were made of the actual ski and actual strut weights with those obtained from the only existing empirical formula and relatively poor correlation was obtained. New empirical weight formulas were established which were shown to provide substantially improved correlations. Rough methods were also provided for the weight estimation of carry-through structure and ski retraction systems.

Two significant conclusions were drawn with regard to future weight prediction:

A. Because all previous hydro-ski installations (with but one exception) were retro-fitted to existing aircraft and were often based on large safety factors, it is obvious that the associated weight data should generally prove to be somewhat pessimistic if used for pre-diction of future system weights.

B. In Section 5 of this report, it is demonstrated that single wave impact loads and associated wetted lengths can be predicted in a rational and accurate manner. As the asso-ciated pressure distribution, shears and bending moments can also be calculated, it follows that systematic analyses can be made to determine:

a) Optimum strut locations relative to the ski;

b) Ski structural requirements for various types of construction
     (solid plate, hollow shells with and without stringers, bulkheads);

c) Corresponding ski weight values.

By repetition of this procedure for various aircraft weights, rational and accurate formulas for ski "weight fractions" could then be derived for prescribed parameter ranges (wave geometry, sink speeds, etc.). Such ideal, minimum weight formulas would clearly serve as invaluable design goals and it is strongly recommended that this approach be followed.

10.9.   RATIONAL DESIGN LOADS FOR HYDRO-SKI SEAPLANE HULLS (SECTION 2)

Section 2 of this report describes the problem areas and their relations that must be analyzed during the earlier phases of hydro-ski seaplane design. One of the significant problem areas is that of the basic sizing of hydro-ski dimensions and the closely related area of hull structural design loads.

In this connection, Section 2 describes a recommended program for the solution of this problem for a particular aircraft configuration. Among other things, this program uses an "inverted" form of the computer program of Section 7, wherein known aircraft motions and ski-wave geometrical relations are used to calculate instantaneous ski loads. By subtracting these loads from the total loads measured in rough water tests of a model, the experimental hull loads can be determined.

This program is of interest for two different reasons:

A. It is of general interest because it can be used as a basis for formulation
     of specification requirements;

B. It is of specific interest in the design of particular hydro-ski seaplanes, es-
     pecially those subject to strut height limitations of any kind.

10.10   ADDITIONAL RECOMMENDATION

At the time that the subject investigation was initiated, the hydro-ski represented the most promising device which could be efficiently applied with confidence to a seaplane configuration for improving its rough water capability. However, during the time frame of this investigation, full-scale flight tests have been conducted on a seaplane with a single small hydrofoil. The results of these tests, presented in Reference 10-7, demonstrate that such a hydrofoil appendage offers even further performance improvements, at lighter weight, as compared with a small hydro-ski installation.

In view of this development, it is recommended that a survey and study be conducted on hydrofoil seaplane technology similar to that undertaken in the present investigation. Since many of the areas covered in the hydro-ski study are equally applicable to hydrofoil design, it is anticipated that much of the work performed herein can be readily applied. Further, the effort required for a seaplane hydrofoil survey would be substantially less than that for the present ski survey because of the more limited available data for both model and full-scale aircraft.

Such a parallel survey, in conjunction with the further hydro-ski programs recommended herein, would ultimately widen the entire field of advanced seaplane technology thereby increasing the number of choices open to the designer. This would surely be reflected in corresponding improvements in future design efforts.

REFERENCES

10-1   NACA TN 3939: "A Theoretical and Experimental Study of Planing Surfaces
        Including Effect of Cross-Section and Planform," by C. L. Shuford, Jr.,
        March 1957.

10-2   NACA TN 3249: "The Hydrodynamic Characteristics of an Aspect-Ratio-0.125
        Modified Rectangular Flat Plate Operating Near a Free Water Surface,"
        by J. A. Ramsen and V. L. Vaughan, Jr., October 1954.

10.3   NACA RM L57I16: "Theoretical and Experimental Investigation of Arbitrary
        Aspect Ratio, Supercavitating Hydrofoils Operating Near the Free Water
        Surface," by V. E. Johnson, Jr., 12 December 1957.

10.4   NASA MEMO 1-5-59L: "The Effect of Beam Loading on Water Impact Loads and
        Motions," by J. S. Mixson, February 1959.

10.5   J. SHIP RESEARCH, VOL. 11. No. 4: "The Impact of a Flat Plate on a Water
        Surface," by J. H. G. Verhagen, December 1967.

10.6   HYDRONAUTICS INC. TR 605-2: "Choking of Strut-Ventilated Foil Cavities"
        by C. Elata, May 1967.

10.7   THURSTON AIRCRAFT CORP. REPORT NO. 6702-3: "Flight Test of the Hydro
        Research Vehicle HRV-1 Equipped with Hydrofoil No. 1 on Strut No. 2, Final
        Summary Report," by D. B. Thurston, February 1967.

APPENDIX A

CORRELATION OF DRAG AND C.P. VALUES FOR A FULLY-WETTED, FLAT PLATE, RECTANGULAR SKI OF ASPECT RATIO, 1/4

A1.   DRAG VALUES

Figure 3 of Reference 3-8 gives the experimental values for the drag coefficients of the subject ski vs. trim angle for four different depth-chord ratios. As described in the text, the drag values at each depth were assumed to be given by the following equation:

$$C_D = C_{DO} + (C_{L1}^2 / \pi A \eta) + C_{L2} \tan \tau$$

where: $$C_{L1} = \frac{2\pi K_2 K_3 A}{(1 + A) + 2K_2} \tau,$$

$$C_{L2} = (8/3) K_3 \sin^2 \tau \cos \tau$$

and where the depth-correction function, K_2 and K_3, are those described in the text.

Suitable values of C_{DO} and η were then established by the following procedure. Using values for a speed of 30 fps, for each data point, the calculated value of $C_{L2} \tan \tau$ was subtracted from the experimental C_D value to give:

$$C_{D\,EXP} - C_{L2} \tan \tau = C_{DO} + (C_{L1}^2 / \pi A \eta)$$

Using the calculated values of $C_{L1}^2 / \pi A$, the "residuals", $C_{DO} + (C_{L1}^2 / \pi A \eta)$, were analyzed by least squares to obtain the "best fit values" of C_{DO} and η. This was done for each depth. The resulting values of C_{DO} and η as functions of depth are shown in Figures A-1 and A-2 of this appendix.

The test drag values included the hydrodynamic drag due to wetting of the ski support strut and this value is reflected in the C_{DO} values obtained herein. The strut drag was assumed to vary linearly with depth and the true ski profile drag was then obtained by

A-1
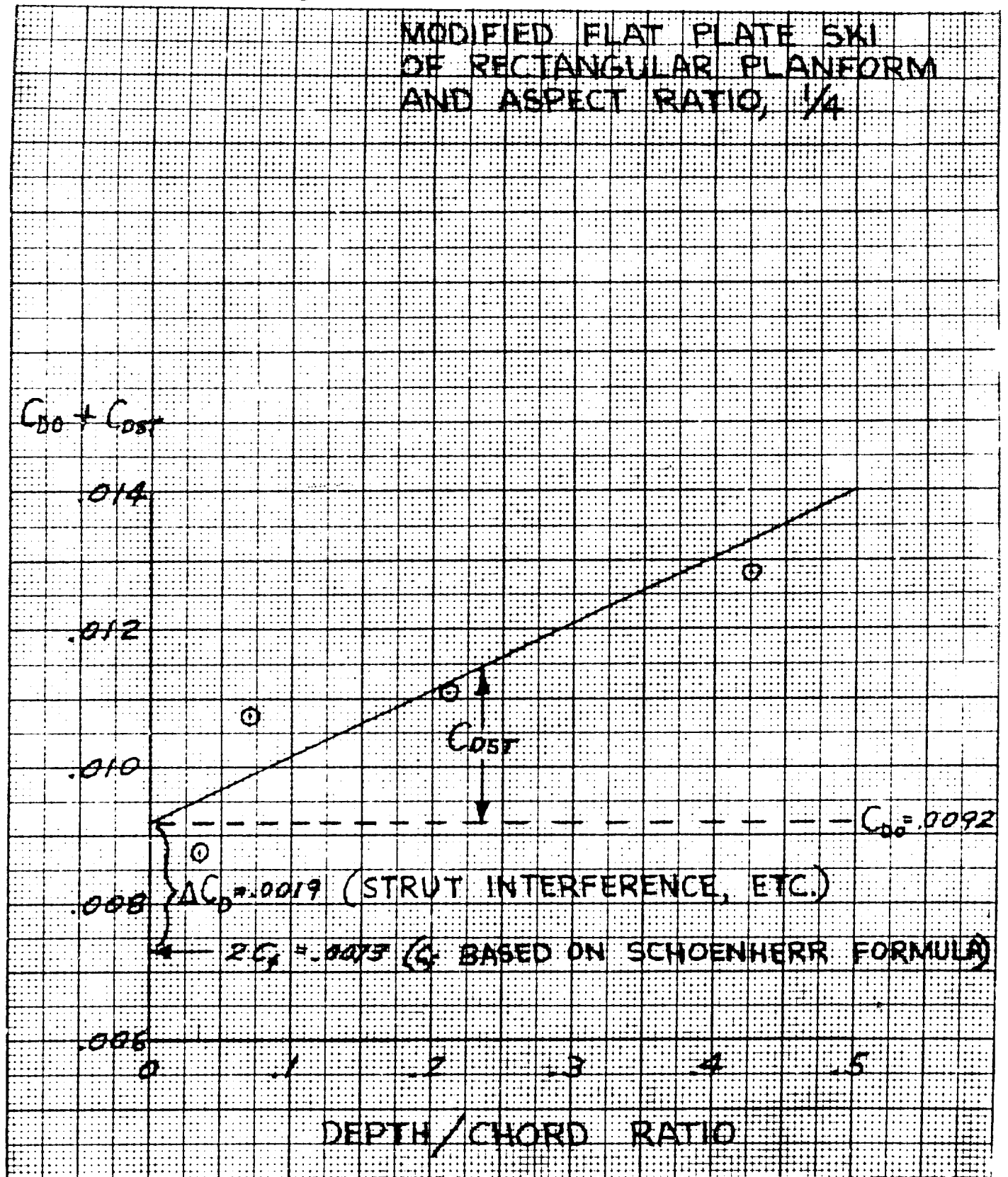
Figure A-1. Ski Profile Drag Plus Strut Drag vs Ski Depth-Chord Ratio
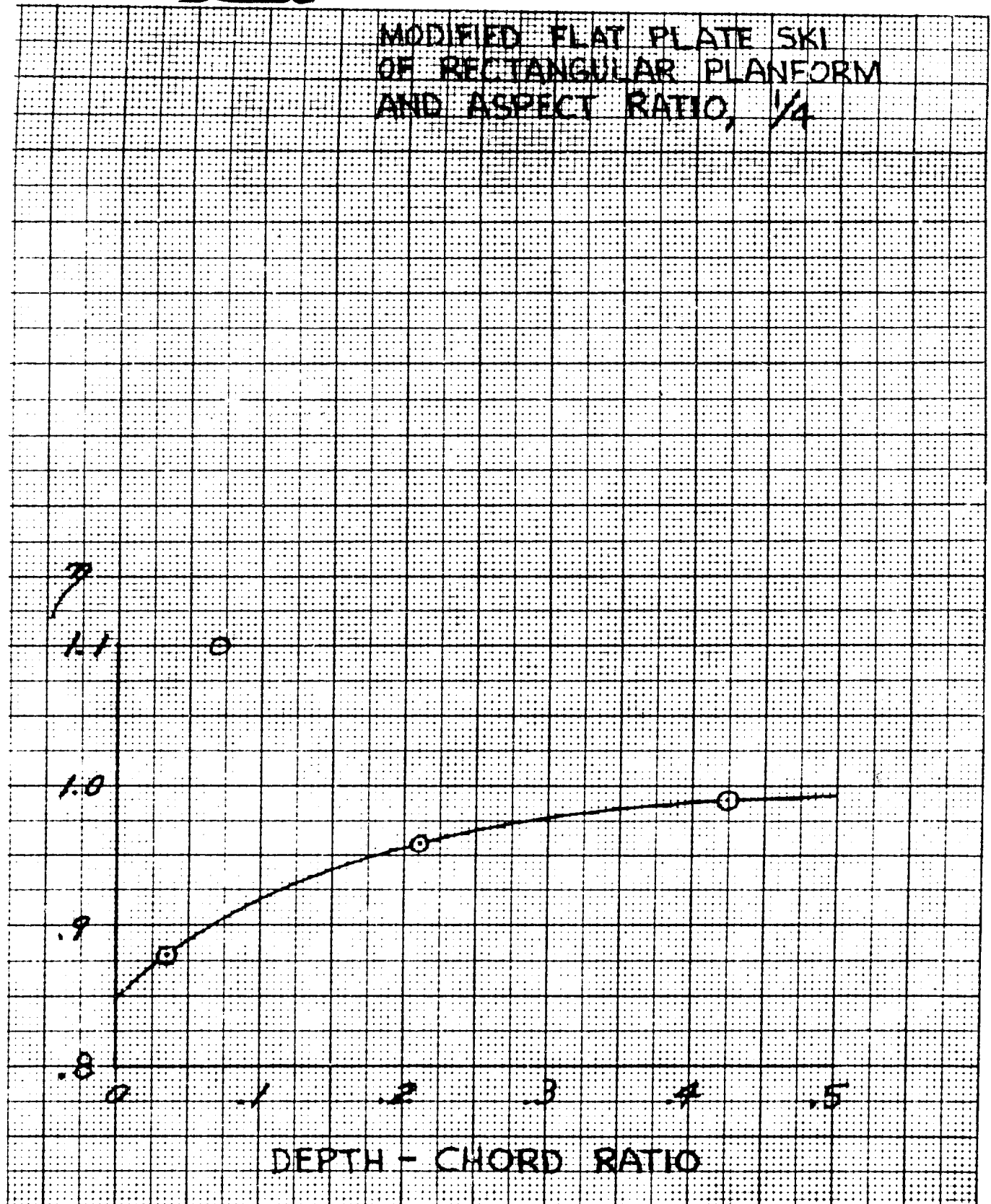
Figure A-2. Hydro-Ski Efficiency Factor vs Depth-Chord Ratio

extrapolation of the C_{DO} values to zero depth, as shown in Figure A-1. This value is C_{DO} = .0092. The skin friction drag, as obtained from the Schoenherr curve for the pertinent test Reynolds Number was: $2C_f$ = .0073. This shows that the ski C_{DO} is reasonable, the difference being attributable to the combination of ski wake drag and strut interference.

Similarly, but except for one point, the η values are considered reasonable and, in fact, the correctness of their asymptote, $\eta \rightarrow 1$ for $d/c \rightarrow \infty$, is considered a distinct validation of the formula proposed herein. *

Figures A-3 through A-6 show the correlation of the experimental polar curves with those calculated from the preceding C_D formula, using the _curve_ values for C_{DO} (inclusive of strut drag) and η . The agreement must be considered remarkable.

A2.   CENTER OF PRESSURE VALUES

Figure 12 (b) of Reference 3-5 shows the variation of center of pressure with trim angle for four different depth-chord ratios as determined in tank tests. Using the experimental lift coefficients given in Figure 2 of Reference 3-8, the experimental c.p. values were first plotted against C_L in Figure A-7. These curves were approximated by the semi-empirical formula:

$$\text{c.p. (\% chord, forward of T.E.)} = (a + \frac{b}{C_{L1}}) \frac{C_{L1}}{C_L} + 50 \frac{C_{L2}}{C_L}$$

where a and b depend on the depth-chord ratio.

Figure A-8 shows the "best fit" values of a and b determined from the test data and Figures A-9, A-10, A-11 and A-12 show the comparison of the experimental c.p. values with those given by the preceding formulas, using the "a" and "b" values from the curves of Figure A-8. The agreement is extremely close.

*This three-term formula obviously has application to low-aspect airfoils. In that connection, it is considered to furnish a distinct improvement over most current formulas which incorrectly lump the cross-flow contribution with the induced drag and thus use only two terms.
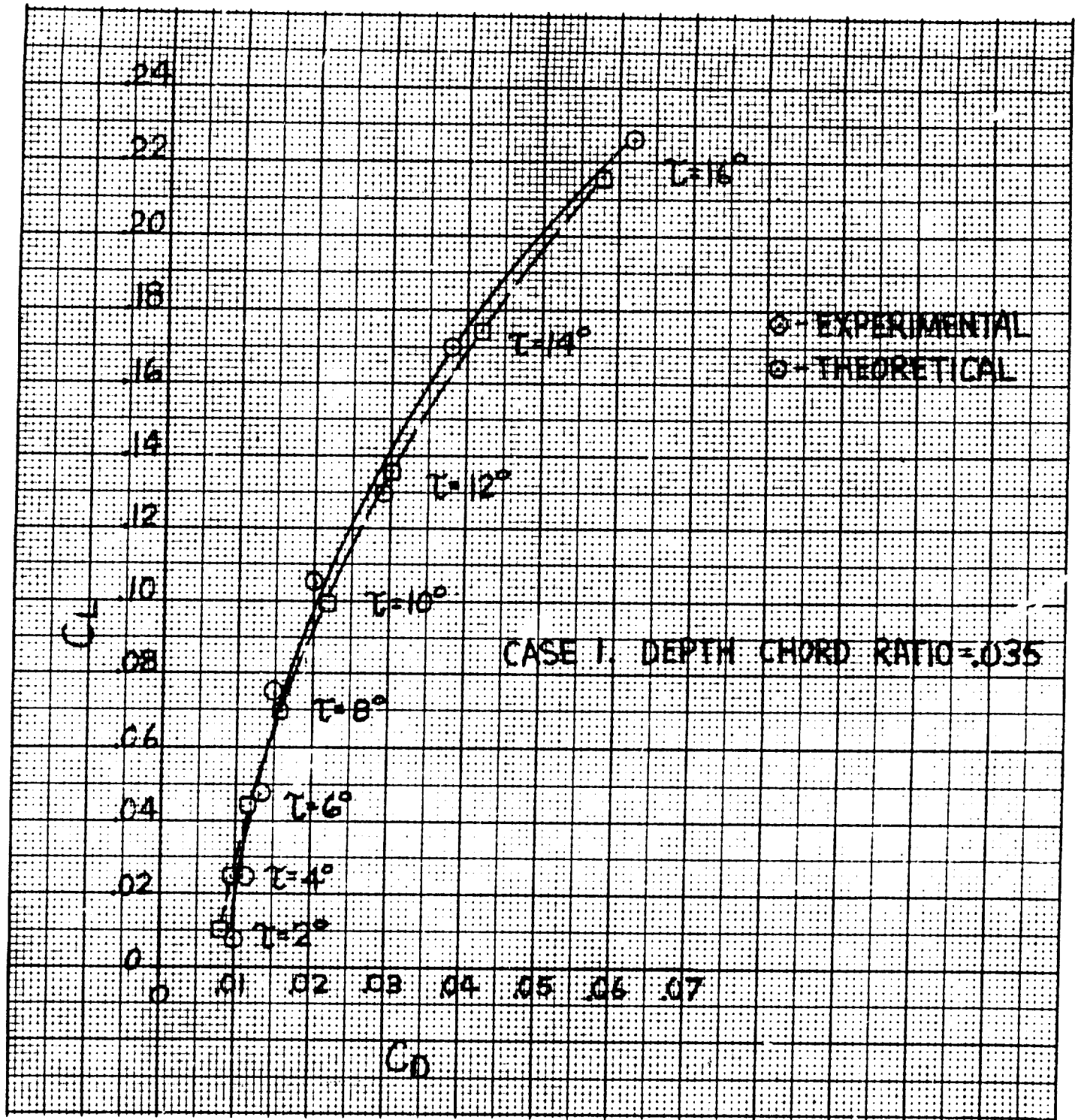
Figure A-3. C_D vs C_L, Modified Flat Plate Ski of Rectangular Planform and Aspect Ratio, 1/4
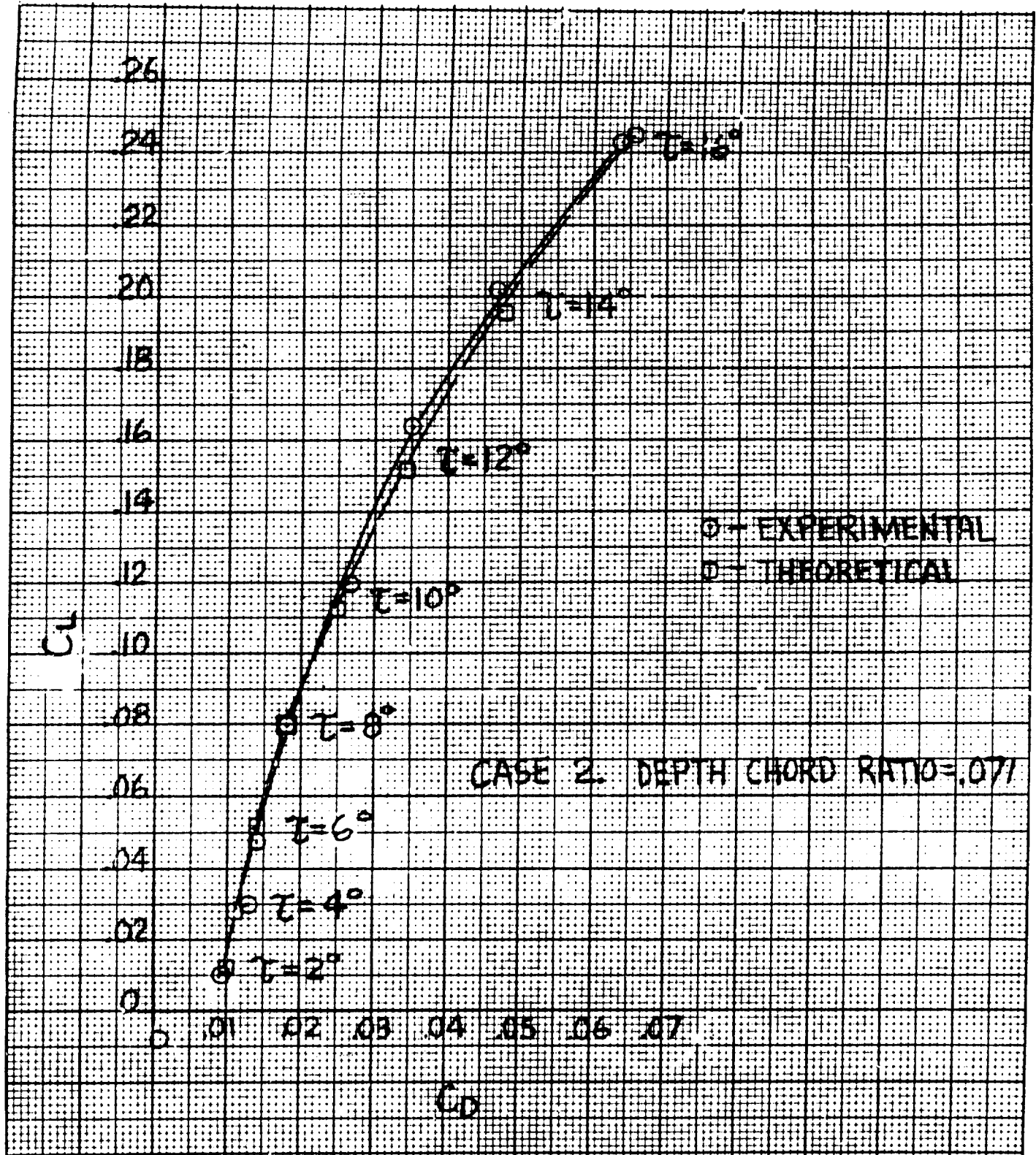
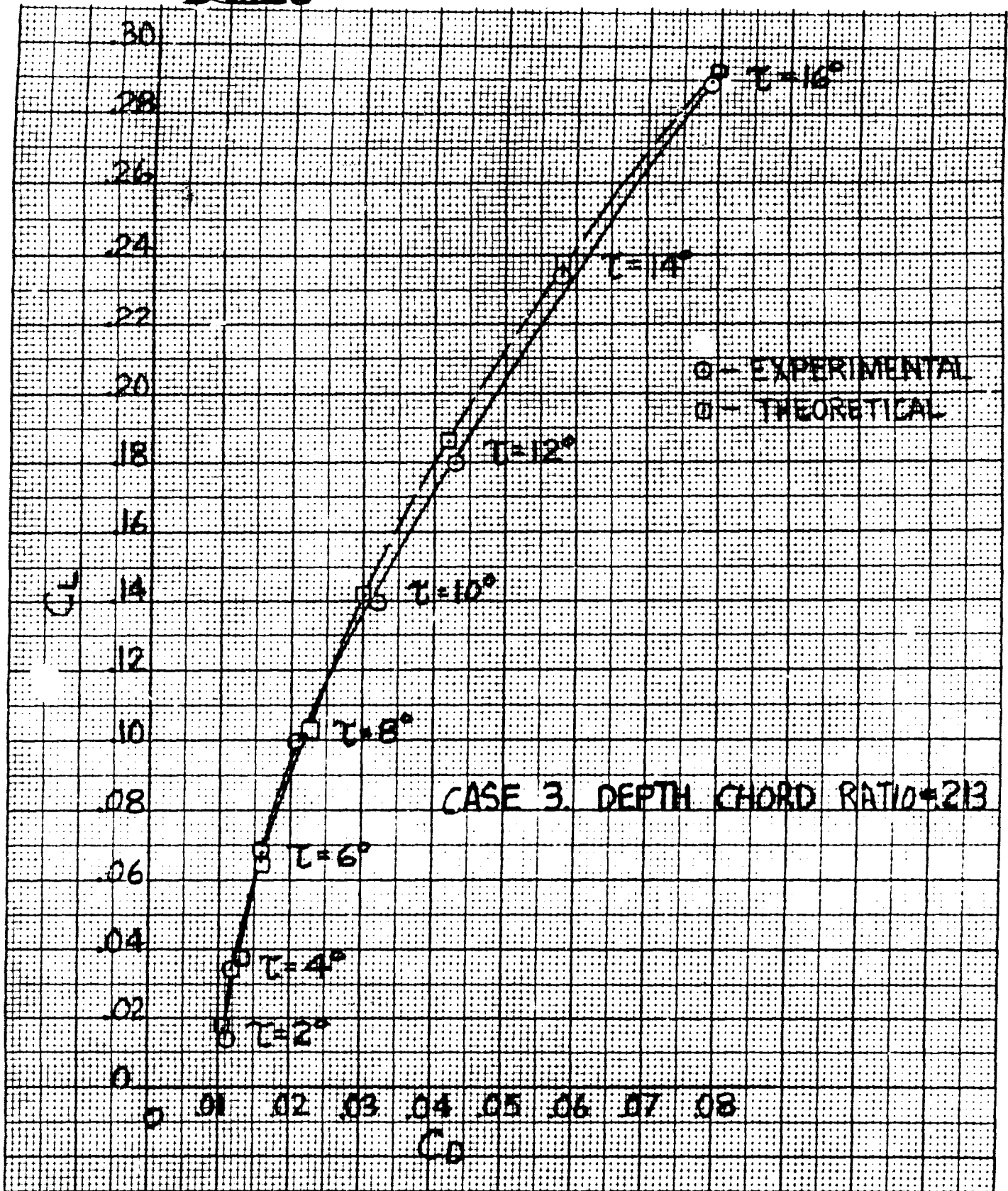Figure A-4. C_D vs C_L, Modified Flat Plate Ski of Rectangular Planform and Aspect Ratio, 1/4

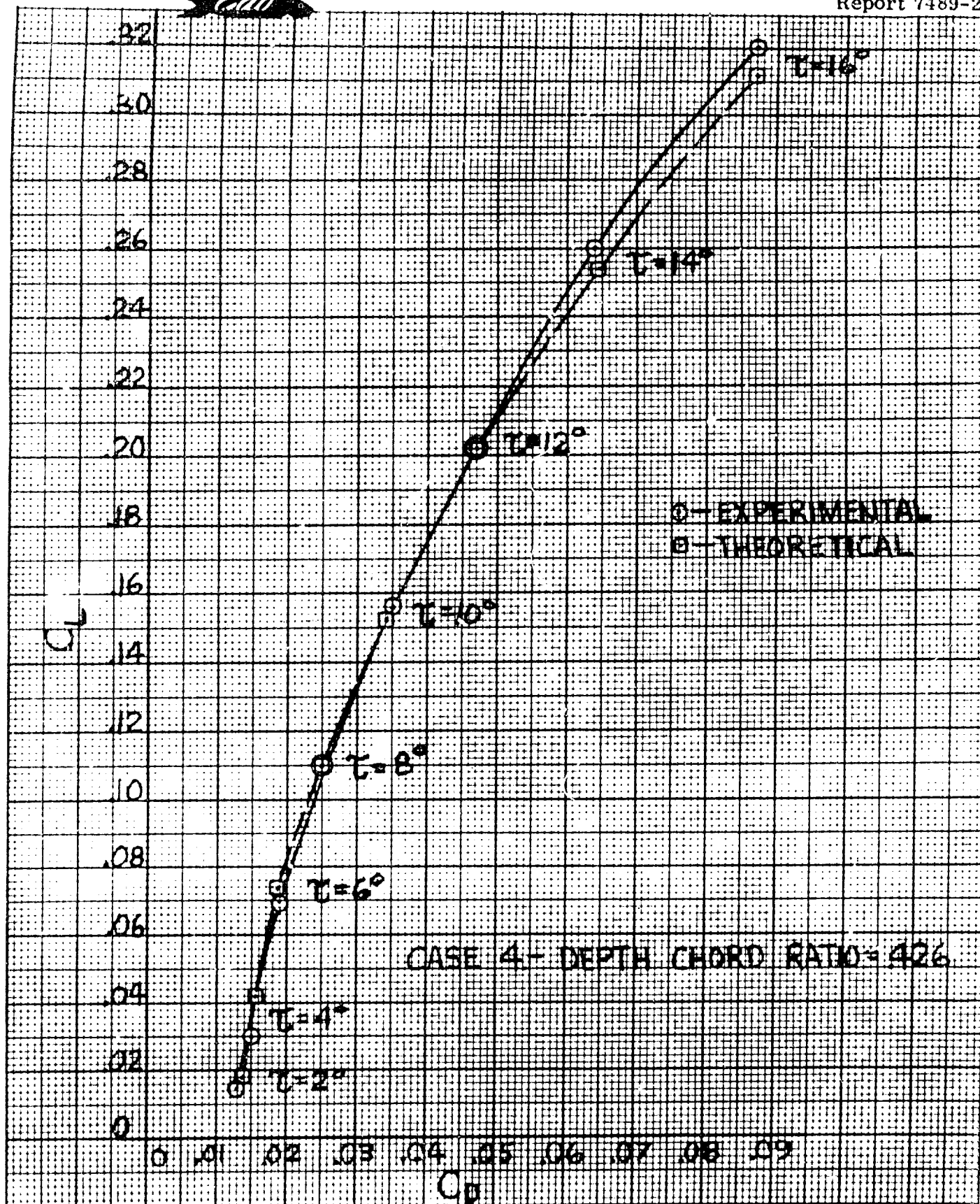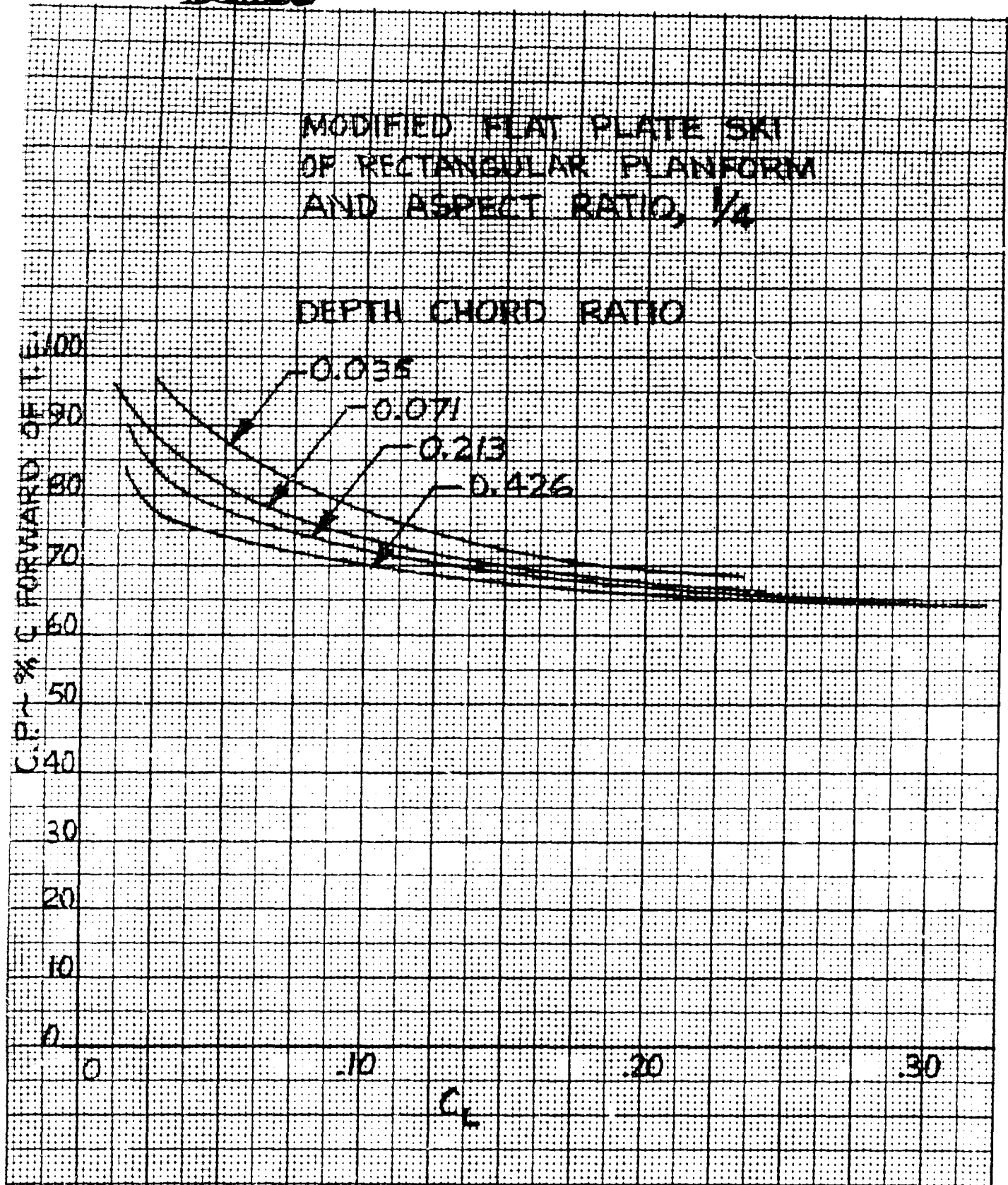Figure A-5. C_D vs C_L, Modified Flat Plate Ski of Rectangular Planform and Aspect Ratio, 1/4

Figure A-6. C_D vs C_L, Modified Flat Plate Ski of Rectangular Planform and Aspect Ratio, 1/4

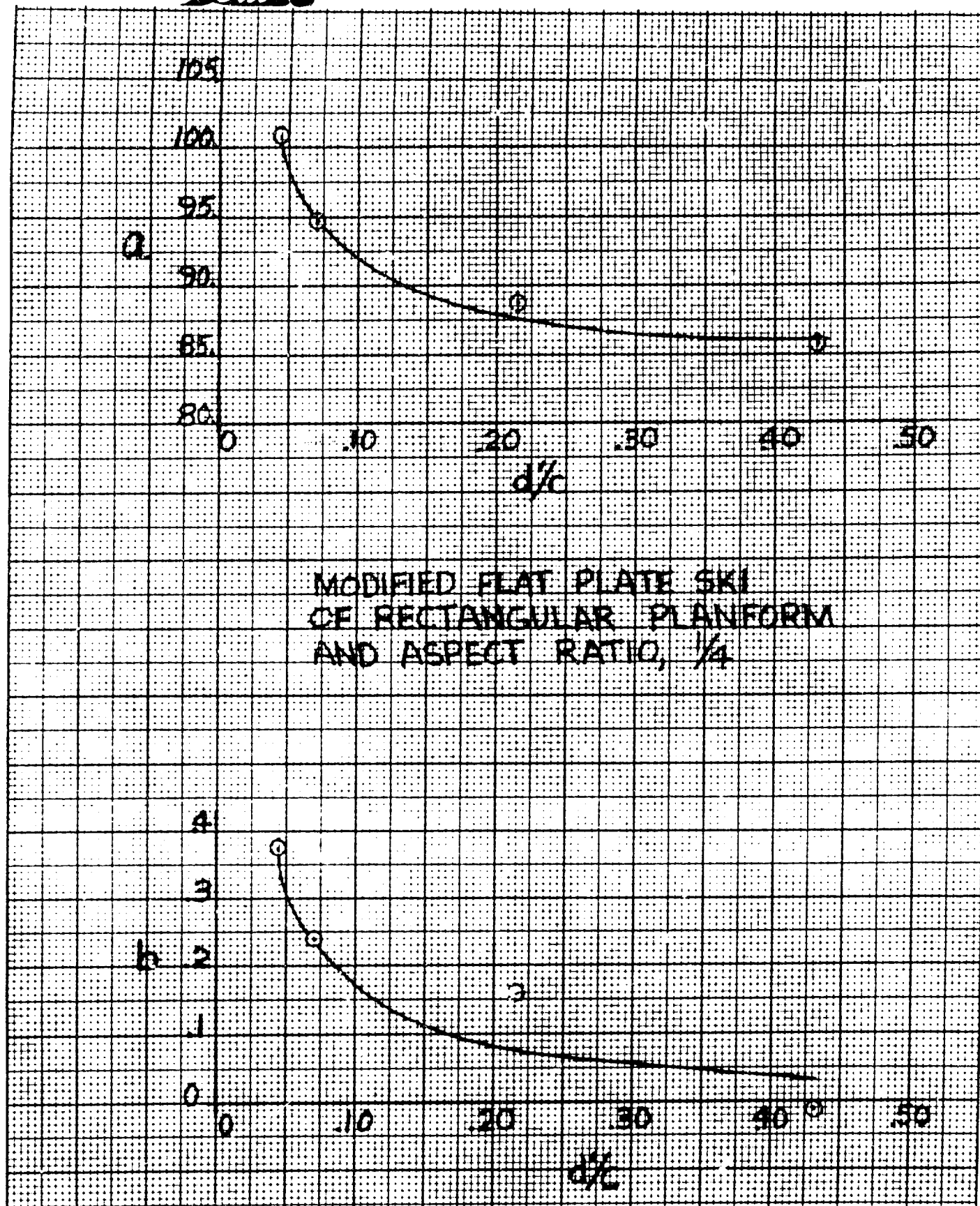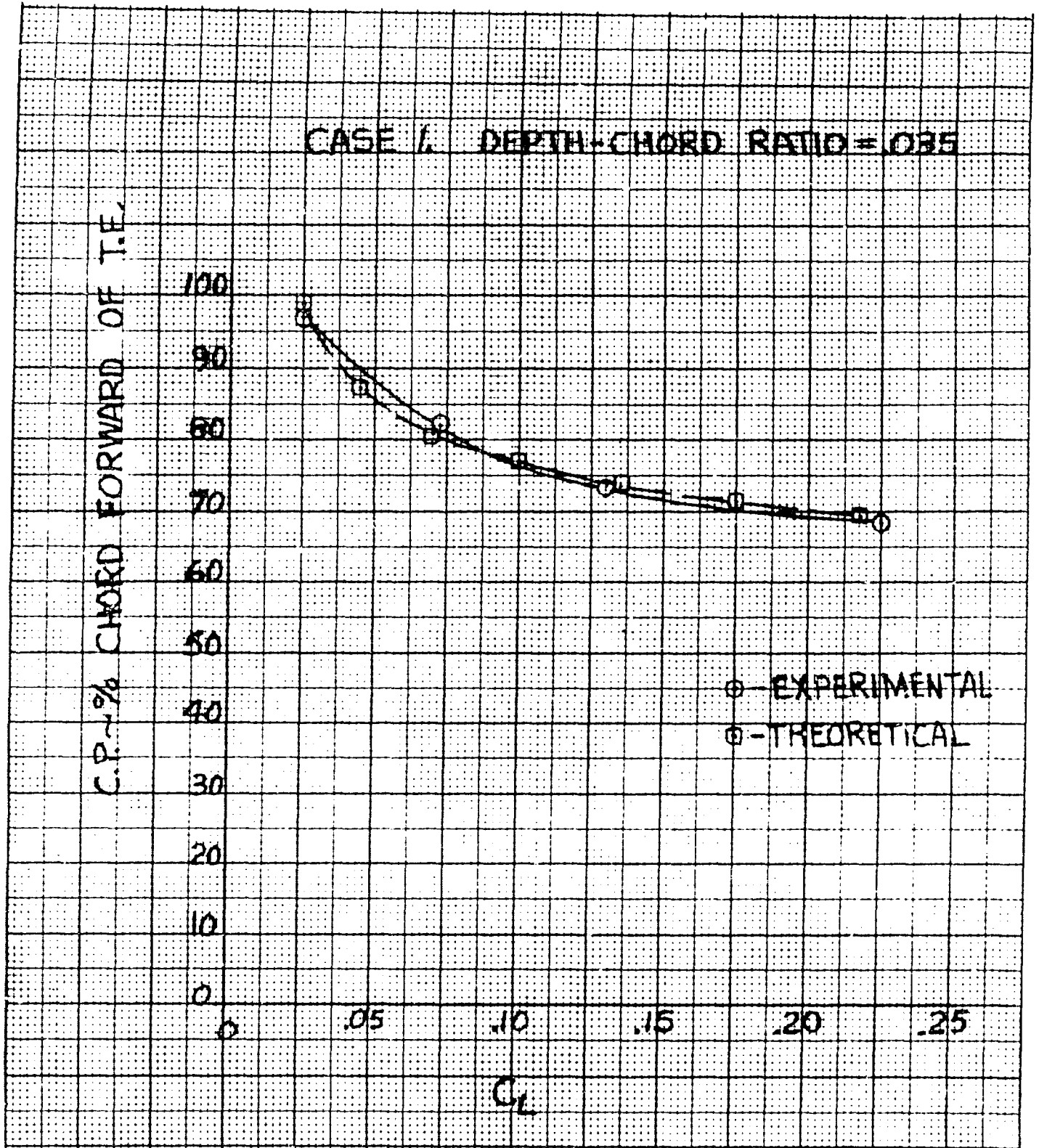Figure A-7. Experimental Center of Pressure vs Lift Coefficient and Depth-Chord Ratio

Figure A-8. Center of Pressure Parameters vs Depth-Chord Ratio

A-10

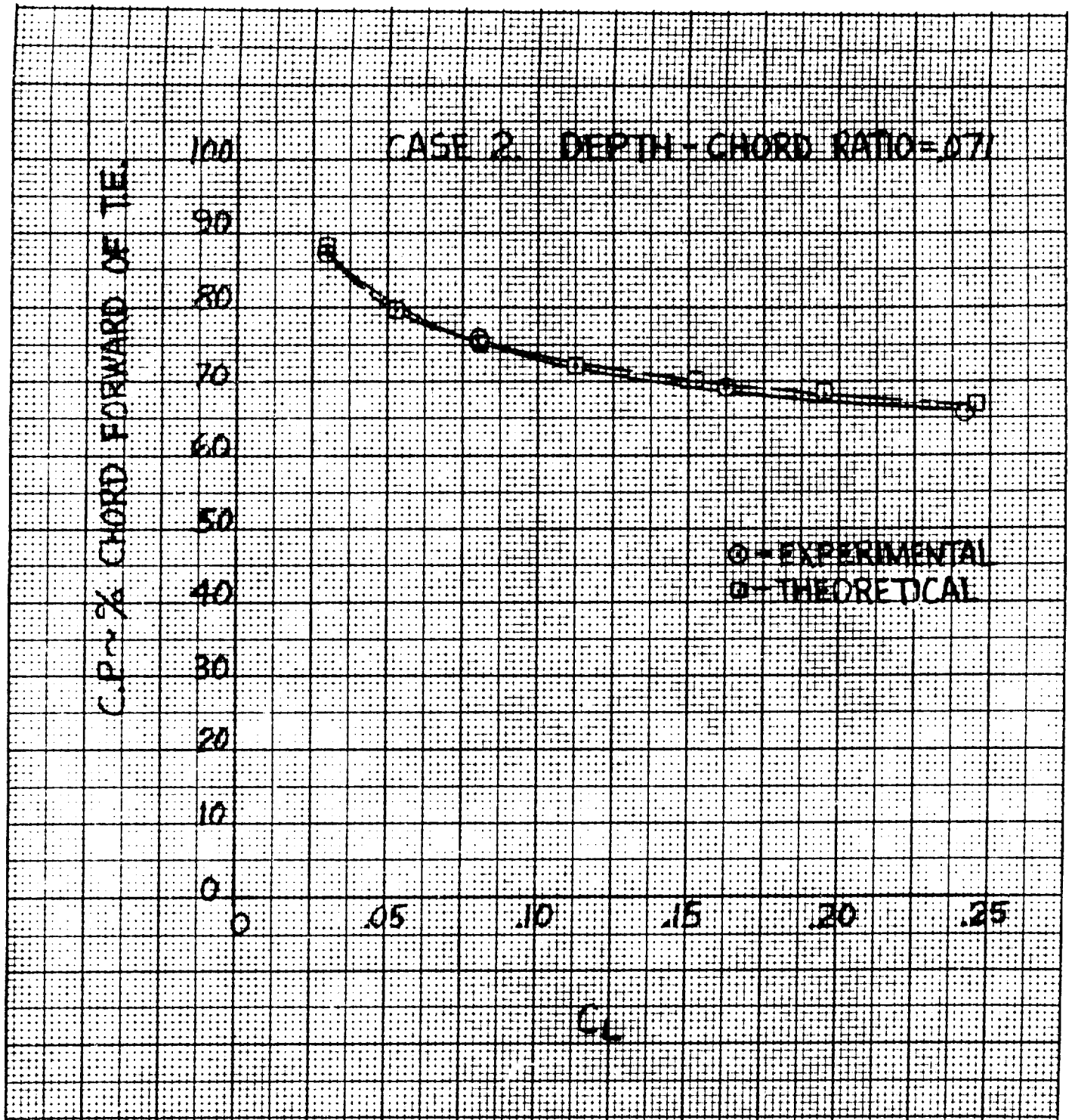Figure A-9. C.P. vs C_L, Modified Flat Plate Ski of Rectangular Planform and Aspect Ratio, 1/4

Figure A-10. C.P. vs C_L, Modified Flat Plate Ski of Rectangular Planform and
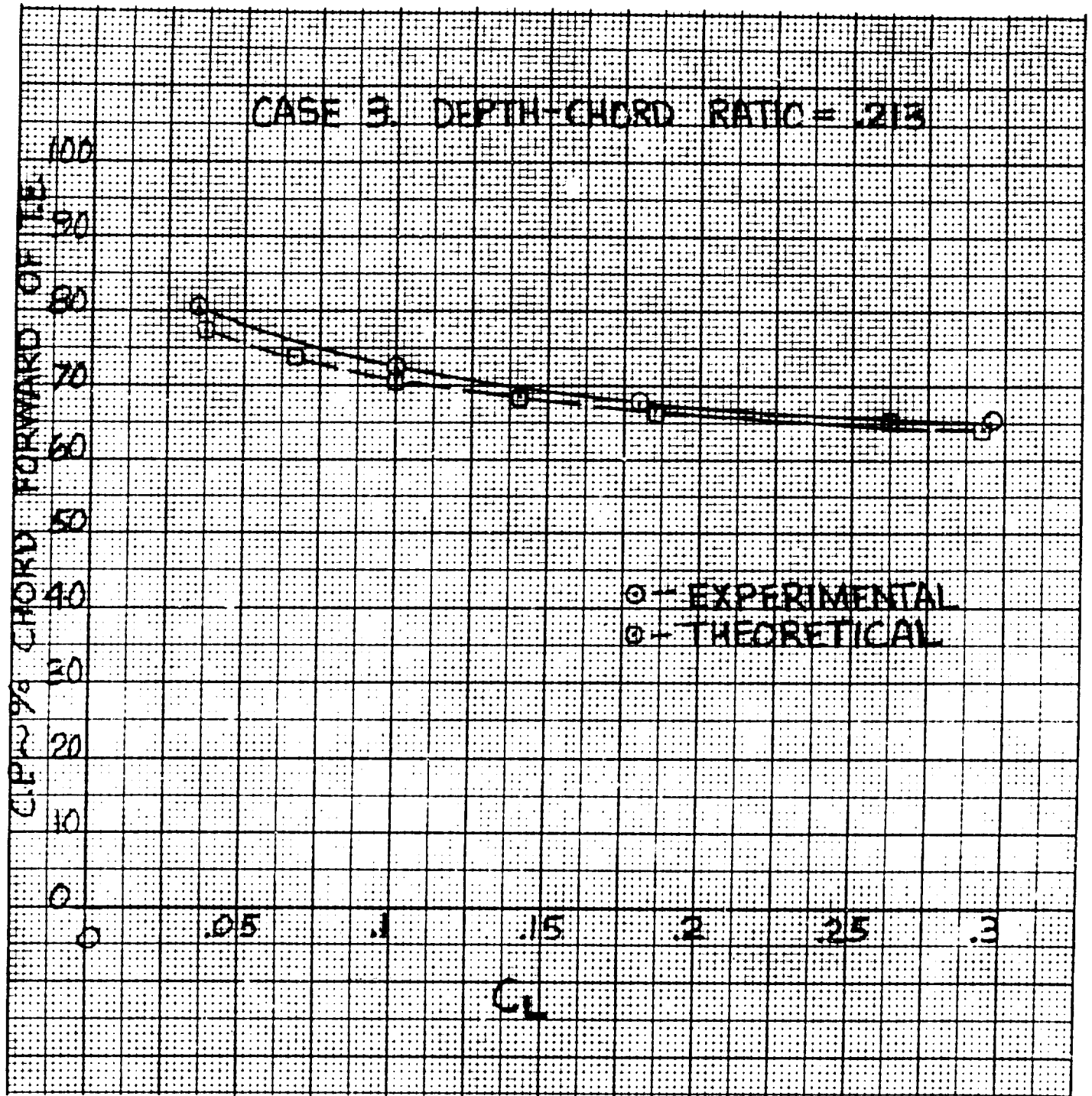Aspect Ratio, 1/4

Figure A-11. C.P. vs C_L, Modified Flat Plate Ski of Rectangular Planform and
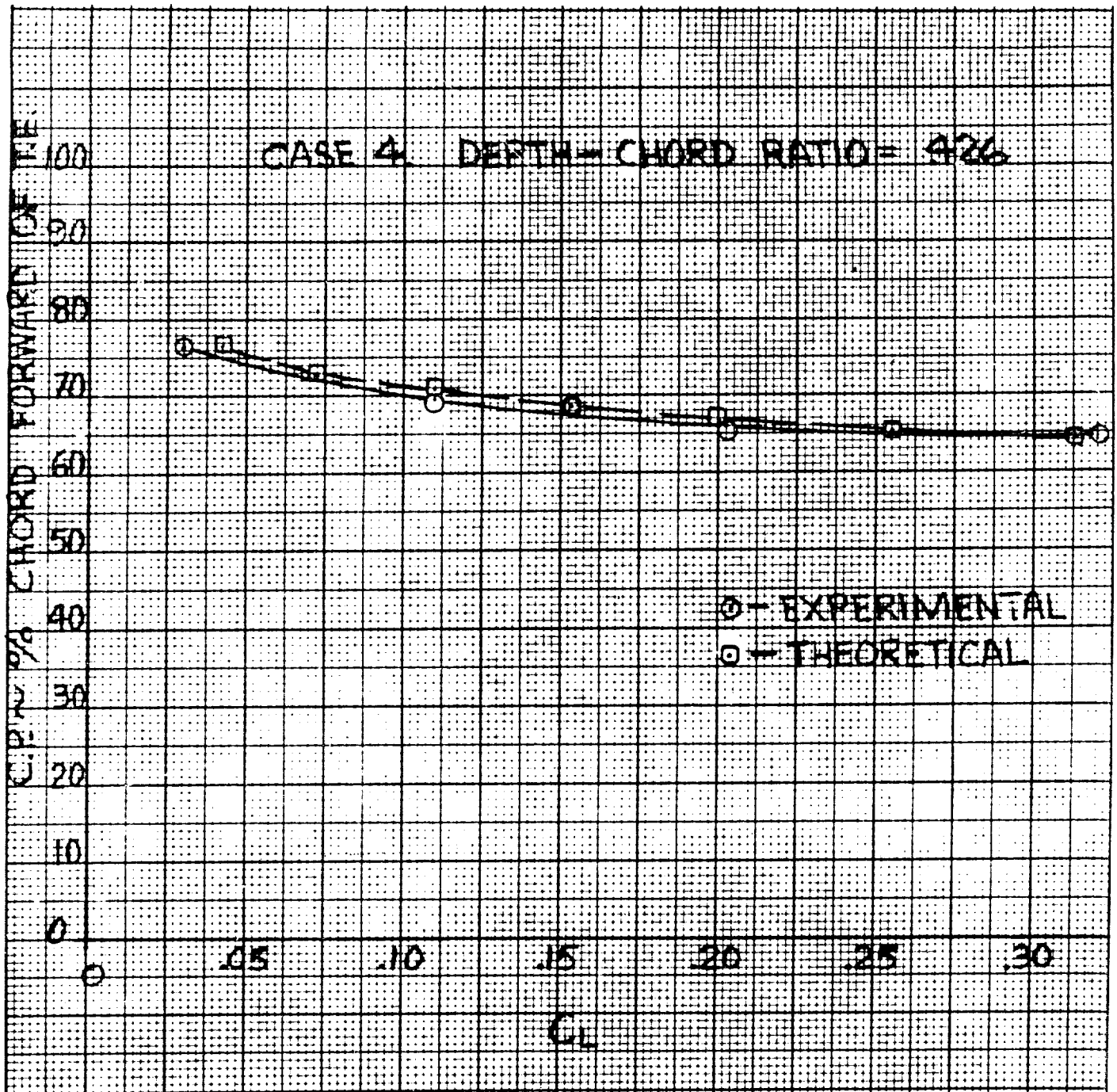Aspect Ratio, 1/4

Figure A-12. C.P. vs C_L, Modified Flat Plate Ski of Rectangular Planform and
Aspect Ratio, 1/4

APPENDIX B

HYDRODYNAMIC CHARACTERISTICS OF SUBMERGED VENTILATED HYDRO-SKIS

B1.   COMPUTER PROGRAM

a) Calculation of C_L

In Reference 3-7, Johnson's equation for the lift coefficient of a fully ventilated rectangular flat plate (hydro-ski) is:

$$C_L = C_{L1} + C_{L2} \tag{B-1}$$

where

$$C_{L1} = \frac{A}{A+1}\, m\,(\alpha - \alpha_i)\, \frac{\cos \alpha}{\cos (\alpha - \alpha_i)} \tag{B-2}$$

and

$$C_{L2} \approx \frac{0.88}{A+1}\, \sin^2 \alpha\, \cos \alpha \tag{B-3}$$

C_{L2} can be calculated directly, but this is not the case for C_{L1}. In the expression for C_{L1}, the quantity, α_i, the induced angle of attack, is given by:

$$\alpha_i = C_{L1} / \pi A \tag{B-4}$$

and, further, the quantity, m, is a complicated function of $(\alpha - \alpha_i)$ and the depth-chord ratio, d/c. In Reference 7, m is shown only in graphical form and, accordingly, Reference 7 uses an iteration technique to determine C_{L1}.

It has been found necessary to retain the use of an iteration technique to determine C_{L1}. To permit use of this technique on a digital computer, the function, $m(d/c, \alpha - \alpha_i)$, was represented as a sub-routine wherein m is obtained by linear interpolation inside of a network of numerical values which has been read from Figure 2, Reference 7. This network (grid) consisted of 112 pairs of values for d/c and $\alpha - \alpha_i$ covering the ranges:

$$0 \leqslant d/c \leqslant 2, \qquad 0 \leqslant \alpha - \alpha_i \leqslant 28°,$$

which was considered to cover the region of most practical interest.

With this technique, the desired values of C_{L1}, α_i, and m (for given values of A, α, and d/c) could then be obtained by iteration between equations (B-2), (B-4) and the sub-routine for m. Further, to ensure rapid convergence, this program was furnished with a reasonable starting value for C_{L1}:

$$C_{L1} = \left[1 + e^{-1.165\,(d/c)}\right]\left(\frac{A}{A+1}\right)\left(\frac{2\pi \sin\alpha \cos\alpha}{4 + \pi \sin\alpha}\right) \quad \text{(B-5)}$$

b) Calculation of C_D and x_{cp}

The calculation for C_D and x_{cp} by Johnson's method utilizes an iteration procedure involving a set of quantities, B_n, which are the Fourier coefficients of the function:

$$f(\theta; a, d/c) = \frac{a + \sqrt{d/c} + (1 - \cos\theta)/2}{\left[a + \sqrt{d/c} + (1 - \cos\theta)/2\right]^2 + d/4c} \quad \text{(B-6)}$$

i.e.,

$$B_o(a, d/c) = (1/\pi)\int_o^\pi f \cdot d\theta$$

$$B_n(a, d/c) = (2/\pi)\int_o^\pi f \cdot \cos n\theta \cdot d\theta \quad \text{(B-7)}$$

These coefficients are shown in chart form in Figure 9, Reference 3-7.

In the computer program, the functions, B_n, were computed by application of Simpson's rule to the integrals in eq. (B-7), the required accuracy being achieved by varying the number of intervals in the Simpson integration formula, as required.

Otherwise, the iteration technique used in the computer program is identical with that used in Johnson's method. For this iteration, the parameter, a, was given the arbitrary starting value of 0.3, irrespective of all other quantities.

c) Program Summary

This computer program as described above, covering the steady-state hydrodynamic characteristics of the ventilated hydro-ski, is a direct conversion of the methods presented in Reference 3-7 and, in principle, should (with negligible inaccuracy) yield exactly the same numerical results. This fact was actually verified by a calculation for one condition (A = 1/4, α = 12°, d/c = .071) as shown by the following results:

Method	C_L	$C_D - C_f$	x_{cp}
Hand Calculation. using Reference 3-7:	.0875	.0186	.347
Computer Program:	.0915	.0194	.359

where x_{cp} is the distance of the center of pressure aft of the L. E., in chord lengths.

It is seen that the agreement is extremely close. It is further assumed that, while not precise, the computer results have an accuracy at least equal to that of the hand calculations.

B2.   CORRELATION WITH EXPERIMENTAL DATA

Reference 8 presents experimental values for the hydrodynamic force and moment coefficients of a ventilated rectangular flat plate of aspect ratio, 1/4, at two depth-chord ratios (.035 and .071). The moment coefficients were first converted to center of pressure values, x_{cp}, representing the distance of the center of pressure aft of the L. E., measured in chords. The experimental values of C_L, C_D, and x_{cp} were then compared with the corresponding values obtained from the computer program ("Johnson values"). This comparison (not illustrated herein) showed certain fairly systematic discrepancies between the two sets of values even though the calculated values successfully duplicated all of the significant trends obtained in the experiments.

It must now be explained that Johnson's theory has, in the past, been very successfully correlated with available experimental data for aspect ratios as low as 1.0 (Reference 3-7). It was therefore supposed initially that the discrepancies found for the A = 1/4 data could be attributed to an aspect ratio effect and, accordingly, that the discrepancies could be eliminated by changing the common denominator, (A + 1), appearing in C_{L1} and C_{L2}. (See eqs. (B-2) and (B-3), above.) However, careful examination of the comparative values showed that much closer correlation could be obtained by use of purely empirical correction factors which are primarily dependent on angle of attack. Specifically, these corrections are as follows:

A) C_L and x_{cp}

It was found necessary to multiple the computed values for both of these quantities by a factor:

$$F_1(\alpha) = 1.55 \sqrt{\sin \alpha}$$

Within the range of the experimental data, this has the effect of appreciably reducing the calculated C_L values and of moving the calculated center of pressure forward.

B) $\underline{C_D}$

It was found necessary to increase the calculated C_D values by a constant value:

$$\Delta C_D = .0040$$

At this time, no theoretical (or other) justification can be offered for the nature or magnitude of these corrections although it is conjectured that they are primarily related to the use of a beveled trailing edge on the model ski used in the experiments.

The preceding correction factors were then incorporated directly into the computer program and a new set of computed values obtained. The comparison of these final computed values with the experimental data is illustrated in Figures B-1 through B-3. It is seen that well-nigh perfect agreement has been obtained. Further, the negligible residual discrepancies are well within the experimental accuracies indicated in Reference 3-8.
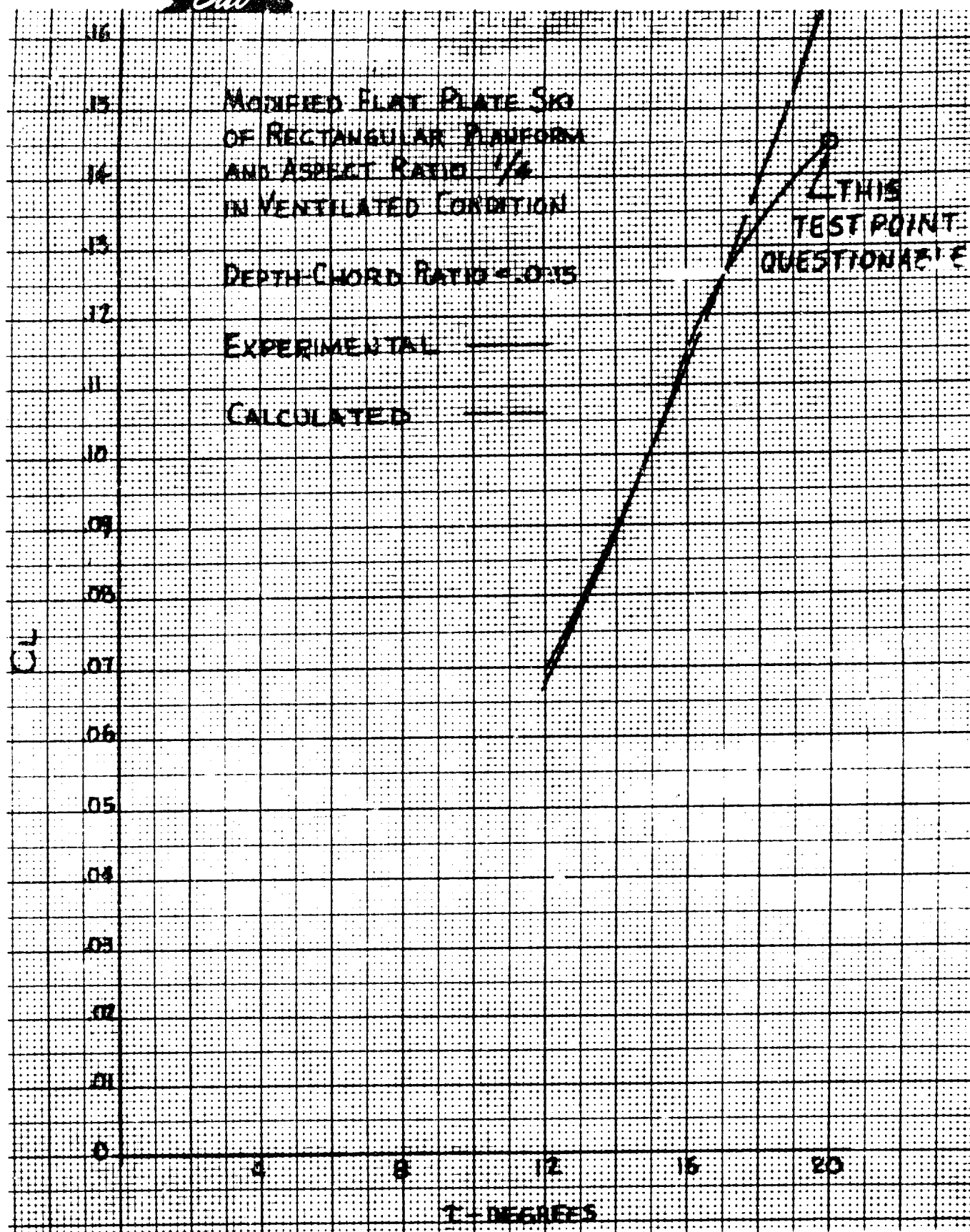
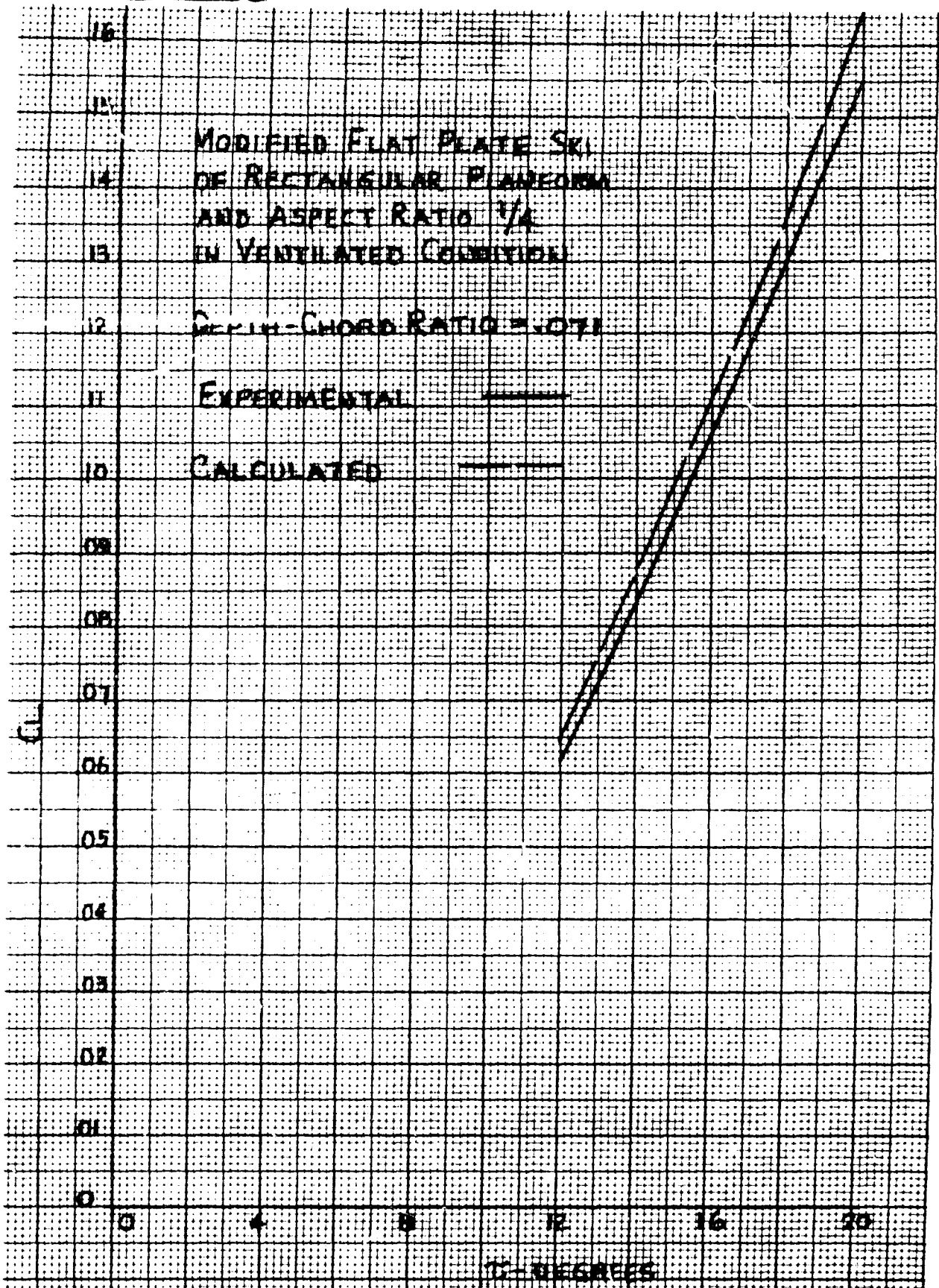Figure B-1(a). Comparison of Calculated and Experimental Lift Coefficients

MODIFIED FLAT PLATE SKI
OF RECTANGULAR PLANFORM
AND ASPECT RATIO 1/4
IN VENTILATED CONDITION

DEPTH-CHORD RATIO = .071

EXPERIMENTAL ————

CALCULATED ——

Figure B-1(b). Comparison of Calculated and Experimental Lift Coefficients
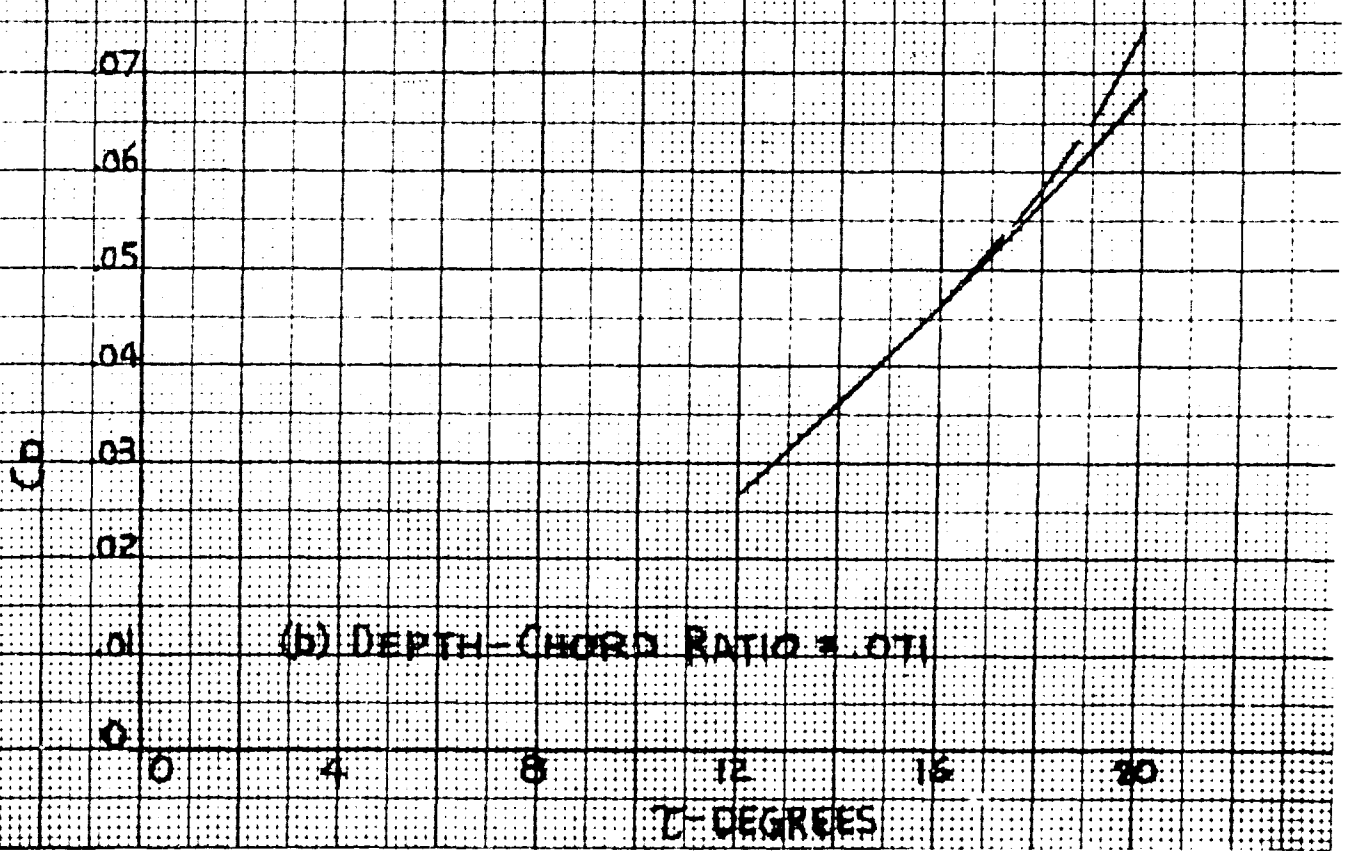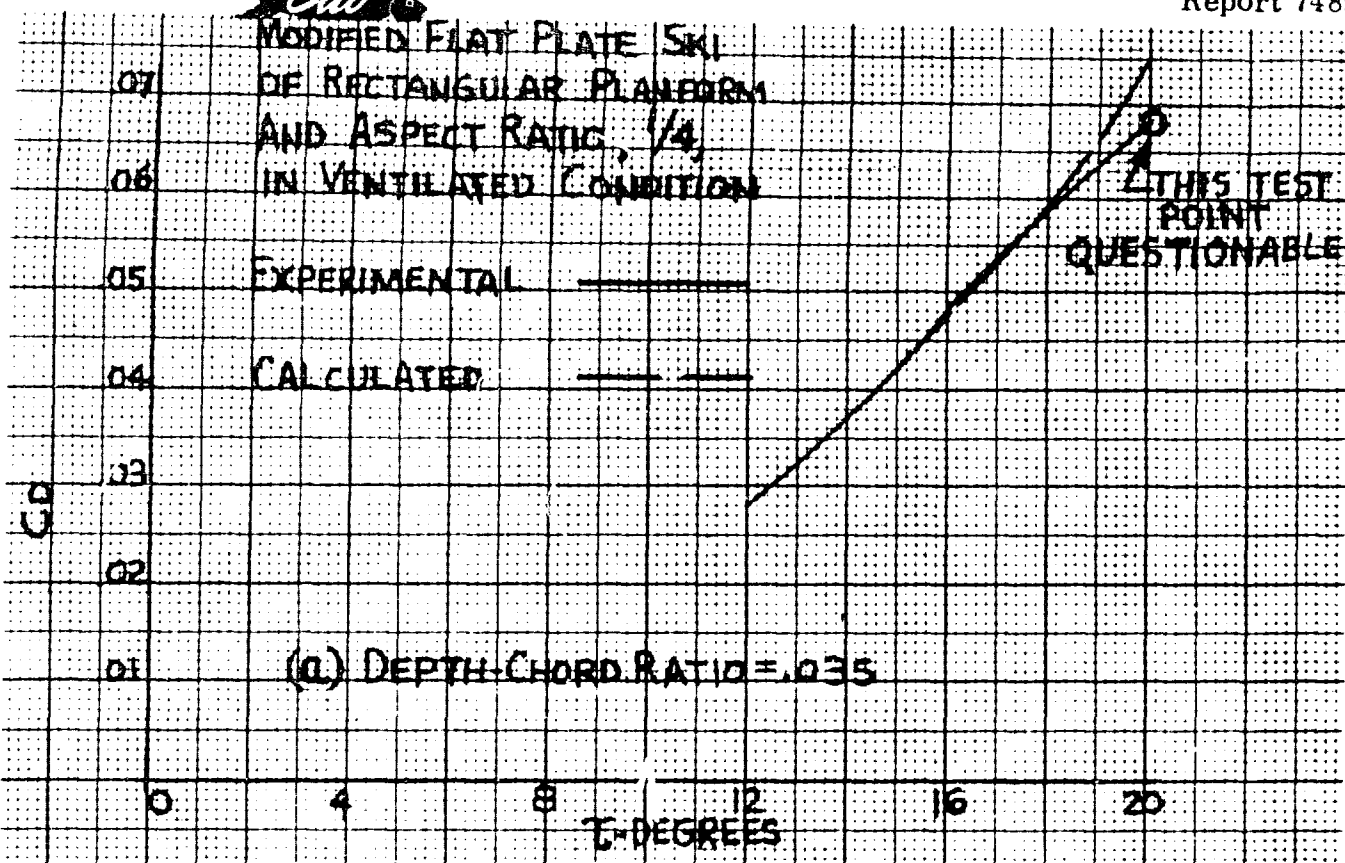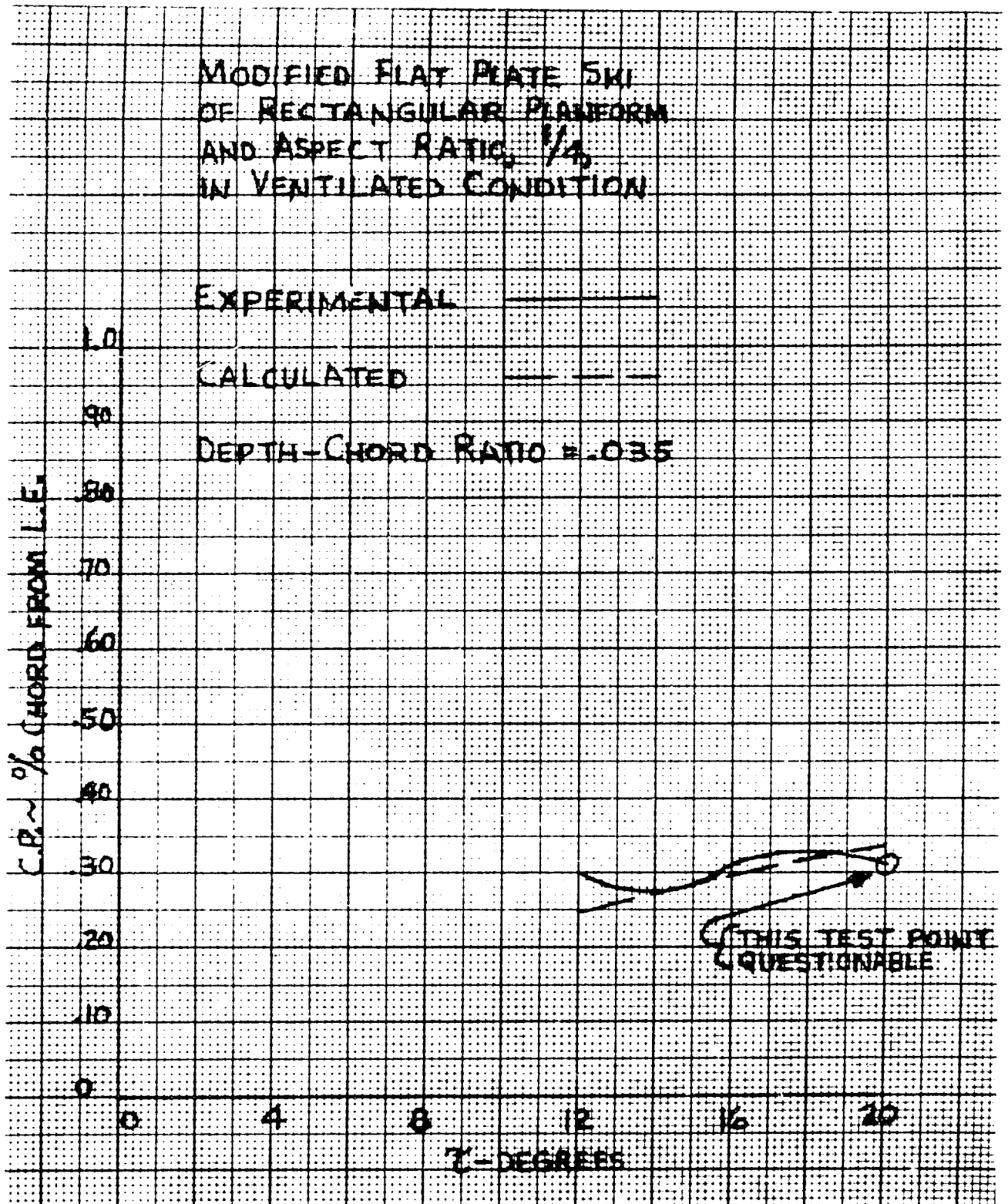
Figure B-2.   Comparison of Calculated and Experimental Drag Coefficients

Figure B-3(a). Comparison of Calculated and Experimental Moment Coefficients

Modified Flat Plate Ski
of Rectangular Planform
and Aspect Ratio, 1/4,
in Ventilated Condition

Experimental ——————
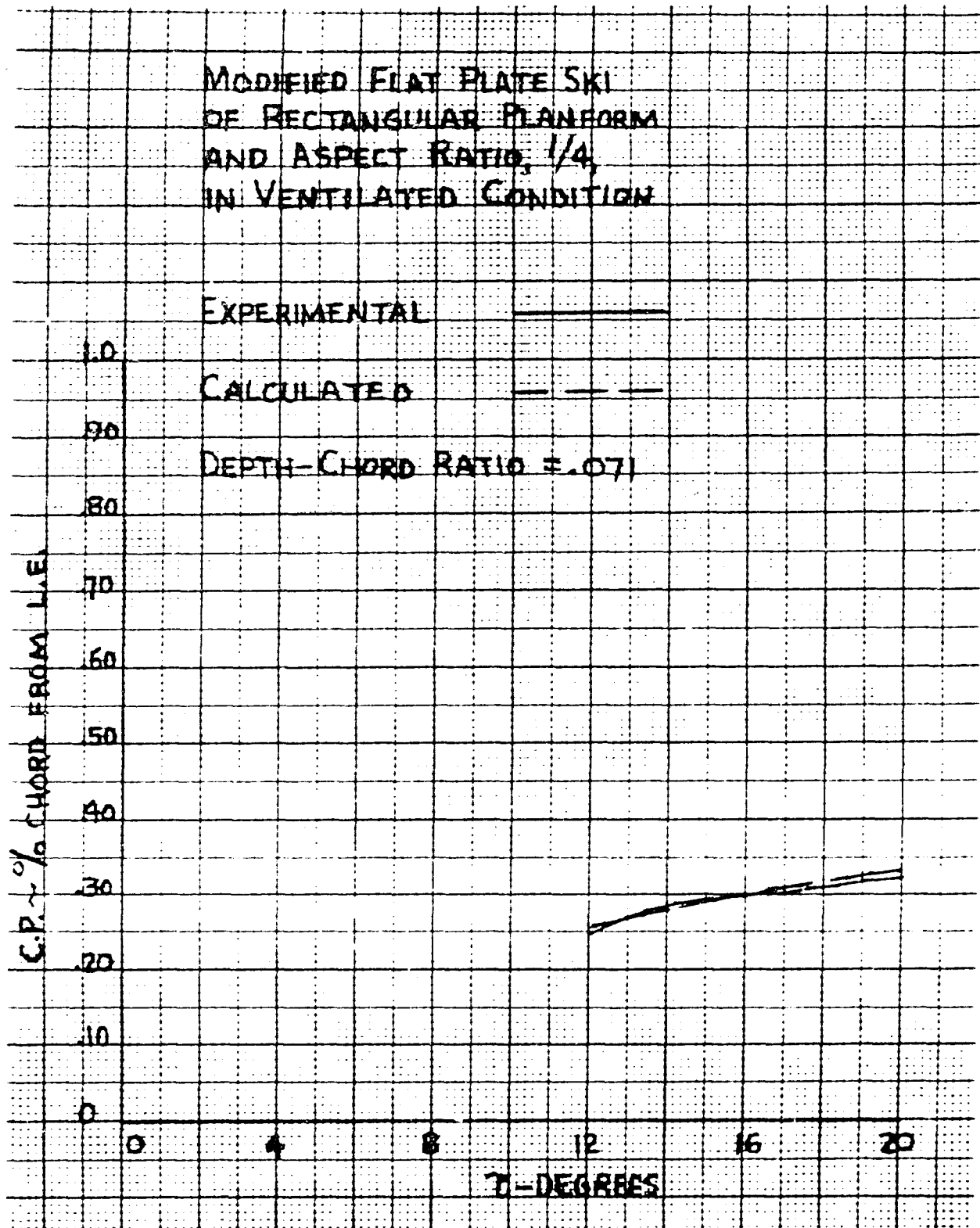
Calculated —— —— ——

Depth-Chord Ratio = .071

Figure B-3(b).   Comparison of Calculated and Experimental Moment Coefficients
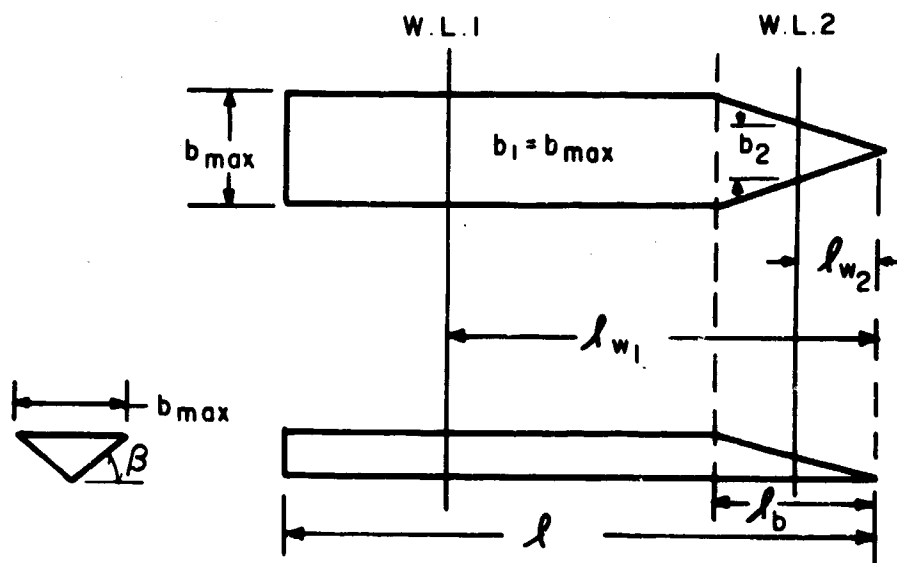
APPENDIX C

PLANING STABILITY DERIVATIVES FOR A SKELETON HYDRO-SKI SEAPLANE

C1. DETERMINATION OF EQUILIBRIUM WETTED SKI LENGTHS

The most general ski shape considered herein has constant deadrise and a planform which is basically rectangular but which may have a triangular trailing edge. The sketch below shows a ski of this type:

Obviously, the rectangular, constant deadrise ski is represented by the special limiting case:

$$l_b = 0$$

By an obvious extension of Shuford's formulas in Reference C-1, the lift coefficient for a constant deadrise ski with triangular trailing edge and wetted length, l_w, is approximated as:

$$C_{LH} = \left[\frac{\pi}{2} \quad \frac{1}{\Lambda + 1} \quad \tau \cos^2 \tau \, (1 - \sin\beta) + \frac{4}{3} \, \sin^2 \tau \cos^3 \tau \, \cos\beta \right]$$

where:

$$\Lambda = l_w / b$$

In this formula, which, in accordance with earlier sections of this report assumes "full wave rise", b is the local beam at the water line. Thus, as shown in the preceding sketch, for water lines occurring on the rectangular portion of the ski:

$$b = b_{max}, \text{ for } l_w \geqslant l_b;$$

while, for water lines on the triangular portion of the ski:

$$b = b_{max} \cdot (l_w / l_b), \text{ for } l_w \leqslant l_b$$

Using the notation:

$$\Lambda = l_w / b_{max}, \qquad \Lambda_b = l_b / b_{max},$$

$$P(\tau, \beta) = (\pi/2) \tau \cos^2 \tau \ (1-\sin \beta),$$

$$Q(\tau, \beta) = (4/3) \sin^2 \tau \ \cos^3 \tau \ \cos \beta$$

the lift coefficient can be written concisely as:

$$C_{LH1} = (\frac{1}{\Lambda+1} P + Q) \text{ for } \Lambda \geqslant \Lambda_b$$

$$C_{LH2} = (\frac{1}{\Lambda_b+1} P + Q) \text{ for } \Lambda \geqslant \Lambda_b$$

It is thus seen that, for a given ski, C_{LH1} depends both on Λ (i.e., on l_w) and τ, whereas C_{LH2} depends only on τ.

The wetted areas corresponding to the two W. L. locations are:

$$S_{W1} = (\Lambda - \frac{1}{2} \Lambda_b) b^2_{max}$$

$$S_{W2} = (1/2) \Lambda^2 / \Lambda_b) b^2_{max}$$

These relations can be used for the determination of the ski wetted length in any specified equilibrium planing condition i.e., for specified trim-speed combinations, as follows. For equilibrium of vertical forces:

C-2

$$L_H = W - L_A = W - C_{LA}(\tau)(\rho_A/2)V_H^2 S_w$$

$$\text{or,} \quad C_{LH}S_W = \frac{W}{(\frac{\rho_w}{2}V^2)} - C_{LA}(\tau)(\rho_A/\rho_w)S_w$$

where $C_{LA}(\tau)$ represents the known lift curve for the airplane. Hence, the alternate equations defining the equilibrium wetted length are:

(1): $\quad \Lambda \geqslant \Lambda_b$:

$$(\frac{P}{\Lambda+1} + Q)(\Lambda - \frac{1}{2}\Lambda_b) = N$$

(2): $\quad \Lambda \leqslant \Lambda_b$:

$$\Lambda = \sqrt{2\Lambda_b}\left\{ N \Big/ \left[(P/\Lambda_b) + Q\right] \right\}^{1/2}$$

where: $\quad N = \left[W/(\rho_{w/2})V_H^2 b_{max}^2 \right] - (\rho_A/\rho_w)(S_w/b_{max}^2)C_{LA}(\tau)$

Note that the first of these equations requires use of the quadratic formula while the second is explicit.

C2.   UNSTEADY HYDRODYNAMIC LIFT FORCE

The instantaneous force acting on the heaving and pitching ski is assumed to be given by the relation:

$$L_H = C_{LH}S_W(\rho_w/2)V_{eq}^2$$

$$= S_{LH}(\rho_w/2)V_{eq}^2$$

where, in accordance with the "equivalent planing velocity" theory (previously validated for one degree of freedom), the "hydrodynamic lift area" depends only on the instantaneous geometry of the ski relative to the (smooth) water surface i.e., on wetted length and ski trim angle, while the "equivalent planing velocity" is a fictitious steady-state horizontal velocity which would produce the same lift force under the instantaneous geometric conditions.

If there were no pitching velocity, V_{eq} would be defined as was done in Section 5.

$$V_{eq} = V_H (1 - \frac{\dot{h}}{V_H} \cot \tau)$$

It is obvious that the actual effect of a pitching velocity (about a transverse axis through the aircraft c.g.) is to induce linear velocities which, at any one instant, vary along the ski's wetted length. This is clearly equivalent to the production of an instantaneous effective ski camber. Further, the effects of such camber on ski lift could presumably be calculated by a suitable adaptation of Johnson's theory, Reference C-2, for submerged cambered, supercavitating hydrofoils. Primarily because of its complexity, this approach was rejected as inexpedient.

Instead, it was assumed that the actual effect, as just described, could be approximated by adding to the "heaving equivalent planing velocity" a term representing the component, normal to the ski keel, of the linear velocity induced at the ski-waterline intersection, i.e., by taking:

$$V_{eq} = V_H (1 - \frac{\dot{h}}{V_H} \cot \tau - \frac{\dot{\tau} a}{V_H} \csc \tau)$$

where the quantity "a" is defined by the following sketch:
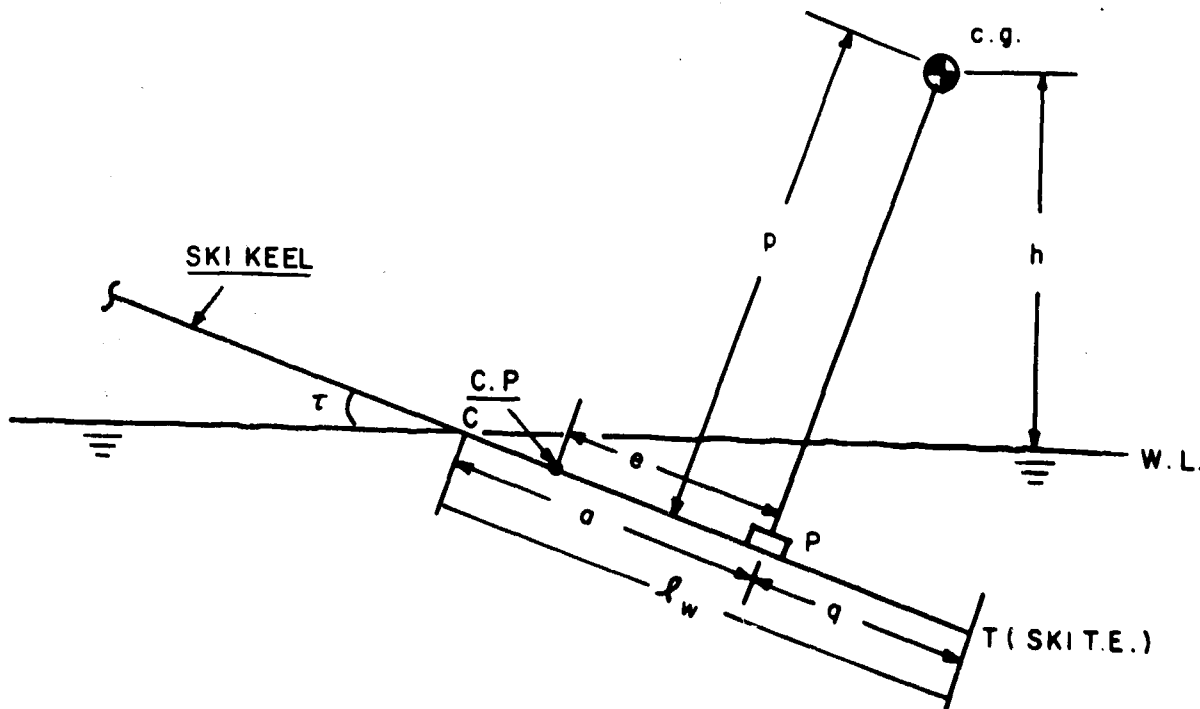
Here, h = heave, instantaneous height of c.g. above W. L., (variable)

p = perpendicular distance from c.g. to ski keel line, positive for ski keel below c.g., (constant for any particular configuration).

q = $\overline{PT}$, measured parallel to ski keel line (constant for any particular configuration).

a = $\overline{PC}$ (where C designates ski-W.L. intersection), measured parallel to ski keel line, positive for P aft of C.

l_w = ski wetted length

By trigonometry, it is found that:

$$a = p \cot \tau - h \csc \tau$$

so that:

$$l_w = q + a$$

$$= q + p \cot \tau - h \csc \tau$$

Hence, the final complete expression for the unsteady hydrodynamic lift force becomes:

$$L_H / (\rho_w / 2) V_H^2 = S_{LH} \left[1 - \cot \tau \, (\dot{h}/V_H) - (p \cot \tau - h \csc \tau) \csc \tau \, (\dot{\tau}/V_H) \right]^2$$

where the alternate values of S_{LH} are:

$$S_{LH} = (\frac{P}{\Lambda + 1} + Q)(\Lambda - \frac{1}{2} \Lambda_b) b^2_{max}, \qquad \Lambda \geqslant \Lambda_b$$

$$S_{LH} = (\frac{P}{\Lambda_b + 1} + Q)(\Lambda^2 / 2 \Lambda_b) b^2_{max}, \qquad \Lambda \leqslant \Lambda_b$$

and

$$\Lambda = l_w / b_{max}, \qquad \Lambda_b = l_b / b_{max}$$

$$P = (\pi/2) \tau \cos^2 \tau \, (1 - \sin\beta)$$

$$Q = (4/3) \sin^2 \tau \, \cos^3 \tau \, \cos\beta$$

C3. UNSTEADY HYDRODYNAMIC PITCHING MOMENT

It is obvious that the "equivalent planing velocity" method utilizes the tacit assumption that the unsteady longitudinal pressure distribution on the ski is the same as in steady flow for the same geometric conditions. It follows automatically that the unsteady center of pressure (c.p.) is the same as the corresponding steady c.p. Consequently, unsteady moment values can be obtained by locating the unsteady lift force at the steady-state c.p. location.

Section 3.2 gives the steady planing c.p. locations for hydro-skis having rectangular and triangular planforms. By a suitable combination of these values, it is possible to devise an approximate expression for a rectangular ski with a triangular T.E. However, the resulting expression for the hydrodynamic pitching moment would then be excessively complex and the corresponding stability derivatives even more so.

Instead of this approach, the c.p. of the rectangular ski with triangular T.E. is arbitrarily assumed to be located at a fixed fraction of the wetted length, namely, at 75% of the wetted length, measured from the trailing edge. Referring back to the preceding sketch, the ski pitching moment is taken as:

$$M_H = e\, L_H / \cos \tau$$

where

$$e + q = .75\, l_w$$

i.e.

$$e = .75\, l_w - q$$

$$= .75\, (q + p \cot \tau - h \csc \tau) - q$$

$$= .75\, (p \cot \tau - h \csc \tau) - .25\, q$$

where, again, p and q are each constant for a particular configuration.

C4. HYDRODYNAMIC STABILITY DERIVATIVES

It is now a straightforward matter to determine all of the hydrodynamic stability derivatives. For this purpose, it is convenient to use logarithmic differentiation.

Thus:

$$L_H = C_{LH} (\rho_w / 2)\, V_{eq}^2\, S_W$$

so that, for example,

$$\frac{L_{Hh}}{L_H} = \frac{C_{LHh}}{C_{LH}} + \frac{2 V_{eq\,h}}{V_{eq}} + \frac{S_{Wh}}{S_W}$$

with corresponding equations for the other three derivatives of L_H and the four derivatives of M_H.

The following results were then obtained:

CASE I. $\Lambda \geqslant \Lambda_b$

Equilibrium Values

A) With P, Q, N as defined above, let:

$$b = \frac{P + (1 - \frac{\Lambda_b}{2}) Q - N}{Q}$$

$$c = \frac{\frac{\Lambda_b}{2} (P + Q) + N}{Q}$$

Then $\Lambda = -\frac{b}{2} + \left|\frac{b}{2}\right| \sqrt{1 + \frac{4c}{b^2}}$

B) $l_w = b_{max} \Lambda$

C) $h = \sin \tau \left[q + p \cot \tau - l_w \right]$

D) $C_{LH} = \left[P/(\Lambda + 1) \right] + Q$

E) $S_W = b^2_{max} (\Lambda - \frac{1}{2} \Lambda_b)$

F) $L_H = C_{LH} S_W (\rho_w/2) V_H^2$

G) $f = \left[.75 (p \cot \tau - h \csc \tau) - .25 q \right] / \cos \tau$

H) $M_H = f L_H$

Stability Derivatives

I.1.a) $\quad L_{Hh} = L_H \left[\dfrac{C_{LHh}}{C_{LH}} + \dfrac{S_{Wh}}{S_W} \right]$

I.1.b) $\quad M_{Hh} = M_H \left[\dfrac{C_{LHh}}{C_{LH}} + \dfrac{S_{Wh}}{S_H} + \dfrac{f_h}{f} \right]$

where: $\quad C_{LHh} = \dfrac{P}{b_{max} (\Lambda + 1)^2 \tau}$

$\quad S_{Wh} = -b_{max}/\tau$

$\quad f_h = -.75/\tau$

I.2.a) $\quad L_{H\tau} = L_H \left[\dfrac{C_{LH\tau}}{C_{LH}} + \dfrac{S_{W\tau}}{S_W} \right]$

I.2.b) $\quad M_{H\tau} = M_H \left[\dfrac{C_{LH\tau}}{C_{LH}} + \dfrac{S_{W\tau}}{S_W} + \dfrac{f_\tau}{f} \right]$

where: $\quad C_{LH\tau} = \dfrac{(\pi/2)(1 - \sin\beta)}{(\Lambda + 1)^2} \dfrac{(p-h)}{b_{max}} \dfrac{(1 - \frac{\tau^2}{2})}{\tau}$

$\quad\quad\quad + \dfrac{(\pi/2)(1 - \sin\beta)}{(\Lambda + 1)} (1 - \frac{3}{2}\tau^2)$

$\quad\quad\quad + (8/3)(\cos\beta)(\tau - \frac{10}{3}\tau^3)$

$\quad S_{W\tau} = -\dfrac{b_{max}(p-h)}{\tau^2}$

$\quad f_\tau = \dfrac{-.75(p-h)}{\tau^2}$

I.3.a) $\quad L_{H\dot{h}} = L_H (-2/V_H \tau)$

I.3.b) $\quad M_{H\dot{h}} = M_H \left(-2/V_H \tau\right)$

I.4.a) $\quad L_{H\dot{\tau}} = L_H \left[-2\,(p-h)/V_H \tau^2\right]$

I.4.b) $\quad M_{H\dot{\tau}} = M_H \left[-2\,(p-h)/V_H \tau^2\right]$

CASE II. $\quad \Lambda \leqslant \Lambda_b$

Equilibrium Values

A) With P, Q, N defined above:

$$\Lambda = \sqrt{\frac{2\Lambda_b(\Lambda_b + 1)\,N}{P + (\Lambda_b + 1)\,Q}}$$

B) $\quad l_w = b_{max}\,\Lambda$

C) $\quad h = \sin\tau \left[q + p\cot\tau - l_w\right]$

D) $\quad C_{LH} = \left[P/(\Lambda_b + 1)\right] + Q \quad \text{(independent of } \Lambda \text{)}$

E) $\quad S_W = (b^2_{max}/2\,\Lambda_b)\,\Lambda^2$

F) $\quad L_H = C_{LH}\,S_W(\rho_w/2)\,V_H^2$

G) $\quad f = \left[.75\,(p\cot\tau - h\csc\tau) - .25\,q\right]/\cos\tau$

H) $\quad M_H = f\,L_H$

C-9

Stability Derivatives

II.1.a) $\quad L_{Hh} = L_H \left[\dfrac{S_{Wh}}{S_W} \right]$

II.1.b) $\quad M_{Hh} = M_H \left[\dfrac{S_{Wh}}{S_W} + \dfrac{f_h}{f} \right]$

where: $\quad S_{Wh} = -\left(\dfrac{b_{max}}{\tau} \right) \left(\dfrac{\Lambda}{\Lambda_b} \right)$

$\quad f_h = -.75/\tau$

II.2.a) $\quad L_{H\tau} = L_H \left[\dfrac{C_{LH\tau}}{C_{LH}} + \dfrac{S_{W\tau}}{S_W} \right]$

II.2.b) $\quad M_{H\tau} = M_H \left[\dfrac{C_{LH\tau}}{C_{LH}} + \dfrac{S_{W\tau}}{S_W} + \dfrac{f_\tau}{f} \right]$

where: $\quad C_{LH\tau} = \dfrac{(\pi/2)(1 - \sin\beta)}{(\Lambda_b + 1)} \left(1 - \dfrac{3}{2}\tau^2\right)$

$\quad\quad\quad + (8/3)(\cos\beta)\left(\tau - \dfrac{10}{3}\tau^3\right)$

$\quad S_{W\tau} = -b_{max}\left(\dfrac{p-h}{\tau^2}\right)\left(\dfrac{\Lambda}{\Lambda_b}\right)$

$\quad f_\tau = -.75\,(p-h)/\tau^2$

II.3.a) $\quad L_{H\dot{h}} = L_H\left(-2/V_H\tau\right)$

II.3.b) $\quad M_{H\dot{h}} = M_H\left(-2/V_H\tau\right)$

II.4.a) $\quad L_{H\dot{\tau}} = L_H\left[\dfrac{-2\,(p-h)}{V_H\,\tau^2}\right]$

II.4.b) $\qquad M_{H\dot{\tau}} = M_H \left[\dfrac{-2(p-h)}{V_H \tau^2} \right]$

It will finally be noted that these results also cover the case of the <u>completely</u> <u>rectangular ski</u>. For the latter geometry, it is only necessary to substitute $\Lambda_b = 0$ <u>in all of the Case I equations</u>.

C5. AERODYNAMIC STABILITY DERIVATIVES

In general, the present treatment of the aerodynamic stability derivatives is similar to that used in the classical analyses of aircraft aerodynamic stability. However, this treatment also assumes that the four static derivatives, $L_{A\tau}$, $M_{A\tau}$, L_{Ah}, M_{Ah}, are known from wind-tunnel tests. It also assumes that the aircraft is of "conventional" aerodynamic and propulsive configuration and that the hull does not contribute to any of the four dynamic (damping) derivatives. Finally, all effects of power on the stability derivatives are neglected.

Before proceeding, it must be pointed out that none of these limitations really restrict the application of the present method. Thus, the dynamic derivatives can actually be measured by the more elaborate tunnel techniques presently available. Similarly, power-on derivatives can be measured by suitable wind-tunnel tests of powered models. Further, in the case of "unconventional" configurations (canards, etc.) the dynamic derivatives can be estimated, if necessary, by approaches similar to those used herein.

The dynamic values of the aerodynamic lift and pitching moment can be written as:

$$L_A = L_{A(t-o)} + L_{At}$$

$$M_A = M_{A(t-o)} + M_{At}$$

where "$(t-o)$" signifies values in the absence of the horizontal tail and "t" signifies the values for the horizontal tail in the presence of the wing.

The "tail-off" values can be written as:

$$L_{A(t-o)} = q_A C_{L\alpha(t-o)} (\alpha_{w\,eff} - \alpha_0) S_w$$

$$M_{A(t-o)} = q_A C_{M\alpha(t-o)} (\alpha_{w\,eff} - \alpha_1) S_w \bar{c}$$

where $\qquad \alpha_{w\,eff} = \alpha_w - (\dot{h}/V_H)$

The horizontal tail contributions can be written as:

$$L_{At} = q_A C_{L \alpha t} \alpha_{teff} S_t$$

$$M_{At} = -q_A l_t C_{L \alpha t} \alpha_{teff} S_t$$

where

$$\alpha_{teff} = \alpha_{weff} + \frac{l_t}{V} \dot{\tau} - \epsilon + i_t$$

In this expression for α_{teff}, it is necessary to account for the effect of "downwash lag," as follows. The downwash angle is written as:

$$\epsilon (t) = \frac{d\epsilon}{d\alpha_w} \alpha'_{weff}$$

where $\epsilon (t)$ is the downwash angle at the tail at time, t, and α'_{weff} is the effective wing angle of attack at the earlier time:

$$t' = t - (l_t / V_H)$$

Then, approximately,

$$\alpha'_{weff} \cong \alpha_{weff} - \frac{l_t}{V_H} \dot{\alpha}_{weff}$$

so that:

$$\alpha_{teff} = \alpha_{weff} + \frac{l_t}{V_H} \dot{\tau} - \frac{d\epsilon}{d\alpha_w} (\alpha_{weff} - \frac{l_t}{V_H} \dot{\alpha}_{weff}) + i_t$$

$$= (1 - \frac{d\epsilon}{d\alpha}) \alpha_{weff} + \frac{l_t}{V_H} (\dot{\tau} + \frac{d\epsilon}{d\alpha_w} \dot{\alpha}_{weff}) + i_t$$

But

$$\alpha_w = \tau + i_w \quad (i_w = \text{wing incidence to ski keel})$$

so that

$$\alpha_{weff} = \tau - (\dot{h}/V_H) + i_w$$

and

$$\dot{\alpha}_{weff} = \dot{\tau} - (\ddot{h}/V_H)$$

Hence

$$\alpha_{teff} = (1 - \frac{d\epsilon}{d\alpha_w})(\tau - \frac{\dot{h}}{V_H} + i_w) + \frac{l_t}{V_H} \left[(1 + \frac{d\epsilon}{d\alpha}) \dot{\tau} - \frac{d\epsilon}{d\alpha} \frac{\ddot{h}}{V_H} \right] + i_t$$

From the preceding expressions, the eight aerodynamic stability derivatives are found to be:

1.a) $\quad L_{Ah} = 0*$

1.b) $\quad M_{Ah} = 0*$

2.a) $\quad L_{A\tau} = q_A \left[C_{L\alpha(t-o)} S_w + (1 - \frac{d\epsilon}{d\alpha_w}) C_{L\alpha t} S_t \right]$

2.b) $\quad M_{A\tau} = q_A \left[C_{M\alpha(t-o)} S_w \bar{c} - (1 - \frac{d\epsilon}{d\alpha_w}) C_{L\alpha t} S_t l_t \right]$

3.a) $\quad L_{A\dot{h}} = -L_{A\tau} / V_H$

3.b) $\quad M_{A\dot{h}} = -M_{A\tau} / V_H$

4.a) $\quad L_{A\dot{\tau}} = (1 + \frac{d\epsilon}{d\alpha_w}) q_A C_{L\alpha t} S_t l_t / V_H$

4.b) $\quad M_{A\dot{\tau}} = -(K + \frac{d\epsilon}{d\alpha_w}) q_A C_{L\alpha t} S_t l_t^2 / V_H *$

In addition to these eight derivatives, it is seen that the "downwash lag" effect contributes two additional terms into the equations, both of which are proportional to $\ddot{h}$. While these terms represent real effects, they will be neglected herein primarily for reasons of consistency. If they were retained, consistency would demand inclusion of all

*The following remarks are of importance in practical application of the preceding results:

    1) In many cases, L_{Ah} and M_{Ah} are not necessarily zero, even approximately. Their actual values are best established by direct wind-tunnel tests for "ground effect."

    2) The values given above for $L_{A\tau}$ and $M_{A\tau}$ are useful for estimation purposes. It is far better, of course, to utilize the values obtained directly from wind-tunnel tests.

    3) In accordance with conventional practice, an empirical factor, K, has been introduced into the expression for $M_{A\dot{\tau}}$ to account for the pitch damping contributions of the wing and the hull. It is standard practice to assume that $K \cong 1.1$.

other terms proportional to $\overset{\cdot}{h}$ and $\overset{\cdot\cdot}{t}$. While such other terms exist and are of importance in flutter analyses, they are customarily neglected in aircraft dynamic stability investigations. By way of further justification, it may be noted that the coefficient:

$$L_{A\overset{\cdot}{h}} = \left(\frac{d\epsilon}{d\alpha_w}\right)\left(\frac{\rho_A}{2}\right)C_{L\alpha t}S_t l_t$$

represents an "added mass" whose value in a typical case is about 2% of the aircraft mass.

REFERENCES

C-1. **NACA TN 3939:** "A Theoretical and Experimental Study of Planing Surfaces Including Effects of Cross-Section and Planform," C. L. Shuford, Jr., March 1957.

C-2. **NACA RM L57I16:** "Theoretical and Experimental Investigation of Arbitrary Aspect Ratio, Supercavitating Hydrofoils Operating Near the Free Water Surfaces," by V. E. Johnson, Jr., 12 December 1957.

APPENDIX D

HYDRO-SKI FORCES AND MOMENTS FOR WAVE RESPONSE COMPUTER PROGRAM

D1.   HYDRO-SKI FORCES

The sketches in Figure D-1 show all of the impact (wetted ski) conditions that can possibly arise while the seaplane is operating in waves. A level water line is shown in each sketch only for simplicity of illustration but the load estimate for each case is intended to be applicable to wave conditions. It will be understanding that, in the force calculations, the resultant velocity vector at the hydro-ski also includes the effect of the rigid-body angular velocity about the aircraft center of gravity. That is, the linear velocity of the hydro-ski center of pressure due to aircraft rotation is vectorially added to the translational velocity so that the hydro-ski is considered to be only in translational motion at any instant.

Case (1)

The necessary conditions for Case (1) are:

a) Leading edge at or above water surface;
b) Trailing edge below water surface;
c) Minimum trim, + 3°;
d) Lower surface only wetted.

This is the conventional impact condition extensively covered in the literature. The instantaneous hydrodynamic load is determined by calculating the resultant velocity component normal to the keel, from which is obtained the equivalent planing velocity for use in conjunction with the Shuford planing lift formula, given in Section 3.2.
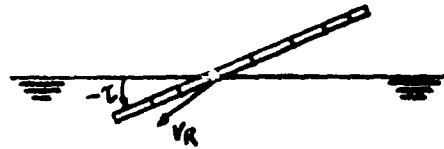
Case (2)

The necessary conditions for Case (2) are:

a) Leading edge at or below water surface;
b) Trailing edge above water;
c) Minimum trim, −3°;
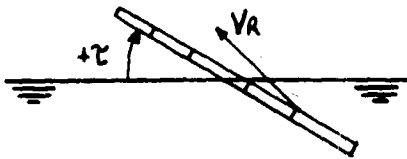d) Lower surface only wetted.

This impact condition is not covered in the literature, either theoretically or empirically. It is therefore accounted for by assuming that, like Case (1), the resultant velocity component normal to the keel defines an equivalent planing velocity, which is calculated by the same method used for Case (1). However, in this case, the equivalent planing velocity vector is directed toward the right in the following sketch:
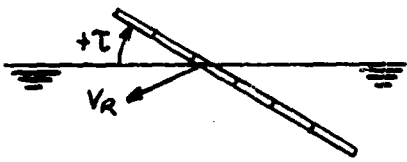
Case (1): Lower Surface Wetted, $\tau > +3°$ Case (2): Lower Surface Wetted, $\tau < -3°$
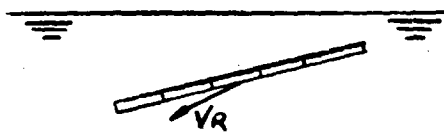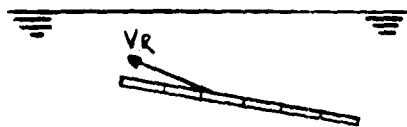
Case (3): Upper Surface Wetted Case (4): Upper Surface Wetted

Case (5): Lower Surface Wetted Case (6): Lower Surface Wetted
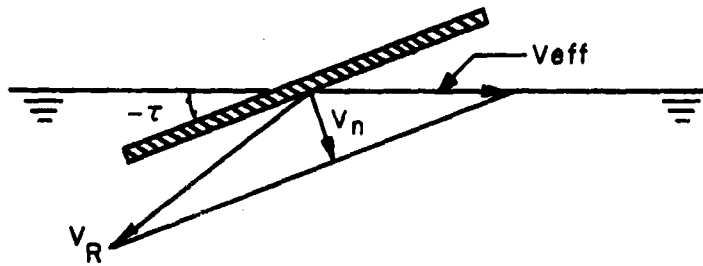
Case (7): Upper Surface Wetted Case (8): Upper Surface Wetted

CASE (9): Lower Surface Wetted, $0 < \tau < +3°$
("Two - Dimensional Impact")

Figure D-1. Sketch Showing Possible Ski-Wave Geometries and Ski Motions in Rough Water

The instantaneous hydrodynamic load is then determined in the same manner as for Case (1). It is recognized that, for this case, the flow around the leading edge is considerably different from that which it would be if "reversed planing" tests were conducted. However, it is reasoned that, since much higher pressures are to be expected in the spray root region at the water line-ski intersection, the error incurred is not significant.

Case (4)

Case (4) is considered before Case (3) as it is easier to visualize the concept used to derive an expression for its hydrodynamic loading.

The necessary conditions for Case (4) are:
a) Leading edge at or below water surface;
b) Trailing edge above water surface;
c) Upper surface only wetted;

Treating the hydro-ski as a flat plate at negative trim moving parallel to the water surface, a reasonable estimate for the vertical component of its "hydraulic" loading can be easily developed by applying the impulse-momentum relationship to the change in velocity direction of the fluid above the leading edge, as indicated in the following sketch:
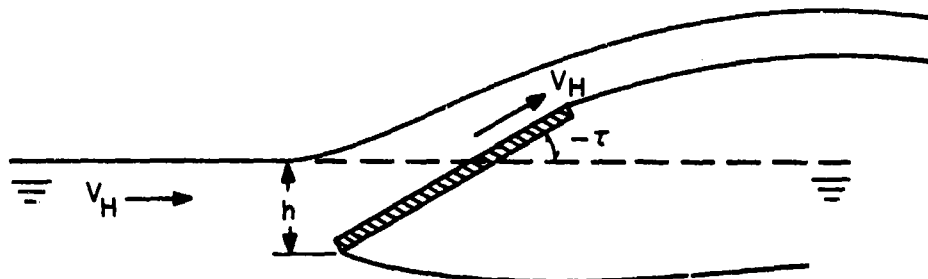
The impulse-momentum relationship is:

$$\left| F \right| \Delta t = M \left| \Delta V \right|$$

or,

$$\left| F \right| = \frac{M}{\Delta t} \left| \Delta V \right|$$

where:

$$\frac{M}{\Delta t} = \text{mass rate of flow}$$

$$\left| \Delta V \right| = \text{velocity increment}$$

For a fluid stratum of thickness h, and a hydro-ski width, b:

$$\frac{M}{\Delta t} = \rho h b V_H$$

Also,

$$\left| \Delta V \right| = V_H \sin(-\tau)$$

With

$$F = L_V = \text{vertical lift component},$$

there is finally obtained:

$$L_V = \rho h b V_H^2 \sin(-\tau)$$

This is taken as the basic expression for the downward force acting on a hydro-ski planing at a negative trim.

As it stands, this basic expression does not account for the detailed nature of the flow past the side edges of the ski. To account for this factor and, also, for possible upper surface deadrise, β_u, this expression is multiplied by a factor:

$$C_D = .88 \sec \beta_u \quad (\beta_u \geqslant 0°)$$

$$C_D = .88 \cos \beta_u \quad (\beta_u \leqslant 0°)$$

The second of these terms is an approximation for the well-known Bobyleff drag coefficient for a wedge in cavity flow and the first is an "ad hoc" estimate for the

$\beta_u < 0°$ case for which no theory presently exists.

For calculating the hydrodynamic load in this case, the velocity parallel to the water surface, V_H, is regarded as the equivalent planing velocity, V_{eq}, corresponding to the resultant velocity component normal to the keel.

Case (3)

The necessary conditions for Case (3) are:

a) Leading edge at or above water surface;
b) Trailing edge below water surface;
c) Upper surface only wetted.

Case (3) is treated by the same approach used for Case (2). That is, the resultant velocity component normal to the keel defines the equivalent planing velocity. It should be noted that the latter is also directed toward the right side of the preceding sketch.

Case (5)

The necessary conditions for Case (5) are:

a) Leading edge at or below water surface;
b) Trailing edge below leading edge;
c) Lower surface only wetted.

This is the conventional submerged supercavitating case which has primarily been studied for high-speed hydrofoil design. The Johnson supercavitating lift formula, corrected for finite depth, is used on this case. (See Section D-3 of this appendix.)

Case (6)

The necessary conditions for Case (6) are:

a) Trailing edge at or below water surface;
b) Leading edge below trailing edge;
c) Lower surface only wetted.

This case is treated in a manner identical to Case (5), that is, depth corrections are still based on the distance from the leading edge to the water surface.

Case (8)

Here again, because it is simpler conceptually, Case (8) is treated prior to Case (7). The necessary conditions for Case (8) are:

a) Leading edge below trailing edge;
b) Trailing edge at or below water surface;
c) Upper surface only wetted.

In this case, it is assumed that the cavity to the lower surface extends to the atmosphere so that ventilated (supercavitated) flow exists. However, when near the water surface, the depth correction factors of Cases (5) and (6) are inapplicable because, unlike Cases (5) and (6), the fluid region on the positive pressure side of the hydro-ski does not extend to infinity.

An approximate solution for this case is therefore established in the following manner:

1) First, the lift coefficient is determined in the same manner as for Cases (5) or (6) at deep draft, for ventilated flow.

2) A generally different lift force is then also calculated by the same method as was employed for Case (4).

3) The lower of the two resulting values of lift force is then selected as being the more correct.

Case (7)

The necessary conditions for Case (7) are:

a) Leading edge at or below water surface;
b) Trailing edge below leading edge;
c) Upper surface only wetted.

The approach in this case is essentially the same as that for Case (8). That is, the deep draft calculation is made in exactly the same manner but the effect of water surface proximity is treated as described for Case (5), where the normal velocity component is used to establish the equivalent planing velocity.

Case (9)

This conventional two-dimensional impact case is used until bow submergence occurs, provided that the initial contact trim angles for Cases (1) and (2) are from −3° to +3°. Further, if the hydro-ski deadrise is less than 10°, the effective deadrise is taken as

10°. The virtual mass values derived by J. D. Pierson in Reference D-1 are used to express the rate of virtual mass growth with keel depth. Pierson's two-dimensional virtual mass values can be approximated by the formula:

$$m_w / (\pi/2) \rho C^2 = .246 \beta^2 - .745 \beta + .802$$

where: C = wetted semiwidth = $(\pi/2)$ z cot β (Wagner wave rise formula);

z = keel draft to undisturbed water line;

β = deadrise angle, radians

The impact force acting on the hydro-ski in this condition is calculated by integration of the hydrodynamic force per unit length over the total wetted length of the hydro-ski. That is, the fundamental expression for the hydrodynamic force per unit length is:

$$\frac{dF}{ds} = m_w \frac{dV_n}{dt} + V_n \frac{dm_w}{dt}$$

where: m_w = virtual water mass per unit length;

V_n = velocity component normal to the keel;

In terms of the local draft, z :

$$\frac{dF}{ds} = m_w \frac{dV_n}{dz} \frac{dz}{dt} + V_n \frac{dm_w}{dz} \frac{dz}{dt}$$

Since $V_n = dz/dt$,

$$\frac{dF}{ds} = m_w V_n \frac{dV_n}{dz} + V_n^2 \frac{dm_w}{dz}$$

When this expression is integrated over the hydro-ski length, it is seen that the first term is related to the magnitude of the total virtual mass and the rate at which the normal velocity varies with draft, (i.e., the acceleration) which can be neglected in hydro-ski impacts. The second term is related to the rate at which the total virtual mass varies with draft. Accordingly, the differential force, dF, on an elemental strip of length, ds, is dependent on the chine-water surface relation at that instant. A strip of water (fixed in the

still fluid) in the "chines-dry" region has a varying virtual mass, while a strip in the "chines wetted" region has a constant virtual mass. The implications of this statement on the total hydro-ski load can be best illustrated by considering a constant trim impact of a rectangular planform hydro-ski having deadrise, with a constant normal velocity component to the keel. In this case, prior to wetting of the chine, since the magnitude of the virtual mass varies with the square of the wetted width, the hydrodynamic impact force increases parabolically with draft. After chine immersion has occurred, the virtual mass associated with the chines-dry region remains constant. However, it is seen that the virtual mass associated with the chines-wetted region varies linearly with the draft, so that under the assumed constant velocity impact, the impact load remains constant until the bow submerges. Finally, an aspect ratio correction, $1 - (b/2l_w)$, is applied to the load calculated by the basic two-dimensional procedure to account for the finite hydro-ski length.

The hydrodynamic load in a "two-dimensional" hydro-ski impact is, therefore:

$$F = V_n^2 \frac{dm_w}{dz} (1 - \frac{b}{2l_w}) \int_o^{l_w} ds$$

$$= V_n^2 \frac{dm_w}{dz} l_w (1 - \frac{b}{2l_w})$$

where: l_w = actual keel wetted length prior to chine immersion; or

wetted keel length corresponding to the draft at which chine immersion occurs.

The growth rate with draft of the virtual mass, dm_w/dz, is evaluated from the analytical expression:

$$m_w/(\pi/2) \rho C^2 = m_w/(\pi^3/8) \rho z^2 \cot^2 \beta = .246 \beta^2 - .745 \beta + .802$$

so that $dm_w/dz = (.246 \beta^2 - .745 \beta + .802)(\pi^3/4) \rho z \cot^2 \beta$

where: z = actual draft, prior to chine immersion, or, after chine immersion, draft at which chine immersion occurs.

D2.   HYDRODYNAMIC MOMENTS

        Associated with the hydrodynamic loads for the nine impact conditions described
above are their respective centers of pressure which are required for calculating hydro-
dynamic moments about the aircraft center of gravity. For some of these conditions, the
analytic expressions for centers of pressure have already been established earlier in this
report; for the remainder, a series of simple and plausible approximations have been made,
as will now be described.

Case (1):

        Shuford formula; see Section 3.2

Case (2):

        0.3 of wetted length forward of ski-water line intersection

Case (3):

        0.3 of wetted length forward of ski trailing edge

Case (4):

        0.3 of wetted length aft of ski leading edge

Cases (5), (6), (7), and (8):

        Computer subroutine, as described in Appendix B.

Case (9):

        2/3 of chines-dry wetted length from ski-water line intersection

D3.   APPROXIMATION FOR JOHNSON'S LIFT FORMULA

        Section 3.4 of this report describes a computer program which "automates"
the calculation of ski lift and moment for the submerged ventilated condition. This program
replaces the "manual" iteration and interpolation procedures required for application of
Johnson's theory. As mentioned in Section 3.4, it was intended to use this program as a
subroutine in the wave response computer program.

        When this was attempted, it was found that the total wave response program ex-
ceeded the capacity of Edo's IBM 1130 Computer. To eliminate this difficulty, the venti-
lated flow subroutine was replaced by another much simpler (and slightly less accurate)
program, developed as follows:

Johnson's expression for C_{L1} is:

$$C_{L1} = \frac{A}{A+1} \, m \, (\alpha - \alpha_i) \, \frac{\cos \alpha}{\cos (\alpha - \alpha_i)} \qquad \text{(D-1)}$$

where $\qquad \alpha_i = C_{L1} / \pi A \qquad$ (D-2)

and m is a complicated function of $\alpha - \alpha_i$ and d/c (depth-chord ratio), shown graphically in Figure 2 of NACA RML57I16.

The quantity, m, is approximated now by the expression:

$$m \cong \pi \left[1 - .344 \, (d/c)^{.2125} \right] - 2.29 \, (\alpha - \alpha_i) \qquad \text{(D-3)}$$

Eqs. (D-1), (D-2), and (D-3) can be solved for C_{L1}:

$$C_{L1} = \pi A \left[\alpha - \psi + \sqrt{\psi^2 - \eta} \right]$$

where:

A $\quad$ = $\quad$ ski aspect ratio (b/l)

α $\quad$ = $\quad$ effective angle of attack

ψ $\quad$ = $\quad$ (1 + Cf cos α) / 2 Ck cos α

η $\quad$ = $\quad$ α / Ck cos α

C $\quad$ = $\quad$ 1 / π (A + 1)

f $\quad$ = $\quad$ $\pi \left[1 - .344 \, (d/c)^{.2125} \right]$

k $\quad$ = $\quad$ 2.29

Johnson's value for C_{L2} is retained:

$$C_{L2} = \left[.88 / (A + 1) \right] \sin^2 \alpha \, \cos \alpha$$

and his expression for the center of pressure is approximated by:

$$X_{c.p.} = (.3125 \, C_{L1} + .5 \, C_{L2}) / C_L$$

where $X_{c.p.}$ is measured from the ski L. E.

REFERENCES FOR APPENDIX D

D-1   Experimental Towing Tank, Stevens Institute of Technology, Note 137:
         "On the Virtual Mass of Water Associated with an Immersing Wedge",
         by J. D. Pierson, (undated).

DOCUMENT CONTROL DATA - R & D

(Security classification of title, body of abstract and indexing annotation must be entered when the overall report is classified)

1. ORIGINATING ACTIVITY *(Corporate author)*	2a. REPORT SECURITY CLASSIFICATION
Edo Corporation College Point	UNCLASSIFIED
	2b. GROUP

3. REPORT TITLE

Survey on Seaplane Hydro-Ski Design Technology Phase 2: Quantitative Study

4. DESCRIPTIVE NOTES *(Type of report and inclusive dates)*

5. AUTHOR(S) *(First name, middle initial, last name)*

Perry, A. Pepper and Leon Kaplan

6. REPORT DATE	7a. TOTAL NO. OF PAGES	7b. NO. OF REFS
28 March 1968	242	62

8a. CONTRACT OR GRANT NO.	9a. ORIGINATOR'S REPORT NUMBER(S)
b. PROJECT NO.	7489-2
c.	9b. OTHER REPORT NO(S) *(Any other numbers that may be assigned this report)*
d.	None

10. DISTRIBUTION STATEMENT

Distribution of this Document is Unlimited

11. SUPPLEMENTARY NOTES	12. SPONSORING MILITARY ACTIVITY
	Office of Naval Research

13. ABSTRACT

This report covers the second part of a two-phase survey and analysis of hydro-ski seaplane technology. It contains quantitative correlations and parametric analyses of significant data used to define optimum hydro-ski size, ski location with respect to the strut and aircraft, ski and strut resistance, ski loads and load factors in waves, strut attachment to the aircraft, effects of strut size and length, and ski installation weight. The Phase I report previously issued, contains qualitative descriptions and correlations of the same information, as well as a complete bibliography of hydro-ski technology.

These two documents contain all of the background knowledge required before conducting general or specific studies of hydro-ski configurations for a given set of design criteria, thereby eliminating the necessity for first reviewing the entire vast literature on seaplane hydro-skis. Simultaneously, they serve to define the state-of-the-art in this field and to indicate those specific areas requiring further investigation and definition.

14 KEY WORDS	LINK A		LINK B		LINK C	
	ROLE	WT	ROLE	WT	ROLE	WT
Hydro-Skis						
Hydrodynamics						
Seaplane						
Bibliography						